SPACE FLIGHT HANDBOOKS
Volume 2
Lunar Flight Handbook

PART 1 - BACKGROUND MATERIAL

Office of Scientific and Technical Information
NATIONAL AERONAUTICS AND SPACE ADMINISTRATION
Washington, D. C. **1963**

CONTENTS

Volume II, Part 1 - Background Material

The preceding contents are Part 1 of Volume II. The remaining two parts of Volume II contain the following:

Volume II, Part 2 - Lunar Mission Phases

Volume II, Part 3 - Mission Planning

FOREWORD

This handbook has been produced by the Space Systems Division of the Martin Company under contract NAS8-5031 with the George C. Marshall Space Flight Center of the National Aeronautics and Space Administration. The Lunar Flight Handbook is considered the second in a series of volumes by various contractors, sponsored by MSFC, treating the dynamics of space flight in a variety of aspects of interest to the mission designer and evaluator. The primary purpose of these books is to serve as a basic tool in preliminary mission planning. In condensed form they provide background data and material collected through several years of intensive studies in each space mission area, such as earth orbital flight, lunar flight, and interplanetary flight.

Volume II, the present volume, is concerned with lunar missions. The volume consists of three parts presented in three separate books. The parts are:

> Part 1 - Background Material
> Part 2 - Lunar Mission Phases
> Part 3 - Mission Planning

The Martin Company Program Manager for this project has been Jorgen Jensen; George Townsend has been Technical Director. Fred Martikan has had the direct responsibility for the coordination of this volume; he has shared the responsibility for the generation of material with Frank Santora.

Additional contributors were Robert Salinger, Donald Kraft, Thomas Garceau, Andrew Jazwinski and Lloyd Emery. The graphical work has been prepared by Dieter Kuhn and Elsie M. Smith. John Magnus has assisted in preparing the handbook for publication. William Pragluski, Don Novak, James Porter, Edward Markson, Sidney Roedel, Wade Foy and James Tyler have made helpful suggestions during the writing of this book.

The assistance given by the Future Projects Office at MSFC and by the MSFC contract management panel, directed by Conrad D. Swanson is gratefully acknowledged.

INTRODUCTION

I. INTRODUCTION

The primary intent of the Lunar Flight Handbook is to introduce the engineer to the flight mechanics aspects of lunar missions. In addition, the handbook material is designed to enable the user to design a lunar mission for any date in this decade.

To fulfill this double purpose while presenting new material in compact form, several guidelines were established and followed in the selection and arrangement of the material.

The format selected for the Lunar Flight Handbook is somewhere between textbooks of celestial mechanics and observational astronomy, and the recent literature in journals and reports. The material presented in the Handbook is intended to provide the link between these two types of publications and to provide a framework for the published articles and reports covering specialized aspects of lunar flight.

The order of the presentation progresses from relatively simple physical concepts to a derivation, or the outline of the derivation, of more detailed results and concepts. More important and useful results are presented analytically, and if possible graphically, while results which depend on the vehicle configuration and operational concepts, such as the use of tracking and communication equipment, have been described in narrative form only. A large number of sketches are included in the text in order to permit a quick grasp and easy visualization of the concepts and techniques of lunar flight.

Frequent reference to outside material is provided to enable the reader to trace numerical values to their source and find references to further material. Frequent reference is made to material in the Orbital Flight Handbook, the companion volume to this Handbook, since the technical material overlaps to some extent. It was attempted to keep the technical level and notation uniform throughout the Handbook. This was no small task if one considers that a number of people were contributing to the Handbook directly and much outside material was reviewed, checked and integrated into the text.

The technical material of the Handbook is arranged into three groups:

(1) Background material. This group, consisting of Chapters II, III and IV, gives the results of astronomy, describes the geometry, the environment, the force models for trajectory calculation, and classifies lunar trajectories and missions. In addition, since all material in the Lunar Flight Handbook is in the metric system of units, conversions to the commonly used English system of units is given.

(2) Lunar mission phases. This group, consisting of Chapters V to X, discusses all possible phases of lunar flight chronologically from earth departure

to re-entry into the earth's atmosphere upon return from the moon. Of special interest is the attempt to catalogue a major portion of circumlunar and approach trajectories to the moon and return trajectories to a degree of accuracy which has not so far been achieved in the published literature.

(3) Mission planning. In the final technical chapter of the Handbook, the previous material is applied to the design of two specific lunar missions to illustrate its use in preliminary design.

The subject material of each technical chapter and some general guidelines for use of the data presented in the Lunar Flight Handbook follow.

Chapter II. PHYSICAL DATA

Chapter II describes the environment of the space vehicles, gives conversion factors between the various systems of units and describes the lunar exploration programs. In the first section, the astronautical constants, or constants describing the gravitational force acting on the space vehicle and the geometry of the celestial bodies, have been discussed. The recently published data on astronautical constants has been summarized, and the best values of these constants, together with a confidence interval determined with the Student's t distribution, have been used for all trajectory calculations in the Handbook. Thus, a standard and nearly consistent set of constants based on recent data has been adopted. Future, more accurate determinations of these astronautical constants will not change any of the graphical trajectory data significantly. Thus, the Handbook will retain its value for preliminary design purposes.

The atmospheric, meteoritic, radiative and thermal environment of the space vehicle and the effect of this environment on the vehicle and its occupants are then discussed. The data on the near-earth environment and earth-moon space environment has been classified and summarized with frequent reference to the Orbital Flight Handbook for details, while the near-moon and lunar surface environment, as deduced from observations and as it is known at the present, has been discussed in much more detail.

Since handbook data is given in the absolute MKS system of units, the various systems of mechanical and thermal units employed for trajectory calculations as well as conversion factors between metric, English and astronomical systems of units are given. Much of the data is in tabular form, but basic definitions and fundamental units with common multiples and submultiples have been listed in the text to provide for convenient conversions between the various systems of units.

The chapter continues with a review of the current status of the U.S. lunar exploration

program to familiarize the reader with the project terminology and with the immense scope of the lunar exploration task. A list of announced space vehicle launches with lunar missions, their trajectories, results and attempted experiments completes the material of Chapter II.

Chapter III. THE EARTH-MOON SYSTEM

Chapter III provides some astronomical background for lunar flight. The various coordinate systems centered at the earth or the moon and used for describing the position of space vehicles are introduced, and transformations between the various moon-centered and trajectory coordinate systems are given. A list of available lunar maps is also included.

The motion of a space vehicle in earth-moon space as interpreted in the three-body and restricted three-body problems of astronomy is discussed. Conclusions that can be drawn from these astronomical results in their application to ballistic space-vehicle trajectories in earth-moon space have been presented in some detail.

Since knowledge of lunar position and orientation is also required for lunar flight, brief descriptions of Delaunay's Hansen's and the Hill-Brown lunar theories are followed by a listing of the available lunar ephemerides and by a method for including lunar librations in trajectory digital computer programs.

Chapter IV. TRAJECTORIES IN THE EARTH-MOON SYSTEM

This chapter introduces, in descriptive form, the nomenclature and classification of lunar missions and trajectories as well as the determination of the trajectories. The restricted three-body problem permits the use of many types of ballistic trajectories for lunar flights. If thrust is available to modify these ballistic trajectories at predetermined points, a wide variety of lunar missions are possible. The most common missions have been described and illustrated by sketches in the text.

The force models, or the physical assumptions, underlying trajectory calculations, have been described in considerable detail in order to show the assumptions involved in the use of particular equations of motion for lunar trajectory calculations. The description starts from simple two-body equations permitting closed-form solutions; it progresses through the "patching" of two-body trajectories around the earth and moon in order to obtain a complete ballistic lunar trajectory; the restricted three-body force model is discussed as a tool to determine trajectories; the n-body force model with earth oblateness and lunar triaxiality is presented in detail; and the chapter concludes with a discussion of the effects of nongravitational forces, such as rocket thrust, atmospheric drag, meteoritic drag, solar radiation pressure, electromagnetic forces, special and general relativistic effects. In most cases the form of the equations of motion has been given or derived and the effect of including the nongravitational forces in lunar trajectories is evalu-

ated. The description of methods for numerical integration of these trajectories on the digital computer round out this section.

The Voice (volume-of-influence calculated envelopes) computation technique, which uses a patched conic force model, and the geometry and nomenclature peculiar to the Voice technique have been introduced in the final section of Chapter IV. This special treatment is necessary since the particular trajectory geometry enables the efficient cataloguing of lunar trajectories to be discussed in the summary of Chapter VI.

Chapter V. EARTH DEPARTURE

This is the first chapter in the chronological description of the separate phases of a lunar mission. The fixed translunar trajectory technique, in which the translunar trajectory has a specified inclination to the moon's orbital plane at injection, the variable translunar trajectory technique, in which the inclination of the translunar trajectory varies with the time of injection, and the translunar injection itself are discussed.

It is demonstrated how the use of parking orbits during earth departure increases the period in which space vehicle launch can take place (i.e., the launch tolerance) and hence provides additional flexibility for the planning of lunar missions. During the injection phase, abort requirements, or the requirements to return the space vehicle to earth as quickly as possible in the event of a malfunction, have been discussed. Abort requirements are mentioned for each phase of lunar flight in the Handbook since they are important for the selection of trajectories and vehicle hardware for manned lunar missions and since many published articles disregard this aspect of lunar missions.

All graphical data for specific numerical examples in the Lunar Flight Handbook reflects launches from Cape Canaveral, Florida, under appropriate launch azimuth restrictions. At present, NASA has announced plans to use this launch site for lunar flights, and in view of the long-range planning and expense of the launch support equipment, these plans are likely to be carried out. Launch from other sites with different launch azimuth restrictions requires a different set of graphs since trajectories have a strong dependence on launch site location.

Chapter VI. EARTH-TO-MOON TRANSFER

Of special note in this chapter is the catalogue of a large portion of circumlunar trajectories to an accuracy which permits the preliminary selection of lunar mission parameters-- a level of accuracy which is unique among presentations of this type. Use of the Voice patched-conic trajectory program, use of trajectory symmetry about the moon's orbital plane as well as a plane perpendicular to it, and use of two equations for extending injection parameters, enables the presentation of a major portion of the circumlunar trajectories launched from Cape

Canaveral in only 83 figures. Typical comparisons of trajectories calculated by use of the Voice technique, the restricted three-body force model, and the n-body force model have been given frequently throughout the Handbook in order to illustrate the remarkable accuracy achievable with the Voice technique.

Navigation during lunar missions has been discussed qualitatively and quantitatively, with examples given for a particularly useful navigation technique for position determination in cislunar space. Tracking and communications, on the other hand, have been described qualitatively, since the actual procedures depend to a great degree on the available equipment as well as on the trajectory. Several techniques for determining midcourse guidance corrections have been discussed and some typical fuel requirements are also given.

Abort requirements and possible abort procedures during the translunar trajectory phase together with abort maneuver graphs for a typical circumlunar mission conclude the material of Chapter VI.

Chapter VII. LUNAR ORBIT

Artificial satellites in orbits around the moon behave in the same fashion as artificial satellites in earth orbits. Only the astronautical constants appearing in the equations and the magnitude of the perturbing forces of the other celestial bodies are different. Hence, satellite data most commonly used in preliminary design such as period, velocity, lunar oblateness effects on the orbit, as well as reconnaissance aspects of lunar orbits, are given analytically and graphically, and the relative magnitude of the various perturbing effects is presented.

The effect of finite rocket burning time on fuel requirements for entry to and exit from lunar orbits has been discussed, and a comparison with Voice trajectory data is made. This supplements the fuel requirements for orbit entry and exit given in the trajectory catalogues of Chapters VI and IX, which is based on an impulsive change of velocity (infinite thrust-to-weight ratio). Finally, lunar orbit determination schemes are described briefly.

Chapter VIII. DESCENT TO AND ASCENT FROM THE LUNAR SURFACE

In this chapter, the vehicle trajectory near the lunar surface has been described: the need to reduce the lunar approach velocity of the space vehicle for most landing missions, the descent burning and ballistic flight phases, any required hovering or translation, landing safety boundaries and abort during each descent or ascent phase are covered. In each case the equations of motion, some methods of trajectory optimization and guidance as well as typical results describe the trajectory phase.

Chapter IX. MOON-TO-EARTH TRANSFER

This chapter gives a catalogue of trajectories from the vicinity of the moon to the vicinity of the earth in 90 figures. Use of symmetry and reinterpretation of moon-to-earth trajectories as earth-to-moon trajectories again enables a significant extension of the catalogued data. The catalogues of Chapters VI and IX thus include a major portion of feasible circumlunar and approach trajectories. Impact as well as specialized periodic trajectories have not been catalogued since they most probably will not be used for lunar exploration in the 1965 to 1970 time period; however, they are described and classified in Chapter IV.

Midcourse guidance and energy requirements during the moon-to-earth transfer phase have been briefly discussed. The description of guidance techniques, navigational techniques and tracking requirements of Chapter VI applies directly to moon-to-earth trajectories.

Chapter X. EARTH RETURN

A description of re-entry into the earth's atmosphere and landing at a specific site completes the chronological description of the lunar mission phases. The problem of timing earth return provides the introduction to the chapter which considers two methods for re-entering the atmosphere and landing.

The first method considers a direct entry of the space vehicle into the earth's atmosphere from the transearth trajectory at speeds near the parabolic speed for earth (or earth escape speed). Equations of motion, characteristics of re-entry trajectories, maneuverability by use of aerodynamic forces and various guidance techniques during this supercircular re-entry are considered.

The second method of re-entry employs a combination of atmospheric and rocket or pure rocket deceleration to establish a circular earth satellite orbit prior to re-entering and landing from circular orbital speed. The requirements on the guidance system and the materials are thus reduced, but a significant amount of fuel is required for the deceleration and deorbit maneuvers.

Chapter XI. MISSION PLANNING

Chapter XI, provides the link between the background and trajectory material presented in Chapters II to X and the planning of a lunar mission on a specific date in the period of 1965 to 1970.

The following material is necessary for the conversion from generalized trajectory data to specific mission dates: transformations from the Voice coordinate system to the selenographic coordinate system, the illumination of the moon by the sun, lunar declination and distance from the earth, and some useful empirical relationships for extending catalogued

trajectory data. Also included are mission planning envelopes, or graphs which give several geometrical trajectory parameters as a function of mission constraints in summary form, thus enabling a ready patching of the translunar, lunar orbit, and transearth trajectories into a complete and continuous trajectory for the mission.

The use of the material in the Handbook and the procedure of planning lunar missions has been illustrated by two sample missions in the final section of the chapter. One mission is a manned lunar exploration mission with a stay of three days on the lunar surface, while the other is an unmanned photographic reconnaissance mission of the moon lasting one month. In addition to illustrating the use of the Handbook material for mission planning, these missions are representative of the type of lunar missions planned for the end of this decade.

CHAPTER II

PHYSICAL DATA

Prepared by:

F. Martikan and R. Salinger
Martin Company (Baltimore)
Aerospace Mechanics Department
March 1963

The purpose of this chapter is to present background data for the discussion of lunar missions--to be more specific, the astrodynamical constants needed for lunar trajectories, a discussion of the space vehicle environment, and of the absolute MKS system of units used in the handbook, together with conversion factors to English units. The astrodynamical constants and near-earth environment have been discussed in the companion volume (Chapter II, Ref. 1), and data from that reference is given in summary form for the convenience of the user. Additional data needed specifically for lunar missions has been included in more detail in Sections A and B. A list of space vehicle launches with lunar missions, their objectives, and the present lunar exploration program of the United States is given at the end of the chapter, in Section D.

A. ASTRONAUTICAL CONSTANTS

The constants of the solar system determined from astronomical observations are accurate enough for the prediction of the positions of celestial bodies. However, for a successful lunar or interplanetary mission, better values for the astronomical unit (AU), the distances, diameters, figures, masses, and other data concerning the earth, moon, sun, and planets are required. As these values should be internally consistent, they depend on the physical model used for the trajectory calculation. In addition, some indication of the uncertainty in the values is necessary since these constants define the ballistic trajectory, and uncertainties in the constants are reflected in trajectory "errors" and "miss distances."

In recent years, several articles on astronautical constants have appeared in the literature (Refs. 2, 3, 4, 5 to name but a few). Of these, Refs. 2 and 3 have aimed at a standardization of the constants for astronautical calculations (although there seem to be small inconsistencies in the data, and no indication of a "standard deviation" or other "confidence interval" is given in the data). Reference 4 is restricted to a statistical analysis of geocentric constants, and the constants in Ref. 5, even though internally consistent, appeared too late for their evaluation and inclusion in the handbook. Reference 5 is reproduced in its entirety as Appendix B of Ref. 1. In addition, the calculation of the lunar ephemeris is based on a different set of constants, which is given in the American Ephemeris (Ref. 6). Since more accurate values of constants will become available in the future from observations of space vehicles, radar echoes, and by other means, most of these constants will be superseded by more accurate values and smaller tolerances. In any case, the best values available should be used in trajectory calculations.

For the trajectories in this handbook and its companion volume, Ref. 1, the recently published data has been summarized, and the best values of the constants have been used. The procedure used for determining the means of the various constants is as follows:

(1) Collect all recent values of a particular constant.

(2) Assume that the various values of the particular constant are of roughly the same accuracy.

(3) Obtain the mean ($\bar{x}$) and variance (σ^2) of this sample,

$$\bar{x} = \frac{1}{n} \sum_{i=1}^{n} x_i, \quad \sigma_{\bar{x}}^2 = \frac{1}{n} \sum_{i=1}^{n} (x_i - \bar{x})^2, \quad \sigma^2 = \frac{n-1}{n} \sigma_{\bar{x}}^2 \quad , \text{ where n is the number}$$

of values for the constant.

(4) Throw out all values deviating from the mean by more than one standard deviation (1σ).

(5) Recompute the mean and use this value as the "adjusted mean" for the constant.

The "confidence interval" of a constant is used here to indicate that the sample interval brackets the true mean or adjusted mean, as computed by the procedure above, some prescribed percentage of the time. For these small samples, the confidence interval has been obtained from the Student's t-distribution. As this procedure has been fully discussed in Chapter II of Ref. 1, no further details will be given here.

In the remainder of this section, the astronautical constants are defined (and discussed, when necessary), and at the end of the section, their values and confidence levels as used in the handbook are summarized. Since, in the broadest sense, all celestial bodies influence the trajectory to some degree, heliocentric and planetocentric constants will be given, together with the geocentric and selenocentric constants which are of primary interest for lunar trajectories.

1. Heliocentric Constants

Planetary observations and theories of planetary motion permit precise computation of the angular position of the planets. Although angular measurements are quite accurate, no distance scale is readily available. Attempts to resolve this problem have led to the comparison of large, unknown interplanetary distances to the largest of the known distances available to man, the equatorial radius R_e of the earth. In the process, solar parallax was defined as the ratio of the earth's equatorial radius to the mean distance to the sun from a fictitious unperturbed planet whose mass and sidereal period are those utilized by Gauss in his computation of the solar gravitation constant (i.e., one astronomical unit, AU). This definition renders unnecessary the revisions in planetary tables as more accurate fundamental constants are made available, since the length (in kilometers) of the astronomical unit can be modified.

In the broadest sense, the solar parallax is the ratio between two sets of units: (1) the astronomical set utilizing the solar mass, the astronomical unit and the mean solar day (which has recently been replaced by the ephemeris day), and (2) the laboratory set, for which the absolute MKS system of units has been adopted in this handbook.

Another important heliocentric quantity is the value of the solar gravitational constant, $\mu_{\odot}$ = $GM_{\odot}$, where G is the universal gravitational constant and $M_{\odot}$ is the mass of the sun. This constant can be determined in both the astronomical and the laboratory units; results from both determinations are given in this subsection.

In 1938 it was internationally agreed (IAU 1938) that to maintain the Gaussian value of the solar gravitational constant or Gaussian constant $K_{\odot}^2$ = $GM_{\odot}$ as determined by Gauss from Kepler's third law in astronomical units.

$$K_{\odot} = \frac{2\pi}{\tau} \sqrt{\frac{\bar{r}_{\odot\oplus}^3}{M_{\odot} + \frac{M_{\oplus}}{M_{\odot}}}} =$$

$$0.017, 202, 098, 95 \ \frac{AU^{3/2}}{\text{solar day}} \qquad (1)$$

where

$\bar{r}_{\odot\oplus}$ = 1 AU

τ = 365.256,383,5 mean solar days

$M_{\odot}$ = solar mass = 1

$\dfrac{M_{\oplus}}{M_{\odot}}$ = ratio of earth and solar masses

= 0.000,002,819

The value of $K_{\odot}$ has nine significant figures by this definition.

The value of $\mu_{\odot}$ = $GM_{\odot}$ (as $K_{\odot}^2$ is usually denoted when measured in laboratory units) can be determined directly by use of the best values for G and $M_{\odot}$. This yields, if we refer to Ref. 2,

$$\mu_{\odot} = 1.3251 (1 \pm 0.0010) \times 10^{20} \ \left[m^3/sec^2\right]$$

$$\mu_{\odot}^{1/2} = 1.1511 (1 \pm 0.0005) \times 10^{10} \ \left[m^3/sec^2\right]^{1/2}$$

The latter value, which corresponds to $K_{\odot}$ measured in laboratory units, is accurate only to the three significant figures as compared to the nine significant figures of the determination of $K_{\odot}$ in astronomical units.

It is thus advantageous to compute in the astronomical system of units, converting only when necessary. This procedure assures that the results will become more accurate as better values for the astronomical unit are obtained and pro-

duces a much lower end figure error due to round-off.

The sun's orbit and such auxiliary constants as the mean obliquity of the ecliptic, its rate of rotation, and lengths of the various years can be found in the American Ephemeris (Ref. 6).

2. Planetocentric Constants

The mass of a planet is its most important property from the standpoint of trajectory analysis; only in the vicinity of a planet will its actual shape influence the trajectory to some degree. From the mass and its shape, some auxiliary quantities such as the radius of a sphere having the equivalent volume can be derived.

Planetary and some lunar data is summarized in tabular form at the end of this subsection. Table 1 presents the gravitational properties of the sun and planets--their masses and gravitational constants μ = GM in absolute MKS, gravitational FPS, and astronomical units. In addition, the radius of action of the particular planet with respect to the sun is given in the same units. The radius of action

$$r^* = r_{\odot p} \left(\frac{M_p}{M_{\odot}}\right)^{2/5} \qquad (2)$$

where $r_{\odot p}$ = distance from sun to planet

defines a spherical region around the planet p which approximates the sphere of influence of the planet in the dynamical system of the planet and the sun. (For more detail, see Subsection B-1b of Chapter IV.) The main significance of the radius of action lies in its use in the "patching" of conic trajectories; inside the sphere of influence, the gravitational attraction of the planet may be neglected as a first approximation to the trajectory, while outside the sphere of influence the gravitational attraction of the planet may be neglected. In the case of the moon, the tabulated radius of action is centered at the moon and defined with respect to the earth, while in the case of the earth-moon system it is centered at the earth-moon barycenter, and the combined masses of the earth and moon are used in its definition with respect to the sun. The last three columns of Table 1 present the sidereal period of revolution, its mean distance from the sun, and the true distance of the planet from the earth on a given date to illustrate the scale of planetary distances and for typical calculations of planetary gravitational attractions near the earth. The data is taken from Refs. 7 and 6, respectively.

Table 2 presents the geometry of the planets. Most celestial bodies are very nearly spherical in shape. However, an oblate ellipsoid can be assumed as a second approximation to the planetary shape, while, for the shape of the moon, a triaxial ellipsoid has been deduced from observations. The oblate ellipsoid is defined by its equatorial radius R_e, its polar radius R_p, or, alternatively, by R_e and its flattening, f, with

$$f = \frac{R_e - R_p}{R_e} \qquad (3)$$

TABLE 1

Gravitational Properties of the Planets

Planet	Mass M 10²⁴ kg	Mass M 10²⁴ slugs	$M_\odot/M_p$	Gravitational Constant μ 10⁶ km³/sec²	10¹⁶ ft³/sec²	10⁻⁹ AU³/solar day²	Radius of Action r* 10⁶ km	10⁹ ft	AU	Sidereal Period of Revolution (yr)	Mean Distance from the Sun to the Planet (AU)	True Distance from Earth (AU) Epoch: December 25.0, 1963
Mercury	0.3257	0.02232	6,100,000 ±65,000	0.021,725	0.076,721	0.048,509	0.11178	0.36674	0.000,747,6	0.2411	0.387	0.8407
Venus	4.8811	0.3345	407,000 ±1300	0.325,581	1.149,78	0.726,987	0.61696	2.0241	0.004,126	0.6156	0.724	1.4076
Earth	5.9758	0.40947	332,440 ±50	0.398,601,5	1.407,648	0.890,033	0.92482	3.03429	0.006,185,0	1.0000	1.0000	0
Earth-Moon	6.0484	0.41444	328,400 ±25	0.403,444	1.424,75	0.900,847	0.92933	3.04898	0.006,215,1	--	--	--
Moon	0.073451	0.0050330	$\frac{M_\oplus}{M_{\mathrm{C}}} = 81.357 \pm 0.010$	0.004,899,4	0.017,302,1	0.010,939,8	0.066282	0.217460	0.000,443,3	0.0748**	--	0.0025
Mars	0.6429	0.04405	3,090,000 ±12,000	0.042,883,0	0.151,440	0.095,753,1	0.57763	1.8951	0.003,863	1.8822	1.53	2.3554
Jupiter	1896.7	129.97	1,047.4 ±0.1	126.515	446.783	282.493	48.141	157.943	0.321,96	11.86	5.20	4.7246
Saturn	567.60	38.89	3500 ±1.7	37.860,4	133.703	84.538,3	54.774	179.70	0.366,31	29.46	9.54	10.4871
Uranus	87.132	5.970	22,800 ±100	5.811,91	20.524,6	12.977,4	51.755	169.80	0.346,13	84.0	19.2	17.9031
Neptune	101.88	6.981	19,500 ±200	6.795,75	23.999,0	15.174,2	86.952	285.28	0.581,51	164.8	30.1	31.0049
Pluto	5.676	0.3889	350,000 ±27,000	0.378,596	1.337,0	0.845,364	35,812	117.49	0.239,5	247.7	39.4	32.5967
Sun	1.9866 x 10⁶	0.13613 x 10⁶	1.00000	132,511	467,960	295,912.208.3*	--	--	--	--	--	0.9835

Underlined digits are questionable.
* Solar gravitational constant is Gaussian value.
** Period of revolution is around earth.

Table 2 also presents the radius of the sphere having the same volume as the oblate ellipsoid,

$$R = \left(R_e^2 \, R_p\right)^{1/3} \qquad (4)$$

to facilitate Keplerian orbit calculations and to illustrate the small planetary asphericities.

Table 3 presents the circular velocity, escape velocity and gravity at the surface of the equivalent sphere (called "sea level") in metric, English and astronomical units, as computed from the following equations:

$$V_{circular} = \sqrt{\frac{\mu}{R}}$$

$$V_{parabolic} = V_{escape} = \sqrt{\frac{2\mu}{R}} \qquad (5)$$

$$g_0 = \frac{\mu}{R^2}$$

Preliminary trajectory calculations use the spherical body assumption (i.e., that the celestial body is spherically symmetric in concentric layers) with the radius R given by Eq (4) and the gravitational potential by $U = \frac{\mu}{r}$, where r is the distance from its center. The gravitational attraction is given by $g = \frac{\partial U}{\partial r} = -\frac{\mu}{r^2}$, where the negative sign denotes an attractive force. Orbital data for the planets and auxiliary quantities can be obtained from Ref. 6. Since the orbits of planets (with the exception of Mercury and Pluto) are very nearly circular and are near the ecliptic plane, another common assumption for preliminary calculations is that planetary orbits are circular and in the ecliptic. Further data on planets and their orbits, together with the sources of this information, has been presented in Chapter III of Kuiper (Ref. 8) and in the references listed in the Bibliography of background material of the Lunar Flight Handbook.

3. Geocentric Constants

The approximation of the earth's shape by a rotating oblate ellipsoid which in the interior is symmetric in ellipsoidal layers is quite good for ascent and descent trajectories as well as short-time orbits around the earth. The further assumption is made that the surface of the oblate ellipsoid is an equipotential surface of the geopotential which consists of the gravitational potential of the earth, $U_{\oplus}$, and the potential of the centrifugal force due to the rotation, $\frac{1}{2} \omega_{\oplus}^2 \, R_\phi^2 \cos^2 \phi'$, where $\omega_{\oplus}$ is the rotational rate of the earth around its axis, R_ϕ is the local radius of the earth, and ϕ' is the geocentric latitude.

The local radius of the oblate ellipsoid R_ϕ as a function of geocentric latitude is given by

$$\frac{R_\phi^2 \cos^2 \phi'}{R_e^2} + \frac{R_\phi^2 \sin^2 \phi'}{R_e^2 (1 - f)^2} = 1$$

which can be expressed to order f^2 as

$$R_\phi \simeq R_e \left[1 - f \sin^2 \phi + \frac{5}{8} f^2 \sin^2 2\phi \right]$$

$$\simeq R_e \left[1 - f \sin^2 \phi' - \frac{3}{8} f^2 \sin^2 2\phi' \right] \qquad (6)$$

where the flattening f is defined by Eq (3), R_e is the earth's equatorial radius, ϕ is the geodetic latitude (as given on maps), and ϕ' is the geocentric latitude. These latter two quantities are related by

$$\tan \phi' = (1 - f)^2 \tan \phi. \qquad (7)$$

A consistent expression for $U_{\oplus}$ is given by

$$U_{\oplus} = \frac{GM_{\oplus}}{r_G} \left[1 - \frac{1}{2} J_2 \left(\frac{R_e}{r_G} \right)^2 (3 \sin^2 \phi' - 1) \right.$$

$$\left. - \frac{1}{8} J_4 \left(\frac{R_e}{r_G} \right)^4 (35 \sin^4 \phi' - 30 \sin^2 \phi' + 3) \right] \qquad (8)$$

where r_G is the distance from the center of the earth (the radius in the geographic coordinate system) $GM_{\oplus} = \mu_{\oplus}$ is the gravitational constant of the earth, and J_2 and J_4 are numerical coefficients which can be expressed in terms of f, R_e, $\mu_{\oplus}$, and $\omega_{\oplus}$. Equations (6) through (8) can be applied to any oblate planet.

The earth's gravitational potential, $U_{\oplus}$, at a point exterior to the earth must satisfy Laplace's equation.

$$\nabla^2 U_{\oplus} \equiv \frac{\partial^2 U_{\oplus}}{\partial x_{\oplus}^2} + \frac{\partial^2 U_{\oplus}}{\partial y_{\oplus}^2} + \frac{\partial^2 U_{\oplus}}{\partial z_{\oplus}^2} = 0 \qquad (9)$$

A solution of this partial differential equation by separation of variables suggests an expansion of $U_{\oplus}$ in terms of spherical harmonics which can be written in the form

$$U_{\oplus} = \frac{\mu_{\oplus}}{r_G} \left\{ 1 + \sum_{n=1}^{\infty} \sum_{m=0}^{n} \left(\frac{R_e}{r_G} \right)^n P_n^m (\sin \phi') \cdot \right.$$

$$\left. \left[C_{n,m} \cos m\lambda + S_{n,m} \sin m\lambda \right] \right\} \qquad (10)$$

where R_e now becomes the earth's mean equatorial radius, λ is the longitude (counted positive to the east through 360°), $C_{n,m}$, $S_{n,m}$ are numerical coefficients, and P_n^m is the associated Legendre polynomial, defined in terms of the Legendre polynomial P_n by

$$P_n^m (x) = (1 - x^2)^{\frac{m}{2}} \frac{d^m}{dx^m} \left[P_n (x) \right] \qquad (11)$$

TABLE 2

Geometry of the Planets

Planet	Equatorial Radius, R_e (km)	(stat mi)	(naut mi)	(ft x 10^7)	1/f	Polar Radius, R_p (km)	(stat mi)	(naut mi)	(ft x 10^7)	Radius of Sphere of Equivalent Volume, R ($R^3 = R_e^2 R_p$) (km)	(stat mi)	(naut mi)	(ft x 10^7)
Mercury	2330 ±10	1448 ±6	1258 ±5	0.7644 ±0.0032	∞*	2330 ±10	1448 ±6	1258 ±5	0.7644 ±0.0032	2330 ±10	1488 ±6	1258 ±5	0.7644 ±0.0032
Venus	6100 ±50	3790 ±30	3290 ±25	2.001 ±0.016	∞*	6100 ±50	3790 ±30	3290 ±25	2.001 ±0.016	6100 ±50	3790 ±30	3290 ±25	2.001 ±0.016
Earth	6378.16 ±0.02	3963.20 ±0.03	3443.93 ±0.02	2.09257 ±164 x 10^{-7}	298.24 ±0.01	6356.77 ±0.05	3949.77 ±0.03	3432.38 ±0.02	2.08555 ±164 x 10^{-7}	6371.02 ±0.05	3958.77 ±0.03	3440.08 ±0.02	2.09023 ±164 x 10^{-7}
Earth-Moon	--	--	--	--	--	--	--	--	--	--	--	--	--
Moon** a	1738.57 ±0.07	1080.30 ±0.04	938.75 ±0.03	0.57040 ±0.00002	--	--	--	--	--	--	--	--	--
b	1738.31 ±0.07	1080.14 ±0.04	938.61 ±0.03	0.57031 ±0.00002	--	1737.58 ±0.07	1079.68 ±0.07	938.22 ±0.03	0.57007 ±0.00002	1738.16 ±0.07	1080.04 ±0.04	938.53 ±0.03	0.57026 ±0.00002
c	1737.58 ±0.07	1079.68 ±0.04	938.22 ±0.03	0.57007 ±0.00002	--	--	--	--	--	--	--	--	--
Mars	3415 ±5	2122 ±3	1844 ±2	1.1204 ±0.0016	75 ±12	3369 ±5	2094 ±3	1819 ±2	1.1055 ±0.0016	3400 ±5	2113 ±3	1836 ±2	1.1155 ±0.0016
Jupiter	71,375 ±50	44,350 ±30	38,539 ±25	23.417 ±0.016	15.2 ±0.1	66,679 ±50	41,432 ±30	36,004 ±25	21.876 ±0.016	69,774 ±50	43,356 ±30	37,675 ±25	22,892 ±0.016
Saturn	60,500 ±50	37,590 ±30	32,670 ±25	19.849 ±0.016	10.2 ± ?	54,560 ±50	33,900 ±30	29,470 ±25	17.990 ±0.016	58,450 ±50	36,320 ±30	31,560 ±25	19.176 ±0.016
Uranus	24,850 ±50	15,440 ±30	13,420 ±25	8.153 ±0.016	14* ± ?	23,070 ±50	14,340 ±30	12,460 ±25	7.571 ±0.016	24,240 ±50	15,060 ±30	13,090 ±25	7.953 ±0.016
Neptune	25,000 ±250	15,530 ±150	13,500 ±130	8.202 ±0.080	58.5 ± ?	24,600 ±250	15,260 ±150	13,270 ±130	8.062 ±0.080	24,870 ±250	15,450 ±150	13,430 ±130	8.159 ±0.080
Pluto	3000 ±500	1860 ±300	1620 ±250	0.984 ±0.16	--	--	--	--	--	3000 ±500	1860 ±300	1620 ±250	0.984 ±0.16
Sun	696,500 ±500	432,800 ±300	376,100 ±250	228.51 ±0.16	--	--	--	--	--	696,500 ±500	432,800 ±300	376,100 ±250	228.51 ±0.16

*Taken from K. A. Ehricke (Ref. 7)

**Moon is best presented by triaxial ellipsoid--a: toward earth
  b: orthogonal to "a" and "c"
  c: along axis of rotation.

TABLE 3

Planetary Circular and Escape Velocities and Planetary Gravity

Planet	Circular Velocity at Sea Level				Escape Velocity at Sea Level				Gravity at Sea Level			
	(km/sec)	(ft/sec)	(stat mi/hr)	(AU/solar day)	(km/sec)	(ft/sec)	(stat mi/hr)	(AU/solar day)	(cm/sec^2)	(ft/sec^2)	$(stat\ mi/hr^2)$	$(AU/solar\ day^2)$
Mercury	3.05361	10,018.4	6,830.73	0.00176444	4.31846	14,168.2	9,660.13	0.00249530	400.212	13.1303	32,228.9	0.199801
Venus	7.30630	23,970.8	16,343.7	0.00422174	10.33266	33,899.8	23,113.5	0.00597043	875.261	28.7159	70,484.5	0.436964
Earth	7.909773	25,950.7	17,693.7	0.00457044	11.18610	36,699.8	25,022.6	0.00646357	982.0214	32.21855	79,081.88	0.4902632
Earth-Moon	--	--	--	--	--	--	--	--	--	--	--	--
Moon	1.678900	5,508.2	3,755.59	0.00097010	2.374831	7,789.8	5,311.23	0.00137194	162.169	5.32049	13,059.38	0.0809608
Mars	3.55141	11,651.6	7,944.27	0.00205208	5.02243	16,477.8	11,234.9	0.00290207	370.951	12.1703	29,872.5	0.185193
Jupiter	42.5818	139,704	95,252.7	0.0246047	60.2196	197,571	134,707	0.0347962	2598.63	85.2569	209,267	1.29734
Saturn	25.4511	83,500.9	56,932.4	0.0147062	35.9932	118,088	80,514.5	0.0207977	1108.26	36.3601	89,247.5	0.553284
Uranus	15.4841	50,800.9	34,637.0	0.00894705	21.8978	71,843.3	48,984.1	0.0126530	989.073	32.4499	79,649.7	0.493784
Neptune	16.5308	54,234.8	36,978.3	0.00955183	23.3780	76,699.6	52,295.2	0.0135083	1098.84	36.0512	88,489.3	0.548584
Pluto	11.23(?)	36,860(?)	25,130(?)	0.00649(?)	15.89(?)	52,130(?)	35,540(?)	0.00918(?)	4209(?)	138.1(?)	338,900(?)	2.101(?)
Sun	436.181	1,431,040	975,709	0.252035	616.853	2,023,795	1,379,860	0.356431	27,315.7	896,186	2,199,730	13.6371

_____ Underlined digits are questionable.

A frequent variant of the form (10) is

$$U_{\oplus} = \frac{\mu_{\oplus}}{r_G} \left\{ 1 + \sum_{n=1}^{\infty} \sum_{m=0}^{n} \left(\frac{R_e}{r_G} \right)^n P_{n,m} (\sin \phi') \cdot \left[A_{n,m} \cos m\lambda + B_{n,m} \sin m\lambda \right] \right\} \quad (12)$$

where

$$P_{n,m}(x) = \left[\frac{(n-m)!}{(n+m)!} \right]^{1/2} P_n^m(x).$$

A simplification of the expressions (10) or (11) to axially symmetric cases removes the bothersome time-dependence of $U_{\oplus}$ by eliminating the longitude λ, which is defined on the rotating earth. The inclusion of λ in $U_{\oplus}$ requires a transformation of the potential to inertial coordinates before it can be used in most trajectory programs. For the axially symmetric earth, $U_{\oplus}$ can be written (in expression which holds to inertial as well as in rotating coordinates):

$$U_{\oplus} = \frac{\mu_{\oplus}}{r_G} \left[1 - \sum_{n=1}^{\infty} J_n \left(\frac{R_e}{r_G} \right)^n P_n (\sin \phi') \right], \quad (13)$$

where $J_n = -C_{n,0}$, $S_{n,0} = 0$. Equation (8), giving $U_{\oplus}$ for an oblate ellipsoidal earth, is a special case of Eq (13) restricted to n = 2 and n = 4. The expressions (10), (12) and (13) were adopted as standard notation by the IAU in 1961. Other expressions used in the literature for $U_{\oplus}$, as well as the equivalent constants in terms of J_n, have been catalogued in Chapter II of Ref. 1.

An analytic expression for the local radius of the earth, R_ϕ, which is consistent with the general forms (10) and (12) of $U_{\oplus}$, is too complex to derive. It is customary to give R_ϕ--describing the radius of the geoid, or mean sea level surface of the earth (which is also an equipotential surface of the geopotential)--in graphical form by superimposing the deviations of the geoid from the oblate ellipsoid characterized by R_e and f on a world map. Since these deviations are less than ±50 meters at any point of the earth, many trajectory calculations retain the simple form (6) for R_ϕ, while using a form for $U_{\oplus}$ which is adequate for the approximation of the trajectory. This is done with the knowledge that R_ϕ and $U_{\oplus}$ are not strictly consistent.

From long-term observations of earth satellites, the values of J_n, n = 2, 3, 4, 5, 6, have been determined relatively well, where $J_1 = 0$ if the center of mass and the origin of the coordinate system coincide, and the oblateness coefficient J_2 is much larger than J_n, $n \geq 3$. Values of $C_{m,n}$ and $S_{m,n}$ together with standard deviations have been obtained up to m, n = 8 from gravity

measurements in Ref. 4 and elsewhere. Values for $\mu_{\oplus}$, J_2 through J_6, R_e and $1/f$ are given in the table of adopted constants at the end of Section A. The oblateness coefficient J_2 is, numerically, by far the largest coefficient of J_n.

The value of $\omega_{\oplus}$ is extremely accurately known from astronomical observations. For the handbooks, the constant value

$$\omega_{\oplus} = 7.292\ 115\ 146 \times 10^{-5} \text{ rad/sec} \quad (14)$$

has been taken, which in turn determines the period of the earth's rotation with respect to a fixed equinox or the sidereal day at 86164.0989 sec. The mean solar day, or period of the earth's rotation with respect to the mean sun, is 24 hr, or 86,400 sec.

4. Selenocentric Constants

Selenocentric constants can be conveniently divided into two categories--those of primary interest in determining the moon's motion, and those determining its shape and gravitational potential.

In the first category, the constants $\bar{r}_{\mathbb{C}}$, the lunar distance, L', the lunar inequality as defined by W. de Sitter (Ref. 8) and the mass ratio $\frac{M_{\oplus}}{M_{\mathbb{C}}} = \frac{\mu_{\oplus}}{\mu_{\mathbb{C}}}$ have been discussed in Chapter II of Ref. 1, and the numerical values are given in the table of adopted constants at the end of this subsection.

The moon has been captured rotationally by the earth, which means that the relatively strong gravitational attraction of the earth has aligned the longest axis of the moon toward the earth in an effect similar to the action of the earth's gravitational torque on a dumbbell-shaped satellite. This has the immediate consequence that the rotational rate of the moon about its axis, $\omega_{\mathbb{C}}$, equals the sidereal mean motion of the moon around the earth. For the Lunar Flight Handbook, the constant value

$$\omega_{\mathbb{C}} = \omega_{\oplus\mathbb{C}} = 2.661\ 699\ 484 \times 10^{-6} \text{ rad/sec} \quad (15)$$

has been adopted, fixing the length of the sidereal lunar month and the sidereal period of revolution of the moon about its axis at $27^d\ 7^h\ 43^m\ 11.^s55$, or 27.321 661 4 days. The eccentricity and inclination of the lunar orbit as well as gravitational torques of the sun and other planets cause the moon to perform a "wobble motion" or librations in its orientation with respect to the earth at a given time in its orbit. These lunar librations are discussed further in Chapter III, Section C. Other examples of rotational capture in the solar system include Mercury, which has been captured by the sun, and possibly Venus, as determined by the recent findings of the Mariner II space vehicle.

Values of $\bar{r}_{\mathbb{C}}$, $\frac{\mu_{\oplus}}{\mu_{\mathbb{C}}}$, and $\omega_{\oplus\mathbb{C}}$ have been determined for the n-body problem (i.e., the motion

of the moon under the attraction of the sun and planets). If the simpler restricted three-body problem is used for trajectory calculations (spherical earth, spherical moon in a circular orbit around the earth, massless space vehicle), then the value of one constant must be changed for consistency with Kepler's third law for this force model, as mentioned in Subsection B-2 of Chapter IV. It is customary to retain the values of $\mu_\oplus$, $\mu_\mathbb{C}$ and $\omega_{\oplus\mathbb{C}}$ and use a mean earth-moon distance of

$$\bar{r}_{\oplus\mathbb{C}} = 384,747.2 \text{ km} \tag{16}$$

instead of the lunar distance $\bar{r}_\mathbb{C} = 384,402$ km.

The distance $\bar{r}_{\oplus\mathbb{C}}$ is also called the lunar unit (LU) and is analogous to the astronomical unit (AU) on the planetary scale of distances. The value of $\bar{r}_{\oplus\mathbb{C}}$ is 0.09% larger than $\bar{r}_\mathbb{C}$, but the restricted three-body force model constants cannot be expected to match observed quantities exactly, as the force model doesn't include all the forces acting on the moon.

Another item of interest in connection with the motion of the moon are the lengths of the lunar months, which have been obtained from Ref. 6 (data is for the epoch 1900.0):

Synodic month $\quad 29\overset{d}{.}530589 \quad 29^d12^h44^m02\overset{s}{.}9$

Tropical month $\quad 27\overset{d}{.}321582 \quad 27^d07^h43^m04\overset{s}{.}7$

Sidereal month $\quad 27\overset{d}{.}321661 \quad 27^d07^h43^m11\overset{s}{.}5$

Anomalistic month $\quad 27\overset{d}{.}554551 \quad 27^d13^h18^m33\overset{s}{.}2$

Draconitic month $\quad 27\overset{d}{.}212220 \quad 27^d05^h05^m35\overset{s}{.}8$

Any variation of these values since 1900 from lunar theory and any observed difference can safely be neglected for most astronautical calculations.

Accurate orbital data for the moon, which involves several additional constants, can be found in Ref. 6. The lunar theory which has been used in obtaining the data, the comparison of theory with observation, and the variables given are discussed in detail in Section C of Chapter III. Some orbital elements--important spherical position coordinates as well as the illumination of the moon by the sun--have been given in Chapter XI up to the year 1970 to enable the planning of lunar missions.

The second category of constants deals with the figure of the moon and its gravitational potential. The asphericity of the moon can be deduced from photographic measurements as well as from physical librations (the small wobble-motion of the moon due to gravitational torques of the sun and planets other than earth), and the data indicates that the moon may best be represented by a triaxial ellipsoid with semiaxes a, b and c. The c axis is assumed to coincide with the rotational axis of the moon, the a axis is directed to the mean center point of the moon (see Subsection A-2 of Chapter III for a definition), and the b axis completes the right-handed

Cartesian coordinate system. Thus, the a, b, and c axes coincide with the selenographic x_s, y_s and z_s axes, respectively. Define moments of inertia of the moon I_a, I_b and I_c about the a, b, and c axes, and assume that the moon is symmetric in concentric ellipsoidal shells. From observation it has been determined that a > b > c. Consequently, $I_a < I_b < I_c$.

Very little data is available on the lunar shape. For the manual, the data given by Alexandrov (Ref. 9), which is based on Yakovkin's observations, Jeffreys' calculations, and the assumptions given in the previous paragraph, has been adopted.

The lengths of the lunar semiaxes depend on the rigid-body motion of the moon and have been calculated as:

	Forced Libration	Free Libration
Semiaxis a (km)	1738.67 ± 0.07	1738.57 ± 0.07
Semiaxis b (km)	1738.21 ± 0.07	1738.31 ± 0.07
Semiaxis c (km)	1737.58 ± 0.07	1737.58 ± 0.07

Values for free libration, adopted by Baker, have also been adopted for the Lunar Flight Handbook. These values are based on the dimensionless moment-of-inertia parameters:

$$\frac{I_c - I_a}{I_b} = 0.000,626,6 \pm 0.000,002,7 \text{ (standard error)}$$

$$\frac{I_a - I_b}{I_c} = 0.000,204.9 \pm 0.000,000,9 \text{ for a forced libration}$$

$$= 0.000,209,8 \pm 0.000,002,2 \text{ for a free libration.}$$

These were calculated by Jeffreys (Ref. 10) from the observational data of Yakovkin. The moments of inertia are given by

$$I_a = \lambda M \ (b^2 + c^2)$$

$$I_b = \lambda M \ (c^2 + a^2) \tag{17}$$

$$I_c = \lambda M \ (a^2 + b^2)$$

where λ is the inhomogeneity factor, which has the value $\lambda = 0.2$ for a constant density model of the moon and $\lambda = 0.199$ for a modified compressional model of the moon having a density gradient caused by the pressure of the outer layers on the interior (Ref. 9). For $\lambda = 0.199$ (exact value) the moments of inertia are:

Moment of Inertia	Forced Libration	Free Libration
I_a (10^{34} kg-m^2)	8.8293 ± 0.0018	8.8298 ± 0.0018
I_b (10^{34} kg-m^2)	8.8317 ± 0.0018	8.8312 ± 0.0018
I_c (10^{34} kg-m^2)	8.8349 ± 0.0018	8.8349 ± 0.0018

Again, the values for free libration have been adopted in this handbook.

The surface of the lunar ellipsoid is given by

$$\frac{x_S^2}{a^2} + \frac{y_S^2}{b^2} + \frac{z_S^2}{c^2} = 1 \tag{18}$$

This expression will be transformed to spherical coordinates $R_{\phi\lambda}$, the selenocentric radius of a surface point, $\phi_{\mathbb{C}}$, the selenographic latitude, and $\lambda_{\mathbb{C}}$, the selenographic longitude in order to obtain an expression for $R_{\phi\lambda}$. Define the flattening of the lunar equator as

$$f' = \frac{a - b}{a} = 0.00015 \tag{19}$$

and the flattening of the lunar prime meridian as

$$f* = \frac{a - c}{a} = 0.00057. \tag{20}$$

The equation of the lunar ellipsoid becomes, in spherical coordinates,

$$\left(\frac{R_{\phi\lambda}}{a}\right)^2 \cdot \left[\cos^2\phi_{\mathbb{C}} \cos^2\lambda_{\mathbb{C}} + \frac{\cos^2\phi_{\mathbb{C}} \sin^2\lambda_{\mathbb{C}}}{(1 - f')^2} + \frac{\sin^2\phi_{\mathbb{C}}}{(1 - f*)^2}\right] = 1 \tag{21}$$

Since both f' and f* are very small, it is sufficiently accurate to solve for $R_{\phi\lambda}$ and subsequently expand by use of the binomial theorem, retaining only first-order terms in f' and f*. The resulting expression for $R_{\phi\lambda}$ is

$$R_{\phi\lambda}(\phi_{\mathbb{C}}, \lambda_{\mathbb{C}}) \simeq a\left[1 - f' \cos^2\phi_{\mathbb{C}} (1 - \cos^2\lambda_{\mathbb{C}}) - f* \sin^2\phi_{\mathbb{C}}\right] \tag{22}$$

The expression for the local radius of the oblate earth--R_ϕ to first order--can be obtained from Eq (22) if $f' \to 0$, $f* \to f$, as can be verified by comparison with Eq (6). Altitude on lunar maps is not given with respect to the ellipsoidal surface, which is defined to first order by Eq (22), and it is not given with respect to a spherical moon, but it is given with respect to an arbitrary spherical lunar datum which is well below the lunar surface and results in positive altitudes for all lunar surface features.

It remains to obtain an expression for the lunar gravitational potential $U_{\mathbb{C}}$ corresponding to its triaxially ellipsoidal shape and for the modified compressional lunar model. Alexandrov (Ref. 9) and Baker, Makemson (Ref. 10) give the lunar potential in the following widely used form:

$$U_{\mathbb{C}} = \frac{\mu_{\mathbb{C}}}{r_S}\left\{1 + \frac{1}{2}\left(\frac{a}{r_S}\right)^2\left[\frac{I_b - I_a}{I_c}\left(1 - 3\frac{y_S^2}{r_S^2}\right)\right.\right.$$

$$\left.\left. + \frac{I_c - I_a}{I_c}\left(1 - 3\frac{z_S^2}{r_S^2}\right)\right]\right\} =$$

$$\frac{\mu_{\mathbb{C}}}{r_S}\left\{1 + \frac{1}{2}\left(\frac{a}{r_S}\right)^2\left[\frac{I_b - I_a}{I_c}(1 - 3\cos^2\beta_{\mathbb{C}})\right.\right.$$

$$\left.\left. + \frac{I_c - I_a}{I_c}(1 - 3\sin^2\phi_{\mathbb{C}})\right]\right\} \tag{23}$$

where r_S is the distance from the center of the moon (the radius in the selenographic coordinate system), y_S and z_S denote components of r_S in selenographic coordinates and $\beta_{\mathbb{C}}$ is the angle between the y_S axis and r_S. Since the y_S axis rotates with the moon, the expression for $U_{\mathbb{C}}$ is in a non-inertial rotating coordinate system.

The transformation from the selenographic coordinate system $x_S y_S z_S$ to the lunar equatorial system $x_{\mathbb{C}} y_{\mathbb{C}} z_{\mathbb{C}}$ is given in Subsection A-2b of Chapter III, from where:

$$y_S = -\sin(\Lambda_S + \omega_{\mathbb{C}} t) x_{\mathbb{C}} + \cos(\Lambda_S + \omega_{\mathbb{C}} t) y_{\mathbb{C}}$$

$$z_S = z_{\mathbb{C}} \tag{24}$$

where Λ_S is an arbitrary initial phase angle between the $x_{\mathbb{C}}$ and x_S axes. The expression for $U_{\mathbb{C}}$ in non-rotating lunar equatorial coordinates becomes, after substitution of Eq (24) into Eq (23) and some mathematical operations

$$U_{\mathbb{C}} = \frac{\mu_{\mathbb{C}}}{r_{\mathbb{C}}}\left\{1 - \frac{1}{2}\left(\frac{a}{r_{\mathbb{C}}}\right)^2\left[\frac{I_b - I_a}{I_c}\left(-\frac{1}{2} + \frac{3}{2}\frac{z_{\mathbb{C}}^2}{r_{\mathbb{C}}^2}\right.\right.\right.$$

$$+ 3\left(\frac{1}{2} - \frac{z_{\mathbb{C}}^2}{2r_{\mathbb{C}}^2} - \frac{y_{\mathbb{C}}^2}{r_{\mathbb{C}}^2}\right)\cos 2(\Lambda_S + \omega_{\mathbb{C}} t)$$

$$\left.+ \frac{3 x_{\mathbb{C}} y_{\mathbb{C}}}{r_{\mathbb{C}}^2}\sin 2(\Lambda_S + \omega_{\mathbb{C}} t)\right)$$

$$\left.\left.+ \frac{I_c - I_a}{I_c}\left(1 - 3\frac{z_{\mathbb{C}}^2}{r_{\mathbb{C}}^2}\right)\right]\right\} \tag{25}$$

where $r_{\mathbb{C}} \equiv r_S$. (The change in subscript has been introduced in order to emphasize that the radius has components in the lunar equatorial coordinate system.)

Another form of the lunar gravitational potential has been given by Jeffreys (Ref. 11, p 140). It is more useful than the forms (23) and (25) because it allows the expression of the lunar potential in a form analogous to Eq (10) for the earth's potential, with the polar flattening of the moon described by the numerical coefficient

$J_2 = -C_{2,0}$ and the lunar equatorial ellipticity by the coefficient $C_{2,2}$. This form is given in the selenographic coordinate system, and, with a slight change in notation for compatibility with Eq (10), it is:

$$U_{\mathbb{C}} = \frac{\mu_{\mathbb{C}}}{r_S} \left\{ 1 + \frac{1}{2} \left(\frac{a}{r_S} \right)^2 \left[J_2 \left(1 - 3 \sin^2 \phi_{\mathbb{C}} \right) \right. \right.$$
$$\left. \left. + 3 C_{2,2} \cos^2 \phi_{\mathbb{C}} \cos 2\lambda_{\mathbb{C}} \right] \right\} \tag{26}$$

where the values of the coefficients are:

$$J_2 = \frac{I_c - \frac{1}{2}(I_a + I_b)}{M_{\mathbb{C}} a^2} = 200 \times 10^{-6}$$

$$C_{2,2} = \frac{I_b - I_a}{4 M_{\mathbb{C}} a^2} = 27 \times 10^{-6} \tag{27}$$

The semiaxis used in Eqs (26) and (27) should be the largest semiaxis, or a, in order to ensure that $U_{\mathbb{C}}$ represents the potential external to the moon. Further forms of the lunar potential use- ful for determining the magnitudes of the earth's perturbation on a lunar satellite orbit are given in Chapter VII.

For the compressional and constant density lunar models, the origin of the selenographic coordinate system is at the mass center of the moon, so that $J_1 = 0$. As in the case of the earth, the oblateness coefficient J_2 is numerically the largest for the moon, with $(J_2)_{\mathbb{C}} \approx \frac{1}{8} (J_2)_{\oplus}$. Oblateness effects on lunar satellite orbits will be discussed further in Chapter VII.

The values for J_2 and $C_{2,2}$ given in Eq (27) are rather crude, so no uncertainties will be given. For calculations in the lunar handbook, the values given by Krause (Ref. 5), together with his un- certainty, will be adopted, even though his values are slightly inconsistent with the values for a, b, c, I_a, I_b, I_c adopted for the handbook. Krause obtains:

$$J_2 = 212.5 \times 10^{-6} \pm 2.9 \times 10^{-6}$$

$$C_{2,2} = 18.8 \times 10^{-6} \pm 1.3 \times 10^{-6} \tag{28}$$

5. Summary of Adopted Constants

The constants needed for trajectory calcula- tions which were given in this section are sum- marized in Table 4. Note is made of the source of each number. The values given, together with the uncertainty and the confidence level have been calculated by Townsend (Ref. 12); they reflect our present knowledge regarding such observa- tions and measurements. The values have been adopted for uniformity in trajectory calculations and in the presentation of results for the handbooks. Better values, with smaller uncertainties and a higher confidence level will appear in the future and should be used in trajectory calculations as

soon as they become available. The data in the handbook will remain valid, as any anticipated future changes in the constants will be too small to be reflected in the graphical data, which is for relatively short-term trajectories. A signifi- cant improvement in the values for selenocentric constants is expected, however, as soon as long- term satellite orbits around the moon can be established and observed.

B. ENVIRONMENTAL DATA

Section A discussed and summarized the astro- nautical constants which in effect determine the gravitational environment of the space vehicle. Section B gives some background on other forces and the atmospheric, radiation, meteoroid, and thermal environment in which the space vehicle finds itself during lunar missions.

Environmental data may be subdivided into (1) data pertaining directly to the celestial body, which includes the near-satellite environment of this body, and (2) data pertaining to space between the celestial bodies, such as cislunar space data, interplanetary, interstellar and intergalactic space data. The dividing line between the two types of environment is not very well defined, especially for celestial bodies without a dense gaseous atmosphere, but the delineation will help in the discussion of environmental data.

For lunar missions near earth, cislunar space and near-moon environmental data is required. As near-earth data has been discussed extensively in Chapter II of Ref. 1, this environment will only be summarized and its applicability to lunar flight discussed. Near-earth data has been ac- cumulated rapidly by earth satellites so a clearer picture of the environment is rapidly becoming available. Much less is known about the cislunar environment (the region beyond the earth's at- mosphere) and the effect of its magnetic field, due to the small number of space probes and the relatively short time that these probes are in cislunar space. The effects of radiation and micrometeoroids have been discussed quite generally in Chapter II of Ref. 1 and are also applicable to cislunar space. The bulk of the data in this section is on the near-moon environ- ment--the lunar surface, its appearance and approximate thermal characteristics, together with a brief discussion of the tenuous lunar at- mosphere.

Much of the environmental data is of a quali- tative nature and intended to provide a classifi- cation and framework into which the numerous sources and articles in this field can be placed. References giving a comprehensive survey and providing a link between the material in this section and the actual sources have been indicated in order to enable the tracing of data required for lunar flight to its source.

The primary concern in this section is to describe the space environment with very slight mention of its effect on the trajectory, people and materials. The modification of the force model (and hence of the trajectory) by the environ- ment has been discussed in Section B of Chapter IV. A recent survey article by Jaffe and Rittenhouse

TABLE 4

Adopted Constants

Quantity	Best Value	Uncertainty	Approximate Confidence Level[b] (%)
General Constants			
Speed of light	[f]299792.5 km/sec	[f]0.1 km/sec	--
Universal grav constant G	$6.670 \times 10^{-11} \frac{m^3}{kg\ sec^2}$	$0.005 \times 10^{11} \frac{nt - m^2}{kg^2}$	--
Heliocentric Constants			--
Solar parallax	[a]8".798	[b]±0.001	90
Astronomical unit	[a]149.53×10^6 km	[a]±0.03	90
$K_{\odot}^2$	[c]0.2959122083 AU^3/solar day^2	[a]±0.010^{-10}	99+
Planetocentric Constants			
Mercury			
Solar mass/mass Mercury	[a]6,100,000	[b]±65,000	70
Equatorial radius	[a]2330 km	[b]±11	70
1/f	?	?	?
Venus			
Solar mass/mass Venus	[a]407,000	[b]±1300	90
Equatorial radius	[a]6100 km (incl. atmosphere)	[b]±12	70
1/f	?	?	?
Earth-Moon			
Solar mass/earth-moon mass	[a]328,450	[b]±25	81
Equatorial radius	--	--	--
1/f	--	--	--
Mars			
Solar mass/mass Mars	[a]3,090,000	[b]±12,000	81
Equatorial radius	[a]3415	[b]±12	88
1/f	[b]75	[b]±12	80
Jupiter			
Solar mass/mass Jupiter	[a]1047.4	[b]±0.1	81
Equatorial radius	[a]71,875 km	[b]±20	50
1/f	[a]15.2	[b]±0.1	50
Saturn			
Solar mass/mass Saturn	[a]3500	[b]±2.0	70
Equatorial radius	[a]60,500 km	[b]±480	50
1/f	[a]10.2	± ?	?

(continued)

NOTE:

[a]Baker's value (Ref. 3)

[b]Townsend's value (Ref. 12)

[c]Gaussian value

[d]Ehricke's value (Ref. 7)

[e]Kaula's value (Ref. 4)

[f]Krause's value (Ref. 5)

TABLE 4 (continued)

Quantity	Best Value	Uncertainty	Approximate Confidence Level[b] (%)
Uranus			
Solar mass/mass Uranus	[a]$22,800$	[b]± 60	50
Equatorial radius	[a]$24,850$	[b]± 50	?
$1/f$	[a]14.0	$\pm$?	?
Neptune			
Solar mass/mass Neptune	[a]$19,500$	[b]± 200	70
Equatorial radius	[a]$25,000$ km	[b]± 2100	50
$1/f$	[a]58.5	$\pm$?	?
Pluto			
Solar mass/mass Pluto	[a]$350,000$	[b]$\pm 27,000$	70
Equatorial radius	[a]3000 km	[b]± 500	20
$1/f$	?	?	?
Geocentric Constants			
$\omega_{\oplus}$ (rad/sec)	[f]$7.292115146 \times 10^{-5}$	(exact)	--
μ (km^3/sec^2)	[e]398601.5	± 9.9	88
J_2	[a]1082.28×10^{-6}	[a]$\pm 0.2 \times 10^{-6}$	95
J_3	[a]-2.30×10^{-6}	[a]$\pm 0.2 \times 10^{-6}$	90
J_4	[a]-2.12×10^{-6}	[a]$\pm 0.5 \times 10^{-6}$	92
J_5	[a]-0.20×10^{-6}	[a]$\pm 0.1 \times 10^{-6}$	88
J_6	[a]-1.0×10^{-6}	[a]$\pm 0.8 \times 10^{-6}$	70
Equatorial radius (km)	[e]6378.163	[e]± 0.021	95
$1/f$	[e]298.24	[e]± 0.01	95
Selenocentric Constants			
$\omega_{\mathbb{C}} = \omega_{\oplus \mathbb{C}}$ (rad/sec)	[f]$2.661699484 \times 10^{-6}$	(exact)	--
Lunar distance (km)	[a]$384,402$ km	[a]± 1 km	88
L'	[a]6.4385	[a]± 0.0015	92
$M_{\oplus}/M_{\mathbb{C}}$	[b]81.357	[b]± 0.01	90
Semiaxis a (km)	[a]1738.57 km	[a]± 0.07 km	50
b (km)	[a]1738.31 km	[a]± 0.07 km	50
c (km)	[a]1737.58 km	[a]± 0.07 km	50
J_2	[f]212.5×10^{-6}	[f]$\pm 2.9 \times 10^{-6}$	50
$C_{2,2}$	[f]18.8×10^{-6}	[f]$\pm 1.3 \times 10^{-6}$	50

(Ref. 13) discusses the behavior of materials in space environments; the 330 references at the end of this article may be consulted for more detailed information.

1. Near-Earth Environment

   a. Atmospheric environment

Three types of near-earth environment can be distinguished--the atmospheric, the radiation, and the meteoroid environment. Due to the many large-scale and local variations in the earth's atmosphere, most trajectory calculations are based on a model atmosphere which is assumed to describe average properties of the actual atmosphere and to obey the perfect gas law

$$\rho = \frac{p\overline{M}}{R*T}$$ (29)

and the hydrostatic differential equation

$$dp = -g\rho\,dh,$$ (30)

where

ρ = the density in kg/m^3

p = the pressure in $newtons/m^2$

T = the temperature in $°K$

$\overline{M}$ = the molecular weight of air

$R*$ = 8.31439×10^3 joules/kg $°K$ is the universal gas constant

g = the acceleration due to gravity in m/sec^2

h = the geometric altitude in meters.

The physical properties for the model atmosphere have been calculated under additional assumptions and by use of satellite observations. They are tabulated as a function of altitude up to 700 km as the 1961 U. S. Standard atmosphere. This tabulation, the history of model atmospheres, and additional background have been presented in Chapter II of Ref. 1 and in the listed references of that chapter. Atmospheric effects on space vehicles with lunar mission objectives at altitudes in excess of 700 km are negligible over the short periods of time the vehicle is at these altitudes, and hence no atmosphere need be assumed for altitudes in excess of 700 km. However, if density data at extreme altitudes is required, Nicolet (Ref. 14) can be used as a guide. The atmosphere up to 700 km can be assumed to rotate with the same angular velocity as the earth to a good degree of accuracy.

The 1961 U. S. Standard model atmosphere represents average atmospheric conditions between the maximum and minimum of the sunspot cycle. The actual atmospheric properties that the space vehicle encounters may differ quite considerably from the model atmosphere. This variability is due primarily to solar radiation and heating, gravitational effects of the sun and moon or tidal motions, as well as viscous and turbulent effects, which have been discussed in Chapter II of Ref. 1. To approximate variability for preliminary engineering design, it is sufficient, in most cases, to introduce a certain percentage dispersion in density about the 1961 U. S. Standard atmosphere.

The main effects of the earth's atmosphere on a space vehicle's trajectory are the aerodynamic forces, and the aerodynamic heating it produces. The parameter relating these two effects is the atmospheric density. Expressions for aerodynamic forces have been given in Subsection B-4b of Chapter IV; they are important in designing parking orbits and waiting orbits (see Chapter V and Chapter V of Ref. 1). Aerodynamic forces and heating define a safe re-entry corridor for earth return, or a region of possible re-entry trajectories within the design limits of the lunar vehicle. This aspect is discussed in Chapters IX of Ref. 1 and briefly mentioned in Chapter X.

   b. Radiation environment

Contrary to the atmospheric effects on the space vehicle, the effect of radiation is damage to man, electronic equipment, and structural components of the space vehicle. Of all the elements in a space vehicle, man and semiconductors have the lowest threshold of damage from ionizing radiation. The radiation dosage to be expected in a near-earth orbit, radiation damage thresholds, and the shielding (which is defined as additional structural material in the vehicle to absorb radiation before it can reach man and electronic equipment) have been discussed extensively in Chapter II of Ref. 1.

Most of the data on penetrating radiation in the near-earth environment has been acquired since 1958, when the first earth satellites and space probes carried radiation-measurement equipment aloft. Little penetrating radiation reaches the surface of the earth, as the atmosphere represents shielding material of approximately 1 kg/cm^2, and, hence, much of the radiation was not detected until satellite experiments could be performed. In fact, many parameters are still poorly known. The space radiation can be classified into five general types:

(1) Van Allen radiation, consisting of high-energy charged particles which have been trapped in the earth's magnetic field. An inner and an outer belt have been distinguished; the outer belt may extend out as far as 10 ER (earth radii). The particle flux of these two belts is affected by geomagnetic storms.

(2) Solar flare radiation, consisting of high-energy protons and electrons which are ejected at certain times from the sun. Half an hour or more after a large chromospheric flare, high-energy protons (and possibly electrons) can be detected on the earth (p 62, Ref. 15).

(3) Cosmic radiation, consisting of atomic nuclei (mostly of hydrogen, but atomic numbers in excess of 30 have been observed) which move with velocities near the speed of light.

(4) Auroral radiation, consisting of electrons and protons emitted by the sun and concentrated near the geomagnetic poles. The electrons supply the energy for the auroral light.

(5) Penetrating electromagnetic radiation of the sun, consisting mostly of X-rays and Y-rays with energies as high as 500 kiloelectron volts and wavelengths as short as $0.02 \overset{\circ}{A}$ ($1\overset{\circ}{A} = 10^{-10}$ meter) having been observed.

More detailed descriptions of these radiations and recent data can be found in Ref. 15, while Chapter II of Ref. 1 includes data on radiation, the type of damage, as well as shielding requirements from these radiations. Table 5 summarizes the space radiations which penetrate at least 10^{-6} kg material per square centimeter. This table has been taken from Ref. 15, pp 70 to 71; additional remarks and sources of the data can be found in this reference. Tabulated are the types of radiation, the particle energy and an indication of the integral spectrum (the slope of the particle flux per energy versus energy curve as a function of energy), or differential spectrum (the distribution of particles as a function of the energy of the particle flux in an increment of energy) as well as the particle flux itself.

In the near-earth environment, radiation hazards occur mainly in the parking and/or waiting orbit phase, in any orbital phase on earth return, and in the near-earth portions of lunar flight, when the vehicle velocity relative to earth is about 10 km/sec. Radiation dosages and shielding requirements during that portion have been given in Chapter II of Ref. 1. The parking and waiting orbit altitudes in Chapter V as well as the orbital phase during earth return in Chapter X can be selected so as to be below the inner Van Allen belt.

Figure 1 illustrates the early phases of a typical lunar mission launched from Cape Canaveral. The doughnut-shaped inner Van Allen belt is shown, with the proton flux indicated by eight cross sections and the geomagnetic equator shown on the earth. The shading indicates the proton flux -- the darker the appearance of the shaded area, the higher the flux. The illustrated trajectory (with a relatively high parking orbit altitude) intersects the fringes of the inner Van Allen belt after injection, but the time spent in the region of high proton flux is very small due to the high initial space vehicle velocities.

Solar flare radiation occurs sporadically, especially during sunspot maxima. The only protection against this type of radiation and against cosmic and solar electromagnetic radiation is the shielding of the space vehicle and the layout of the equipment so as to provide maximum protection to the vulnerable men and electronic equipment. For launches from Cape Canaveral, the auroral radiation can be neglected, since the parking and waiting orbits will not reach the regions near the geomagnetic poles.

c. Meteoroid environment

Meteoroids are small astronomical bodies which are generally in highly eccentric orbits around the sun. They range in dimension from several meters (extremely rare) to dust particles or micrometeorites as small as one micron in diameter. Beyond the earth's atmosphere, meteoroids may present a hazard to space vehicles. As pointed out by a sample calculation in Subsection B-4d of Chapter IV, the force on the space vehicle due to meteoroids is relatively small and can be neglected in all but the most precise trajectory calculations. However, of major concern is the possibility of a meteoroid collision with the space vehicle resulting in penetration or even puncture of the skin of the vehicle or fuel tank. Puncture of the skin causes a loss of pressurization or fuel, which may require an abort of the mission.

Data concerning average meteoroid fluxes, encounter probabilities and penetration has been given in Chapter II of Ref. 1. Also listed there are the more common meteoroid penetration models and a typical model for evaluating meteoroid effects on propellant storage vessel design.

Meteoroid showers are phenomena which are observed on earth and tend to recur annually. They result from swarms of meteoroids which are roughly in the same solar orbit. When a meteoroid shower is observed on earth, all meteoroids seem to come from the same area in the sky, known as its "quadrant." Data on meteor showers observed on earth has been given on page 99 of Ref. 15. It can be assumed that many other showers may be expected in space and that the value of the micrometeorite flux is enhanced in and near the meteoroid shower.

2. Cislunar Space Environment

In cislunar space, the solar flare radiation, cosmic radiation, the penetrating electromagnetic radiation from the sun, and the meteoroid environment must be considered. The qualitative description and summary of Subsection B-1 regarding these areas apply, as does the referenced quantitative material in Chapter II of Ref. 1 and in Ref. 15. In general, increasingly less reliable data is available than for the near-earth environment. In the list of lunar probes in Section D, some of the vehicle-borne experiments and results have been listed.

3. Lunar Environment

The figure of the moon has been discussed in some detail in Subsection A-4 of Chapter II and its motion in space in Section C of Chapter III. Still to be discussed are lunar topography as deduced by observation of the moon with telescopes, the photographs and maps which have resulted from these observations, the thermal environment on the lunar surface, the type of surface, and the lunar atmosphere. Since many lunar observations have been made by telescopes, Table 6, showing the smallest lunar features visible from earth with perfect optics and under excellent viewing conditions (see Wilkins and Moore, Ref. 16, p 349) gives an idea of the finest lunar surface detail that can be observed.

TABLE 5
Penetrating Radiations in Space

Radiation	Particle Energy or Photon Energy	Flux
Protons		(protons/cm^2-sec)
Auroral--altitudes > 100 km	Integral spectrum, 100 kev < E < 800 kev, varies between E^{-1} and E^{-4}	Normally 10^4 to 10^6 with E > 100 Mev
Van Allen--±40° from integral-invariant equator, altitudes from 10^3 to 8 x 10^3 km	E$^{-0.8}$ integral spectrum above 40 Mev; no radiation observed with E > 700 Mev	Up to ～10^4
Solar-flare--relativistic	E > 1 Bev and usually < 10 Bev	Usually 10 to 10^2; occasionally to ～10^4
Solar-flare--nonrelativistic	From 30 to 300 Mev, E^{-1} to E^{-6} integral spectrum; for typical large solar-flare event, max-intensity integral spectrum might be represented by 3 x 10^{10} E^{-4} protons/cm^2 sec, where E is proton energy in Mev; should not be applied below 30 Mev	Usually 10^2 but occasionally to ～10^4
Cosmic rays--interplanetary space	E$^{-1.5}$ integral spectrum for E > 10 Bev	2 ± 0.3 for E > 40 Mev near max of sunspot cycle; probably increases to ～5 near sunspot min
Cosmic-ray ("splash") albedo-- <10 Earth radii	1 to 10 Mev	～1 near top of atmosphere
Electrons		(electrons/cm^2-sec)
Auroral--from 100 to 1000 km altitudes	<50 kev; spectrum highly variable; integral spectrum >4 kev between E^{-1} and E$^{-2.5}$; 1 observation showed nearly mono-energetic 6-kev stream	Up to 10^{11} to 10^{13} average ～10^5 to 10^7
Van Allen radiation	Integral spectrum ranges from E^{-3} to E^{-6}	Up to ～10^8 for E > 20 kev
Solar-flare--magnetic latitudes > 60°	～100 Mev	Probably < 10^2
Neutrons		(neutrons/cm^2-sec)
Cosmic-ray albedo	E$^{-0.9}$ differential spectrum for 0.1 ev < E < 100 kev, E^{-2} differential spectrum for 1 Mev < E < 1 Bev	～1
X- and Y-Rays		(photons/cm^2-sec)
Electron bremsstrahlung		
Auroral zone	～E^{-4} integral spectrum for E > 30 kev	10 to 10^3 above absorbing atmosphere
Low-latitude visible aurora	E$^{-2.5}$ integral spectrum, ～100 kev	10^3 to 10^5
Atmosphere below radiation belt near 100 km, usually between magnetic latitudes 50 and 60°	10 to 500 kev; theoretical spectrum,	～10^4
Van Allen belt	20 to 50 kev with an energy flux of 10^{-7} erg/cm^2-sec	
Nuclear Y-rays from atmosphere above polar caps	E > 100 kev	～10^3 initially
Solar flares Above 100 km on sunlit hemisphere	5 to 80 kev with an energy flux of 10^{-2} to 10^{-5} erg/cm^2-sec)	
	～500 kev with an energy flux of 10^{-4} erg/cm^2-sec	

TABLE 6

Smallest Lunar Features Visible from
Earth Assuming Perfect Optics and
Excellent Viewing Conditions

| Aperture of Telescope (cm) | Diameter of Smallest Crater (km) | Smallest Cleft | |
		Minimum Width (km)	Minimum Length (km)
15.2	2.4	0.13	1.1
30.5	1.2	0.06	0.5
91.4 (Lick Observatory)	0.4	0.02	0.18
508 (Mt. Palomar Observatory)	0.07	0.005	0.03

However, the necessary excellence of the view-
ing conditions can be illustrated by the fact that
photographs have not shown craters less than 1
km in diameter on the moon, and hence visual ob-
servations are the primary source for small de-
tails on the lunar surface.

a. Lunar topography

About 100,000 formations on the surface of the
moon have been described. In order to discuss
these formations, the nomenclature in general
use for lunar features is introduced in this sub-
section. The problem of classification has been
taken up by Blagg and Saunders (Ref. 17) and
Blagg and Müller (Ref. 18) for those wishing
more detail, and another system has been pro-
posed by Bobrovnikoff (Ref. 19), which is
claimed to be more detailed than those of Refs.
17 and 18.

The moon as viewed from earth is characterized
by light and dark areas. In general, the lighter
the appearance of the lunar surface, the higher its
elevation.

The dark areas are called "maria," or seas.
They are, in general, low plains with some small
irregularities (compare the surface elevation con-
tours as given on the USAF lunar aeronautical
charts, one of which is reproduced as Fig. 2 in
the present chapter). The term "maria" is re-
stricted to larger areas. The terms "lacus"
(lake) and "sinus" (bay) are applied to smaller
dark features on the lunar surface, while the
term "palus" (marsh) describes regions of inter-
mediate coloration.

The boundaries between the dark maria and the
lighter-colored "continents" and "mountains" are
generally quite sharp. The continents have not
been given names, except for a few "capes" which
jut out into the maria.

Mountains on the moon usually are named after
terrestrial mountains or after scientists; smaller
mountains are designated by suffixing a small
Greek letter to the name of a large mountain in
their vicinity, i.e., Stadius Y. They occur as
"chain mountains" in mountain ranges, "ridges,"
"cellular ring formations" or "domes," which are
small, rounded mountains. The vertical relief of
the lunar surface can be determined in two steps:

(1) Determine the relative height by measur-
ing the length of a mountain's shadow (a
technique which is quite accurate as long
as there are mountains in the particular
region of the moon by determining the
altitudes by scanning the photographic

negative of the moon with a photometer
and noting the brightness (photometric
method), by making direct measurement
at or near the limb, or by other methods.

(2) Determine absolute heights by measuring
the selenographic locations of these points
very accurately and correcting for the
projection and the refraction of the earth's
atmosphere.

For more detail, Fielder (Ref. 20) can be con-
sulted. From these observations, the vertical re-
lief of the lunar surface has been found to be high.

Some peaks near the lunar south pole exceed an
altitude of 9000 meters above the neighboring val-
leys. This compares with an elevation of 12,000
meters of the Island of Mindanao above the Philip-
pine trench on earth, which has almost four times
the radius of the moon. The slopes are usually
gentle, with angles less than those on earth. How-
ever, in the Jura mountains, slopes average as
much as 45°. The maximum elevation in this re-
gion is about 6000 meters above Sinus Iridum
(Ref. 21).

Very characteristic features of the lunar sur-
face are the "walled enclosures", the larger of
which have been referred to as "walled plains"
and the smaller of which are called "craters" by
Bobrovnikoff. Walled enclosures consist of a
plain surrounded by mountains which slope rela-
tively steeply inward (up to a 20° slope, which
locally may exceed 45°, as for Copernicus, Ref.
21) and somewhat more gently outward (5° to 10°
overall for Copernicus, Ref. 21). They are
named primarily after scientists and philosophers,
but smaller craters are named after a larger one
in the vicinity by suffixing a capital Latin letter,
i.e., "Mösting A." Walled enclosures may have
one or more central peaks, or they may be without
one. The walled plains are quite irregular in
shape--hexagonal, quadrangular, triangular, or
oval--with the maximum linear dimension from
about 300-60 km. Craters are much more cir-
cular in shape, and range in diameter from 60 km
down to the limit of the present optical resolution,
which is of the order of 1 km. The craters may
be large and submerged, as is Stadius, large and
partially filled, or small craterlets ranging in
size down to blowholes or "pits," which are the
smallest observed craters. There are also such
features as confluent craters and crater chains.

Associated with some craters, and named after
them, are "fractures," which range in size from
large valleys to fault lines (caused when part of
the lunar surface has subsided relative to the
surrounding), clefts or rills, and cracks, which
consist of a large number of small craters joined
together in a chain.

At the time of full moon, "rays", or white
streaks which seem to originate from a crater
can be observed on the moon, their brightness
depending on the phase of the moon. The most
prominent is the system of rays associated with
the crater Tycho. These ray systems can be clas-
sified as radial ray systems, tangential ray sys-
tems, ray systems in certain directions, or as
"bright spots."

Lunar surface features may merge into one
another, as in the following sequences of features

listed by Bobrovnikoff (Ref. 19), for example:

> Maria, walled plains, craters, craterlets, crater chains, valleys;
>
> Mountain ranges, isolated peaks, mounds, domes, pits.

In a similar fashion, mountain ranges on the moon are connected with maria, while isolated peaks occur in or near walled plains and craters, as mentioned previously.

During the history of observing the moon (since Galileo's time), no clear-cut changes of the lunar surface have been observed. Changes in small lunar surface features (those several km in extension) depend on such conditions of visibility as the phase of the moon, the libration, the resolving power of the telescope, atmospheric refraction, cloud cover, and the subjective interpretation of the observer. These changes are mostly observed as variations in the brightness and color of small craters, the observation of something looking like a mist, and the appearance of flashes, i.e., any apparent changes in physical relief. Real changes of physical relief must occur due to the impact of meteorites, but no such observation can be safely attributed to that cause (Ref. 19, p 62). The lunar surface must also change due to the pressure of tidal motions inside the moon (Ref. 20, p 127).

Much more material on lunar topography and the nature of the lunar surface can be found in Bobrovnikoff (Ref. 19), Fielder (Ref. 20), Firsoff (Ref. 21), and the bibliography listed in each of these references. In addition, the present theories on the origin of the lunar features, and questions of selenology (which form the lunar counterpart of geology on earth), such as the composition of the interior, the type of surface, the pattern of tectonic grids, and the divisions of selenological time are discussed in Refs. 19 through 21. Our knowledge of the moon's topography and interior will increase vastly in the near future as the planned lunar missions of Ranger, Surveyor, and Apollo spacecraft return scientific data to earth. Until such time, many of the present theories should be regarded as provisional. An illustration of the actual photographically observed lunar topography can be found in the Lunar Aeronautical Chart, which has been reproduced as Fig. 2. Other lunar maps and series of lunar maps prepared in the same fashion are listed in Subsection A-2g of Chapter III.

b. Lunar photometry

In integrated photometry, the total emission of a celestial body is measured. The brightness of the full moon under standard conditions is usually given in stellar magnitudes (mag). In the visual region (average wavelength 5280 Å), the latest determination is by Nikonova (1949) who finds -12.67 mag, and in the photographic region (average wavelength 4250 Å) Bobrovnikoff gives an average value of -11.55 mag, ±0.09 mag; the color index of the moon, or the difference between the two, is +1.12 mag. The amount of light from the full moon under standard conditions is 0.342 ± 0.011 lux (Bobrovnikoff, p 66). Integrated phase curves of the moon, or the variation of the lunar brightness with the phase, have been given by

Bobrovnikoff on p 67. The albedo, or reflecting power of the lunar surface, can be defined in two ways: (1) the spherical albedo of the moon or the ratio of the light of the sun scattered in all directions by the lunar hemisphere to the total light, is 0.073; (2) the average geometric albedo of the moon, or ratio between the average brightness of the disk at full moon and the brightness of a white screen of the same size normal to the incident solar rays, is 0.105 (Bobrovnikoff).

In detailed photometry, the emission of light from a small area is measured. Actually, this is to be regarded as the average emission of light over the various surface materials, slopes and the microfeatures or unevenness of the surface in that small area. The moon can be studied in detail due to its nearness to earth, and many photometric studies of lunar details have been made. Of course, the brightness of the lunar feature depends on the directions to the sun and to the observer on earth. If one defines photometric coordinates $(\alpha_P, \epsilon_P, i_P)$ of a point P whose brightness is measured by reference to the following sketch:
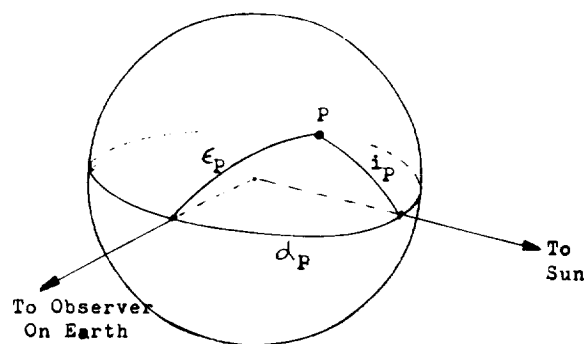
where i_P is the angle of incidence of the solar rays, ϵ_P is the angle of reflection of these rays to the observer on earth, and α_P is the phase angle of the sun with respect to earth, then the brightness of P can be expressed in the form

$$\rho* = \rho*_0 \, f \, (i_P, \epsilon_P, \alpha_P). \tag{31}$$

In Eq (31), $\rho*$ is called the "brightness factor," or the ratio of the brightness of the diffusing surface at point P to the brightness of a white screen of the same size placed normally to the sun, and it can be directly compared with the brightness of terrestrial objects. The normalized factor f depends on the photometric coordinates of P such that f = 1 when $i_P = 0°$, $\epsilon_P = 0°$ and $\alpha_P = 0°$.

Hence $\rho*_0$, or the normal albedo, is the value of ρ for an object near the center of the full moon. It should be remarked that the brightness of every detail of the moon reaches its maximum at full moon, and at that time the brightness of structurally similar details does not depend on the solar position with respect to them, i.e., f = 1 when i = ϵ

(see Bobrovnikoff, Ref. 19, p 68). The following table of normal albedos ρ_0^* of lunar features has been taken from Kuiper (Ref. 8, p 236) and was obtained from a catalogue of 104 normal visual albedos which were reduced to absolute values:

Location	ρ_0^*
Darkest spot (inside Oceanus Procellarum $\lambda_{\mathbb{C}} = 60°$, $\phi_{\mathbb{C}} = +27°$)	0.051
Maria (seas)	0.065
Paludes (marshes)	0.091
Mountain regions	0.105
Crater bottoms	0.112
Bright rays	0.131
Brightest spot (Aristarchus)	0.176

The ratio of brightness between the brightest and darkest points is 3.45, which corresponds to 1.34 stellar magnitudes.

One can observe the ashen light on the moon; this is sunlight which reaches the observer from the dark hemisphere of the moon after having been reflected from the earth. It is about 4000 times fainter than moonlight. Seasonal and diurnal variation has been detected in the brightness (see Fielder, Ref. 20, p 55). In addition, there is observational evidence from spectroscopic data that there are luminescent substances on the moon.

The surface of the moon seems to be quite varied in color. These colors range from the greenish tint of the maria to yellow and orange hues on the continents and mountains. These shades have also been photographed and are represented on many of the lunar maps listed in Subsection A-2g of Chapter III. However, measurements of lunar color by photography through filters yield a surprisingly small coloration range (see Bobrovnikoff, Ref. 19, p 71).

c. Temperature of the lunar surface

If the moon is assumed to be a black body in thermal equilibrium, its temperature is given by the Stefan-Boltzmann law:

$$W_{\mathbb{C}} = \sigma T^4 \qquad (32)$$

where $W_{\mathbb{C}}$ watts/m^2 is the total amount of radiated power by unit area of the lunar area whose temperature is to be calculated, T is the absolute temperature in °K, and $\sigma = 5.67 \times 10^{-8}$ watts/ m^2-(°K)^4 is the Stefan-Boltzmann constant. Let $r_{\odot\mathbb{C}}$ be the distance of the moon from the sun. The total radiated solar power crossing a sphere of radius $r_{\odot\mathbb{C}}$ is $4\pi r_{\odot\mathbb{C}}^2 W_{\mathbb{C}}$, and, by definition of the solar constant S, the total radiated

power crossing a sphere of radius $\bar{r}_{\odot\oplus} = 1$ AU is $4\pi \bar{r}_{\odot\oplus}^2 S$. From conservation of energy,

$$W_{\mathbb{C}} = \left(\frac{\bar{r}_{\odot\oplus}}{r_{\odot\mathbb{C}}}\right)^2 S \qquad (33)$$

and the temperature of the lunar surface area becomes

$$T = \left(\frac{\bar{r}_{\odot\oplus}}{r_{\odot\mathbb{C}}}\right)^{1/2} \left(\frac{S}{\sigma}\right)^{1/4} \qquad (34)$$

For S = 1379 watts/m^2 (Allen, Ref. 22) and $r_{\odot\mathbb{C}} = \bar{r}_{\odot\oplus}$ it follows that T $\simeq$ 394.5° K = 121.5° C. This value should be regarded as the maximum temperature that the lunar surface can attain, since in practice some energy can flow to the interior of the moon, and some energy is reflected.

The temperature of the moon is a very difficult quantity to measure. Lunar temperatures have been determined by investigating the emitted light of the moon at various wavelengths (radiometric measurements). Problems arise with the resolution of the measuring instrument and the penetration of the radiation into the lunar surface as well. Thus one can at best obtain an average temperature over some area at some estimated depth below the lunar surface, and the temperature of certain lunar rocks, i.e., a specific local temperature, cannot be determined.

Variations of the lunar surface temperature depend on the thermal inertia constant,

$$K = (\lambda \rho c)^{-1/2} \qquad (35)$$

where λ (cal/cm^2-sec) is the thermal conductivity of the surface material, ρ (grams/cm^3) is its density, and c (cal/gram) is the specific heat per unit mass, all measured in cgs units. Optical lunar observations indicate that K $\simeq$ 1000. However, Muncey (Ref. 23) has postulated that λ and c vary with the absolute temperature in vacuo, and K for 300° K $\simeq$ 27° C should be between 200 and 300.

Radiometric observations of lunar surface temperatures indicate a maximum temperature of about 130° C and a very unreliable minimum of -153° C depending on the phase of the moon. Some recent measurements by Mezger and Strassl (Ref. 29) indicate a subsurface equilibrium temperature which is independent of the phases. Lunar surface isotherms which were obtained by Geoffrion, et al. (Ref. 25) have been given as a function of phase in Space and Planetary Environments (Ref. 26). A rough estimate of average lunar surface temperatures as a function of the lunar day (1 lunar day = 1 synodic month = $29^d 12^h 44^m 2^s.9$) has been given in Fig. 3. The data in Fig. 3 is based on Pettit and Nicholson's data (Ref. 27) under the assumptions that the temperature variations in latitude and longitude

are identical (i. e. , the surface isotherms are circular) and that the ecliptic and lunar equatorial planes coincide; the solar irradiation at the subsolar point has been taken as given by the solar constant, $S = 1396.4$ watts/m^2.

d. Lunar magnetic field

The instrumentation on the Soviet Lunik II space vehicle did not detect a lunar magnetic field. These measurements put an upper limit on the lunar magnetic field of 3×10^{-4} gauss, which compares to a field strength of 0.6 gauss in the polar region of the earth. Thus the lunar field is very weak compared to the earth's. However, one can still assume that the magnetic field on the lunar surface is of the order of 2.5×10^{-5} gauss, due to the general interplanetary magnetic field, rising to a maximum of 4×10^{-4} gauss at periods of high solar activity (Ref. 26, p 102).

e. Lunar surface characteristics

The structure of the surface and the subsurface layers of the maria, continents, and mountains varies according to different theories about the origin of the major surface features. One theory postulates the volcanic origin of these features, while another postulates meteoritic origin. The spectroscopic, radiometric, radar and radio data on the moon suggest a surface cover of dust or finely ground powder, but there is disagreement on the thickness of the dust layer. It is assumed to vary in thickness from a few millimeters to several meters, although some small areas on the moon seem to be substantially free from dust cover (Bobrovnikoff, Ref. 19, p 106). Both the meteoritic and volcanic theories predict a layer of dust.

The behavior of the dust is also open to question. Theories range from an extremely loose top layer held in suspension by electrostatic forces and subject to migration (Gold, Ref. 28) to a layer of dust grains cemented together (Whipple, Ref. 29). The vacuum welding effect found by Roche (Ref. 30) predicts a strong tendency of particles to adhere to each other when disturbed by seismic quakes. In Ref. 26, p 111, it is stated that theoretical considerations suggest "dust on the lunar surface which is cemented into a porous, low-density matrix, weak compared to sedimentary rocks on earth but strong compared to earth dust and not subject to migration."

The microfeatures (i. e. , unobservably small features) of the lunar surface are also open to question. Radar measurements seem to indicate both a smooth and rough surface on the decimeter scale (see Ref. 26, p 112), while the photometric interpretations of Sytinskaya (Ref. 31) indicate a mean dimension of these microfeatures of the order of several millimeters to several centimeters.

f. Natural resources on the moon

A good reference on lunar natural resources is Ref. 26,pp 114 to 121 and the listed sources. The conclusion in that reference is that limited amounts of useful materials may be present on the lunar surface. One of these useful materials could be water. Due to the low vapor pressure of water at $-150°$ C, it could remain in the solid state at zero pressure for millions of years. Such surface conditions exist in some lunar areas which remain in perpetual shadow. There might also be large ice deposits sealed off beneath the lunar surface. It has been predicted that the volatile materials associated with earth volcanism such as H_2O, H_2S, CO_2 and SO_2 have been concentrated near the margins of the circular maria.

g. Lunar atmosphere

The lunar atmosphere must be extremely rarefied, as determined from such observational evidence as sharp surface shadows, sudden star occultation and the absence of refraction phenomena during solar eclipses. Jeans (Ref. 32) was able to show from considerations of kinetic theory that, under certain assumptions, if the root-mean-square velocity $\sqrt{(\overline{V^2})}$ of the individual molecules of a planet's atmosphere is 0.2 V_p, where V_p is the parabolic or escape velocity of the planet, then atmospheric dissipation periods of 100 million years can be expected. The low value of $V_p = 2.375$ km/sec for the moon as compared to the earth's value of $V_p = 11.186$ km/sec would then suggest that only molecules with a high molecular weight such as SO_2, CO_2, H_2S can be retained by the moon for long periods of time. Some radiogenic krypton, xenon, argon, radon and helium should be continually released from the lunar interior, and some gases may be released during the vaporization of ice deposits. However, the latter would escape rather rapidly due to the low value of V_p. Hence,the composition of the lunar atmosphere is open to question. The following table, taken essentially from Fielder (Ref. 20 , p 115), gives maximum densities of the lunar atmosphere as established by various methods:

Observation	Method	Source	Maximum Density of the Lunar Atmosphere (atmospheres)
1	Absence of twilight	Russel, Dugan and Stewart (Ref. 33)	$< 10^{-4}$
2	Photography of twilight in green light with a polarimeter	Lipski (Ref. 34)	$< 10^{-4}$
3	Photography of twilight in yellow light with a 20-cm coronograph	Lyot and Dollfus (Ref. 35)	$< 10^{-8}$
4	Photography of twilight in orange light, with a 20-cm coronograph and a polariscope	Dollfus (Ref. 36)	$< 10^{-9}$
5	Refraction of radio waves in the lunar ionosphere	Elsmore and Whitfield (Ref. 37)	$< 10^{-12}$
6	Refraction of radio waves in the lunar ionosphere	Costain, Elsmore and Whitfield (Ref. 38)	$< 10^{-13}$

In general, the minimum density on the lunar surface is assumed to be the same as that of the interplanetary medium. However, Öpik and Singer (Ref. 39) have postulated zero pressure due to the repulsion of ionized gas molecules by the positively changed lunar surface. Under these circumstances a maximum lunar atmospheric density of 10^{-12} atmospheres can be assumed (Bobrovnikoff), compared to 10^{-13} atmospheres assumed in Ref. 26.

Locally the atmospheric density may exceed these values due to very rare gaseous discharges. There have been observations of haziness near some features, notably of a "volcanic eruption" in the crater Alphonsus observed by Kozyrev (Ref. 40). Again, from kinetic theory considerations, most of these gases quickly escape from the moon.

Due to the absence of a lunar atmosphere, the surface of the moon is bombarded much more frequently by meteorites, micrometeorites, cosmic rays and high-energy solar radiation (such as X-rays and γ-rays) than the earth. The radiation and meteoritic environment near the lunar surface is probably not much different from that in cislunar space, since such an atmosphere can provide no shielding.

h. Summary

The lunar environmental data has been discussed in narrative form for this handbook because of its importance for lunar flight. The major references used for this discussion have been Refs. 8, 19, 20, 21 and 26, and the sources indicated in these references. If it is desired to trace the lunar environmental information to the source, the major references which give the source should be consulted. All numerical data on the lunar environment has been either referenced to the major reference or to the source itself to allow further checking of numerical data.

Our present ideas about surface conditions on the moon can be summarized as follows (see also Bobrovnikoff, Ref. 19, p 108):

(1) The lunar surface has a rough microrelief with many small pits, depressions and elevations.

(2) The vertical relief (macrorelief) is high, but the slopes are generally gentle.

(3) The lunar surface consists of dust (probably radioactive) which is cemented into a porous, low-density matrix not subject to migration.

(4) There is no appreciable atmosphere, the upper limit on atmospheric density being 10^{-12} atmospheres.

(5) Locally, gases must be escaping, and seismic quakes must be rather common.

(6) The temperature variations are extremely great, from a maximum of about +130° C near the subsolar point to a minimum of about -150° C.

(7) There is no appreciable lunar magnetic field.

(8) There is no shielding of the lunar surface from the bombardment of meteorites, micrometeorites, particles and radiation which affect the structure, texture and composition of the surface.

Some lunar environmental data, as it was acquired by the space vehicles listed in Section D of this chapter, has already been incorporated in the present writeup. It should be mentioned again that planned space vehicle flights into the vicinity of the moon and exploration of the lunar surface will yield much more data and may modify our present ideas on the near-moon environment.

C. SYSTEMS OF UNITS AND CONVERSION TABLES

Throughout the Lunar Flight Handbook the absolute MKS system of units, which is based on the meter as the basic unit of length, the kilogram as the basic unit of mass, and the second as the basic unit of time, has been used. In order to be able to compare the handbook data with that presented elsewhere, the systems of units in common use and conversion factors between the units are presented in summary form in this section. More information on units and conversions can be found in Judson (Ref. 41). It is important that this or later references be consulted, since the metric equivalents of the U.S. foot, and U.S. pound (avoirdupois) have recently been changed slightly by act of Congress. Another good reference on units of measurement is Green (Ref. 42), who also discusses electrical systems of units. Astronomical units have been discussed to some extent by Herrick, Baker, and Hilton (Ref. 2) and in the standard textbooks of astronomy.

1. Systems of Mechanical and Astronomical Units.

The unit force in an absolute system of units gives unit acceleration to unit mass, while the unit force in a gravitational system of units gives the acceleration of g_0 to a unit mass (see Table 7).

There are two types of gravitational units; choice of either depends on whether the unit of mass is numerically equal to the unit mass in the absolute system (Type 2) or differs from it by a factor g_0 (Type 1).

TABLE 7
Systems of Mechanical Units

Property	Metric				English		
	1 Absolute MKS $F = Ma$	2 Absolute CGS $F = Ma$	3 *** Gravitational MKS Type 1 $F = Ma$	4 *** Gravitational MKS Type 2 $F = \frac{M}{g_0}a$	5 Absolute FPS $F = Ma$	6 *** Gravitational FPS Type 1 $F = Ma$	7 *** Gravitational FPS Type 2 $F = \frac{M}{g_0}a$
Length	meter (m)	centimeter (cm)	meter (m)	meter (m)	foot (ft)	foot (ft)	foot (ft)
Mass	kilogram (kg)	gram (g)	*kgf sec²/m	kilogram (kg)	pound (lb)	**slug = $\frac{lbf\ sec^2}{ft}$	pound (lb)
Time	second (sec)	sec	sec	sec	sec	sec	sec
Force	newton (nt) = $\frac{kg\ m}{sec^2}$	dyne = $\frac{g\ cm}{sec^2}$	*kilogram force (kgf)	*kilogram force (kgf)	poundal (pdl) = $\frac{lbf}{sec^2}$	**pound force (lbf)	**pound force (lbf)
Energy	joule = nt-m	erg = dyne-cm	*kgf-m	*kgf-m	pdl-ft	**lbf-ft	**lbf-ft
Power	watt = $\frac{joule}{sec}$ = $\frac{nt-m}{sec}$	$\frac{erg}{sec}$ = $\frac{dyne-cm}{sec}$	$\frac{*kgf-m}{sec}$	$\frac{*kgf-m}{sec}$	$\frac{pdl-ft}{sec}$	$\frac{**lbf-ft}{sec}$	$\frac{**lbf-ft}{sec}$
Pressure	10^{-2} millibar (mb) = $\frac{nt}{m^2}$	10^{-3} millibar (mb) = $\frac{dyne}{cm^2}$	$\frac{*kgf}{m^2}$	$\frac{*kgf}{m^2}$	$\frac{pdl}{ft^2}$	$\frac{**lbf}{ft^2}$	$\frac{**lbf}{ft^2}$

*The numbers associated with these units are only $\frac{1}{g_0} = \frac{1}{9.80665}$ (exact) as large as the numbers associated with corresponding units of system 1.

**The numbers associated with these units are only $\frac{1}{g_0} = \frac{1}{32.17404855}$ as large as the numbers associated with corresponding units of system 5.

***All gravitational units are based on the standard acceleration due to gravity, g_0, no matter where the force measurement takes place. This weight, thrust, etc., in the vicinity of the moon is given in terms of g_0, not the lunar acceleration of gravity.

(1) The absolute MKS system of units in column 1, which is used by physicists, has been employed throughout the Lunar Flight Handbook.

Auxiliary units, related to the basic units in the table by powers of 10, are defined by the following standard pre-prefixes and abbreviations

tera:	10^{12}	T
giga:	19^{9}	G
mega:	10^{6}	M
kilo:	10^{3}	k
hecto:	10^{2}	h
deka:	10^{1}	da
deci:	10^{-1}	d
centi:	10^{-2}	c
milli:	10^{-3}	m
micro:	10^{-6}	μ
nano:	10^{-9}	n
pico:	10^{-12}	p
femto:	10^{-15}	f
atto:	10^{-18}	a

Both basic and auxiliary units will be used in the Handbook, whichever are more convenient in describing the quantity in question.

(2) The gravitational MKS system of units in column 4 of the preceding table is in general use in Europe. The word "kilogram" is very often used as the unit of both mass and force. Consequently, the expression "kilogram" is ambiguous, although its meaning as a unit of mass or force is usually clear from the context. To avoid confusion, it is desirable to denote the basic unit of mass by "kilogram" and the basic unit of force by "kilogram force" as has been done in the table above. The same remark applies to derived units such as "gram," "metric ton," etc.

(3) The gravitational MKS system of units in column 3 of the preceding table is used by European aeronautical engineers.

(4) The gravitational FPS system of units in column 7 is in general use in the U.S. The word "pound" is very often used interchangeably as a unit of force and mass, and consequently its meaning is ambiguous. To avoid confusion, the basic unit of mass has been designated "pound" and the basic unit of force has been designated "pound force" in the preceding table. Again, the same remark applies to derived units such as "ounce" and "ton."

(5) The gravitational FPS system of units in column 6 is used by American aeronautical engineers. The basic unit of mass in this system of units is the slug. One slug corresponds to g_0 pounds (mass), so that the mass M expressed in slugs is M/g_0, where M is the mass expressed in pounds (mass).

Astronomers frequently use systems of units which are adapted to calculations in dynamical astronomy. A comparison of two common systems of astronomical units with the absolute MKS system is given in Table 8.

TABLE 8

Systems of Astronomical Units

Property	Absolute MKS $F = \dfrac{G M_1 M_2}{r^2}$	Astronomical	
		Type 1 $F = \dfrac{K_\odot^2 M_2}{r^2}$	Type 2 $F = \dfrac{K_\odot^2 M_2}{r^2}$
Length	Meter (m)	Astronomical unit (AU) *1 AU = 149.53 x 10^9 m	AU
Mass	Kilogram (kg)	Solar mass ($M_\odot$) *1 $M_\odot$ = 1.9866 x 10^{30} kg	**$M_\odot$
Time	Second (sec)	Mean solar day (MSD) 1 MSD = 86,400 sec	*$t_\odot$ = 58.13244087 MSD
Universal gravitational constant G or solar gravitational constant $K_\odot$	*G = 6.670 x 10^{-11} m^3/kg sec^2	*$K_\odot$ = 0.01720209895 $\dfrac{(AU)^{3/2}}{MSD}$	$K_\odot$ = 1 $\dfrac{(AU)^{3/2}}{t_\odot}$
Force	Newton = 1 kg · m/sec^2	$\dfrac{M_\odot (AU)}{(MSD)^2}$	** $\dfrac{M_\odot (AU)}{t_\odot^2}$
Angular velocity	Radian/sec	$\dfrac{radian}{MSD}$	$\dfrac{radian}{t_\odot}$

*Value adopted in the handbook. For further details see Section A.

**If the mass M_2 is an appreciable fraction of $M_\odot$, i.e., $\dfrac{M_2}{M_\odot} > 10^{-6}$,

then quite frequently the unit of mass is chosen as M = ($M_\odot$ + M_2),

and the unit of force becomes $\dfrac{M (AU)}{t_\odot^2}$.

The astronomical system of units, Type 1, has been defined because the angular motion of the planets and moons can be determined much more accurately by observation than their distances. As long as all calculations are performed in astronomical units, they are very accurate. At the end of the calculations one can make the transformation to the absolute MKS laboratory units (see Subsection A-1).

The astronomical system of units, Type 2, has been introduced in order that the mean motion (or average angular velocity) of the earth around the sun has magnitude 1.

In both systems of astronomical units, the dynamical system consists of a spherical earth in an elliptical orbit around a spherical sun, so that two-body results apply. It is also possible to construct other sets of astronomical units by use of other planets or comets and the sun, or of moons around planets. The earth case is of particular interest in lunar flight problems when applied to the dynamical system of a spherical moon in an elliptic orbit around the earth. For the earth-moon system, the unit of length becomes the lunar unit (*1 LU = 384,747.2 km) and unit of mass the earth's mass (*$M_\oplus$ = 5.9758 x 10^{24} kg). The unit of time in a Type 1 astronomical system is the mean solar day (MSD) and the gravitational constant of the earth becomes:

$$*K_\oplus = \frac{2\pi}{\tau} \sqrt{\frac{\bar{r}_{\oplus\text{☾}}}{M_\oplus + \dfrac{M_\text{☾}}{M_\oplus}}} =$$

$$0.228570389 \ \frac{(LU)^{3/2}}{MSD}$$

where

$$\bar{r}_{\oplus\text{☾}} = 1 \text{ LU}$$

*The values adopted in the lunar handbook have been used for the calculations.

*τ = 27.3216614 mean solar days

$M_\oplus$ = 1 earth mass

$\dfrac{*M_\text{☾}}{M_\oplus}$ = $\dfrac{1}{81.357}$ = 0.012291505 (exact).

The unit of time in a Type 2 astronomical system is $t_\oplus$ = 4.37501990 MSD; therefore, the gravitational constant of the earth becomes $K_\oplus = 1\dfrac{(LU)^{3/2}}{t_\oplus}$

2. Length, Velocity, Acceleration and Volume/Capacity Unit Conversions

a. Defined relations

Meter (m) = 1,650,763.73 wavelengths of the orange-red radiation of Krypton-86: the fundamental metric unit of length.

Foot (ft) = 0.3048 m (exact): the fundamental U.S. unit of length.

Second (sec) = 1/86400 mean solar day: the fundamental unit of civil time.

Velocity units: length/time.

Acceleration units: length/$(time)^2$.

Volume (or capacity) units: $(length)^3$.

The fundamental unit of volume is one cubic meter (m^3) or the unit of volume equal to a cube with edges 1 m in length.

The fundamental metric unit of capacity is the liter (ℓ), which is equal to the volume of 1 kg of pure water at its maximum density near 4° C and under standard atmospheric pressure of 760 mm Hg. 1 ℓ = 1000.028 (cm^3).

The gallon is a unit of liquid capacity equal to 231 cubic inches (in ^{3}).

b. Length conversions

Table 9 lists conversion factors for standard units of length.

TABLE 9
Length Conversions

	Astronomical Units	International Nautical Miles	Statute Miles	Meters	International Yards	International Feet	International Inches
1 Astronomical Unit =	1	$80.737,90 \times 10^6$	$92.911,52 \times 10^6$	149.5266×10^9	$163.524,3 \times 10^9$	490.5728×10^9	$588.687,4 \times 10^{10}$
1 International Nautical Mile =	$1.238,575 \times 10^{-8}$	1	$1.150,779,447$	1852^*	$2025.371,828$	$6076.115,485$	$72.913,385,826$
1 Statute Mile =	$1.076,292 \times 10^{-8}$	$0.868,976,242$	1	1609.344^*	1760^*	5280^*	$63,360^*$
1 Meter =	$0.668,777,3 \times 10^{-11}$	$0.539,956,803 \times 10^{-3}$	$0.621,371,192 \times 10^{-3}$	1	$1.093,613,298$	$3.280,839,895$	$39.370,078,740$
1 International Yard =	$0.611,528,9 \times 10^{-11}$	$0.493,736,501 \times 10^{-3}$	$0.568,181,818 \times 10^{-3}$	0.9144^*	1	3^*	36^*
1 International Foot =	$0.203,843,3 \times 10^{-11}$	$0.164,578,833 \times 10^{-3}$	$0.189,393,939 \times 10^{-3}$	0.3048^*	$0.333,333,333$	1	12^*
1 International Inch =	$0.169,869,4 \times 10^{-12}$	$0.137,149,028 \times 10^{-4}$	$0.157,828,282 \times 10^{-4}$	0.0254^*	$0.027,777,777$	$0.083,333,333$	1

$$1 \text{ micron} = 10^{-6} \text{ meter}, \quad 1 \text{ Angstrom unit} = 10^{-10} \text{ meter}$$

c. Velocity conversions

Table 10 lists conversion factors for standard units of velocity.

TABLE 10
Velocity Conversions

	Astronomical Units per Mean Solar Day	Astronomical Units per Sidereal Day	International Nautical Miles per Hour	Statute Miles per Hour	Kilometers per Hour	Meters per Second	Feet per Second
1 Astronomical Unit per Mean Solar Day =	1	$1.002,737,90$	$3.364,078 \times 10^6$	$3.871,313 \times 10^6$	$6.230,273 \times 10^6$	$1.730,632 \times 10^6$	$5.677,928 \times 10^6$
1 Astronomical Unit per Sidereal Day =	$0.997,269,57$	1	$3.354,892 \times 10^6$	$3.860,743 \times 10^6$	$6.213,260 \times 10^6$	$1.725,907 \times 10^6$	$5.662,424 \times 10^6$
1 International Nautical Mile per Hour =	$0.297,258,2 \times 10^{-6}$	$0.298,072,1 \times 10^{-6}$	1	$1.150,779,447$	1.852^*	$0.514,444,444$	$1.687,809,856$
1 Statute Mile per Hour =	$0.258,310,3 \times 10^{-6}$	$0.259,017,5 \times 10^{-6}$	$0.868,976,242,6$	1	$1.609,344^*$	$0.447,040^*$	$1.466,666,666$
1 Kilometer per Hour =	$0.160,506,6 \times 10^{-6}$	$0.160,946,1 \times 10^{-6}$	$0.539,956,803,4$	$0.621,371,192$	1	$0.277,777,777$	$0.911,344,415$
1 Meter per Second =	$0.577,823,6 \times 10^{-6}$	$0.579,405,5 \times 10^{-6}$	$1.943,844,491$	$2.236,936,288$	$3,600^*$	1	$3.280,839,895$
1 Foot per Second =	$0.176,210,6 \times 10^{-6}$	$0.176,602,8 \times 10^{-6}$	$0.592,483,800$	$0.681,818,181$	$1.097,280^*$	0.3048^*	1

— Underlined digits are questionable.
* Denotes exact conversion factor.

d. Acceleration conversions

Table 11 lists conversion factors for standard units of acceleration.

TABLE 11
Acceleration Conversions

	Astronomical Units per Mean Solar Day^2	Astronomical Units per Sidereal Day^2	International Nautical Miles per Hour^2	Statute Miles per Hour^2	Kilometers per Hour^2	Meters per Second^2	International Feet per Second^2
1 Astronomical Unit per Solar Day^2 =	1	$1.005,483,40$	$1.401,700 \times 10^5$	$1.613,047 \times 10^5$	$2.595,989 \times 10^7$	$20,030,36$	$65,715,76$
1 Astronomical Unit per Sidereal Day^2 =	$0.994,546,60$	1	$1.394,056 \times 10^5$	$1.604,250 \times 10^5$	$2.581,832 \times 10^7$	$19,922,23$	$65,358,38$
1 International Nautical Mile per Hour^2 =	$0.713,419,4 \times 10^{-5}$	$0.717,332,1 \times 10^{-5}$	1	$1.150,779,447$	1.852^*	$1.428,012,44 \times 10^{-4}$	$4.688,360,731 \times 10^{-4}$
1 Statute Mile per Hour^2 =	$0.619,944,7 \times 10^{-5}$	$0.623,344,2 \times 10^{-5}$	$0.868,976,242,6$	1	$1.609,344^*$	$1.241,777,778 \times 10^{-4}$	$4.074,074,074 \times 10^{-4}$
1 Kilometer per Hour^2 =	$0.385,209,6 \times 10^{-5}$	$0.387,321,9 \times 10^{-5}$	$0.539,956,803,4$	$0.621,471,192$	1	$0.771,604,938,2 \times 10^{-4}$	$2.531,512,964 \times 10^{-4}$
1 Meter per Second^2 =	$0.049,923,97$	$0.050,197,70$	$0.699,784,017,6 \times 10^4$	$0.805,297,064,9 \times 10^4$	$12,960^*$	1	$3.280,839,895$
1 International Foot per Second^2 =	$0.015,216,82$	$0.015,300,26$	$0.213,294,168,6 \times 10^4$	$0.245,245,245,2 \times 10^4$	$0.395,020,800$	0.3048^*	1

e. Volume and capacity conversions

Table 12 lists conversion factors for standard units of volume and capacity.

TABLE 12

Volume and Capacity Unit Conversions

	Cubic Inches	Cubic Feet	Cubic Meters	Liters	Gallons
1 Cubic Inch	1*	5.787037×10^{-4}	1.6387064×10^{-5}	0.01638661	0.004329004
1 Cubic Foot	1,728*	1	0.028316846592 *	28.31605	7.480519
1 Cubic Meter	61,023.74*	35.31467*	1	999.972	264.172
1 Liter	61.02545	0.03531566	1.000028×10	1	0.2641794
1 Gallon (U.S.)	231*	0.1336806	3.7854118×10^{-3}	3.785306	1

*Denotes exact conversion factor

3. Angular conversions

Table 13 lists conversion factors for standard units of angular measurement.

TABLE 13

Angular Unit Conversions

	Revolutions	Radians	Degrees	Minutes of Arc	Seconds of Arc	Angular Mils
1 Revolution =	1	6,283,185,307	360.0*	21,600.0*	1,296,000.0*	6400*
1 Radian =	0.159,154,943	1	57.295,779,511	3,437.746,771	206,264.806,236	1018.591636
1 Degree =	$2.777,777,777 \times 10^{-3}$	$1.745,329,252 \times 10^{-2}$	1	60.0*	3,600.0*	17.777,777,77
1 Minute of Arc =	$4.629,629,629 \times 10^{-5}$	$2.908,882,086 \times 10^{-4}$	$1.666,666,666 \times 10^{-2}$	1	60.0*	0.296,296,296
1 Second of Arc =	$7.716,049,382 \times 10^{-7}$	$4.848,136,812 \times 10^{-6}$	$2.777,777,777 \times 10^{-4}$	0.016,666,666	1	$4.938,271,605 \times 10^{-3}$
**1 Angular Mil =	$1.5625 \times 10^{-4*}$	$9.817,477,040 \times 10^{-4}$	$5.6250 \times 10^{-2*}$	3.375*	202.5*	1

*Denotes exact conversion factor.

**The "angular mil" should be differentiated from the milliradian,
which is often designated "mil" in targeting, and the "mil" which
is a unit of length corresponding to 0.001 inch. From the table,
1 angular mil = 0.981,747,704 milliradian

4. Mass and Force Unit Conversions

a. Defined relations

Kilogram (kg) the mass of the international proto-
type kilogram: the fundamental metric unit
of mass in the absolute MKS system of units.

Pound avoirdupois (lb) = 0.45359237 kg (exact):
the fundamental U.S. unit of mass in the
absolute FPS system of units.

Unit force in an absolute system of units is a unit
which gives unit acceleration to unit mass:

1 newton (nt) = 1 kg-m/sec^2

1 poundal (pdl) = 1 lb-ft/sec^2

Unit force in a gravitational system of units is a
mass unit multiplied by g_0, where g_0 =
9.80665 m/sec^2 (exact) is the standard ac-
celeration due to gravity, the adopted sea
level value for 45° latitude. In U.S. units

g_0 = $32.17404855 + \text{ft/sec}^2$ (derived value).

1 kilogram force (kgf) = $9.80665 \text{ kg-m/sec}^2$
= 9.80665 nt

1 pound force (lbf) = $32.17404855 + \text{lb-ft/sec}^2$
= 32.17404855 + pdl

b. Derived mass unit conversions

Table 14 lists conversion factors for mass
units.

c. Derived force and mass unit conversions

1 kgf	= 2.204622621 + lbf

1 lbf   = 0.45359237 kgf = 4.448176256 +
newtons

1 newton = 10^5 g-cm/sec^2 = 10^5 dynes

1 newton = 0.101972661 + kgf

1 newton = 0.224811235 + lbf

1 newton = 7.23301387 + pdl

1 pdl = 0.1382549543 + newtons

1 pdl = 0.31080950 + lbf

1 kg = 0.101972661 + kgf sec²/m

1 lb = 0.0310809501 + lbf sec²/ft = 0.0310809501 slugs.

TABLE 14
Derived Mass Conversions

	Solar Mass	Earth Mass	Moon Mass	Slugs	Kilograms	Pounds (avdp)	Ounces (avdp)
1 Solar Mass =	1	332,440	27,646,600	$1.361,25 \times 10^{29}$	$1.986,6 \times 10^{30}$	$4.379,70 \times 10^{40}$	$70.075,3 \times 10^{30}$
1 Earth Mass =	$3.088,062 \times 10^{-6}$	1	81.358	$4.094,2 \times 10^{23}$	$5.975,0 \times 10^{24}$	$13.172,6 \times 10^{24}$	210.76×10^{24}
1 Moon Mass =	$3.697,320 \times 10^{-8}$	$1.229,14 \times 10^{-2}$	1	$5.032,3 \times 10^{21}$	$7.344,0 \times 10^{22}$	$16.191,0 \times 10^{22}$	259.06×10^{22}
1 Slug =	$7.346,18 \times 10^{-29}$	$0.244,25 \times 10^{-23}$	$0.198,72 \times 10^{-21}$	1	14.593,902,876	32.174,048,556	514,784,777.0
1 Kilogram =	$5.033,73 \times 10^{-31}$	$0.167,36 \times 10^{-24}$	$0.136,16 \times 10^{-22}$	$6.852,176,612 \times 10^{-2}$	1	2.204,622,621	35.273,961,94
1 Pound (avdp) =	$2.283,26 \times 10^{-31}$	$0.759,15 \times 10^{-25}$	$0.617,63 \times 10^{-23}$	$3.108,095,016 \times 10^{-2}$	0.453,592,37	1	16.0
1 Ounce (avdp) =	$1.427,04 \times 10^{-32}$	$0.474,47 \times 10^{-26}$	$0.386,01 \times 10^{-24}$	$1.942,559,385 \times 10^{-3}$	$0.283,495,231 \times 10^{-2}$	0.062,5	1

—Underlined digits are questionable.

*Denotes exact conversion factor.

$g_0 = 9.80665 \dfrac{\text{meters}}{\text{sec}} = 32.174,048,556$ ft/sec²

5. Energy Unit Conversions

a. Derived conversion factors between mechanical units of energy

1 joule = 1 nt-m = 1 kg-m²/sec²

1 joule = 10^7 erg = 10^7 g-cm²/sec²

1 joule = 0.101972661 + kgf m

1 joule = 0.7375621493 + lbf ft

1 erg = 10^{-7} joule = 10^{-7} kg-m²/sec²

1 pdl ft = 0.04214011007 + joule

1 pdl ft = 0.0310809501 + lbf ft

1 kgf m = 9.80665 joules

1 lbf ft = 32.17404855 + pdl ft

1 lbf ft = 1.35581794 + joules

b. Defined conversion factors from thermal to mechanical units of energy

1 kilocalorie or kilogram calorie (kg-cal) = $\dfrac{1}{860}$ kilowatt-hours (kw hr)

1 kg-cal = $\dfrac{1}{0.45359237}$ Btu = 3.98320719 + Btu

1 watt-sec = 1 joule

c. Derived conversion factors from thermal to mechanical units of energy

1 kwhr = 3.6×10^6 joules

1 kg-cal = 1000 calories

1 kg-cal = 4186.046511 + joules = 4186.046511 + kg m²/sec²

1 metric ton = 1000* kilogram

1 ton = 2000* pound (avdp) = 907.18474* kilograms

1 kg-cal = 426.8579495 + m-kgf

1 kg-cal = 3087.469937 + ft-lbf

1 Btu = 0.2519957611 + kg-cal

1 Btu = 778.0292165 + ft-lbf

1 Btu = 25032.34980 + lb-ft²/sec²

1 Btu = 1054.866068 + joules

1 joule = 2.388888888 + x 10^{-4} kg-cal

1 joule = 9.479876444 + x 10^{-4} Btu

d. Atomic energy units

The "electron volt" is defined as the amount of work done on one electron by a potential difference of 1 volt; the charge on the electron is taken as 4.80286×10^{-10} electrostatic units of charge.

1 electron volt (EV) = 1.60206×10^{-12} erg

1 kilo-electron volt (kEV) = 10^3 EV

1 mega-electron volt (MEV) = 10^6 EV

1 billion electron volt (BEV) = 10^9 EV

1 erg = 6.24196×10^{11} EV

1 lbf-ft = 8.46297×10^{18} EV

1 kg-cal = 2.6116×10^{22} EV

6. Pressure Unit Conversions

a. Defined units

One atmosphere is defined as the standard pressure (of the earth's atmosphere) at sea level and under $g_0 = 9.80665$ m/sec². It corresponds

to the sea level pressure of the 1959 ARDC and the 1961 U.S. Standard Model Atmospheres.

One millimeter of mercury (mm Hg) is the pressure that a column of mercury 1 millimeter (10^{-3} m) in height exerts at 0° C and under g_0 = 9.80665 m/sec^2.

One inch of mercury (in. Hg) is the pressure that a column of mercury 1 inch in height exerts at 32° F and under g_0 = 32.17404855 + ft/sec^2.

One bar is a unit of pressure corresponding to a force of 10^6 dynes per square centimeter (or 10^5 nt/m^2). Usually, pressure is given in terms of millibars (mb), where 1 mb = 10^{-3} bar.

b. Conversion factors between pressure units

1 nt/m^2	= 10^{-4} nt/cm^2
1 nt/m^2	= 10^{-2} millibar (mb)
1 nt/m^2	= 0.101972661 + kgf/m^2
1 nt/m^2	= 0.67196908 - pdl/ft^2
1 nt/m^2	= 0.020885437 + lbf/ft^2
1 nt/m^2	= 1.4503776- x 10^{-4} lbf/in.^{2}
1 kgf/m^2	= 9.80665 (exact) nt/m^2
1 pdl/ft^2	= 1.48816371 + nt/m^2
1 lbf/ft^2	= 47.8802515 - nt/m^2
1 lbf/in.^{2}	= 6894.756 + nt/m^2
1 atmosphere	= 101,325.00 nt/m^2
1 atmosphere	= 10,332.275 kgf/m^2
1 atmosphere	= 68,087.267 pdl/ft^2
1 atmosphere	= 2116.2170 lbf/ft^2
1 atmosphere	= 14.695951 + lbf/in.^{2}
1 atmosphere	= 760 mm Hg
1 atmosphere	= 29.921260 in. Hg
1 atmosphere	= 1013.2500 mb

7. Temperature Unit Conversions

a. Defined relations

$$t(°C) = T(°K) - T_i(°K)$$

$$T(°R) = 1.8\,T(°K)$$

$$t(°F) - t_i(°F) = T(°R) - T_i(°R)$$

where

$$T_i(°K) = 273.16° K$$

$$t_i(°F) = 32° F$$

b. Derived relations

$$t_i(°C) = 0° C$$

$$T_i(°R) = 491.688° R$$

$$t(°C) = \frac{T(°R) - T_i(°R)}{1.8} = \frac{t(°F) - t_i(°F)}{1.8}$$

$$T(°R) = 1.8\ t(°C) + 273.16(°C)$$

$$= t(°F) - t_i(°F) + 491.688° R$$

$$t(°F) - 32° F = 1.8\,t(°C) = 1.8\ T(°K)$$

$$- 273.16(°K)$$

where

°C = degrees in thermodynamic centigrade (Celsius) scale

°K = degrees in thermodynamic Kelvin scale

°R = degrees in thermodynamic Rankine scale

the subscript "i" denotes the freezing point of water.

D. SUMMARY OF LUNAR EXPLORATION PROGRAMS AND RESULTS

In the United States, the National Aeronautics and Space Administration has been established by Congress to direct the nation's civilian space program which up to the time of writing includes the entire announced U. S. lunar exploration program. Table 15 summarizes the current U. S. lunar spacecraft programs, while Table 16 lists all announced U. S. and Soviet space vehicle launches with lunar mission objectives. The data presented in the first table has been taken partially from Ref. 43, while the data for the second table has been obtained from Refs. 43, 44 and 45 and many lesser sources.

TABLE 15

Current U.S. Lunar Spacecraft Programs

Project	Contractors	Description	Status
Apollo, NASA	North American, command and mission modules, systems integration; MIT, guidance development; Collins Radio, telecommunications; Minneapolis-Honeywell, stabilization and control; AiResearch, environmental control; Radioplane, parachute recovery; Lockheed Propulsion Company, escape tower rocket; Marquardt, reaction controls; Grumman, lunar excursion module (LEM); Avco, heat shield, etc.	Three-man spacecraft for earth-orbital, lunar-orbital and landing missions. Boosters: Saturn for earth orbits, Saturn C-5 for lunar rendezvous, NOVA for direct flight. Spacecraft has three modules: command module, 4.5×10^4 newtons, 3.5 m high; service module, 20.5×10^4 newtons, 7 m high; lunar excursion vehicle, 13×10^4 newtons, 6 m high; total weight 38×10^4 newtons. An idea of the magnitude of this lunar program may be gained in that, by the first launch, about 20,000 companies and 150,000 to 200,000 scientists and engineers will have been involved. The total cost is estimated at $20 billion.	Earth orbital shots scheduled 1964 to 1965, lunar orbits 1966, lunar landing 1967 to 1968. Lunar orbit rendezvous mission profile has been selected.
Lunar Logistics Vehicle (LLV), NASA	Grumman, Northrop Space Technology Laboratories submitted feasibility studies, contract award expected early 1963; Pratt and Whitney, variable-thrust RL-10 liquid hydrogen engine.	3300-newton spacecraft "bus" to carry support payloads to the moon, initially boosted by Saturn C-1B; later 9×10^4-newton "bus" boosted by Saturn C-5. Seven specific payloads will be studied.	Development expected to begin in 1963 after congressional approval of fiscal year 1964 budget. Cost is expected to run to $500 million.
Ranger, NASA	JPL, prime contractor; Aeronutronic, capsule; Hercules, retrorocket.	1300-newton instrument capsule with seismometer will be hard-landed on the moon. Before impact, a TV camera tapes pictures of the lunar surface. The booster is an Atlas-Agena B combination.	Research and development stage. First two Rangers failed to launch from earth orbit; Ranger III launched January 26, 1962, but failed to impact the moon and is in solar orbit; Ranger IV impacted on the moon April 26, 1962; Ranger V, launched October 18, 1962, had a power failure after 8 hours and 44 minutes; it failed to impact the moon and is in solar orbit. A total of 9 more Rangers are planned for 1962 to 1963, and there may be as many as 15 additional Ranger shots. At the time of writing, the program has been temporarily halted for an extensive review of the many failures.
Surveyor, NASA	Hughes, prime contractor; Martin, SNAP II nuclear power generator.	3300-newton spacecraft lands 400 to 1300 newton instruments on the moon. Booster: Atlas-Centaur lunar orbiting vehicle is planned.	First lunar flights planned for 1964--seven soft landing vehicles and five lunar orbiting vehicles for transmitting pictures of the lunar surface.

TABLE 16

Data on U.S. and Soviet Space Vehicle Launches with Lunar Mission Objectives
(Chronological listing)

Definitions of success, partial success, failure are given below:

Success: major mission objective was achieved.

Partial success: yielded scientific information.

Failure: yielded no scientific information on major mission objective. No mission will be stated for failures.

1. Pioneer O (U.S.) 17 August 1958, failure. Propulsion failure of the first stage.

2. Pioneer I (U.S.) 11 October 1958, partial success..

   Pioneer I, a lunar probe, reached a distance of 113,000 km from earth. It carried an ionization chamber to measure cosmic radiation, and the returned data gave a qualitative peak of radiation in space.

3. Pioneer II (U.S.), 8 November 1958, failure.

4. Pioneer III (U.S.), 6 December 1958, partial success.

   The mission objective was to place a scientific payload on an earth escape trajectory into the vicinity of the moon. The space vehicle failed to achieve earth escape velocity; it achieved a maximum distance of about 100,000 km from earth.

   On-board instruments included two Geiger-Mueller counters. Cosmic ray data from Pioneer III revealed the existence of a second Van Allen radiation belt at a higher altitude than that discovered by the Explorer I earth satellite. The region of high-intensity radiation was found to consist of two concentric belts around the earth.

5. Lunik I (U.S.S.R.) 2 January 1959, success.

   This lunar probe was probably an attempt to impact. Pericynthion distance (closes approach to the moon) of 7500 km was achieved about 36 hr after launch. After lunar passage, the space vehicle went into a solar orbit between earth and Mars with the following characteristics:

Period	=	450^d
Eccentricity	=	0.148
Inclination	=	15.18°
Perihelion	=	146.4×10^6 km = 0.9791 AU
Aphelion	=	197.2×10^6 km = 1.319 AU

   On-board instruments included:

   Magnetometer
   Twin Geiger-Mueller counters
   Nitrium spectral analyzer
   Skin and chamber temperature thermocouples
   Micrometeorite erosion gauge
   Sodium vapor discharge device (which released, for tracking purposes, a sodium cloud 100 km in diameter at a distance of 115,000 km from earth).

   The total vehicle weight was 14,435 newtons.

   The purpose of the vehicle was to measure intensities of radiation and cosmic rays. Actual measurements of the moon included magnetic field strength, gravitational forces, cosmic ray intensity, sediment evaluation of the lunar craters, properties of the moon's inner strata and optical teletransmission of the moon's surface.

6. Pioneer IV (U.S.), 3 March 1959, success.

   This lunar probe passed the moon at a distance of approximately 60,000 km because the injection velocity was 84 m/sec below the planned velocity of 11,166 m/sec. The vehicle continued on to a solar orbit between earth and Mars with the following characteristics:

Period	=	$397^d.75$
Eccentricity	=	0.067
Inclination to the earth's equator	=	29.9°

$$\text{Perihelion} = 147.6 \times 10^6 \text{ km} = 0.9871 \text{ AU}$$

$$\text{Aphelion} = 173.7 \times 10^6 \text{ km} = 1.162 \text{ AU}$$

$$\text{Inclination to ecliptic} = 1.5°$$

On-board instruments included:

> 2 Geiger-Mueller counters
> A photoelectric sensor
> A despin mechanism

The total space vehicle weight was 60 newtons.

Primary mission objectives were to:

> Achieve an earth-moon trajectory
> Determine the physical limits of the Van Allen radiation belts
> Determine the extent of radiation in the vicinity of the moon
> Test the operation of a photoelectric sensor

During the 8 hr of its battery life, this payload transmitted to earth new information on the extent and nature of cosmic radiation in space, indicating variations on both the extent and intensity of the high-altitude Van Allen radiation belt.

The first Van Allen radiation belt was found to consist of high energy protons and low energy electrons, while the second belt consists primarily of low energy protons after shielding.

Data was received to a range of 650,000 km.

7. Lunik II (U.S.S.R.), 12 September 1959, success.

Lunik II impacted on the moon in a triangular area bounded by the Mare Tranquillitatis, Mare Serenitatis, and Mare Vaporum after covering the earth-moon distance of $r_{\oplus\mathcal{C}} = 381,100$ km in $35^h 2^m 24^s$ from launch to impact. The selenocentric velocity of the space vehicle 5 hr before impact was 2317 m/sec, and at impact it was about 3315 m/sec. The last stage of the rocket also impacted on the moon.

The guidance system of Lunik II functioned only during the initial powered phase of flight.

The mission objectives of Lunik II were to investigate:

> The magnetic fields of the earth and moon
> Radiation belts around the earth
> Intensity and variations in cosmic radiation
> Heavy nuclei in cosmic radiation
> Gas components of interplanetary substance
> Meteoritic particles

The results of the flight included discovery that

(1) The moon has no magnetic field or radiation belt of charged particles.

(2) The moon is enveloped by a belt of low energy ionized gases which might resemble an ionosphere.

8. Lunik III (U.S.S.R.), 4 October 1959, success.

Lunik III carried scientific equipment, including both photographic and television systems to the vicinity of the moon. It passed close to it, so oriented as to photograph the part of the lunar surface that is hidden from the earth.

Photography continued for 40 minutes and images were later televised to earth. The plates and their interpretation were subsequently published by the U.S.S.R. Academy of Sciences as an Atlas of the Moon's Far Side.

Lunik III passed within 7000 km of the moon's south pole at its pericynthion on 6 October 1959.

Its initial orbital parameters were:

$$\text{Nodal period} = 16^d.2$$

$$\text{Eccentricity} = 0.8$$

$$\text{Inclination} = 76.8°$$

Perigee distance = 40,671 km
                     Apogee distance   = 469,306.4 km

9. Lunar Orbiter I (U.S.) 26 November 1959, failure.

    The booster for all Lunar Orbiters was an Atlas-Able combination.

10. Pioneer V (U.S.), 11 March 1960, success.

    The primary mission of Pioneer V was to record space data within approximately 80×10^6 km from
    the earth. It went into a solar orbit between Earth and Venus with the following characteristics:

                Period   = $311^d_.6$
                Eccentricity   = 0.104
                Inclination to
                  ecliptic   = 3.35°
                Perihelion   = 120.5×10^6 km = 0.8059 AU
                Aphelion   = 148.5×10^6 km = 0.9931 AU

On-board instruments included:

        High energy radiation counter to measure high energy radiation, particularly from the sun
        Ionization chamber and a Geiger-Mueller tube to measure the total radiation flux
          encountered
        Micrometeorite counter
        Search coil magnetometer
        Photoelectric cell "aspect indicator" designed to send a signal when the device directly
          faced the sun
        The total weight of the spacecraft was 100 newtons

Important experimental accomplishments of this cislunar and interplanetary space probe were:

    (1) Discovery of large electrical current system in the outer atmosphere, namely, a
         "ring" current of 5 million amperes, 40,000 km in diameter, exists 65,000 km
         from earth.

    (2) Discovery that the earth's magnetic field at times extends out as far as 100,000 km
         and oscillates with solar flare activity.

    (3) Discovery of interplanetary magnetic field which fluctuates in intensity in relation
         to solar flare activity.

    (4) Achievement of the first radio communication over interplanetary distances.

    (5) Discovery that the planar angle of the interplanetary magnetic field forms a large
         angle with the plane of the ecliptic.

    (6) Discovery that the Forbush decrease does not depend on presence of earth's mag-
         netic field.

    (7) Discovery of penetrating radiation beyond the Van Allen belts. The conclusion is
         that radiation will be a major hazard for manned flight between earth and Venus.

11. Lunar Orbiter II (U.S.), 25 September 1960, failure.

12. Lunar Orbiter III (U.S.), 15 December 1960, failure.

13. Ranger I (U.S.), 23 August 1961, failure.

    The mission objective was to make highly elliptical earth orbits near minimum three-body velocity
    for earth escape. Ranger I was injected into a parking orbit around earth. It was planned to inject
    the space vehicle from parking orbit by a velocity impulse of about 3200 m/sec into the desired tra-
    jectory. However, the actual velocity impulse was only 73 m/sec, which resulted in a low altitude
    earth orbit and caused the vehicle to re-enter the atmosphere after one week. During this time, the
    on-board instruments functioned flawlessly.

    The planned experiments and instruments for Rangers I and II are:

Subjects of Experiment	Instruments and Measurements
Fields, charged particles and solar X-rays	Electrostatic analyzer for solar plasma
	Semiconductor detectors and thin-walled Geiger-Mueller counter

Subjects of Experiment	Instruments and Measurements
	Ionization chamber
	Triple-coincidence telescopes
	Rn vapor magnetometer
	X-ray scintillation detectors
Hydrogen geocorona	Lyman-alpha telescope
Interplanetary dust	Micrometeorite composite detectors

14. Ranger II (U.S.), 18 November 1961, failure.

Ranger II had the same mission objectives and on-board instruments as Ranger I. Its injection rocket from earth parking orbit failed and it re-entered the earth's atmosphere after 9 hr.

15. Ranger III (U.S.), 26 January 1962, partial success.

The mission of Rangers III, IV and V was to impact the moon to land a scientific package.

Ranger III used an earth parking orbit. However, the injection velocity was too high. Pericynthion was reached 51 hr after launch. The lunar distance at that time was 36,785 km and the selenocentric velocity was 1872 m/sec. It continued into a solar orbit with the following characteristics:

Period $= 406\overset{d}{.}4$

Perihelion distance $= 147.12 \times 10^6$ km $= 0.9839$ AU

Aphelion distance $= 173.90 \times 10^6$ km $= 1.163$ AU

The mission objectives and experiments planned for Rangers III, IV and V were to:

(1) Collect γ-ray data in flight and in the vicinity of the moon.

(2) Relay to earth, by a vidicon TV camera, photos of the lunar surface.

(3) Place an instrumented transmitting capsule containing a seismometer on the lunar surface to relay seismic data to earth.

(4) Determine the radar reflectivity of the moon by a radar altimeter.

(5) Develop spacecraft and space flight technology.

The weight of Rangers III, IV and V was in the vicinity of 3000 newtons.

16. Ranger IV (U.S.), 23 April 1962, partial success.

Ranger IV was launched at 2050 UT, 23 April 1962, and impacted on the moon at 1250 UT, 26 April 1962, after a flight time of 63 hr. It failed to perform any of its planned experiments.

17. Ranger V (U.S.), 18 October 1962, failure.

The space vehicle was launched at 1659 UT. Ranger V had a power failure 8^h46^m after launch, and it missed the moon by 725 km on 21 October, continuing into a solar orbit. The Ranger program was temporarily halted for a program review in view of the fact that 5 firings were either failures or, at best, partial successes.

E. REFERENCES

1. "Orbital Flight Handbook," ER 12684, Martin Company, Space Systems Division, (Baltimore), 1963.

2. Herrick, S., Baker, R.M.L., Jr. and Hilton, C. G., "Gravitational and Related Constants for Accurate Space Navigation," Eighth International Astronautical Congress, Barcelona, 1957 (Proceedings), Springer Verlag (Vienna), 1958, pp 197 to 235.

3. Makemson, M. W., Baker, R.M.L., Jr. and Westrom, G. B., "Analysis and Standardization of Astrodynamic Constants," Journal of Astronautical Sciences, Vol. 8, No. 1, Spring 1961, pp 1 to 13.

4. Kaula, W. M., "A Geoid and World Geodetic System Based on a Combination of Gravimetric, Astrogeodetic, and Satellite Data," Journal of Geophysics Res. Vol. 66, June 1961, pp 1799 to 1811; also NASA Technical Note TN D-702, May 1961.

5. Krause, H. G. L., "On a Consistent Set of Astrodynamic Constants," George C. Marshall Space Flight Center Report MTP-P & VE-F 62-12 (NASA) (Huntsville, Alabama), 1963.

6. "American Ephemeris and Nautical Almanac," published annually by the Nautical Almanac Office, United States Naval Observatory, Washington, D. C. (obtainable from the Superintendent of Documents, U. S. Government Printing Office, Washington 25, D. C.).

7. Ehricke, K. A., "Space Flight," Van Nostrand (Princeton, New Jersey), 1960.

8. deSitter, W. and Brouwer, D., "On the System of Astronomical Constants," Bulletin of the Astronomical Institutes of the Netherlands, Vol. VIII, No. 307, 8 July 1938, pp 213 to 231.

9. Alexandrov, I., "The Lunar Gravitational Potential," Advances in the Astronautical Sciences, Vol. 5, Plenum Press, New York, 1960, pp 320 to 324.

10. Baker, R.M.L., Jr. and Makemson, M. W., "An Introduction to Astrodynamics," Academic Press (New York), 1960.

11. Jeffreys, H., "The Earth, Its Origin, History, and Physical Constitution," Fourth ed., Cambridge University Press, 1959.

12. Townsend, G. E., "Analysis of Heliocentric, Planetocentric, Geocentric and Selenocentric Constants," ER 12201, Martin Company, Space Systems Division (Baltimore), June 1962.

13. Jaffe, L. D. and Rittenhouse, J. B., "Behavior of Materials in Space Environments," ARS Journal, Vol. 32, No. 3, March 1962, pp 320 to 345.

14. Nicolet, M., "Density of the Heterosphere Related to Temperature," SAO Special Report No. 75, Smithsonian Astrophysical Observatory (Cambridge, Massachusetts), 1961.

15. Johnson, F. S., editor, "Satellite Environment Handbook," Stanford University Press (Stanford, California), 1961.

16. Wilkins, H. P. and Moore, P., "The Moon," Macmillan (New York, 1955.

17. Blagg, M. A. and Saunder, S. A., "Collated List of Lunar Formations Named or Lettered in the Maps of Neison, Schmidt, Mädler," Lunar Nomenclature Committee of the International Association of Academies, 1913, p 196.

18. Blagg, M. A. and Müller, K., "Named Lunar Formations," International Astronomical Union, 1935.

19. Bobrovnikoff, N. T., "Natural Environment of the Moon," WADC Phase Technical Note 847-3, Wright Air Development Center (Dayton, Ohio), June 1959, ASTIA Document No. AD 242177.

20. Fielder, G., "Structure of the Moon's Surface," Pergamon Press (New York), 1961.

21. Firsoff, V. A., "Surface of the Moon, Its Structure and Origin," Hutchinson and Company, Ltd. (London), 1961.

22. Allen, C. W., "Astrophysical Quantities" (London), 1955.

23. Muncey, R. W., "Calculation of Lunar Temperature," Nature, Vol. 181, 24 May 1958, pp 1458 to 1459.

24. Mezger, P. S. and Strassl, H., "The Thermal Radiation of the Moon at 1420 MC/S," Planetary and Space Science, Vol. 1, 1959, pp 213 to 226.

25. Geoffrion, A. R., Korner M. and Sinton, W. M., "Isothermal Contours of the Moon," Lowell Observatory Bulletin No. 106, 1960.

26. Valley, S. L., editor, "Space and Planetary Environments," AFCRL-62-270, Air Force Surveys in Geophysics No. 139, GRD Air Force Cambridge Research Laboratories (Bedford, Massachusetts), January 1962.

27. Pettit, E. and Nicholson, S. B., "Lunar Radiation Temperatures," Astrophysical Journal, Vol. 71, 1930, p 102, and Astrophysical Journal, Vol. 91, 1940, p 408.

28. Gold, Q., "Dust on the Moon," Vistas in Astronautics, Vol. 2, 1959, pp 261 to 266.

29. Whipple, F. L., "On the Lunar Dust Layer," Vistas in Astronautics, Vol. 2, 1959, pp 267 to 272.

30. Roche, R. A., "The Importance of High Vacuum in Space Environment Simulation," Vistas in Astronautics, Vol. 2, 1959, pp 22 to 27.

31. Sytinskaya, N. N., "Probable Dimensions of Microfeatures of the Lunar Surface," ARS Journal (Russian Supplement), Vol. 32, No. 3, March 1962, pp 488 and 489.

32. Jeans, J., "Dynamical Theory of Gases," Dover Publications, Inc., 1954.

33. Russell, H. N., Dugan, R. S. and Stewart J. Q., "Astronomy," Ginn and Company, 1945.

34. Lipski, Y. N., "On the Existence of a Lunar Atmosphere," Dokl Akad. Nauk., Vol. 65, 1949, pp 465 to 468.

35. Lyot, B. and Dollfus, A., "Recherche d'une Atmosphére au Voisinage de la Lune," Comptes Rendus d'Academie de Science, Vol. 229, 1949, pp 1277 to 1280.

36. Dollfus, A., "Nouvelle, Recherche d'une Atmosphére au Voisinage de la Lune," Comptes Rendus d'Academie de Science, Vol. 234, 1952, pp 2046 to 2049.

37. Elsmore, B. and Whitfield, G. R.,"Lunar Occultation of a Radio Star and the Derivation of an Upper Limit for the Density of the Lunar Atmosphere," Nature, Vol. 176, 1955, pp 457 to 458.

38. Costain, C. H., Elsmore, B. and Whitfield, G. R., "Radio Observations of a Lunar Occultation of the Crab Nebula," Monthly Notices of the Royal Astronomical Society, Vol. 116, 1956, pp 380 to 385.

39. Öpik, E. J. and Singer, S. F., "Escape of Gases from the Moon," Journal of Geophysical Research, Vol. 65, 1960, pp 3065 to 3070.

40. Kozyrev, N. A., "Observations of a Volcanic Process on the Moon," Sky and Telescope, Vol. 18, 1959, pp 184 to 186.

41. Judson, L. V., "Units of Weight and Measure (United States Customary and Metric), Definitions and Tables of Equivalents," National Bureau of Standards Miscellaneous Publications 233 (Washington), December 20, 1960.

42. Green, M. H., "International and Metric Units of Measurement," Chemical Publishing Company, Inc. (New York), 1961.

43. "Astrolog--Current Status of U.S. Missile and Space Programs Plus All Orbiting Satellites," Missiles and Rockets, Vol. 11, No. 10, 3 September 1962, pp 19 to 30.

44. Stafford, W. H. and Croft, R. M., "Artificial Earth Satellites and Successful Solar Probes, 1957 to 1960," NASA Technical Note TN D-601, March 1961.

45. Cummings, C. I., et al., "The Ranger Program," JPL Technical Report 32-141, Jet Propulsion Laboratory (Pasadena, California), September 1961.

46. Kuiper, G. and Middlehurst, B. M., editors, "Planets and Satellites," University of Chicago Press (Chicago), 1961.

ILLUSTRATIONS

LIST OF ILLUSTRATIONS

Fig. 1. Inner Van Allen Belt Proton Flux and Initial
Portions of a Typical Lunar Trajectory
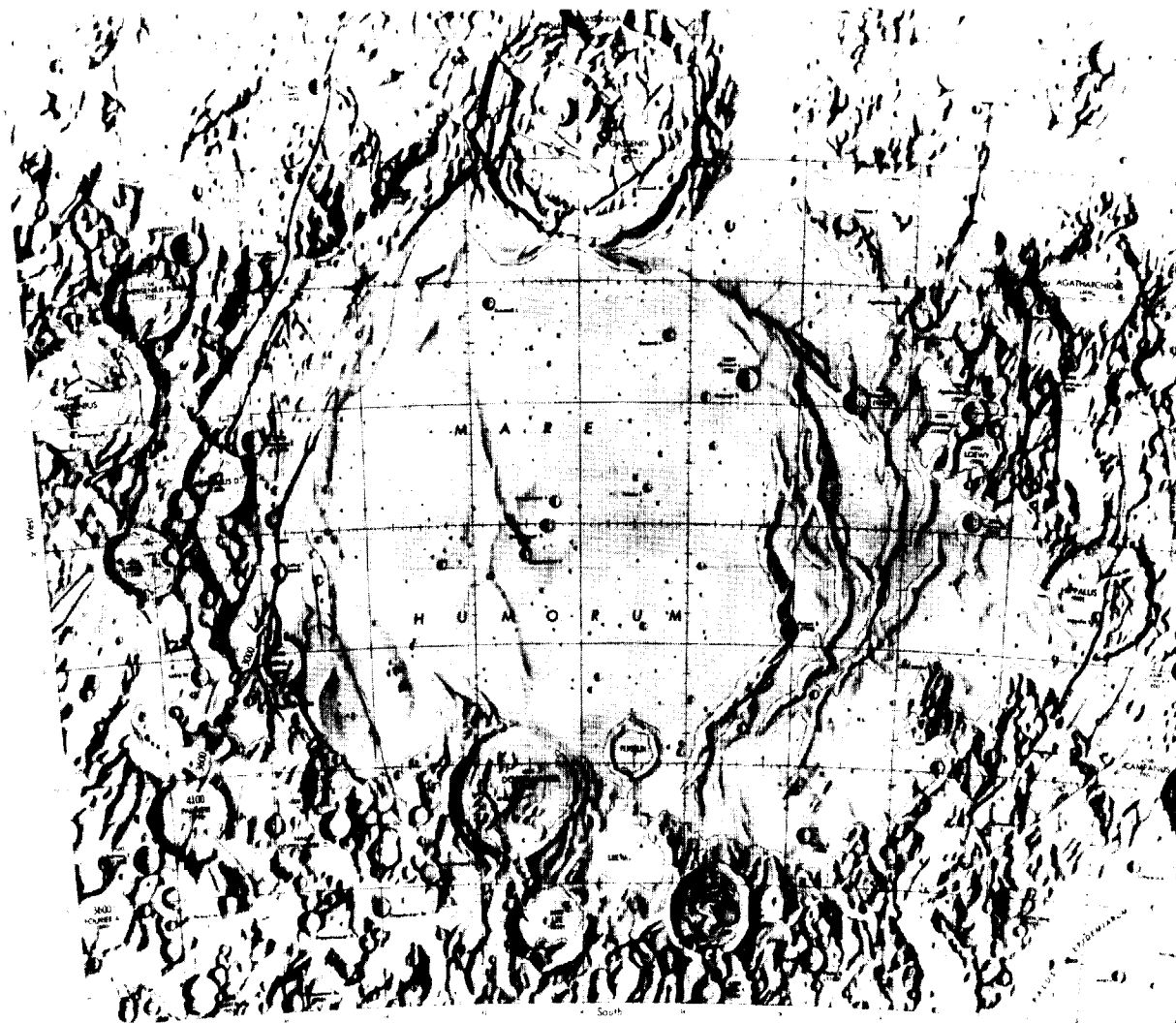
Fig. 2.   Lunar Chart Of The Mare Humorum Region

Fig. 3. Estimate Of Average Lunar Surface Temperatures

Lunar time

Midnight   Sunrise   Noon   Sunset   Midnight

Equator
0
25° Latitude
45°
55°
68°
80°

TEMPERATURE (°K)

TEMPERATURE (°F)

EARTH DAYS
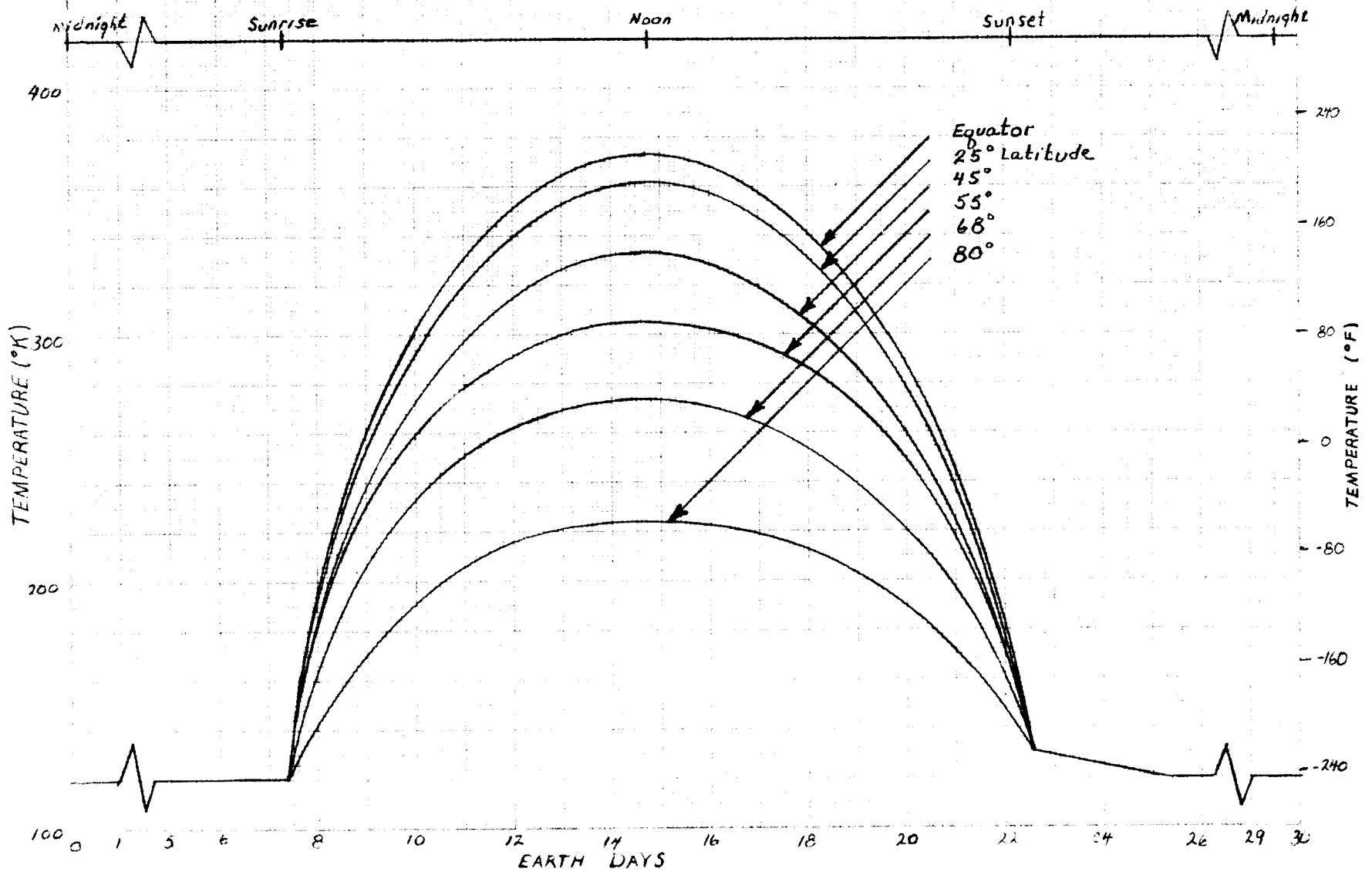
CHAPTER III

THE EARTH-MOON SYSTEM

Prepared by:

F. O. Martikan, F. Santora, and R. Salinger
Martin Company (Baltimore)
Aerospace Mechanics Department
March 1963

This chapter is an introduction to the kinematics and dynamics of the earth-moon system. This introduction is necessary before any actual trajectory programs or trajectories can be discussed, in order to present a clear understanding of the geometry, the various coordinate systems, the vocabulary and previous work in celestial mechanics peculiar to the earth-moon system.

Section A introduces coordinate systems useful for various aspects of earth to moon flight such as tracking, motion in space, guidance, lunar reconnaissance and attitude control. Emphasis is placed on the selenographic or moon-centered rotating coordinate system and transformation from geocentric or earth-centered inertial to selenographic coordinates. A list of current lunar maps is also given. Section B introduces the classical three-body and restricted three-body problems of astronomy and their application to the dynamical system of the earth, moon, and space vehicle. Valuable qualitative as well as quantitative trajectory information can be obtained from the restricted three-body problem. However, the application of the restricted three-body problem to the classification of lunar missions and its adaptation for trajectory calculations will be deferred to Chapter IV. Section C discusses the very complex motion of the moon, some theories used to find this motion, and the adaptation of these theories in generating lunar ephemerides for observations and simulation of the moon in accurate trajectory computer programs.

A. GEOMETRY AND COORDINATE SYSTEMS

In the description of the motion of the moon and of vehicles in the earth-moon space many different coordinate systems have been employed depending on the particular problem of motion to be solved. Several coordinate systems are used in lunar flight problems since several different disciplines such as geography, astronomy, aerodynamics, kinematics, dynamics, and numerical analysis enter into the problem with each discipline having evolved its own techniques and sets of coordinates. Some of the more commonly employed coordinate systems are described in the following pages according to their origin of coordinates, the principal directions and the fundamental plane; transformation equations between the major systems are given. The coordinate systems are further classified into (1) earth-centered coordinates, (2) selenographic coordinates, (3) trajectory coordinates, and (4) vehicle-centered coordinates.

Before a detailed discussion of the various coordinate systems is attempted, some basic definitions of the principal time systems will be given since time usually enters the description of motion or observation of celestial bodies and space vehicles as the independent variable. The fundamental time unit is the sidereal day, or the period of revolution of the earth about its axis with respect to the stars. This time system is known as sidereal time (ST). Mean solar time (MST) or civil time is defined with respect to the position of a fictitious mean sun which moves uniformly along the equator and hence is a function of the earth's rotation and its orbital motion as well. The difference between mean solar time and apparent solar time, the latter being based on the apparent position of the sun, never exceeds 16 minutes. Universal time (UT), sometimes referred to as Greenwich mean time, is the mean solar time referred to the Greenwich (prime) meridian. However, the above listed clock times reflect the variability in the rotational rate of the earth due to tidal friction and irregularities from unknown sources. A uniform mathematical time which is defined by the apparent annual motion of the sun in true orbital longitude rather than the rotation of the earth, is the ephemeris time (ET) or Newtonian time. The mathematical theory of ephemeris time has been developed, and the values

$$\Delta T = ET - UT \qquad (1)$$

are given in the American Ephemeris (Ref. 1), which is published annually, or in the Explanatory Supplement (Ref. 2) up to the year of publication. The fundamental epoch from which ephemeris time is measured is 1900 January 0, Greenwich mean noon in UT which is simultaneously 1900 January 0, 12^h ET in ET. At that instant $\Delta T \equiv 0$. From past observations ΔT is approximately $+35^s$ in 1962 and the change in ΔT is generally less than 1^s between years (Ref. 1, page vii). A discussion of time systems is given in Ref. 3.

1. Earth-Centered Coordinates

a. Geographic system

The origin of the geographic coordinate system is the earth's center and the fundamental plane is the equatorial plane. Longitude λ is measured either east or west from the Greenwich (prime) meridian and the geocentric latitude ϕ' is the angle measured along a meridian from the equatorial plane, positive if north and negative if south of the equatorial plane. The local radius of the earth, R_ϕ, is the third spherical coordinate. (See following sketch.)

The latitude used on maps is the geodetic latitude ϕ which is defined as the angle between the equatorial plane and a normal to the reference ellipsoid which most nearly describes the mean sea level surface of the earth. The greatest difference between ϕ' and ϕ is approximately 0.19° at $\phi' = 45°$. In addition, there is an astronomical latitude ϕ^* which is the angle between the local vertical (as determined by the local gravitational field and affected by the centrifugal force) and the equatorial plane. The difference between ϕ and ϕ^* is called "station error" and is usually negligible. The geographic coordinate system is not an inertial one since it rotates around the earth's axis z_G at a constant angular velocity $\vec{\omega}_\oplus$. A

rectangular geographic coordinate system with origin at the center of the earth has its x_G-axis in the direction of $\lambda = 0$, $\phi = 0$, the z_G-axis toward the north pole, and the y_G-axis completing the right-handed coordinate system in the equatorial plane.
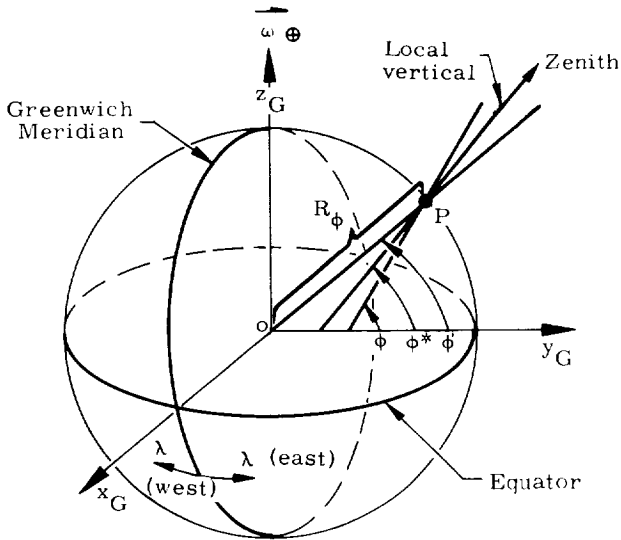

b. Topocentric system

Electronic and optical observations of space vehicles will be generally made from the surface of the earth. It is therefore advantageous to define a topocentric or local coordinate system with origin at the observer and the plane of the horizon as the fundamental plane. The x_h-axis of the rectangular topocentric system is directed to the south (unit vector $\hat{x}_h$), the y_h-axis is directed to the east (unit vector $\hat{y}_h$), and the z_h-axis is directed to the astronomical zenith (unit vector $\hat{z}_h$). The astronomical zenith $\hat{z}_h$ is in the direction of the local vertical and the horizon is a plane perpendicular to z_h. The azimuth, A, is defined as the angle from north measured positive clockwise in the horizon plane and the elevation, ϵ, as the angle measured from this plane toward the zenith. The range r_P, or distance from the observer to the vehicle, is the third spherical coordinate (see the following sketch). The topocentric system is not inertial since it rotates with the earth.

c. Equatorial system

The origin is generally taken at the earth's center and the fundamental plane is the true equatorial plane of the earth. The $x'_\oplus$-axis is directed toward the true vernal equinox (unit vector $\hat{x}'_\oplus$)
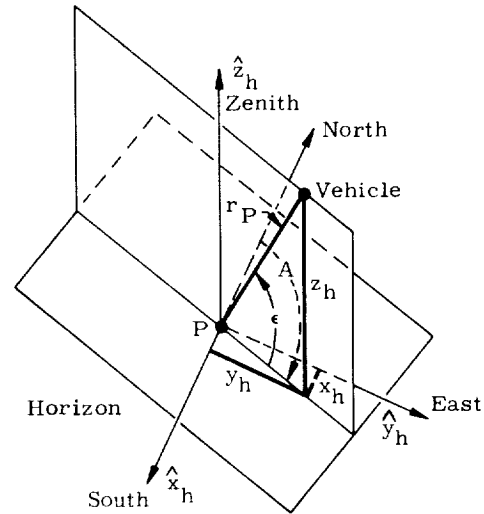
the $z'_\oplus$-axis directed toward the north celestial pole (unit vector $\hat{z}'_\oplus$) and the $y'_\oplus$-axis directed so as to form a right-handed coordinate system (unit vector $\hat{y}'_\oplus$). Since the equator and the vernal equinox are not inertially fixed due to the precession and nutation of the earth's axis, the "equator and equinox" of a certain date should be specified in precision work. The true equinox takes into account the nutation and precession of the earth while the mean equinox ignores the nutation. Define a coordinate system $x_\oplus$, $y_\oplus$, $z_\oplus$ with the same origin as the $x'_\oplus$, $y'_\oplus$, $z'_\oplus$ system, except that the $x_\oplus$-axis points toward the mean equinox and $x_\oplus y_\oplus$-plane is the mean equatorial plane of the earth (see following sketch).
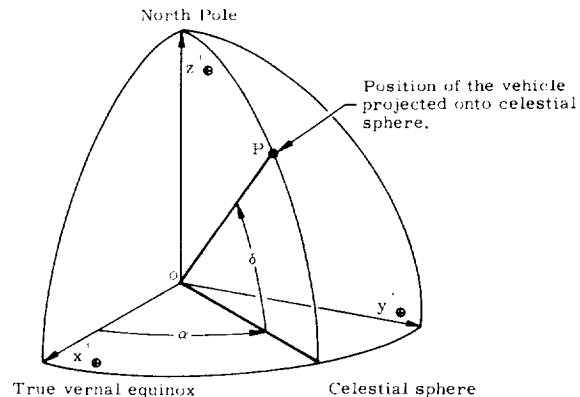

α = right ascension, measured east from the true vernal equinox along the celestial equator. The right ascension may be measured either in degrees or hours (1 hr = 15°).

δ = declination, measured from the true celestial equator to the radius vector of object, positive toward the north, negative toward the south.

In Ref. 1 the coordinates are usually referred to the mean equator and equinox of the beginning of the appropriate year. For the case of the sun, the celestial longitude referred to the true equator and equinox of a certain date is not given but is obtained by applying a reduction factor, which is tabulated in the Ephemeris, to the celestial longitude referred to the mean equinox and equator of the same date. This reduction is the sum of the precession in longitude from the beginning of the year to date, the nutation in longitude and the correction for aberration. For a definition of celestial longitude see the next coordinate system. A standard reference for the mean equator and equinox used for comparison of data from various sources is 1950.0.

d. Ecliptic system

The origin is generally taken as the earth's center and the fundamental plane is the ecliptic, or plane of the earth's orbit around the sun. The x_ϵ-axis is directed to the true vernal equinox (unit vector $\hat{x}_\epsilon$), the z_ϵ-axis is directed along the normal to the ecliptic plane (unit vector $\hat{z}_\epsilon$), and the y_ϵ-axis is directed so as to form a right-handed coordinate system (unit vector $\hat{y}_\epsilon$) (see the following sketch).
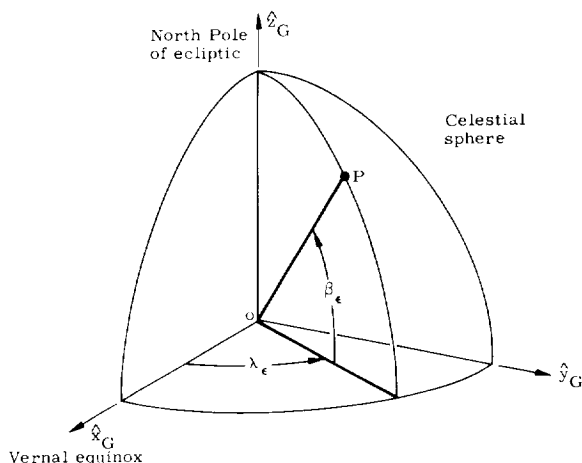
λ_ϵ = celestial longitude, measured positive east along the ecliptic from the true vernal equinox

β_ϵ = celestial latitude, measured from the ecliptic to the radius vector of the object

The equatorial and ecliptic coordinate systems are defined in terms of directions from a particular origin and not by the origin itself, which may be taken at the earth's center, the sun's center, the moon's center, or translated anywhere. We introduce a double subscript notation to define the coordinate system as well as the origin. If the origin of the ecliptic and equatorial coordinate systems is taken at the center of the earth, then there is a single subscript "$\oplus$" or "ϵ". However, if the origin is taken at the center of the moon, for instance, then we use two subscripts separated by a comma "$\oplus$, $\mathbb{C}$" or "ϵ, $\mathbb{C}$", respectively. A

double subscript without the comma indicates the position of the object denoted by the second subscript in the coordinate system of the first. If the origin of the coordinate system has been translated to another place, then a third subscript will denote the object whose position is given. Thus $r_{\oplus \Delta}$ is the distance of the vehicle from the center of the earth in a geocentric equatorial coordinate system while $r_{\oplus, \mathbb{C} \to \Delta}$ is the distance of the vehicle from the center of the moon in a selenocentric equatorial system.

Transformations between the various earth-centered coordinate systems will not be given here since this subject is treated more properly in Chapter XI of Ref. 3.
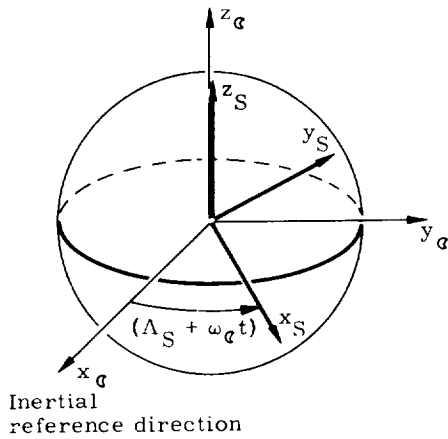
2. Selenographic Coordinate System

a. Definitions

The selenographic coordinate system is fixed with respect to the moon and rotates with it. The north pole of the moon is toward the direction of the lunar angular velocity vector $\vec{\omega}_{\mathbb{C}}$, and the lunar equatorial plane is perpendicular to $\vec{\omega}_{\mathbb{C}}$. Selenographic latitude $\phi_{\mathbb{C}}$ is measured from the lunar equator, positive toward the north, i.e., in the hemisphere containing Mare Serenitatis, and negative toward the south. Selenographic longitude $\lambda_{\mathbb{C}}$ is measured east and west from the lunar prime meridian $\lambda_{\mathbb{C}} = 0$ which passes through the mean center point of the moon. East, or the positive direction for $\lambda_{\mathbb{C}}$, is toward the hemisphere containing Mare Crisium. The mean center of the lunar disk is the point on the lunar surface intersected by the moon-earth line if the moon is at the mean ascending node when the node coincides either with the mean perigee or mean apogee. It is located in the Sinus Medii, a specified distance from the crater Mösting A (see Fig. 1). Orientation of these cardinal directions for astronautical calculations is in accordance with a resolution adopted by the International Astronomical Union general assembly, 1961. Sometimes, notably in the American Ephemeris (Ref. 1), $\lambda_{\mathbb{C}}$ is measured eastward from the prime meridian through 360°. For the primary purpose of astronomical observations, longitude on the moon is sometimes measured from the lunar prime meridian positive toward the west through 360°.

The axes in the selenographic coordinate system are designated by x_S, y_S, z_S with origin at the center of the moon. The z_S-axis points to the north pole of the moon's equatorial plane. The x_S- and y_S-axes lie in the moon's equatorial plane, the x_S-axis being directed to the lunar prime meridian and y_S completing the right-handed coordinate system. Unit vectors $\hat{x}_S$, $\hat{y}_S$, $\hat{z}_S$ are defined in the direction of the x_S-, y_S- and z_S axes.

b. Transformation from lunar equatorial to selenographic coordinates

In addition it is useful to define a selenocentric lunar equatorial coordinate system which does not rotate with the moon. The axes in this system are designated by $x_{\mathbb{C}}$, $y_{\mathbb{C}}$, $z_{\mathbb{C}}$ with origin at the center of the moon. The $z_{\mathbb{C}}$- and z_S-axes coincide. The $x_{\mathbb{C}}$-axis is in the moon's equatorial plane directed toward an inertial reference direction which will be specified each time this coordinate system is used, and the $y_{\mathbb{C}}$-axis completes the right-handed coordinate system. (See following sketch.)

Inertial
reference direction

If the angle between the $x_{\mathbb{C}}$- and x_S-axes at time $t = 0$ is Λ_S, then at any subsequent time t it will be $(\Lambda_S + \omega_{\mathbb{C}} t)$. Hence the transformation from selenocentric lunar equatorial to selenographic coordinates is given by

$$
\begin{Bmatrix} x_S \\ y_S \\ z_S \end{Bmatrix} = \begin{bmatrix} \cos(\Lambda_S + \omega_{\mathbb{C}} t) & \sin(\Lambda_S + \omega_{\mathbb{C}} t) & 0 \\ -\sin(\Lambda_S + \omega_{\mathbb{C}} t) & \cos(\Lambda_S + \omega_{\mathbb{C}} t) & 0 \\ 0 & 0 & 1 \end{bmatrix} \begin{Bmatrix} x_{\mathbb{C}} \\ y_{\mathbb{C}} \\ z_{\mathbb{C}} \end{Bmatrix}
$$

$$
= \begin{bmatrix} T(\Lambda_S + \omega_{\mathbb{C}} t) \end{bmatrix} \begin{Bmatrix} x_{\mathbb{C}} \\ y_{\mathbb{C}} \\ z_{\mathbb{C}} \end{Bmatrix} \tag{2}
$$

and the inverse transformation is:

$$
\begin{Bmatrix} x_{\mathbb{C}} \\ y_{\mathbb{C}} \\ z_{\mathbb{C}} \end{Bmatrix} = \begin{bmatrix} \cos(\Lambda_S + \omega_{\mathbb{C}} t) & -\sin(\Lambda_S + \omega_{\mathbb{C}} t) & 0 \\ \sin(\Lambda_S + \omega_{\mathbb{C}} t) & \cos(\Lambda_S + \omega_{\mathbb{C}} t) & 0 \\ 0 & 0 & 1 \end{bmatrix} \begin{Bmatrix} x_S \\ y_S \\ z_S \end{Bmatrix}
$$

$$
= \begin{bmatrix} T(\Lambda_S + \omega_{\mathbb{C}} t) \end{bmatrix}^{-1} \begin{Bmatrix} x_S \\ y_S \\ z_S \end{Bmatrix} \tag{3}
$$

The origin of the lunar equatorial system in the present case was taken at the center of the moon, but it may be translated anywhere just as in the equatorial and ecliptic coordinate systems (subsection 1c and 1d)

c. Rotation from equatorial to selenographic coordinates

The rotation from selenocentric equatorial coordinates $x'_{\oplus,\mathbb{C}}$, $y'_{\oplus,\mathbb{C}}$, $z'_{\oplus,\mathbb{C}}$, to selenographic coordinates x_S, y_S, z_S consists of a rotation about $z'_{\oplus,\mathbb{C}}$ through the angle Ω', a rotation about $\mathbb{C} N$ through the angle $i_{\mathbb{C}}$, and finally a rotation about $\hat{z}_S$ through the angle Λ_M (see following sketch). A further rotation to an inertial coordinate system $x_{\oplus,\mathbb{C}}$, $y_{\oplus,\mathbb{C}}$, $z_{\oplus,\mathbb{C}}$ with the x-axis directed to the mean equinox of date or to the mean equinox at epoch (a specified date) may be performed, but the difference between true equinox and mean equinox of date or of a recent epoch is small and can usually be neglected in preliminary design work.

The rotations are defined by the following matrix equation:

$$
\begin{Bmatrix} x_S \\ y_S \\ z_S \end{Bmatrix} = \begin{bmatrix} \cos \Lambda_M & \sin \Lambda_M & 0 \\ -\sin \Lambda_M & \cos \Lambda_M & 0 \\ 0 & 0 & 1 \end{bmatrix} \cdot \begin{bmatrix} 1 & 0 & 0 \\ 0 & \cos i_{\mathbb{C}} & \sin i_{\mathbb{C}} \\ 0 & -\sin i_{\mathbb{C}} & \cos i_{\mathbb{C}} \end{bmatrix}
$$

$$
\cdot \begin{bmatrix} \cos \Omega' & \sin \Omega' & 0 \\ -\sin \Omega' & \cos \Omega' & 0 \\ 0 & 0 & 1 \end{bmatrix} \begin{Bmatrix} x'_{\oplus,\mathbb{C}} \\ y'_{\oplus,\mathbb{C}} \\ z'_{\oplus,\mathbb{C}} \end{Bmatrix} \tag{4}
$$

$$
= \begin{bmatrix} T(\Lambda_M) \end{bmatrix} \cdot \begin{bmatrix} T(i_{\mathbb{C}}) \end{bmatrix} \cdot \begin{bmatrix} T(\Omega') \end{bmatrix} \cdot \begin{Bmatrix} x'_{\oplus,\mathbb{C}} \\ y'_{\oplus,\mathbb{C}} \\ z'_{\oplus,\mathbb{C}} \end{Bmatrix}
$$

and the transformation to unit vectors in the selenographic coordinate system can be obtained by matrix multiplication and replacing the coordinates by unit vectors in the coordinate directions:

$$
\hat{x}_S = \hat{x}'_{\oplus,\mathbb{C}} (\cos \Lambda_M \cos \Omega' - \sin \Lambda_M \sin \Omega' \cos i_{\mathbb{C}}
$$
$$
+ \hat{y}'_{\oplus,\mathbb{C}} (\cos \Lambda_M \sin \Omega' + \sin \Lambda_M \cos \Omega' \cos i_{\mathbb{C}})
$$
$$
+ \hat{z}'_{\oplus,\mathbb{C}} (\sin \Lambda_M \sin i_{\mathbb{C}}) \tag{5}
$$

$$\hat{y}_S = \hat{x}'_{\oplus,\mathbb{C}} (-\sin \Lambda_M \cos \Omega'$$
$$- \cos \Lambda_M \sin \Omega' \cos i_{\mathbb{C}})$$
$$+ \hat{y}'_{\oplus,\mathbb{C}} (-\sin \Lambda_M \sin \Omega'$$
$$+ \cos \Lambda_M \cos \Omega' \cos i_{\mathbb{C}})$$
$$+ \hat{z}'_{\oplus,\mathbb{C}} (\cos \Lambda_M \sin i_{\mathbb{C}})$$

$$\hat{z}_S = \hat{x}'_{\oplus,\mathbb{C}} (\sin \Omega' \sin i_{\mathbb{C}})$$
$$+ \hat{y}'_{\oplus,\mathbb{C}} (-\cos \Omega' \sin i_{\mathbb{C}}) + \hat{z}'_{\oplus,\mathbb{C}} \cos i_{\mathbb{C}}$$

(5)

The inverse rotation from x_S, y_S, z_S coordinates to $x'_{\oplus,\mathbb{C}}$, $y'_{\oplus,\mathbb{C}}$, $z'_{\oplus,\mathbb{C}}$ coordinates is given by the inverse of the product of the transformation matrices, which in turn is the product of the inverses of the individual matrices in reverse order:

$$\begin{Bmatrix} x'_{\oplus,\mathbb{C}} \\ y'_{\oplus,\mathbb{C}} \\ z'_{\oplus,} \end{Bmatrix} = \left[T^{-1}(\Omega') \right] \cdot \left[T^{-1}(i_{\mathbb{C}}) \right] \cdot \left[T^{-1}(\Lambda_M) \right] \begin{Bmatrix} x_S \\ y_S \\ z_S \end{Bmatrix}$$

(6)

$$= \begin{bmatrix} \cos \Omega' & -\sin \Omega' & 0 \\ \sin \Omega' & \cos \Omega' & 0 \\ 0 & 0 & 1 \end{bmatrix} \cdot \begin{bmatrix} 1 & 0 & 0 \\ 0 & \cos i_{\mathbb{C}} & -\sin i_{\mathbb{C}} \\ 0 & \sin i_{\mathbb{C}} & \cos i_{\mathbb{C}} \end{bmatrix}$$
$$\cdot \begin{bmatrix} \cos \Lambda_M & -\sin \Lambda_M & 0 \\ \sin \Lambda_M & \cos \Lambda_M & 0 \\ 0 & 0 & 1 \end{bmatrix} \begin{Bmatrix} x_S \\ y_S \\ z_S \end{Bmatrix}$$

(6)

The values of $i_{\mathbb{C}}$ and Ω' are tabulated to the nearest 0.001° in Ref. 1 for intervals of 10 days and referred to the true equator of the earth and equinox of date.

In order to carry out the transformations Eqs (4), (5) or (6), values of $\sin \Lambda_M$ and $\cos \Lambda_M$ are needed in terms of tabulated quantities. It is convenient to choose as the tabulated quantity the displacement of the earth-moon line from the mean center of the moon, or libration of the moon in longitude and latitude. This is given in Ref. 1 as the earth's selenographic longitude and latitude (ℓ, b) to the nearest 0°01, which represents 300 meters on the moon's surface. Librations will be discussed in detail in Section C-2 of the present chapter.

True vernal equinox

Moon's equatorial plane

Earth's equatorial plane

Moon's prime meridian
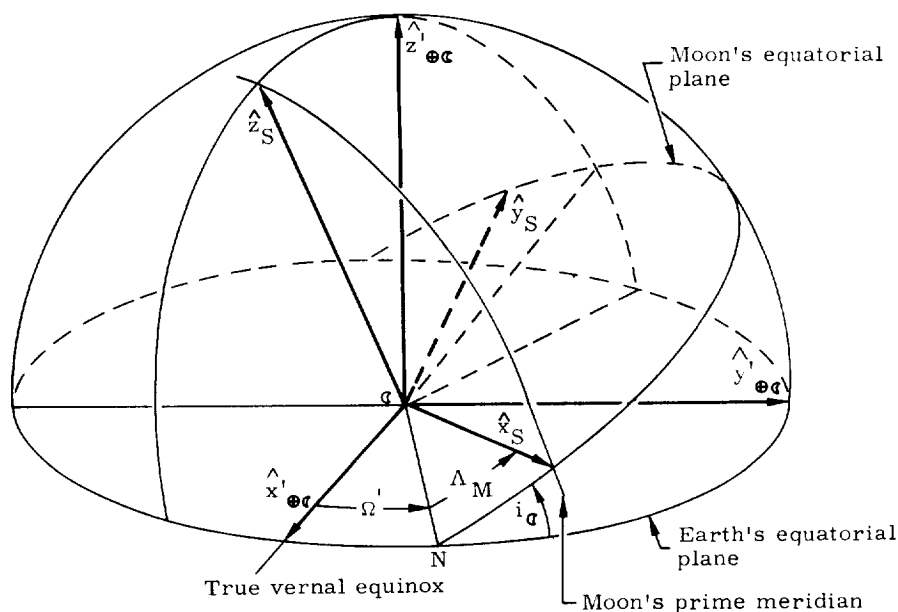
Ω' = right ascension of the moon's ascending node measured from the true equinox of date.

$i_{\mathbb{C}}$ = inclination of the lunar equator to the earth's equator.

Λ_M = angle in the lunar equatorial plane from the ascending node to the lunar prime meridian.

Let $\hat{L}$ be a unit vector along the earth-moon line. The components of $\hat{L}$ in the selenocentric equatorial coordinate system $x'_{\oplus,\mathbb{C}}$, $y'_{\oplus,\mathbb{C}}$, $z'_{\oplus,\mathbb{C}}$ are:

$$L_x = -\cos \delta \cos \alpha$$
$$L_y = -\cos \delta \sin \alpha \qquad (7)$$
$$L_z = -\sin \delta$$

where α is the right ascension of the moon and δ the declination of the moon. If the librations in longitude are ℓ and latitude b (see following sketch), then we obtain, by applying the law of cosines to the spherical triangle with sides b, ℓ, d, $\cos d = \cos b \cos \ell$ so that

$$\hat{x}_S \cdot \hat{L} = \cos d = \cos b \cos \ell \qquad (8)$$

$$\hat{y}_S \cdot \hat{L} = \cos b \sin \ell \qquad (9)$$

If we take the expression for $\hat{x}_S \cdot \hat{L}$ and $\hat{y}_S \cdot \hat{L}$ from Eqs (5) and (7), substitute it in Eqs (8) and (9) and simplify the results, then the following expressions for $\sin \Lambda_M$ and $\cos \Lambda_M$ in terms of tabulated quantities are obtained:

$$\sin \Lambda_M = \frac{\cos \ell}{\cos b}\left[\cos i_{\mathbb{C}} \cos \delta \sin (\Omega' - \alpha)\right.$$

$$\left. - \sin i_{\mathbb{C}} \sin \delta \right]$$
$$- \frac{\sin \ell}{\cos b}\left[\cos \delta \cos (\Omega' - \alpha)\right] \qquad (10)$$

$$\cos \Lambda_M = \frac{\sin \ell}{\cos b}\left[\cos i_{\mathbb{C}} \cos \delta \sin (\Omega' - \alpha)\right.$$

$$\left. - \sin i_{\mathbb{C}} \sin \delta\right]$$
$$- \frac{\cos \ell}{\cos b}\left[\cos \delta \cos (\Omega' - \alpha)\right] \qquad (11)$$

The right ascension α, declination δ and horizontal parallax, $\pi_{\mathbb{C}}$, of the moon are obtained from Ref. 1 and can be used to find the rectangular geocentric equatorial coordinates of the moon (see sketch on the following page).

Let the magnitude of $\vec{r}_{\oplus\mathbb{C}}$ be $r_{\oplus\mathbb{C}}$, then:

$$x'_{\oplus\mathbb{C}} = r_{\oplus\mathbb{C}} \cos \delta \cos \alpha$$
$$y'_{\oplus\mathbb{C}} = r_{\oplus\mathbb{C}} \cos \delta \sin \alpha$$
$$z'_{\oplus\mathbb{C}} = r_{\oplus\mathbb{C}} \sin \delta \qquad (12)$$

and $r_{\oplus\mathbb{C}}$ is found from the tabulated lunar horizontal parallax $\pi_{\mathbb{C}}$ by: $r_{\oplus\mathbb{C}} = \dfrac{R_e}{\pi_{\mathbb{C}}}$ where R_e is

Plane parallel to earth's equatorial plane

Earth-moon line

$\alpha - 180°$

Moon's prime meridian

True vernal equinox

Moon's equatorial plane
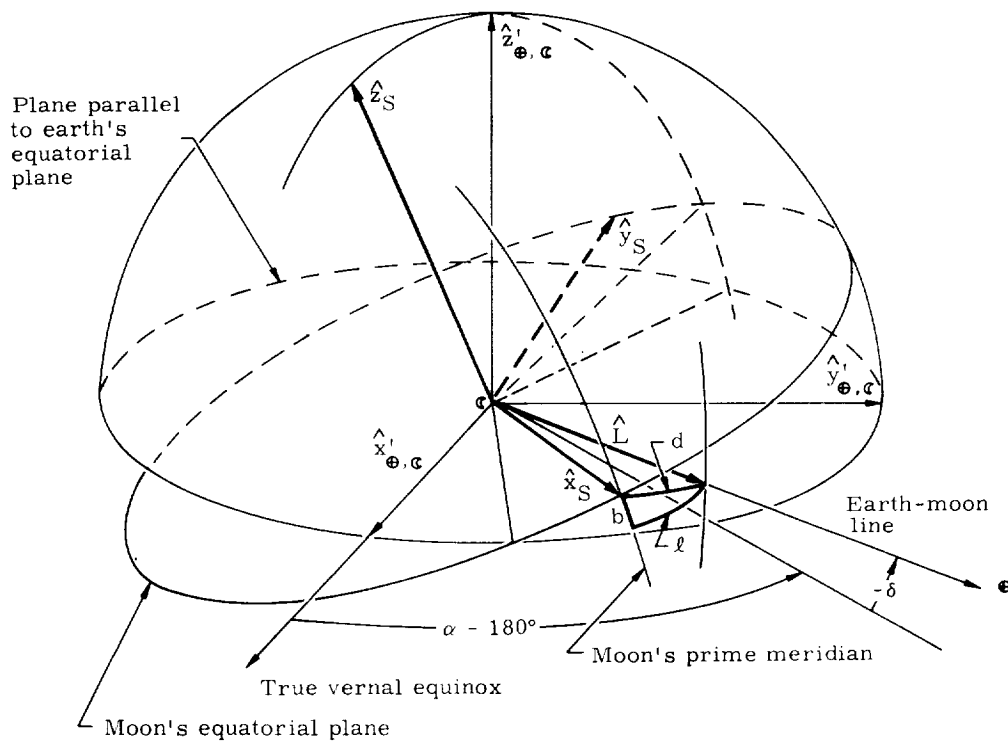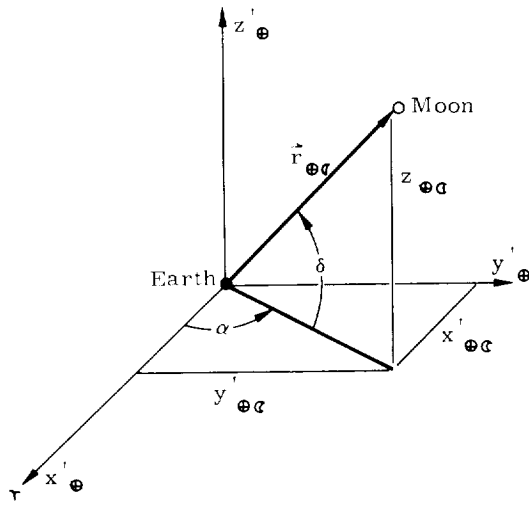
the earth's equatorial radius. By making the necessary substitutions for sin α, cos α, sin δ and cos δ Eqs (10) and (11) become:

$$\sin \Lambda_M = \frac{\cos \ell}{r_{\oplus\mathbb{C}} \cos b} \left[\cos i_{\mathbb{C}} (x'_{\oplus\mathbb{C}} \sin \Omega' \right.$$
$$\left. - y'_{\oplus\mathbb{C}} \cos \Omega') - z'_{\oplus\mathbb{C}} \sin i_{\mathbb{C}} \right]$$
$$+ \frac{\sin \ell}{r_{\oplus\mathbb{C}} \cos b} \left[x'_{\oplus\mathbb{C}} \cos \Omega' \right.$$
$$\left. + y'_{\oplus\mathbb{C}} \sin \Omega' \right] \qquad (13)$$

$$\cos \Lambda_M = \frac{\sin \ell}{r_{\oplus\mathbb{C}} \cos b} \left[\cos i_{\mathbb{C}} (x'_{\oplus\mathbb{C}} \sin \Omega' \right.$$
$$\left. - y'_{\oplus\mathbb{C}} \cos \Omega') - z'_{\oplus\mathbb{C}} \sin i_{\mathbb{C}} \right]$$
$$- \frac{\cos \ell}{r_{\oplus\mathbb{C}} \cos b} \left[x'_{\oplus\mathbb{C}} \cos \Omega' \right.$$
$$\left. + y'_{\oplus\mathbb{C}} \sin \Omega' \right] \qquad (14)$$

With sin Λ_M and cos Λ_M known, the rotations indicated by Eqs (4), (5) and (6) can be carried out. This transformation has also been discussed in Koskela (Ref. 4), Baker (Ref. 5) and Kalensher (Ref. 6).

d. Vehicle position in selenographic coordinates

The selenographic coordinate system has a nearly constant angular velocity $\vec{\omega}_{\mathbb{C}}$ about the z_S axis and its origin is translated by the vector $\vec{r}_{\oplus\mathbb{C}}$ from the origin of the geocentric equatorial system. Before the vehicle position can be given in the selenographic coordinate system, the following quantities are defined by reference to the following sketch:

The position vector of the vehicle in the geocentric equatorial system,

$$\vec{r}_{\oplus\Delta} = x'_{\oplus\Delta} \hat{x}'_{\oplus} + y'_{\oplus\mathbb{C}} \hat{y}'_{\oplus} + z'_{\oplus\mathbb{C}} \hat{z}'_{\oplus} \qquad (15)$$

The position vector of the center of the moon in the geocentric equatorial system,

$$\vec{r}_{\oplus\mathbb{C}} = x'_{\oplus\mathbb{C}} \hat{x}'_{\oplus} + y'_{\oplus\mathbb{C}} \hat{y}'_{\oplus} + z'_{\oplus\mathbb{C}} \hat{z}'_{\oplus} \qquad (16)$$

The position vector of the vehicle referred to the selenocentric equatorial coordinates, i.e., in equatorial coordinates translated to the center of the moon,

$$\vec{r}_{\oplus,\mathbb{C}\to\Delta} = x'_{\oplus,\mathbb{C}\to\Delta} \hat{x}'_{\oplus} + y'_{\oplus,\mathbb{C}\to\Delta} \hat{y}'_{\oplus}$$
$$+ z'_{\oplus,\mathbb{C}\to\Delta} \hat{z}'_{\oplus} \qquad (17)$$

The position vector of the vehicle in selenographic coordinates,

$$\vec{r}_{S\Delta} = x_{S\Delta} \hat{x}_S + y_{S\Delta} \hat{y}_S + z_{S\Delta} \hat{z}_S \qquad (18)$$

Note from the sketch below that

$$\vec{r}_{\oplus,\mathbb{C}\to\Delta} = \vec{r}_{\oplus\Delta} - \vec{r}_{\oplus\mathbb{C}} \qquad (19)$$

and

$$\vec{r}_{S\Delta} = \vec{r}_{\oplus,\mathbb{C}\to\Delta} \qquad (20)$$

The position of the vehicle in selenographic coordinates, $(x_{S\Delta}, y_{S\Delta}, z_{S\Delta})$, in terms of selenocentric equatorial coordinates, $(x'_{\oplus,\mathbb{C}\to\Delta}, y'_{\oplus,\mathbb{C}\to\Delta}, z'_{\oplus,\mathbb{C}\to\Delta})$, can be found by the rotation given in Eq (4)

True vernal equinox
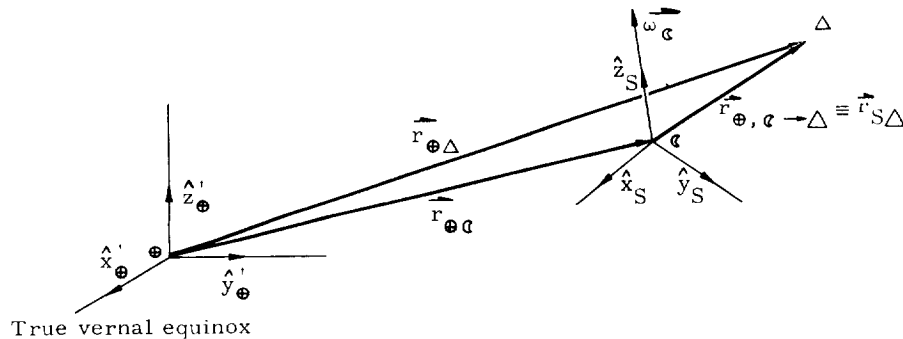
$$\begin{Bmatrix} x_{S\Delta} \\ y_{S\Delta} \\ z_{S\Delta} \end{Bmatrix} = \begin{bmatrix} T(\Lambda_M) \end{bmatrix} \cdot \begin{bmatrix} T(i_{\mathbb{C}}) \end{bmatrix} \cdot \begin{bmatrix} T(\Omega') \end{bmatrix} \begin{Bmatrix} x'_{\oplus,\mathbb{C}\to\Delta} \\ y'_{\oplus,\mathbb{C}\to\Delta} \\ z'_{\oplus,\mathbb{C}\to\Delta} \end{Bmatrix}, \quad (21)$$

and in terms of geocentric equatorial coordinates by use of Eqs (15) through (18):

$$\begin{Bmatrix} x_{S\Delta} \\ y_{S\Delta} \\ z_{S\Delta} \end{Bmatrix} = \begin{bmatrix} T(\Lambda_M) \end{bmatrix} \cdot \begin{bmatrix} T(i_{\mathbb{C}}) \end{bmatrix} \cdot \begin{bmatrix} T(\Omega') \end{bmatrix} \begin{Bmatrix} x'_{\oplus\Delta} - x'_{\oplus\mathbb{C}} \\ y'_{\oplus\Delta} - y'_{\oplus\mathbb{C}} \\ z'_{\oplus\Delta} - z'_{\oplus\mathbb{C}} \end{Bmatrix} \quad (22)$$

The matrix multiplication indicated by Eq (22) can be performed to yield the position of the vehicle in selenographic coordinates when the position of the vehicle and of the moon in geocentric equatorial coordinates as well as the parameters $i_{\mathbb{C}}$, Ω', Λ_M $(\alpha, \delta, \pi_{\mathbb{C}}, \ell, b)$ of the moon are known:

$$x_{S\Delta} = (x'_{\oplus\Delta} - x'_{\oplus\mathbb{C}})(\cos\Lambda_M \cos\Omega'$$
$$- \sin\Lambda_M \sin\Omega' \cos i_{\mathbb{C}}) + (y'_{\oplus\Delta}$$
$$- y'_{\oplus\mathbb{C}})(\cos\Lambda_M \sin\Omega' + \sin\Lambda_M \cos\Omega' \cos i_{\mathbb{C}})$$
$$+ (z'_{\oplus\Delta} - z'_{\oplus\mathbb{C}})(\sin\Lambda_M \sin i_{\mathbb{C}}) \quad (23)$$

$$y_{S\Delta} = (x'_{\oplus\Delta} - x'_{\oplus\mathbb{C}})(-\sin\Lambda_M \cos\Omega'$$
$$- \cos\Lambda_M \sin\Omega' \cos i_{\mathbb{C}}) + (y'_{\oplus\Delta}$$
$$- y'_{\oplus\mathbb{C}})(-\sin\Lambda_M \sin\Omega'$$
$$+ \cos\Lambda_M \cos\Omega' \cos i_{\mathbb{C}}) + (z'_{\oplus\Delta}$$
$$- z'_{\oplus\mathbb{C}})(\cos\Lambda_M \sin i_{\mathbb{C}}) \quad (24)$$

$$z_{S\Delta} = (x'_{\oplus\Delta} - x'_{\oplus\mathbb{C}})(\sin\Omega' \sin i_{\mathbb{C}})$$
$$+ (y'_{\oplus\Delta} - y'_{\oplus\mathbb{C}})(-\cos\Omega' \sin i_{\mathbb{C}})$$
$$+ (z'_{\oplus\Delta} - z'_{\oplus\mathbb{C}}) \cos i_{\mathbb{C}} \quad (25)$$

The selenographic longitude and latitude of a vehicle and the altitude of the vehicle above the moon's surface are illustrated in the following sketch and can be calculated from Eqs (21) and (22) as follows:

Selenographic latitude:

$$\phi_{\mathbb{C}} = \sin^{-1}\left(\frac{z_{S\Delta}}{r_{S\Delta}}\right), \quad -90° \le \phi_{\mathbb{C}} \le +90° \quad (26)$$
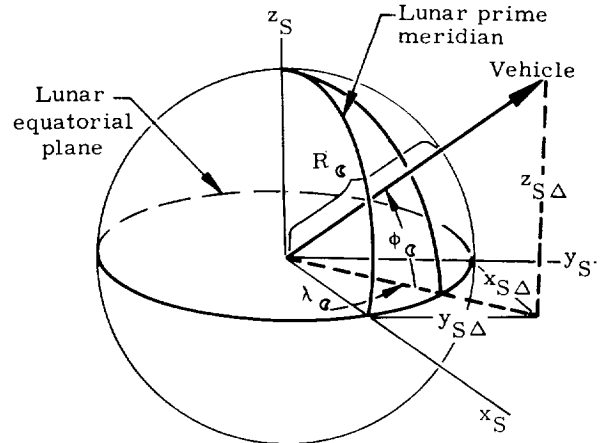
Selenographic longitude:

$$\lambda_{\mathbb{C}} = \sin^{-1}\left(\frac{y_{S\Delta}}{\left[x_{S\Delta}^2 + y_{S\Delta}^2\right]^{1/2}}\right) =$$
$$\cos^{-1}\left(\frac{x_{S\Delta}}{\left[x_{S\Delta}^2 + y_{S\Delta}^2\right]^{1/2}}\right), -180° \le \lambda_{\mathbb{C}} \le 180° \quad (27)$$

Altitude of the vehicle above surface of moon:

$$h_{\mathbb{C}} = r_{S\Delta} - R_{\mathbb{C}} \quad (28)$$

where $R_{\mathbb{C}}$ is the mean radius of the moon and $r_{S\Delta}$ is the magnitude of the vector $\vec{r}_{S\Delta}$.

e. Vehicle velocity in selenographic coordinates

Before we give an expression for the vehicle velocity, we have to introduce some notation and make some definitions.

Let a dot over a symbol denote differentiation with respect to time, i.e.,

$$\dot{x} = \frac{dx}{dt}, \quad \ddot{x} = \frac{d^2x}{dt^2}.$$

In addition, define the following velocities:

The vehicle velocity vector in the geocentric equatorial coordinate system,

$$\dot{\vec{r}}_{\oplus\Delta} = \dot{x}'_{\oplus\Delta}\hat{x}'_{\oplus} + \dot{y}'_{\oplus\Delta}\hat{y}'_{\oplus} + \dot{z}'_{\oplus\Delta}\hat{z}'_{\oplus} \quad (29)$$

The velocity vector of the moon in the geocentric equatorial system,

$$\dot{\vec{r}}_{\oplus\mathbb{C}} = \dot{x}'_{\oplus\mathbb{C}}\hat{x}'_{\oplus} + \dot{y}'_{\oplus\mathbb{C}}\hat{y}'_{\oplus} + \dot{z}'_{\oplus\mathbb{C}}\hat{z}'_{\oplus} \quad (30)$$

The velocity vector of the vehicle in the selenocentric equatorial system,

$$\dot{\vec{r}}_{\oplus,\mathbb{C}\to\Delta} = \dot{x}'_{\oplus,\mathbb{C}\to\Delta}\hat{x}'_{\oplus} + \dot{y}'_{\oplus,\mathbb{C}\to\Delta}\hat{y}'_{\oplus}$$
$$+ \dot{z}'_{\oplus,\mathbb{C}\to\Delta}\hat{z}'_{\oplus} \quad (31)$$

The velocity vector of the vehicle in the seleno-graphic system is

$$\dot{\vec{r}}_{S\Delta} = \dot{x}_{SA}\hat{x}_S + \dot{y}_{SA}\hat{y}_S + \dot{z}_{SA}\hat{z}_S \qquad (32)$$

Differentiation of Eq (19) yields

$$\dot{\vec{r}}_{\oplus\Delta} = \dot{\vec{r}}_{\oplus\mathbb{C}} + \dot{\vec{r}}_{\oplus,\mathbb{C}\to\Delta} \qquad (33)$$

However,

$$\dot{\vec{r}}_{\oplus,\mathbb{C}\to\Delta} = \dot{\vec{r}}_{SA} + \vec{\omega}_{\mathbb{C}} \times \vec{r}_{SA} \qquad (34)$$

due to the rotation of the selenographic system with respect to the geocentric inertial coordinate system. Hence, the velocity in selenographic coordinates can be written,

$$\dot{\vec{r}}_{SA} = \dot{\vec{r}}_{\oplus\mathbb{C}} - \dot{\vec{r}}_{\oplus\Delta} - \vec{\omega}_{\mathbb{C}} \times \vec{r}_{SA} \qquad (35)$$

where

$$\vec{\omega}_{\mathbb{C}} \times \vec{r}_{SA} = \begin{vmatrix} \hat{x}_S & \hat{y}_S & \hat{z}_S \\ 0 & 0 & \omega_{\mathbb{C}} \\ x_{SA} & y_{SA} & z_{SA} \end{vmatrix} = \begin{array}{l} -\omega_{\mathbb{C}} y_{SA}\hat{x}_S \\ + \omega_{\mathbb{C}} x_{SA}\hat{y}_S \end{array} \qquad (36)$$

The velocity components of the vehicle in selenographic coordinates $(\dot{x}_{SA},\ \dot{y}_{SA},\ \dot{z}_{SA})$ in terms of geocentric equatorial velocity components of the moon and vehicle as well as selenographic vehicle position are:

$$\left\{\begin{array}{c} \dot{x}_{SA} \\ \dot{y}_{SA} \\ \dot{z}_{SA} \end{array}\right\} = \left[T(\Lambda_M)\right] \cdot \left[T(i_{\mathbb{C}})\right] \cdot \left[T(\Omega')\right] \left\{\begin{array}{c} \dot{x}'_{\oplus\Delta} - \dot{x}'_{\oplus\mathbb{C}} \\ \dot{y}'_{\oplus\Delta} - \dot{y}'_{\oplus\mathbb{C}} \\ \dot{z}'_{\oplus\Delta} - \dot{z}'_{\oplus\mathbb{C}} \end{array}\right\}$$

$$+ \left\{\begin{array}{c} \omega_{\mathbb{C}} y_{SA} \\ -\omega_{\mathbb{C}} x_{SA} \\ 0 \end{array}\right\} \qquad (37)$$

which can be multiplied to yield:

$$\dot{x}_{SA} = (\dot{x}'_{\oplus\Delta} - \dot{x}'_{\oplus\mathbb{C}})(\cos \Lambda_M \cos \Omega'$$

$$- \sin \Lambda_M \sin \Omega' \cos i_{\mathbb{C}})$$

$$+ (\dot{y}'_{\oplus\Delta} - \dot{y}'_{\oplus\mathbb{C}})(\cos \Lambda_M \sin \Omega' \qquad (38)$$

$$+ \sin \Lambda_M \cos \Omega' \cos i_{\mathbb{C}})$$

$$+ (\dot{z}'_{\oplus\Delta} - \dot{z}'_{\oplus\mathbb{C}})(\sin \Lambda_M \sin i_{\mathbb{C}}) + \omega_{\mathbb{C}} y_{SA}$$

$$\dot{y}_{SA} = (\dot{x}'_{\oplus\Delta} - \dot{x}'_{\oplus\mathbb{C}})(-\sin \Lambda_M \cos \Omega'$$

$$- \cos \Lambda_M \sin \Omega' \cos i_{\mathbb{C}})$$

$$+ (\dot{y}'_{\oplus\Delta} - \dot{y}'_{\oplus\mathbb{C}})(- \sin \Lambda_M \sin \Omega' \qquad (39)$$

$$+ \cos \Lambda_M \cos \Omega' \cos i_{\mathbb{C}})$$

$$+ (\dot{z}'_{\oplus\Delta} - \dot{z}'_{\oplus\mathbb{C}})(\cos \Lambda_M \sin i_{\mathbb{C}}) - \omega_{\mathbb{C}} x_{SA}$$

$$\dot{z}_{SA} = (\dot{x}'_{\oplus\Delta} - \dot{x}'_{\oplus\mathbb{C}})(\sin \Omega' \sin i_{\mathbb{C}})$$

$$+ (\dot{y}'_{\oplus\Delta} - \dot{y}'_{\oplus\mathbb{C}})(-\cos \Omega' \sin i_{\mathbb{C}}) \qquad (40)$$

$$+ (\dot{z}'_{\oplus\Delta} - \dot{z}'_{\oplus\mathbb{C}})(\cos i_{\mathbb{C}})$$

   f. Vehicle acceleration in selenographic
       coordinates

The acceleration of the vehicle in selenocentric equatorial coordinates can be obtained by differentiation of both sides of Eq (33).

$$\ddot{\vec{r}}_{\oplus\Delta} = \ddot{\vec{r}}_{\oplus\mathbb{C}} + \ddot{\vec{r}}_{\oplus,\mathbb{C}\to\Delta} \qquad (41)$$

where, by differentiation of Eq (34) with respect to time in the geocentric equatorial coordinate system, and if we assume that $\dot{\vec{\omega}}_{\mathbb{C}} = 0$

$$\ddot{\vec{r}}_{\oplus,\mathbb{C}\to\Delta} = \ddot{\vec{r}}_{SA} + 2\vec{\omega}_{\mathbb{C}} \times \dot{\vec{r}}_{SA} + \vec{\omega}_{\mathbb{C}} \times (\vec{\omega}_{\mathbb{C}} \times \vec{r}_{SA}).$$
$$\qquad (42)$$

The vehicle acceleration in selenographic coordinates can be obtained by solving for $\ddot{\vec{r}}_{SA}$ from Eqs (41) and (42):

$$\ddot{\vec{r}}_{SA} = \ddot{\vec{r}}_{\oplus\Delta} - \ddot{\vec{r}}_{\oplus\mathbb{C}} - 2\vec{\omega}_{\mathbb{C}} \times \dot{\vec{r}}_{SA} - \vec{\omega}_{\mathbb{C}} \times (\vec{\omega}_{\mathbb{C}} \times \vec{r}_{SA})$$
$$\qquad (43)$$

where

$$\vec{\omega}_{\mathbb{C}} \times \dot{\vec{r}}_{SA} = -\omega_{\mathbb{C}} \dot{y}_{SA}\hat{x}_S + \omega_{\mathbb{C}} \dot{x}_{SA}\hat{y}_S \qquad (44)$$

and

$$\vec{\omega}_{\mathbb{C}} \times (\vec{\omega}_{\mathbb{C}} \times \vec{r}_{SA}) = -\omega_{\mathbb{C}}^2 x_{SA}\hat{x}_S - \omega_{\mathbb{C}}^2 y_{SA}\hat{y}_S . \qquad (45)$$

The components of vehicle acceleration in selenographic coordinates $(\ddot{x}_{SA},\ \ddot{y}_{SA},\ \ddot{z}_{SA})$ in terms of the moon's and vehicle's geocentric equatorial components of acceleration as well as selenographic vehicle position and velocity are:

$$
\begin{Bmatrix} \ddot{x}_{S\Delta} \\ \ddot{y}_{S\Delta} \\ \ddot{z}_{S\Delta} \end{Bmatrix} = \left[T(\Lambda_M) \right] \cdot \left[T(i_{\mathbb{C}}) \right] \cdot \left[T(\Omega') \right] \begin{Bmatrix} \ddot{x}'_{\oplus}\, \Delta^-\, \ddot{x}'_{\oplus\mathbb{C}} \\ \ddot{y}'_{\oplus}\, \Delta^-\, \ddot{y}'_{\oplus\mathbb{C}} \\ \ddot{z}'_{\oplus}\, \Delta^-\, \ddot{z}'_{\oplus\mathbb{C}} \end{Bmatrix}
$$

$$
+ \begin{Bmatrix} 2\omega_{\mathbb{C}}\, \dot{y}_{S\Delta} \\ -2\omega_{\mathbb{C}}\, \dot{x}_{S\Delta} \\ 0 \end{Bmatrix} + \begin{Bmatrix} \omega_{\mathbb{C}}^{2}\, x_{S\Delta} \\ \omega_{\mathbb{C}}^{2}\, y_{S\Delta} \\ 0 \end{Bmatrix}. \qquad (46)
$$

g. Lunar maps

Several lunar map series exist which represent the lunar surface to the best of our present knowledge:

USAF Lunar Atlas (edited by Dr. Gerard P. Kuiper). This atlas contains 280 photographs of the moon, sheet size 16 x 20 inches, scale 2.54 m to the lunar diameter or about 12.7 km to the cm and bound in a looseleaf ring binder. The photographs were from a collection of lunar plates taken at Mt. Wilson, Lick, Yerkes and McDonald Observatories in the United States and the Pic du Midi Observatory in France.

Orthographic Atlas of the Moon (edited by Dr. Gerard P. Kuiper), supplement No. 1 to the USAF Lunar Atlas. This volume contains 60 plates from the USAF Lunar Atlas which carry the orthographic grid established from a control net of 5000 points. Grid spacing is approximately 1.25 cm on the published copy. Meridians and parallels are printed in color at 2° intervals on each of the sheets which are bound in an 18 in. x 24 in. post-type hardback cover.

Rectified Lunar Atlas, supplement No. 2 to the USAF Lunar Atlas. This atlas consists of photographs of the entire visible hemisphere of the moon, rectified by projection on a globe 91.4 cm in diameter. Each of thirty fields on the globe were rephotographed at three different illuminations, corresponding to full moon, early morning and late afternoon.

USAF Lunar Mosaic. The lunar mosaic is a composite photograph of the moon made from the best imagery selected from photographs taken at Yerkes, McDonald and Mt. Wilson Observatories. The photography has been fitted to an orthographic projection which portrays the moon at mean libration as a sphere in true perspective. It is published in two sizes, LEM 1, scale 1:5,000,000 (lunar diameter 69 cm) and LEM 1A, scale 1:10,000,000 (lunar diameter 34 cm).

Lunar Aeronautical Charts (LAC Series). The Lunar Aeronautical Charts consist of a coordinated series requiring a total of 144 charts to cover the entire moon. Approximately 80 charts can be produced of the visible surface (59% of the total). Surface features are shown by a combination of shaded relief, contours and tones representing surface color variations. A spherical figure of the moon is assumed with a radius of $R_{\mathbb{C}} = 1738$ km. Elevations are shown by 300-m approximate contours and referenced to the datum which was taken at 1735.4 km. The scale is 1:1,000,000 (10 km to the cm), and the sheet size is 22 in. x 29 in.

Atlas of the Moon's Far Side. This atlas, issued by the USSR Academy of Sciences and published in the United States by Interscience Publishers, gives the results of the Lunik III reconnaissance of the lunar far side. The volume gives a description of the interpretative technique used and 30 integrated photographs of the moon's far side obtained by the space vehicle camera. The results include a catalog of 498 formations classified according to the reliability of the observation and 4 maps drawn to scale 1:10,000,000.

Topographic Lunar Maps. This series of maps, prepared by the Army Map Service, is on a scale of 1:2,500,000. It shows surface features by a combination of shaded relief, contours and tones representing surface color variations. The moon is assumed to be a sphere with $R_{\mathbb{C}} = 1737.988$ km and the vertical datum of the 500-m approximate contour lines is based on an elevation of 7000 m at the center of the crater Möshing A. A complete listing of lunar formations derived from "Named Lunar Formations" (1935) by M. Blagg and K. Müller is included on the back of the map. One sheet, Mare Nectaris--Mare Imbrium, 113 x 134 cm has been published.

3. Trajectory Coordinates

The position of a vehicle in earth-moon space can be given either in geocentric, geographic, or topocentric coordinates. Similarly, its position and velocity may be given in the selenocentric, selenographic or topocentric coordinate systems when the vehicle is near the moon. For tracking, for instance, it is convenient to use a topocentric system centered at the station since the tracking measurements and errors are given in that system. In the same manner several specialized coordinate systems have been evolved for various trajectory digital computer programs.

a. Typical rectangular coordinate systems.

The choice of coordinate systems for trajectory computations depends to a large degree on the force model and the dynamical system as well as on the method used for integrating the equations of motion. A great simplification of motion in earth-moon space is achieved when in the dynamical system the spherical earth and moon are assumed to move in circular orbits around the common center of mass (barycenter) which is taken as inertially fixed. The coordinate systems of the Martin Simplified Lunar Trajectory Digital Program, Ref. 7, which uses the force model described above, will be given here.

A basic coordinate system in the digital program has its origin at the barycenter and rotates at the constant rate $\omega_{\oplus\mathbb{C}}$ of the earth-moon system (see following sketch). The x_R-axis is directed toward the moon, the z_R-axis coincides with the angular momentum vector of the earth-moon system, and the y_R-axis completes the right-handed Cartesian coordinate system.

Consider another coordinate system with origin at the barycenter and axes x_0, y_0, z_0. At time $t = 0$ the x_R-axis is rotated by an angle Φ from the x_0-axis, and subsequently the angular

z axes are up
out of the plane
of the paper
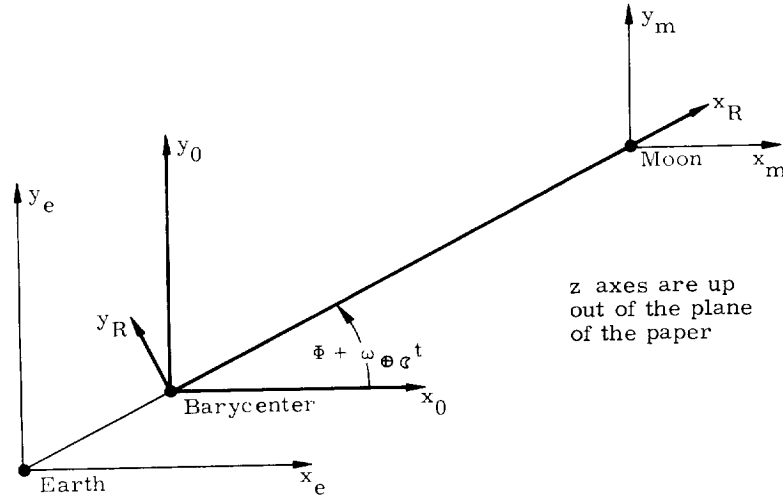
displacement of the rotating x_R -axis from the x_0 axis is $(\Phi + \omega_{\oplus\mathbb{C}} t)$. A third coordinate system, parallel to the nonrotating x_0, y_0, z_0 system but centered at the earth, will be denoted by x_e, y_e, z_e, and a fourth, moon-centered nonrotating coordinate system has axes x_m, y_m, z_m (see preceding sketch). Transformations from the nonrotating systems to the rotating coordinate system involve the same rotation through the angle $(\Phi + \omega_{\oplus\mathbb{C}} t)$ about the z-axis given by the matrix

$$\left[T (\Phi + \omega_{\oplus\mathbb{C}} t) \right] = $$

$$\begin{bmatrix} \cos (\Phi + \omega_{\oplus\mathbb{C}} t) & -\sin (\Phi + \omega_{\oplus\mathbb{C}} t) & 0 \\ \sin (\Phi + \omega_{\oplus\mathbb{C}} t) & \cos (\Phi + \omega_{\oplus\mathbb{C}} t) & 0 \\ 0 & 0 & 1 \end{bmatrix} \quad (47)$$

and a translation which can be obtained by using the definition of the barycenter (see also Chapter IV). Position in the nonrotating systems is related to position in the rotating system by

$$\begin{Bmatrix} x_0 \\ y_0 \\ z_0 \end{Bmatrix} = \left[T (\Phi + \omega_{\oplus\mathbb{C}} t) \right] \begin{Bmatrix} x_R \\ y_R \\ z_R \end{Bmatrix} , \quad \begin{Bmatrix} x_e \\ y_e \\ z_e \end{Bmatrix} = $$

$$\left[T (\Phi + \omega_{\oplus\mathbb{C}} t) \right] \cdot \begin{Bmatrix} x_R + \nu \ \bar{r}_{\oplus\mathbb{C}} \\ y_R \\ z_R \end{Bmatrix} , \quad (48)$$

$$\begin{Bmatrix} x_m \\ y_m \\ z_m \end{Bmatrix} = \left[T (\Phi + \omega_{\oplus\mathbb{C}} t) \right] \begin{Bmatrix} x_R - \bar{r}_{\oplus\mathbb{C}} (1 - \nu) \\ y_R \\ z_R \end{Bmatrix} ,$$

where $\bar{r}_{\oplus\mathbb{C}}$ is the mean distance between the centers of the earth and moon, and $\nu = \dfrac{M_{\mathbb{C}}}{M_{\mathbb{C}} + M_{\oplus}}$

is the ratio of the mass of the moon to the total mass of the earth and moon.

It remains to relate the x_e y_e z_e system to the geographic x_G y_G z_G system which rotates about the z_G -axis at the constant angular velocity $\omega_{\oplus}$. The earth-moon orbital plane (x_e y_e -plane) is inclined to the earth's equatorial plane (x_G y_G -plane) at the constant angle i_{em} and their line of intersection does not rotate in inertial space. Since the initial value of Φ is arbitrary, we may assume that the intersection between the two planes is coincident with the y_e -axis. Thus Φ locates the moon in its orbit at time t = 0. Similarly we locate the Greenwich meridian (x_G -axis) relative to this intersection at time t = 0 by the angle Λ_G which is defined as the angle from the y_e - axis to the y_G -axis in the earth's equatorial plane (see following sketch).

The transformation from the x_e y_e z_e coordinate systems to the x_G y_G z_G system consists first of a rotation about the y_e -axis through the angle $(-i_{em})$ and then of a rotation about the z_G -axis through the angle $(\Lambda_G + \omega_{\oplus} t)$.

With $\left[T (-i_{em}) \right] = \left[T (i_{em}) \right]^{-1}$, the coordinate transformations between the various coordinate systems are given by,

$$\begin{Bmatrix} x_G \\ y_G \\ z_G \end{Bmatrix} = $$

$$\left[T (\Lambda_G + \omega_{\oplus} t) \right] \left[T (i_{em}) \right]^{-1} \begin{Bmatrix} x_e \\ y_e \\ z_e \end{Bmatrix}$$
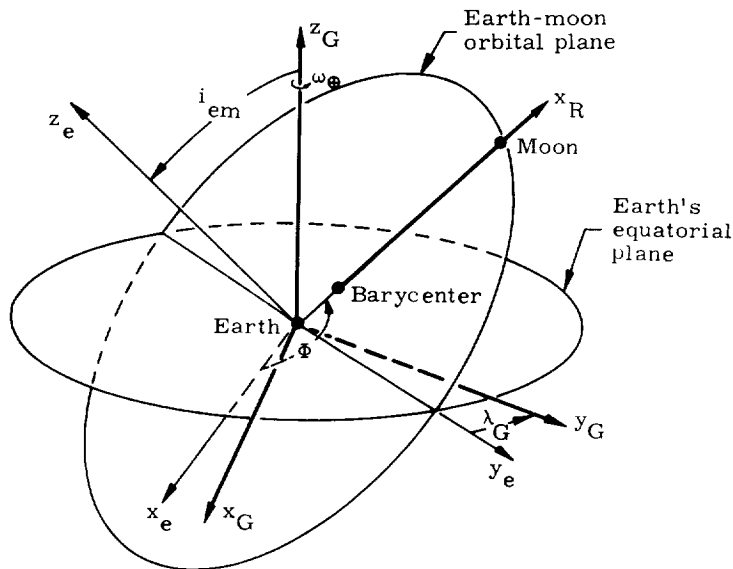
$$= \left[T\,(\Lambda_G + \omega_\oplus t)\right]\left[T\,(i_{em})\right]^{-1}$$

$$\left[T\,(\Phi + \omega_{\oplus\mathbb{C}}\,t)\right]\begin{Bmatrix} x_R \\ y_R \\ z_R \end{Bmatrix} \qquad (49)$$

where

$$\left[T\,(\Lambda_G + \omega_\oplus t)\right] =$$

$$\begin{bmatrix} \cos(\Lambda_G + \omega_\oplus t) & \sin(\Lambda_G + \omega_\oplus t) & 0 \\ -\sin(\Lambda_G + \omega_\oplus t) & \cos(\Lambda_G + \omega_\oplus t) & 0 \\ 0 & 0 & 1 \end{bmatrix}, \quad (50)$$

$$\left[T\,(i_{em})\right]^{-1} =$$

$$\begin{bmatrix} \cos i_{em} & 0 & -\sin i_{em} \\ 0 & 1 & 0 \\ \sin i_{em} & 0 & \cos i_{em} \end{bmatrix}, \qquad (51)$$

and

$$T\left[\Phi + \omega_{\oplus\mathbb{C}}\,t\right]\text{is given by Eq (47).}$$

The angles i_{em}, Φ and Λ_G are determined for any specific launch time $t = 0$ from the ephemerides of the earth and moon.

b. VOICE coordinate system

The coordinate system and force model used in the VOICE lunar trajectory program will be discussed in detail under that heading (Section IV C). Like the previous system, it is essentially based on the moon's orbital plane (MOP) as a fundamental plane and the lines of intersection of

the trajectory planes with the MOP as reference directions. The earth-moon line as well as the earth and moon equatorial planes are defined with respect to this basic system.

c. Orbit plane system

Consider the dynamical system of a vehicle with negligible mass and one central spherical attracting body. It can be shown that in this case the vehicle moves in a fixed plane through the center of the attracting body which is known as the orbit plane.

The Cartesian coordinate systems given in Subsection 3a are essentially orbit plane systems with axes in and perpendicular to the orbit plane. Let us define an additional coordinate system with origin at the center of the attracting body and the z_P-axis normal to the orbit plane. The x_P-axis may be directed to perifocus, the closest approach to the central body, and denoted by x_ω, or to the ascending node and denoted by x_Ω. The y_P-axis is in the orbit plane, directed so as to complete the right-handed system. The unit vectors $\hat{x}_P$, $\hat{y}_P$ and $\hat{z}_P$ are in the x_P, y_P, z_P directions, respectively (see following sketch).

III-12
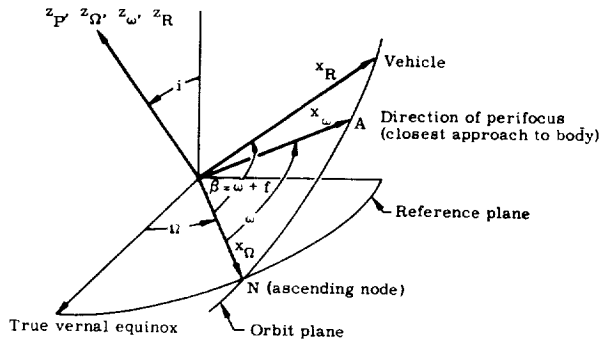
The orientation of the orbit plane may be given in terms of the orientation angles i, $0 \leq i < 180°$, inclination between the orbit plane and the reference plane measured from due east on the reference plane, Ω', longitude of the ascending node measured from the true vernal equinox, and ω, the argument of perifocus as measured from the ascending node. The angles i_{em}, Ω_G, and Φ given in Section 3a can similarly be regarded as orientation angles.

Since there are three second-order equations of motion for the vehicle, there are six constants of integration which enter into the solution of the equations of motion. These constants may be given in terms of initial position x_P, y_P, z_P and initial velocity $\dot{x}_P$, $\dot{y}_P$, $\dot{z}_P$ at time t_0 or in terms of six orbital elements, which do not involve the coordinates, velocity components, or time. In case of elliptic orbits customary sets of elements at epoch, t_0, are:

Ω' longitude of the ascending node

i   inclination

ω argument of perifocus

a   semi-major axis

e   eccentricity

T_ω time of perifocal passage

The time of perifocal passage, T_ω may be replaced as an element by ℓ_0, the mean anomaly at an arbitrarily chosen epoch t_0, which is given by $\ell_0 = n(t_0 - T_\omega)$, where n is the mean motion of the vehicle in its orbit plane. Another set of elements is:

Ω' longitude of the ascending node

i   inclination

$\tilde{\omega}$ $= \Omega + \omega$, longitude of perifocus

n   mean motion

e   eccentricity

ϵ_0 $= \tilde{\omega} + \ell_0$, mean longitude at epoch

Typical elements of a parabolic or hyperbolic orbit at epoch, t_0 are:

Ω' longitude of the ascending node

i   inclination

ω argument of perifocus

q   perifocus distance

e   eccentricity

T_ω time of perifocal passage

while for a circular orbit only four elements are required at epoch t_0,

Ω' longitude of the ascending node

i   inclination

r   orbital radius

T_Ω time of ascending nodal crossing

since the eccentricity vanishes and the argument of perigee is undefined.

These elements remain constant for the dynamical system described at the beginning of the present section. In astronomy the concept of orbital elements is used even if other forces act on the vehicle, provided that they are small compared to the central force directed toward the attracting body. In this case the elements change slowly with time, and osculating elements at time t_0 are defined as the orbital elements of the vehicle if all forces except the central force due to the spherical attracting body were removed at t_0.

It has been found through experience that the orbital elements of a space vehicle are useful for descriptive purposes and to calculate approximate energy requirements only, but not suited to the analytical development of orbit determination and to precision work. In the latter case rectangular coordinates are more useful.

4. Vehicle--Centered Coordinates

In problems involving aerodynamic forces, stability, control and guidance of a space vehicle, it is sometimes convenient to introduce a body-axis system fixed in the vehicle with origin at its instantaneous center of gravity, the x_b-axis along the longitudinal axis of the vehicle in the forward direction, the y_b-axis directed laterally to the right and the z_b-axis completes the right-handed Cartesian system by being directed downward (see following sketch).
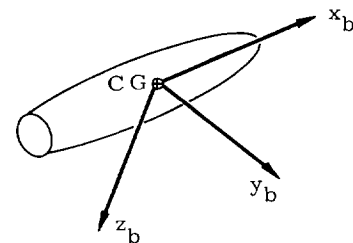
Additional specialized sets of axes which are required for particular equipment in the vehicle such as accelerometers, telescopes, rocket engines, etc. as well as transformations between the body axes and other coordinate systems will be discussed when they are used in the manual.

B. MOTION IN EARTH-MOON SPACE

The discussion in this section is based essentially on results of classical astronomy with Moulton's Celestial Mechanics (Ref. 8) used as the primary reference. Derivations that are important in the discussion of various force models used in the lunar trajectory digital programs, as well as special solutions of the equations of motion useful for space vehicle missions in earth-moon space are given. The material here is also introductory to a more complicated description of the motion of celestial bodies and vehicles in space which may be necessary for precision trajectories.

Assume a dynamical system of n bodies, which are homogeneous in spherical layers and move under the influence of their mutual gravitational attraction. The determination of the motion of these bodies reduces to finding 6n integrals of the 3n second-order simultaneous differential equations, and is known as the n-body problem. The gravitational attraction between celestial bodies is the most important force affecting their motion due to their enormous size and mass. The assumption of spherical celestial bodies is actually quite a good one. The equatorial semiaxes of the ellipsoidal earth model differ by only 21.4 km from the polar semiaxes with the radius of the equivalent sphere being 6371.02 km. The three dynamically determined semiaxes of the moon differ by at most 0.7 km from their arithmetic mean of 1738.5 km. The effect of asphericity of the earth on the motion of the moon at a mean distance of 384,402 km from the earth is thus very minor, even for comparatively long periods of time.

The effect of the asphericity of the earth and moon on the space vehicle will be important only when the space vehicle moves in the vicinity of these celestial bodies as will be shown later. Any irregularities in the shape of the sun and planets are completely negligible in earth-moon space over time periods of a week since these bodies are millions of kilometers away. Consider the two-body problem, n=2. Six integrals of the differential equations of motion can be found by considering the motion of the center of mass, and the other six constants of integration introduced by integrating the equations of motion of one body relative to the other.

The three initial coordinates and the initial velocity of one body with respect to the other, or 6 orbital elements, determine the motion of the two bodies completely. The motion of the smaller body takes place in a fixed plane through the center of the massive body which is known as the orbit plane.

For n > 2, however, only ten of the 6n integrals which are required in order to solve the problem completely have been found. If the dynamical system of n bodies which are homogeneous in spherical layers is subject to no forces except their mutual attractions, six of these integrals show that the center of mass (barycenter) exhibits rectilinear motion at constant speed, three more state that the angular momentum of the system is constant, and the tenth is simply an expression of the conservation of kinetic and potential energy. These

10 integrals are the only ones known since Bruns has proved that, when rectangular Cartesian coordinates are chosen as the dependent variables, there are no new algebraic integrals of existing functions. Also, Poincaré has demonstrated that use of orbital elements as the dependent variables yields no new uniform transcendental integrals even when the masses of all bodies except one are very small. However, the general system can be reduced still further by the mathematical trick of eliminating nodal position and time which reduces the requirement to 6 further integrals in the case n=3.

1. Three-body Problem

For lunar flight trajectories the problem of three bodies, n=3, which is concerned with the motion of a vehicle in the environment of the earth-moon system, is of primary interest. Although a general solution to the problem (which requires 18 arbitrary constants or integrals) has not as yet been found, there are a number of important results which have been established if the initial positions and velocities of the bodies satisfy certain conditions. While some of these special cases have not been found in nature, there are nevertheless some applications, for instance the libration point satellite buoys proposed by Buchheim and discussed further in Chapter IV. These special cases can be classified into: (1) study of the properties of motion of an infinitesimal body (i.e., one that is attracted by finite masses but in turn is assumed not to attract them) when it is attracted by two finite bodies which revolve in circles around their common center of mass; (2) construction of particular solutions for the motion of three finite bodies such that the ratios of their mutual distances are constants.

The former method will be discussed in the next section while, for the latter case, special methods will be described and references will be given here.

There are three special solutions for the case of 3 finite bodies: the three bodies at the vertices of an equilateral triangle, three bodies in a straight line, and the trivial case of the three bodies all at one point. The two nontrivial solutions are described among other places, in Moulton (Ref. 8) on pages 309-318 and in Finlay-Freundlich (Ref. 9).

a. Conditions for circular three-body orbits

Lagrange has shown that it is possible for three finite bodies to move in elliptical orbits around their common center of mass. The special case of circular orbits discussed in Ref. 8 will be presented in the following. Assume that the three bodies move in a common plane. Take the origin of coordinates at the common center of mass (barycenter) and the $x_0 y_0$-plane as the plane of motion. Let the masses of the three bodies be M_1, M_2, M_3 and let G denote the universal gravitational constant. Then the differential equations of motion are:

$$\ddot{x}_{0i} = \frac{1}{M_i} \frac{\partial U}{\partial x_{0i}} \qquad , \; i = 1, \, 2, \, 3$$

$$\ddot{y}_{0i} = \frac{1}{M_i} \frac{\partial U}{\partial y_{0i}} \tag{56}$$

where

$$U = G \frac{M_1 M_2}{r_{1,\,2}} + G \frac{M_2 M_3}{r_{2,\,3}} + G \frac{M_3 M_1}{r_{3,\,1}} \tag{57}$$

is the gravitational potentia, work function, or negative gravitational potential energy, of the dynamical system, and $r_{i,\,j}$ denotes the distance between the centers of M_i and M_j.

The motion of the system can be referred to axes $x_R \, y_R$ with origin at the barycenter and rotating with the uniform angular velocity ω_R with respect to the $x_0 \, y_0$ axes by the transformation

$$\begin{Bmatrix} x_{0i} \\ y_{0i} \\ z_{0i} \end{Bmatrix} = \begin{bmatrix} \cos \omega_R t & -\sin \omega_R t & 0 \\ \sin \omega_R t & \cos \omega_R t & 0 \\ 0 & 0 & 1 \end{bmatrix} \begin{Bmatrix} x_{Ri} \\ y_{Ri} \\ z_{Ri} \end{Bmatrix} \tag{58}$$

Substitution of Eq (58) into Eq (56) yields, after simplification:

$$\left. \begin{array}{l} \ddot{x}_{Ri} - 2\omega_R \dot{x}_{Ri} - \omega_R^2 \, x_{Ri} - \dfrac{1}{M_i} \dfrac{\partial U}{\partial x_{Ri}} = 0 \\[2mm] \ddot{y}_{Ri} + 2\omega_R \dot{y}_{Ri} - \omega_R^2 \, y_{Ri} - \dfrac{1}{M_i} \dfrac{\partial U}{\partial y_{Ri}} = 0 \end{array} \right\} \tag{59}$$

If the bodies are moving in circles around the origin with the angular velocity ω_R, their coordinates with respect to the rotating axes are constant and their time derivatives vanish. Equations (59) become, if we take the derivatives of the potential with respect to the coordinates as indicated and drop the time derivatives of x_{Ri} and y_{Ri},

$$\left. \begin{array}{l} -\omega_R^2 \, x_{R1} + GM_2 \dfrac{(x_{R1} - x_{R2})}{r_{1,\,2}^3} \\[4mm] \qquad + GM_3 \dfrac{(x_{R1} - x_{R3})}{r_{1,\,3}^3} = 0 \\[5mm] -\omega_R^2 \, x_{R2} + GM_1 \dfrac{(x_{R2} - x_{R1})}{r_{1,\,2}^3} \\[4mm] \qquad + GM_3 \dfrac{(x_{R2} - x_{R3})}{r_{2,\,3}^3} = 0 \end{array} \right\} \tag{60}$$

$$\left. \begin{array}{l} -\omega_R^2 \, x_{R3} + GM_1 \dfrac{(x_{R3} - x_{R1})}{r_{1,\,3}^3} \\[4mm] \qquad + GM_2 \dfrac{(x_{R3} - x_{R2})}{r_{2,\,3}^3} = 0 \end{array} \right\}$$

and three similar equations with x_R replaced by y_R.

The converse is also true, i.e., if the six equations (Eqs (60)) are satisfied, then the bodies move in circles around the origin with the uniform angular velocity ω_R. The system equations (Eqs (60)) can be reduced further by use of the condition that the origin is at the center of mass

$$\left. \begin{array}{l} M_1 \, x_{R1} + M_2 \, x_{R2} + M_3 \, x_{R3} = 0 \\[2mm] M_1 \, y_{R1} + M_2 \, y_{R2} + M_3 \, y_{R3} = 0 \end{array} \right\} \tag{61}$$

to yield after simplification:

$$\left. \begin{array}{l} -\omega_R^2 + GM_2 \dfrac{(x_{R1} - x_{R2})}{r_{1,\,2}^3} \\[4mm] \qquad + GM_3 \dfrac{(x_{R1} - x_{R3})}{r_{1,\,3}^3} = 0 \\[5mm] -\omega_R^2 \, x_{R2} + GM_1 \dfrac{(x_{R2} - x_{R1})}{r_{1,\,3}^3} \\[4mm] \qquad + GM_3 \dfrac{(x_{R2} - x_{R3})}{r_{2,\,3}^3} = 0 \\[5mm] -\omega_R^2 \, y_{R1} + GM_2 \dfrac{(y_{R1} - y_{R2})}{r_{1,\,2}^3} \\[4mm] \qquad + GM_2 \dfrac{(y_{R1} - y_{R3})}{r_{1,\,3}^3} = 0 \\[5mm] -\omega_R^2 \, y_{R2} + GM_1 \dfrac{(y_{R2} - y_{R1})}{r_{1,\,2}^3} \\[4mm] \qquad + GM_3 \dfrac{(y_{R2} - y_{R3})}{r_{2,\,3}^3} = 0 \end{array} \right\} \tag{62}$$

Equations (61) and (62) are the necessary and sufficient conditions for the existence of solutions in which the orbits of the three bodies are circles.

b. Equilateral triangle solutions

It remains to find solutions to the system of algebraic equations (Eqs (61) and Eqs (62)). It can be shown that the system is satisfied if the three bodies lie at the vertices of an equilateral triangle.

In that case $r = r_{1, 2} = r_{2, 3} = r_{1, 3}$, and the system becomes:

$$M_1 x_{R1} + M_2 x_{R2} + M_3 x_{R3} = 0$$

$$\left(\frac{M_2}{r^3} + \frac{M_3}{r^3} - \frac{\omega_R^2}{G}\right) x_{R1} - \frac{M_2}{r^3} x_{R2}$$

$$- \frac{M_3}{r^3} x_{R3} = 0$$

$$\left(\frac{M_1}{r^3} + \frac{M_3}{r^3} - \frac{\omega_R^2}{G}\right) x_{R2} - \frac{M_1}{r^3} x_{R1}$$

$$- \frac{M_3}{r^3} x_{R3} = 0 \qquad (63)$$

$$M_1 y_{R1} + M_2 y_{R2} + M_3 y_{R3} = 0$$

$$\left(\frac{M_2}{r^3} + \frac{M_3}{r^3} - \frac{\omega_R^2}{G}\right) y_{R1} - \frac{M_2}{r^3} y_{R2}$$

$$- \frac{M_3}{r^3} y_{R3} = 0$$

$$\left(\frac{M_1}{r^3} + \frac{M_3}{r^3} - \frac{\omega_R^2}{G}\right) y_{R2} - \frac{M_1}{r^3} y_{R1}$$

$$- \frac{M_3}{r^3} y_{R3} = 0$$

The system of equations (Eqs (63)) is linear and homogeneous in $x_{R1}, x_{R2}, \ldots, y_{R3}$ and for a nontrivial solution to exist, the determinant of the coefficients must vanish. By defining $M = M_1 + M_2 + M_3$ this condition turns out to be

$$M^2_3 \left(M - \frac{\omega_R^2 r^3}{G}\right)^4 = 0 \text{ from which}$$

$$\omega_R^2 = \frac{MG}{r^3} \qquad (64)$$

Then two of the x_{Ri} and two of the y_{Ri} are arbitrary, and the equations have a solution compatible with $r_{i, j} = r$. Therefore, the equilateral triangular configuration with proper initial components of velocity is a particular solution of the three-body problem.

c. Straight line solutions

We can find a special solution to the system equations (Eqs (61) and (62)) by assuming $y_{R1} = y_{R2} = y_{R3} = 0$, i.e., all bodies are on the x_R-axis. Let them lie in the order M_1, M_2, M_3 from the negative end of the axis toward the positive. Then $x_{R3} > x_{R2} > x_{R1}$ and $r_{1, 2} = x_{R2} - x_{R1} = r$, and the

system of equations (Eqs (61) and (62)) become:

$$M_1 x_{R1} + M_2 (x_{R1} + r) + M_3 x_{R3} = 0$$

$$\frac{M_2}{r^2} + \frac{M_3}{\left(x_{R3} - x_{R1}\right)^2} + \frac{\omega_R^2}{G} x_{R1} = 0 \qquad (65)$$

$$-\frac{M_1}{r^2} + \frac{M_3}{\left(x_{R3} - x_{R1} - r\right)^2} + \frac{\omega_R^2}{G}\left(r + x_{R1}\right) = 0$$

Elimination of x_{R3} and ω_R^2 yields

$$M_2 + (M_1 + M_2) x_{R1} + \frac{M_3^3 \left(r + x_{R1}\right)}{\left(M x_{R1} + M_2 r\right)^2}$$

$$- \frac{M_3^3 x_{R1}}{\left(M x_{R1} + M_2 r + M_3 r\right)^2} = 0 \qquad (66)$$

a quintic equation for x_{R1} whose coefficients are all positive. Therefore, there is no real positive root but there is at least one real negative root, and consequently at least one solution of the problem.

Instead of adopting x_{R1} as the unknown, $A = x_{R3} - x_{R2}$ may be used. The distance x_{R1} must be expressed in terms of this new variable. The relations among x_{R1}, x_{R2}, x_{R3} and A are

$$M_1 x_{R1} + M_2 x_{R2} + M_3 x_{R3} = 0$$

$$x_{R2} - x_{R1} = r$$

$$x_{R3} - x_{R2} = A$$

from which

$$x_{R1} = -\frac{\left[r \left(M_2 + M_3\right) + M_3 A\right]}{M} \qquad (67)$$

Substitution of Eq (67) into Eq (66) letting $r = 1$, and subsequent simplification yields:

$$\left(M_1 + M_2\right) A^5 + \left(3 M_1 + 2 M_2\right) A^4$$

$$+ \left(3 M_1 + M_2\right) A^3$$

$$- \left(M_2 + 3 M_3\right) A^2 - \left(2 M_2 + 3 M_3\right) A$$

$$- \left(M_2 + M_3\right) = 0 \qquad (68)$$

which is Lagrange's quintic equation in A. Equation (68) has only one real positive root since the coefficients change sign only once. The only A valid in the problem for the chosen order of the masses is positive; hence, the solution of Eq (68) is unique and gives the location of the three bodies

in the straight line solution. Two more distinct straight line solutions can be obtained by cyclically permuting the order of the three bodies.

Moulton (Ref. 8) also discusses special solutions in which the orbits of the three bodies are conic sections with $e \neq 0$.

2. Restricted Three-Body Problem

If the mass of one of the three bodies is small compared to that of the other two, in fact so small that it does not influence the motion of the more massive bodies, then the determination of the motion of the small body is known as the restricted three-body problem. Since the mass of any space vehicle in earth-moon space ($M_\triangle =$ order of 10^5 kg or less) is very small compared to that of the earth ($M_\oplus = 5.9758 \times 10^{24}$ kg) or that of the moon ($M_{\mathbb{C}} = 7.3451 \times 10^{22}$ kg), this approximation is permissible for the study of motion in earth-moon space. In addition, we assume that the earth and moon rotate in circular orbits around their common center of mass with the angular velocity $\omega_{\oplus\mathbb{C}}$. This is not quite true since the eccentricity of the moon's orbit around the earth is about 0.055 and, hence, the angular velocity varies with the moon's orbital position. Non-gravitational forces such as atmospheric drag, electromagnetic forces, meteoritic drag, and solar radiation pressure may become important for unorthodox space vehicle shapes even though they can be utterly neglected in the motion of celestial bodies. Thrust forces will also be neglected in the following discussion. The equations of motion of the space vehicle and some results of the restricted three-body problem will be presented in this section with the discussion following that given by Moulton (Ref. 8, pages 278-307). General characteristics of lunar flight trajectories have been deduced from the restricted three-body problem, notably by Egorov (Ref. 10) and Buchheim (Ref. 11). We will discuss these applications to lunar flight missions in detail in the next chapter.

a. Equations of motion

Let the origin of coordinates be at the center of mass (barycenter) of the earth-moon system, and let the direction of the axes be so chosen that the $x_0 y_0$-plane is the plane of their motion. (See Section A-3.) Denote the masses of the earth and moon by $M_\oplus$ and $M_{\mathbb{C}}$ and the universal gravitational constant by G. Let the coordinates of $M_\oplus$, $M_{\mathbb{C}}$ and the vehicle be $(x_{0\oplus}, y_{0\oplus}, 0)$; $(x_{0\mathbb{C}}, y_{0\mathbb{C}}, 0)$; and $(x_{0\triangle}, y_{0\triangle}, z_{0\triangle})$, respectively, so that the distance of the vehicle from the earth and moon is, respectively:

$$r_{\oplus\triangle} = \left[\left(x_{0\triangle} - x_{0\oplus}\right)^2 + \left(y_{0\triangle} - y_{0\oplus}\right)^2 + \left(z_{0\triangle}\right)^2\right]^{1/2}$$

$$r_{\mathbb{C}\triangle} = \left[\left(x_{0\triangle} - x_{0\mathbb{C}}\right)^2 + \left(y_{0\triangle} - y_{0\mathbb{C}}\right)^2 + z_{0\triangle}^2\right]^{1/2}$$

Note that the vehicle is not restricted to motion in the $x_0 y_0$-plane. (See following sketch.)

Then the equations of motion of the vehicle are:
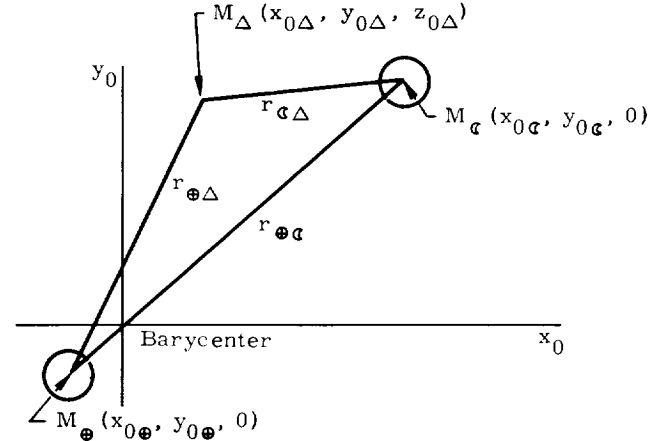
$$\ddot{x}_{0\triangle} = -GM_\oplus \frac{(x_{0\triangle} - x_{0\oplus})}{r_{\oplus\triangle}^3} - GM_{\mathbb{C}} \frac{(x_{0\triangle} - x_{0\mathbb{C}})}{r_{\mathbb{C}\triangle}^3}$$

$$\ddot{y}_{0\triangle} = -GM_\oplus \frac{(y_{0\triangle} - y_{0\oplus})}{r_{\oplus\triangle}^3} - GM_{\mathbb{C}} \frac{(y_{0\triangle} - y_{0\mathbb{C}})}{r_{\mathbb{C}\triangle}^3}$$

$$\ddot{z}_{0\triangle} = -GM_\oplus \frac{z_{0\triangle}}{r_{\oplus\triangle}^3} - GM_{\mathbb{C}} \frac{z_{0\triangle}}{r_{\mathbb{C}\triangle}^3} \tag{69}$$

Let the motion of the bodies be referred to a new system of axes (x_R, y_R, z_R) having the same origin as the old, and rotating in the $x_0 y_0$-plane in the same direction as the earth-moon system with the uniform angular velocity $\omega_{\oplus\mathbb{C}}$. The transformation from the inertial to the moving coordinate system is given by Eq (58). After computing the velocity and acceleration in the rotating coordinate system and substituting into Eqs (69), the equations of motion of the vehicle in the rotating coordinate system became:

$$\ddot{x}_{R\triangle} - 2\omega_{\oplus\mathbb{C}}\dot{y}_{R\triangle} = \omega_{\oplus\mathbb{C}}^2 x_{R\triangle}$$
$$- \frac{GM_\oplus\left(x_{R\triangle} - x_{R\oplus}\right)}{r_{\oplus\triangle}^3} - \frac{GM_{\mathbb{C}}\left(x_{R\triangle} - x_{R\mathbb{C}}\right)}{r_{\mathbb{C}\triangle}^3}$$

$$\ddot{y}_{R\triangle} + 2\omega_{\oplus\mathbb{C}}\dot{x}_{R\triangle} = \omega_{\oplus\mathbb{C}}^2 y_{R\triangle}$$

$$- \frac{GM_\oplus (y_{R\triangle} - y_{R\oplus})}{r_{\oplus\triangle}^3} - \frac{GM_\mathbb{C} (y_{R\triangle} - y_{R\mathbb{C}})}{r_{\mathbb{C}\triangle}^2}$$

$$\tag{70}$$

$$\ddot{z}_{R\triangle} = - \frac{GM_\oplus z_{R\triangle}}{r_{\oplus\triangle}^3} - \frac{GM_\mathbb{C} z_{R\triangle}}{r_{\mathbb{C}\triangle}^3}$$

The direction of the $x_R y_R$-axes can be chosen so that the x_R-axis is in the direction of the moon (see sketch on page 11); then $y_{R\oplus} = 0$, $y_{R\mathbb{C}} = 0$, and the equations of motion of the vehicle simplify to:

$$\ddot{x}_{R\triangle} - 2\omega_{\oplus\mathbb{C}} \dot{y}_{R\triangle} = \omega_{\oplus\mathbb{C}}^2 x_{R\triangle}$$

$$- \frac{GM_\oplus (x_{R\triangle} - x_{R\oplus})}{r_{\oplus\triangle}^3} - \frac{GM_\mathbb{C} (x_{R\triangle} - x_{R\mathbb{C}})}{r_{\mathbb{C}\triangle}^3}$$

$$\ddot{y}_{R\triangle} + 2\omega_{\oplus\mathbb{C}} \dot{x}_{R\triangle} = \omega_{\oplus\mathbb{C}}^2 y_{R\triangle} \tag{71}$$

$$- \frac{GM_\oplus y_{R\triangle}}{r_{\oplus\triangle}^3} - \frac{GM_\mathbb{C} y_{R\triangle}}{r_{\mathbb{C}\triangle}^3}$$

$$\ddot{z}_{R\triangle} = - \frac{GM_\oplus z_{R\triangle}}{r_{\oplus\triangle}^3} - \frac{GM_\mathbb{C} z_{R\triangle}}{r_{\mathbb{C}\triangle}^3}$$

where

$$r_{\oplus\triangle} = \left[\left(x_{R\triangle} - x_{R\oplus} \right)^2 + y_{R\triangle}^2 + z_{R\triangle}^2 \right]^{1/2} \tag{72}$$

and

$$r_{\mathbb{C}\triangle} = \left[\left(x_{R\triangle} - x_{R\mathbb{C}} \right)^2 + y_{R\triangle}^2 + z_{R\triangle}^2 \right]^{1/2} \tag{73}$$

For the particular force model (circular orbits of earth and moon about the barycenter) and the coordinate system (rotating system with the x_R-axis along the earth-moon line) chosen, $x_{R\oplus}$ and $x_{R\mathbb{C}}$ have become constants, and the equations of motion do not involve time explicitly.

The equations of motion (Eqs (71)) of the space vehicle are of sixth order and require six integrals for the determination of the three-dimensional motion of the vehicle; if it moves in the earth-moon plane, then the last equation of Eqs (71) vanishes, and only four integrals are required for the determination of the two-dimensional motion of the vehicle. In general, solutions of the equations of motion (Eqs (71)) are obtained by step-by-step integration with six vehicle initial conditions in the three-dimensional case as well as the initial positions of the earth and moon given.

b. Jacobi's integral and implications

Equations (71) admit an integral first given by Jacobi and which has been discussed by Hill in his Lunar Theory. Let

$$W = \frac{1}{2} \omega_{\oplus\mathbb{C}}^2 \left(x_{R\triangle}^2 + y_{R\triangle}^2 \right) + \frac{GM_\oplus}{r_{\oplus\triangle}} + \frac{GM_\mathbb{C}}{r_{\mathbb{C}\triangle}} \tag{74}$$

then Eqs (71) can be written in the form

$$\left. \begin{array}{l} \ddot{x}_{R\triangle} - 2\omega_{\oplus\mathbb{C}} \dot{y}_{R\triangle} = \dfrac{\partial W}{\partial x_{R\triangle}} \\[2mm] \ddot{y}_{R\triangle} + 2\omega_{\oplus\mathbb{C}} \dot{x}_{R\triangle} = \dfrac{\partial W}{\partial y_{R\triangle}} \\[2mm] \ddot{z}_{R\triangle} = \dfrac{\partial W}{\partial z_{R\triangle}} \end{array} \right\} \tag{75}$$

If these equations are multiplied by $2\dot{x}_{R\triangle}$, $2\dot{y}_{R\triangle}$ and $2\dot{z}_{R\triangle}$, respectively, and added, the resulting equation can be integrated, since W is a function of $x_{R\triangle}$, $y_{R\triangle}$, and $z_{R\triangle}$ alone, and this gives Jacobi's integral:

$$\left(\dot{x}_{R\triangle} \right)^2 + \left(\dot{y}_{R\triangle} \right)^2 + \left(\dot{z}_{R\triangle} \right)^2 = V_{R\triangle}^2 = 2W - C$$

$$V_{R\triangle}^2 = \omega_{\oplus\mathbb{C}}^2 \left(x_{R\triangle}^2 + y_{R\triangle}^2 \right) + \frac{2GM_\oplus}{r_{\oplus\triangle}}$$

$$+ \frac{2GM_\mathbb{C}}{r_{\mathbb{C}\triangle}} - C \tag{76}$$

where $V_{R\triangle}$ is the magnitude of the velocity of the vehicle in the rotating coordinate system and C is the Jacobian constant. We can obtain some qualitative and quantitative information from trajectories in the earth-moon system from Jacobi's integral.

When the constant of integration C has been determined numerically from the initial conditions, $x_{R\triangle}$, $y_{R\triangle}$, $z_{R\triangle}$, $\dot{x}_{R\triangle}$, $\dot{y}_{R\triangle}$, $\dot{z}_{R\triangle}$, Eq (76) determines the velocity $V_{R\triangle}$ of the vehicle at all points in the rotating coordinate system; and conversely, for a given $V_{R\triangle}$, Eq (76) gives the locus of points accessible to the space vehicle. In particular, $V_{R\triangle} = 0$ in Eq (76) defines surfaces of zero relative velocity. On one side of these surfaces the velocity $V_{R\triangle}$ will be real and on the other side imaginary; or, in other words, the space vehicle can move on the real side of this surface only. Thus the surfaces of zero relative velocity indicate the regions of space to which the space vehicle is constrained.

The equation of the surfaces of zero relative velocity for an arbitrary point $x_{R\triangle}$, $y_{R\triangle}$, $z_{R\triangle}$ denoting the space vehicle can be obtained by letting $V_{R\triangle} = 0$ in Eq (76):

$$\omega_{\oplus\mathbb{C}}^2(x_{R\Delta}^2 + y_{R\Delta}^2) + \frac{2GM_\oplus}{r_{\oplus\Delta}} + \frac{2GM_\mathbb{C}}{r_{\mathbb{C}\Delta}} = C \quad (77)$$

where $r_{\oplus\Delta}$ and $r_{\mathbb{C}\Delta}$ are given by Eqs (72) and (73). Since only the squares of $y_{R\Delta}$ and $z_{R\Delta}$ enter into Eq (77), the surfaces defined are symmetrical with respect to the $x_R y_R$ and $x_R z_R$-planes. We obtain the intersection of the surfaces (Eq (77)) with the $x_R y_R$-plane or the trace in the $x_R y_R$-plane by letting $z_{R\Delta} = 0$ in that equation:

$$\omega_{\oplus\mathbb{C}}^2 (x_{R\Delta}^2 + y_{R\Delta}^2)$$

$$+ \frac{2GM_\oplus}{\left[\left(x_{R\Delta} - x_{R\oplus}\right)^2 + y_{R\Delta}^2\right]^{1/2}} \quad (78)$$

$$+ \frac{2GM_\mathbb{C}}{\left[\left(x_{R\Delta} - x_{R\mathbb{C}}\right)^2 + y_{R\Delta}^2\right]^{1/2}} = C$$

The curves (Eq (78)) are shown, not to scale, in Fig. 2, and from them the general characteristics of motion in the moon's orbital plane can be deduced.

The values of C in Fig. 2 are numerically in the order $C_1 > C_2 > C_3 > \ldots$. For initial conditions corresponding to $C = C_1$, the vehicle can move either in a closed region about the earth or in a closed region about the moon: it remains a satellite of the earth or the moon. If the initial conditions correspond to $C = C_3$, the vehicle can move within a closed contour around the earth-moon system such that motion from earth to moon is possible. The limiting case separating earth or moon orbits from earth-moon or moon-earth trajectories is represented by $C = C_2$. For the value $C = C_5$, the vehicle can escape entirely from the earth-moon system since the region of possible vehicle motion is open behind the moon. The value $C = C_4$ separates the earth-moon or moon-earth trajectories from possible escape trajectories from the earth-moon system. Besides these inner bounds of vehicle motion there are, for the same C values, closed outer boundaries around the earth-moon system beyond which motion is also possible. A vehicle coming from very far away with $C > C_4$ cannot approach the earth or moon any closer than the outer boundary of the $C = C_4$ contour of Fig. 2. When $C = C_4$ the inner and outer branches of the curve of zero relative velocity coalesce. For $C < C_4$ a vehicle starting near the earth or moon can escape from the system and one starting from a remote point can reach either body. As C decreases to C_5 and beyond, the opening in the contour behind the moon widens. When $C = C_6$

the contour also begins to open behind the earth and when $C = C_7$ the only portions of the plane excluded from motion of a vehicle are the interiors of 2 kidney-shaped regions above and below the x_R-axis. As C decreases further to a value of C_8, the regions of exclusion shrink to two points, each completing an equilateral triangle with the earth and moon. No region of the $x_R y_R$-plane is excluded if $C < C_8$.

The points at which the contours corresponding to $C = C_2$, C_4 and C_6 coalesce together with the 2 points for which $C = C_8$ are called double points. From the equation for the surfaces of zero relative velocity (Eq (77)) and from the traces of these surfaces in the $x_R y_R$, $x_R z_R$ and $y_R z_R$-planes such as Fig. 2, it can be seen that all the double points are in the $x_R y_R$-plane. Hence it it sufficient to consider the trace in the $x_R y_R$-plane, Eq (78), for the determination of the double points. These double points are of interest as critical points of the curves:

$$F(x, y) = \omega_{\oplus\mathbb{C}}^2\left(x_{R\Delta}^2 + y_{R\Delta}^2\right)$$

$$+ \frac{2GM_\oplus}{\left[\left(x_{R\Delta} - x_{R\oplus}\right)^2 + y_{R\Delta}^2\right]^{1/2}}$$

$$+ \frac{2GM_\mathbb{C}}{\left[\left(x_{R\Delta} - x_{R\mathbb{C}}\right)^2 + y_{R\Delta}^2\right]^{1/2}} - C = 0 \quad (79)$$

The condition for a critical point is that the first derivatives of Eq (78) with respect to $x_{R\Delta}$ and $y_{R\Delta}$ be zero, i.e.:

$$\omega_{\oplus\mathbb{C}}^2 x_{R\Delta} - \frac{GM_\oplus (x_{R\Delta} - x_{R\oplus})}{\left[\left(x_{R\Delta} - x_{R\oplus}\right)^2 + y_{R\Delta}^2\right]^{3/2}}$$

$$- \frac{GM_\mathbb{C}\left(x_{R\Delta} - x_{R\mathbb{C}}\right)}{\left[\left(x_{R\Delta} - x_{R\mathbb{C}}\right)^2 + y_{R\Delta}^2\right]^{3/2}} = 0$$

$$\omega_{\oplus\mathbb{C}}^2 y_{R\Delta} - \frac{GM_\oplus y_{R\Delta}}{\left[\left(x_{R\Delta} - x_{R\oplus}\right)^2 + y_{R\Delta}^2\right]^{3/2}}$$

$$\quad (80)$$

$$- \frac{GM_\mathbb{C} y_{R\Delta}}{\left[\left(x_{R\Delta} - x_{R\mathbb{C}}\right)^2 + y_{R\Delta}^2\right]^{3/2}} = 0$$

It should be noted that Eqs (80) are identical to the equations of motion (Eqs (71)) with $z_{R\Delta} = 0$, and which can be written:

$$\ddot{x}_{RA} - 2\omega_{\oplus\mathbb{C}}\dot{y}_{RA} = \frac{1}{2}\frac{\partial F\left(x_{RA}, y_{RA}\right)}{\partial x_{RA}}$$

$$\ddot{y}_{RA} - 2\omega_{\oplus\mathbb{C}}\dot{x}_{RA} = \frac{1}{2}\frac{\partial F\left(x_{RA}, y_{RA}\right)}{\partial y_{RA}} \qquad (81)$$

Since at the critical points

$$\frac{\partial F}{\partial x_{RA}} = 0, \quad \frac{\partial F}{\partial y_{RA}} = 0$$

and since we are on a surface of zero relative velocity

$$V_{RA} = \left[\dot{x}_{RA}^2 + \dot{y}_{RA}^2\right]^{1/2} = 0$$

we obtain from Eqs (81)

$$\ddot{x}_{RA} = 0, \quad \ddot{y}_{RA} = 0.$$

Hence the coordinates of the vehicle at the critical points satisfy the differential equations and it will remain at the critical point unless it is disturbed by forces from outside of the dynamical system. We proceed to obtain the critical points. The second equation of Eq (80) is satisfied by $y_{RA} = 0$ and the double points on the x_R-axis or the straight line solutions to the problem are given by:

$$\omega_{\oplus\mathbb{C}}^2 x_{RA} - \frac{GM_\oplus\left(x_{RA} - x_{R\oplus}\right)}{\left[\left(x_{RA} - x_{R\oplus}\right)^2\right]^{3/2}}$$

$$\qquad (82)$$

$$- \frac{GM_\mathbb{C}\left(x_{RA} - x_{R\mathbb{C}}\right)}{\left[\left(x_{RA} - x_{R\mathbb{C}}\right)^2\right]^{3/2}} = 0$$

If, as in Ref. 8, the units are normalized such that the sum $M = M_\oplus + M_\mathbb{C}$ is the unit of mass and the distance between the earth and moon or lunar unit (LU) is the unit of length, then the double points can be given in a convenient form. Let the double points on the x_R-axis be denoted by x_{Ri}, x_{RM} and x_{Re} which correspond to C_2, C_4 and C_6, respectively. Then from Moulton (Ref. 8, pages 292-293), for $M_\mathbb{C}$ small compared to $M_\oplus$ and hence small ν, the three straight line solutions can be obtained by expressing them as power series in $\nu^{1/3}$ and determining the coefficients. The result is:

$$x_{Ri} - x_{R\mathbb{C}} = \left(\frac{\nu}{3}\right)^{1/3} - \frac{1}{3}\left(\frac{\nu}{3}\right)^{2/3} - \frac{1}{9}\left(\frac{\nu}{3}\right) + \cdots$$

$$x_{RM} - x_{R\mathbb{C}} = \left(\frac{\nu}{3}\right)^{1/3} + \frac{1}{3}\left(\frac{\nu}{3}\right)^{2/3} - \frac{1}{9}\left(\frac{\nu}{3}\right) + \cdots$$

$$x_{Re} - x_{R\mathbb{C}} = 2 - \frac{7}{12}\nu - 23\frac{(7)^2}{12^4}\nu^3 + \cdots$$

$$\qquad (83)$$

in LU, and where $\nu = \frac{M_\mathbb{C}}{M} = 0.01214226$.

Since $x_{R\mathbb{C}} = (1 - \nu)$ LU, the double points in terms of distances along the x_R-axis are:

$$x_{Ri} = 0.83741 \quad LU$$

$$x_{RM} = 1.15524 \quad LU$$

$$x_{Re} = 1.00506 \quad LU$$

For this force model of the earth-moon system (see Chapter IV, Section B), a consistent value is 1 LU = 384, 747.2 km. Hence, in MKS units

$$x_{Ri} = 322,190 \quad km$$

$$x_{RM} = 444,480 \quad km$$

$$x_{Re} = -386,690 \quad km$$

Substituting these values into Eq (78) with $y_{RA} = 0$, C_2, C_4 and C_6 can be found. These values are:

$$C_2 = 3.34367 \left(\frac{km}{sec}\right)^2$$

$$C_4 = 3.322621 \left(\frac{km}{sec}\right)^2$$

$$C_6 = 3.15895 \left(\frac{km}{sec}\right)^2$$

From Eq (80), the double points corresponding to C_8 are found to be equidistant from the earth and moon, and form an equilateral triangle with these two and with coordinates

$$x_{RS} = 187,702 \quad km$$

$$y_{RS} = \pm 333,201 \quad km$$

The value of C_8 from this equilateral triangle solution is:

$$C_8 = 3.13365 \left(\frac{km}{sec}\right)^2.$$

These values of C_2, C_4, C_6 and C_8 can be made more meaningful if the velocity of a vehicle near the earth is calculated using these values. For the calculations, the positions of the vehicle will be chosen as 100 km and 1000 km from the surface of the earth on the x_R-axis both adjacent and opposite to the moon. If the equatorial radius of the earth (6, 378.2 km) is used, these coordinates are:

$$x_{\Delta 1} = 1,006.5 \text{ km} \qquad \text{Case I:} \qquad \begin{array}{l}\text{100 km above} \\ \text{surface of earth} \\ \text{adjacent to moon}\end{array}$$

$x_{\triangle 2} = 2,706.5\,\text{km}$ Case II: 1000 km above surface of earth adjacent to moon

$x_{\triangle 3} = -11,149.9\,\text{km}$ Case III: 100 km above surface of earth opposite to moon

$x_{\triangle 4}$ -12,049.9 km Case IV: 1000 km above surface of earth opposite to moon

The following sketch shows the position of the five double points.
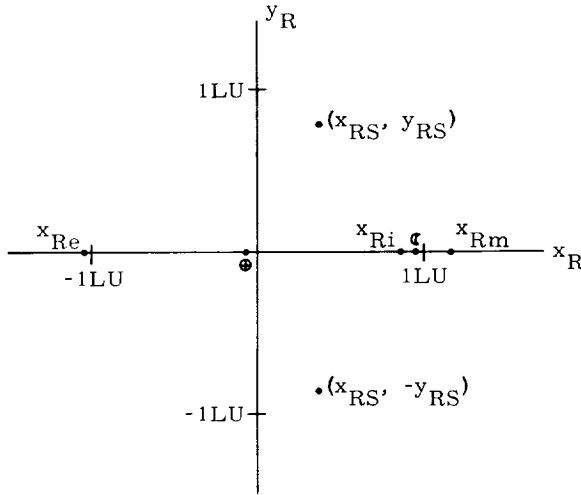
The velocities are then found from Jacobi's integral to be:

	I	II	III	IV
$C_2 = 3.34367$	10942.2	10233.3	10942.2	10233.2
$C_4 = 3.32621$	10943.4	10234.6	10943.4	10234.6
$C_6 = 3.15895$	10951.1	10242.8	10951.1	10242.8
$C_8 = 3.13365$	10952.3	10244.1	10952.3	10244.1

The magnitude of $V_{R\triangle}$ is the same regardless of direction although it is seen to vary from point to point (Cases I to IV correspond to different points). From Eq (76), Fig. 2 and the preceding sketch, it follows that on a circle with small radius about the earth, the velocity is relatively insensitive to position on the circle. This is also evident from the table by comparing Cases I and II (altitude 100 km, radius 6478.2 km with positions adjacent and opposite to the moon) where the difference is too small to detect. According to Egorov at an altitude of 200 km (radius 6578.2 km), the variations in $V_{R\triangle}$ are of order less than 0.01 m/sec and by comparing Cases II and IV (altitude 1000 km, radius 7378.2 km with positions adjacent and opposite to the moon), the variations are of order 0.1 m/sec. The radius of the circle around the earth has a very pronounced effect on the required

$V_{R\triangle}$. A change in altitude from 100 to 1000 km lowers the values of the critical $V_{R\triangle}$'s by 709 m/sec, indicating that the minimum required injection velocity for lunar trajectories is quite sensitive to the injection altitude.

The table also reveals that the velocities corresponding to C_4 are lower than those corresponding to C_6; therefore, it is easier to escape from the vicinity of the earth by projecting toward the moon than it is by projecting away from the moon. The large qualitative difference between the $C = C_2$ and $C = C_4$, as well as the $C = C_6$ and $C = C_8$ contours of Fig. 2, should be compared with the small differences in projection velocities, indicating the sensitivity of lunar trajectories to initial velocities.

The velocities $V_{R\triangle}$ given in table are measured in the rotating $x_R y_R z_R$ coordinate system and are defined as

$$V_{R\triangle}^2 = \dot{x}_{R\triangle}^2 + \dot{y}_{R\triangle}^2 + \dot{z}_{R\triangle}^2 \tag{84}$$

while velocities in lunar trajectories are usually given in the earth-centered $x_e y_e z_e$ coordinate system defined as

$$V_{e\triangle}^2 = \dot{x}_{e\triangle}^2 + \dot{y}_{e\triangle}^2 + \dot{z}_{e\triangle}^2 \tag{85}$$

The transformation between the velocity components is

$$\begin{Bmatrix} \dot{x}_{e\triangle} \\ \dot{y}_{e\triangle} \\ \dot{z}_{e\triangle} \end{Bmatrix} = \left[T\left(\Phi + \omega_{\oplus\mathbb{C}}\, t\right) \right] \begin{Bmatrix} \dot{x}_{R\triangle} - \omega_{\oplus\mathbb{C}}\, y_{R\triangle} \\ \dot{y}_{R\triangle} + \omega_{\oplus\mathbb{C}}\,(x_{R\triangle} + \bar{r}_{\oplus\mathbb{C}}\, v) \\ \dot{z}_{R\triangle} \end{Bmatrix} \tag{86}$$

where $\left[T\left(\Phi + \omega_{\oplus\mathbb{C}}\, t\right) \right]$ is given by Eq (47).

Equations (84) to (86) show that $V_{e\triangle}$ depends on $V_{R\triangle}$, the position of the vehicle, as well as the direction of $V_{R\triangle}$. Since the magnitude of each $V_{R\triangle}$ in the previous table is independent of direction to each such value of $V_{R\triangle}$, there would correspond a range of values of $V_{e\triangle}$.

c. Stability of the double points

The five double points given here are special solutions of the equations of motion and are analogous to the special solutions of the three-body problem (see Section B-1). The question of stability of these five points is of importance; i.e., will the vehicle stay near the point if given a small displacement and velocity (stable solution) or will it rapidly depart from that point (unstable solution)? These small displacements and velocities may be regarded as due to small forces neglected in the present model, which

means that the space vehicle will actually remain near the stable double points but depart rapidly from the unstable ones. It can be shown (Ref. 8, pp 299 to 305 and Ref. 11, pp 7-25 to 7-28) that the straight-line solutions are unstable, while the equilateral triangle solutions are stable.

Equilateral triangle solutions have been observed in the solar system. With the Sun and Jupiter considered as the massive bodies, asteroids have been discovered at approximately the equilateral point and with a mean angular velocity equal to that of Jupiter (Ref. 12; p 243). Buchheim (Ref. 11) has proposed to establish satellites at the equilateral triangle points of the earth-moon system which could serve as space buoys.

It has been suggested by Moulton (Ref. 8) that the phenomenon of gegenschein, a hazy patch of light opposite to the sun, is caused by meteors temporarily trapped in unstable periodic orbits around the straight-line point opposite to the sun in the sun-earth system.

C. MOTION OF THE MOON

The position of the moon and its orientation in space are of paramount importance in lunar flight: the position is important in determining the required injection conditions, as well as the exact value of the gravitational force of the moon on the vehicle during flight, and the position together with the particular orientation of the moon are important for landings at specified lunar sites. For these reasons, the orbit of the moon assumed in the discussion of the three-body and restricted three-body problems is not accurate enough for precision trajectories, and a consideration of neglected forces in that model and a comparison with astronomical observations of the moon is necessary. It has been observed that the mean period of the moon's rotation about its axis is equal to its sidereal period of revolution around the earth. Because of this fact and since lunar vehicles originate and are observed from earth, it is advantageous to define the orientation of the moon with respect to earth. The moon rotates at a very nearly constant rate about its axis while its orbital angular velocity varies slightly due to the eccentricity of the lunar orbit. Thus, during different orbital positions of the moon, some areas on either side of the moon become visible. Similarly, the rotational axis of the moon is inclined by about 6.7° to the normal of the moon's orbital plane and areas beyond the north and south poles of the moon become visible from earth at various times. These apparent side-to-side and tilting movements of the moon which occur periodically, are known as optical librations. In addition, the gravitational attractions of the sun and planets on the triaxially ellipsoidal figure of the moon cause a slight wobble of the rotational axis of the moon which is called physical libration. At any given time, lunar librations are determined by the moon's precise   . orbital motion, its rotational rate, and dynamical effects of its asymmetrical figure.

The first part of this section discusses very briefly the methods used for computing the position of the moon, the comparison between computed and observed positions, and the tabulated lunar ephemerides. The latter part is devoted to

a brief discussion of lunar librations and to an approach for determining librations in a digital computer trajectory program which has stored positional data of the moon in geocentric equatorial coordinates.

1. Lunar Theory

Lunar theory in celestial mechanics is generally understood to be the analytical theory of the motion of the moon. The gravitational attraction of the earth and sun, and the earth's and lunar asphericity, as well as gravitational attractions of the planets as they affect the motion of the moon are considered. The methods employed in various lunar theories differ, but at present three methods, those of Delaunay, Hansen, and Hill-Brown, are referred to most frequently. A detailed discussion of these and other lunar theories can be found in Ref. 13. The brief discussion of lunar theories given here follows Refs. 13 and 14, as well as Ref. 2. The discussion is restricted to the "main problem" of lunar theory, which is the three-body problem of astronomy as applied to finding the motion of the spherical moon under the gravitational attraction of the spherical earth and sun.

a. Delaunay's lunar theory

Choose an inertial right-handed Cartesian coordinate system with origin at the center of mass of the dynamical system earth, moon, sun and axes $x'_0 \, y'_0 \, z'_0$. Let the mass of the earth be $M_\oplus$ with position $x'_{0\oplus} \, y'_{0\oplus} \, z'_{0\oplus}$. The position of the moon with mass $M_\mathbb{C}$ in this coordinate system is given by $x'_{0\mathbb{C}}, \, y'_{0\mathbb{C}}, \, z'_{0\mathbb{C}}$ and that of the sun with mass $M_\odot$ by $x'_{0\odot}, \, y'_{0\odot}, \, z'_{0\odot}$. The equations of motion of the moon are (compare with Eqs 56 and 57):

$$\left.\begin{aligned}
\ddot{x}'_{0\mathbb{C}} &= \frac{1}{M_\mathbb{C}} \frac{\partial U}{\partial x'_{0\mathbb{C}}} \\
\ddot{y}'_{0\mathbb{C}} &= \frac{1}{M_\mathbb{C}} \frac{\partial U}{\partial y'_{0\mathbb{C}}} \\
\ddot{z}'_{0\mathbb{C}} &= \frac{1}{M_\mathbb{C}} \frac{\partial U}{\partial z'_{0\mathbb{C}}}
\end{aligned}\right\} \qquad (87)$$

where

$$U = \frac{G M_\oplus M_\mathbb{C}}{r_{0,\oplus \to \mathbb{C}}} + \frac{G M_\oplus M_\odot}{r_{0,\oplus \to \odot}} + \frac{G M_\mathbb{C} M_\odot}{r_{0,\mathbb{C} \to \odot}} \qquad (88)$$

is the gravitational potential (work function) which is the negative of the gravitational potential energy of the dynamical system.

Since the three-body equations of motion (Eq (87)) cannot be solved in closed form, successive approximations must be used to obtain solutions in analytical form.

In the earth, moon, sun configuration $r_{0,\oplus \to \mathbb{C}}$ is small compared to $r_{0,\oplus \to \odot}$ or $r_{0,\mathbb{C} \to \odot}$ while $M_\odot$ is large compared to

$M_\oplus + M_\text{☾}$, and the earth-moon barycenter approximates unperturbed motion around the sun very well. It is, therefore, helpful to introduce coordinates of the moon relative to the earth,

$$x_{\oplus\text{☾}} = x'_{0\text{☾}} - x'_{0\oplus}$$

$$y_{\oplus\text{☾}} = y'_{0\text{☾}} - y'_{0\oplus} \tag{89}$$

$$z_{\oplus\text{☾}} = z'_{0\text{☾}} - z'_{0\oplus},$$

and coordinates of the sun relative to the earth-moon barycenter,

$$x_{0\,☉} = x'_{0☉} - \frac{M_\oplus x'_{0\oplus} + M_\text{☾} x'_{0\text{☾}}}{M_\oplus + M_\text{☾}}$$

$$y_{0\,☉} = y'_{0☉} - \frac{M_\oplus y'_{0\oplus} + M_\text{☾} y'_{0\text{☾}}}{M_\oplus + M_\text{☾}} \tag{90}$$

$$z_{0\,☉} = z'_{0☉} - \frac{M_\oplus z'_{0\oplus} + M_\text{☾} z'_{0\oplus}}{M_\oplus + M_\text{☾}}$$

The precise orientation of the axes need not be specified for this discussion, but, for agreement with previous notation, $x_{\oplus\text{☾}}$, $y_{\oplus\text{☾}}$, $z_{\oplus\text{☾}}$ are equatorial coordinates of the moon referred to the mean equator and equinox. After making the necessary transformations, the equations of motion (Eq (87)) become

$$\ddot{x}_{\oplus\text{☾}} = \frac{M_\oplus + M_\text{☾}}{M_\oplus M_\text{☾}} \frac{\partial U}{\partial x_{\oplus\text{☾}}}$$

$$\ddot{y}_{\oplus\text{☾}} = \frac{M_\oplus + M_\text{☾}}{M_\oplus M_\text{☾}} \frac{\partial U}{\partial y_{\oplus\text{☾}}} \tag{91}$$

$$\ddot{z}_{\oplus\text{☾}} = \frac{M_\oplus + M_\text{☾}}{M_\oplus M_\text{☾}} \frac{\partial U}{\partial z_{\oplus\text{☾}}}$$

It remains to express U in terms of the new coordinates. Let $r_{\oplus\text{☾}}^2 = x_{\oplus\text{☾}}^2 + y_{\oplus\text{☾}}^2 + z_{\oplus\text{☾}}^2$ be the square of the distance from the earth to the moon, $r_{\oplus☉}^2 = x_{0☉}^2 + y_{0☉}^2 + z_{0☉}^2$ be the square of the distance from the earth to the sun with components in the respective coordinate systems (the earth-moon barycenter is very close to the earth), and S the angle at earth between the earth-moon and earth-sun lines (see following sketch). Then, as in Ref. 14, page 270, $r_{0,\oplus \to \text{☾}}^{-1}$, $r_{0,\oplus \to ☉}^{-1}$ and $r_{0,\text{☾} \to ☉}^{-1}$ can be expressed in terms of $r_{\oplus\text{☾}}$, $r_{\oplus☉}$ and Legendre polynomials of cos S, P_n (cos S), to yield for the gravitational potential:

$$U = G\left[\frac{M_\oplus M_\text{☾}}{r_{\oplus\text{☾}}} + \frac{(M_\oplus + M_\text{☾}) M_☉}{r_{\oplus☉}}\right.$$

$$+ \frac{M_\oplus M_\text{☾} M_☉}{M_\oplus + M_\text{☾}} \frac{r_{\oplus\text{☾}}^2}{r_{\oplus☉}^3} P_2 (\cos S)$$

$$+ \frac{M_\oplus M_\text{☾} M_☉ (M_\oplus - M_\text{☾})}{(M_\oplus + M_\text{☾})^2} \frac{r_{\oplus\text{☾}}^3}{r_{\oplus☉}^4} P_3 (\cos S) \tag{92}$$

$$+ \frac{M_\oplus M_\text{☾} M_☉ (M_\oplus^2 - M_\oplus M_\text{☾} + M_\text{☾}^2)}{(M_\oplus + M_\text{☾})^3}$$

$$\left. \frac{r_{\oplus\text{☾}}^4}{r_{\oplus☉}^5} P_4 (\cos S) + \ldots \right]$$
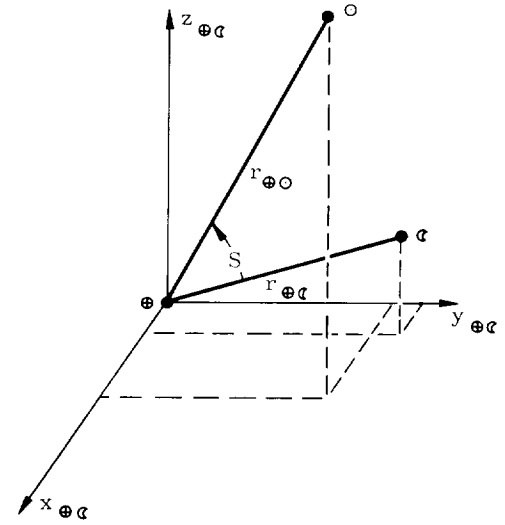
The equations of motion of the moon (Eq (91)) can now be written in the form

$$\ddot{x}_{\oplus\text{☾}} + \frac{G(M_\oplus + M_\text{☾})}{r_{\oplus\text{☾}}^3} x_{\oplus\text{☾}} = \frac{\partial R}{\partial x_{\oplus\text{☾}}}$$

$$\ddot{y}_{\oplus\text{☾}} + \frac{G(M_\oplus + M_\text{☾})}{r_{\oplus\text{☾}}^3} y_{\oplus\text{☾}} = \frac{\partial R}{\partial y_{\oplus\text{☾}}} \tag{93}$$

$$\ddot{z}_{\oplus\text{☾}} + \frac{G(M_\oplus + M_\text{☾})}{r_{\oplus\text{☾}}^3} z_{\oplus\text{☾}} = \frac{\partial R}{\partial z_{\oplus\text{☾}}}$$

where, if we substitute the expressions for the Legendre polynomials,

$$R = \frac{G M_☉}{r_{\oplus☉}} \left[\left(\frac{r_{\oplus\text{☾}}}{r_{\oplus☉}}\right)^2 \left(-\frac{1}{2} + \frac{3}{2}\cos^2 S\right)\right.$$

$$\tag{94}$$

$$\left. + \frac{M_\oplus - M_\text{☾}}{M_\oplus + M_\text{☾}} \left(\frac{r_{\oplus\text{☾}}}{r_{\oplus☉}}\right)^3 \cdot \left(-\frac{3}{2}\cos S + \frac{5}{2}\cos^3 S\right)\right.$$

$$+ \frac{M_\oplus^2 - M_\oplus M_\mathbb{C} + M_\mathbb{C}^2}{(M_\oplus + M_\mathbb{C})^2} \left(\frac{r_{\oplus\mathbb{C}}}{r_{\oplus\odot}}\right)^4 \left(\frac{3}{8} - \frac{15}{4} \cos^2 S\right. \tag{94}$$

$$\left.\left. - \frac{35}{8} \cos^4 S\right) + \ldots \right].$$

In this expression for R the term $\dfrac{G(M_\oplus + M_\mathbb{C})M_\odot}{M_\oplus M_\mathbb{C} \, r_{\oplus\odot}}$

has been omitted since it is independent of $x_{\oplus\mathbb{C}}$, $y_{\oplus\mathbb{C}}$ and $z_{\oplus\mathbb{C}}$.

The second term on the left-hand side of the equations of motion (Eq (93)) is due to the gravitational attraction of the moon by the earth, and R is the disturbing function which in this case is due to the gravitational attraction of the sun by the earth. If $R \equiv 0$ the intermediate orbit, or first approximation to the path of the moon, is an ellipse.

The expression for R may be modified further by using Kepler's third law for the motion of the earth-moon barycenter,

$$G(M_\odot + M_\oplus + M_\mathbb{C}) = n_\odot^2 a_\odot^3, \tag{95}$$

where $n_\odot$ and $a_\odot$ are the sun's mean motion and semimajor axis, respectively. If we ignore the mass of the earth and moon compared to that of the sun, and that of the moon with respect to the earth, then we obtain after some manipulations:

$$R = n_\odot^2 a_\mathbb{C}^2 \left[\left(\frac{r_{\oplus\mathbb{C}}}{a_\mathbb{C}}\right)^2 \left(\frac{a_\odot}{r_{\oplus\odot}}\right)^3 \left(-\frac{1}{2} + \frac{3}{2}\cos^2 S\right)\right.$$

$$+ \frac{a_\mathbb{C}}{a_\odot} \left(\frac{r_{\oplus\mathbb{C}}}{a_\mathbb{C}}\right)^3 \left(\frac{a_\odot}{r_{\oplus\odot}}\right)^4 \left(-\frac{3}{2}\cos S + \frac{5}{2}\cos^3 S\right)$$

$$\tag{96}$$

$$+ \left(\frac{a_\mathbb{C}}{a_\odot}\right)^2 \left(\frac{r_{\oplus\mathbb{C}}}{a_\mathbb{C}}\right)^4 \left(\frac{a_\odot}{r_{\oplus\odot}}\right)^5 \left(-\frac{3}{8} - \frac{15}{4}\cos^2 S\right.$$

$$\left.\left. - \frac{35}{8}\cos^4 S\right) + \ldots \right] = R_1 + R_2 + R_3 + \ldots$$

In Delaunay's lunar theory the orbit of the earth around the sun is a fixed ellipse in a fixed plane. The expression (Eq (96)) for R can now be expanded in terms of elliptic elements of the moon's and sun's orbits. Delaunay's series for R consists of one constant and 320 periodic terms (Ref. 13).

The method of variation of parameters, also known as variation of elements and variation of arbitrary constants, is used in the solution of the lunar equations of motion. Consider the case $R = 0$. Then the instantaneous coordinates and velocity components of the moon allow the determination of a unique set of six orbital elements

for the intermediate orbit of the moon which are constants of the motion. In actual motion $R \neq 0$ and the orbital elements vary with time for the true orbit. The requirement of the method is that the coordinates and velocity components expressed in terms of the elements and time have the same form for the intermediate (R = 0) and the true ($R \neq 0$) orbit. For the actual motion, one can obtain six first-order differential equations (called variation of parameter equations) which give the time-variation of the elements and are fully equivalent to the equations of motion (Eq (93)). The procedure calls for integration of the variation of parameter equations to obtain the orbital elements as functions of time and expressed as sums of trigonometric series. Finally the coordinates as well as velocity components may be obtained as functions of time by a coordinate transformation.

Delaunay chooses a set of elements so that the system of differential equations takes the canonical form:

$$\left.\begin{array}{ll}
\dfrac{dL}{dt} = \dfrac{\partial \tilde{F}}{\partial e}, & \dfrac{d\ell}{dt} = -\dfrac{\partial \tilde{F}}{\partial L} \\[2ex]
\dfrac{dG}{dt} = \dfrac{\partial \tilde{F}}{\partial g}, & \dfrac{dg}{dt} = -\dfrac{\partial \tilde{F}}{\partial G} \\[2ex]
\dfrac{dH}{dt} = \dfrac{\partial \tilde{F}}{\partial h}, & \dfrac{dh}{dt} = -\dfrac{\partial \tilde{F}}{\partial H}
\end{array}\right\} \tag{97}$$

These canonical elements or Delaunay variables are, in terms of μ and the elliptic elements given in section A-3.

$$L = (\mu a)^{1/2}$$

$$G = (\mu a)^{1/2} (1 - e^2)^{1/2}$$

$$H = (\mu a)^{1/2} (1 - e^2)^{1/2} \cos i \tag{98}$$

$$h = \Omega$$

$$g = \omega$$

$$\ell_0 = \int n \, dt + \ell , \text{ the mean anomaly at any}$$
$$\text{time}$$

and

$$\tilde{F} = \frac{\mu^2}{2L^2} + R \tag{99}$$

is the Hamiltonian of the system.

The variation of parameter equations (Eq (97)) cannot be solved in closed form, just as one cannot solve in closed form the equations of motion of the three-body problem, and some approximation procedure has to be used. The coefficients of the disturbing function R are expanded in power series in $e_\mathbb{C}$, $\sin \frac{1}{2} i_{\epsilon m}$, $e_\odot$ and $\dfrac{a_\mathbb{C}}{a_\odot}$ (and not explicitly in canonical elements), while the general

argument is a function of the angles h, g, ℓ referring to the moon's orbit, and the mean anomaly of the sun $\ell_\odot$. During the integration, powers of $\dfrac{n_\odot}{n_\mathbb{C}}$ appear as part of the power series.

The principle of Delaunay's method consists of introducing a force function

$$\overline{F} = \frac{\mu^2}{2\,L^2} + P_1 + Q_1 \cos\theta, \qquad (100)$$

where P_1 denotes the nonperiodic terms in the expansion of R, and $Q_1 \cos\theta$ is one single periodic term selected from the expansion of R. Delaunay then integrated the canonical equations by using $\overline{F}$ instead of $\widetilde{F}$ by applying a canonical transformation to new canonical variables L', G', H', ℓ', g' and h'. This transformation is applied to $\widetilde{F}$ and the term $Q_1 \cos\theta$ has disappeared from R. Delaunay used a succession of canonical transformations (or contact transformations) until the coefficients of the periodic series became sufficiently small to be neglected.

By use of this method Delaunay has obtained a literal solution to the main problem of lunar theory which was presented in two volumes. His results may be readily extended to include other effects on the motion of the moon (Ref. 13).

The utilization of systems of differential equations in canonical form has the advantage that general rules can be established governing transformations from one set of variables to another, which is helpful if one considers the large number of transformations required. One drawback to Delaunay's method is the slow convergence of the coefficients in powers of $\dfrac{n_\odot}{n_\mathbb{C}} = 0.00748$ in the case of the moon. Convergence in terms of the other parameters is generally satisfactory.

b. Hansen's lunar theory

Hansen considers the motion of the moon in its instantaneous orbit plane and starts with the variation of parameters differential equations. For the orbital elements Ω, i, ω, a, e and ℓ_0 these equations, which are equivalent to Delaunay's canonical equations (Eq (97)) (Refs. 3 and 14), become

$$\frac{d\Omega}{dt} = \frac{1}{na^2 (1-e^2)^{1/2} \sin i} \frac{\partial R}{\partial i}$$

$$\frac{di}{dt} = \frac{\cot i}{na^2 (1-e^2)^{1/2}} \frac{\partial R}{\partial \omega}$$

$$- \frac{1}{na^2 (1-e^2)^{1/2} \sin i} \frac{\partial R}{\partial \Omega} \qquad (101)$$

$$\frac{d\omega}{dt} = \frac{(1-e^2)^{1/2}}{na^2 e} \frac{\partial R}{\partial e} - \frac{\cot i}{na^2 (1-e^2)^{1/2}} \frac{\partial R}{\partial i}$$

$$\frac{da}{dt} = \frac{2}{na} \frac{\partial R}{\partial \ell_0}$$

$$\frac{de}{dt} = \frac{1-e^2}{na^2 e} \frac{\partial R}{\partial \ell_0} - \frac{(1-e^2)^{1/2}}{na^2 e} \frac{\partial R}{\partial \omega}$$

$$\frac{d\ell_0}{dt} = -\frac{2}{na} \frac{\partial R}{\partial a} - \frac{1-e^2}{na^2 e} \frac{\partial R}{\partial e} \qquad \begin{matrix}(101)\\ \text{(continued)}\end{matrix}$$

These equations have been derived in Chapter IV of Ref. 3.

In Hansen's method, the plane of the sun need not be fixed, and the fixed plane of reference may be chosen as the ecliptic of a given date or any other plane inclined at a small angle to the ecliptic. However, the motion of the sun must be known.

Consider first the motion of the moon in its instantaneous orbit plane. Define an intermediate orbit in the plane of the moon's instantaneous orbit and one focus at the origin. Let it have constant elements n, a, e and mean anomaly nz where z is a variable with units of time. Let the elements of the intermediate orbit satisfy $\tilde{n}^2 \tilde{a}^3 = G(M_\oplus + M_\mathbb{C})$ and let its perigee have a forward motion $\tilde{n}y$ in the plane of the orbit where y is an unknown constant depending on the attraction of the moon. Impose the additional condition that the point on the intermediate orbit with true anomaly $\tilde{f}$ and radius $\tilde{r}$ lies on the actual radius to the moon. If the true radius to the moon is r, then put

$$r = \tilde{r}(1+k), \qquad (102)$$

where k is the fraction of the lunar radius between the intermediate and lunar orbits. The motion of the moon in the instantaneous plane of the orbit can be given as soon as z and k are determined in terms of time and the introduced constants. In the determination of k and z a single function W of the variable elements is used. Hence, in Hansen's method, the angular perturbations in the plane of the orbit are added to the mean anomaly of the intermediate orbit and the radial perturbations are expressed by the ratio of the true and intermediate radius vectors.

Next the differential equations for the latitude of the moon above the fixed reference plane are obtained by considering the motion of the instantaneous orbit plane.

The motion of the instantaneous orbit plane is independent of the motion of the moon in that plane. Finally, by a transformation of coordinates it can be shown that some very small corrections have to be added to the true orbital longitude in the instantaneous orbit in order to

obtain the true orbital longitude $(\Omega + \omega + f)$ referred to a fixed direction in a fixed reference plane. The differential equations are solved by successive approximations, with the expansion of R in terms of elliptic elements and time being now somewhat different from the form used by Delaunay since the sun's orbit is not fixed.

The slow convergence of the coefficients in powers of $\dfrac{n_\odot}{n_\mathbb{C}}$ has been overcome by starting with assumed numerical values of all parameters entering into the theory as obtained from observation. If the observations improve, then small changes in these values have to be taken into account. Tables based on Hansen's lunar theory were introduced into the calculation of the lunar ephemeris in 1862 (Ref. 14).

c. Hill-Brown lunar theory

Both Delaunay's and Hansen's lunar theories consider the motion of the moon in the osculating plane, or the plane which at each instant contains the origin of coordinates, the radius and velocity vectors of the moon. The method of variation of parameters is then used to obtain the motion of the moon. The Hill-Brown lunar theory, on the other hand, uses rectangular coordinates referred to axes moving with the constant angular velocity of the sun's mean motion, $n_\odot$. Advantages in using rectangular coordinates are: the development of R in terms of elliptic elements is unnecessary, and the perturbations are obtained in a form more immediately suitable for ephemeris calculations (Ref. 14).

The theory begins with the expansion of those perturbations that depend on $\dfrac{n_\odot}{n_\mathbb{C}}$ with the following simplifications in the original equations:

(1) The disturbing function R is given by R_1 only (see Eq (96)) which means that $\dfrac{a_\mathbb{C}}{a_\odot}$ is neglected in the series expansion.

(2) The moon is assumed to move in the plane of the ecliptic ($i_{\epsilon m} = 0$).

(3) The sun's orbit about the earth-moon barycenter is circular ($e_\odot = 0$, $a_\odot = r_{\oplus\odot}$).

The remaining differential equations thus give all terms depending on $\dfrac{n_\odot}{n_\mathbb{C}}$ and $e_\mathbb{C}$, and the terms depending on $e_\mathbb{C}$ may be eliminated by obtaining a particular solution of those equations.

Choose an ecliptic coordinate system with origin at the center of the earth as in Section A-1 and the $x_{\epsilon\mathbb{C}}$, $y_{\epsilon\mathbb{C}}$ axes in the fixed plane of the ecliptic. By assumption (2) above $z_{\epsilon\mathbb{C}} = 0$.

The results of Section C-1a carry over directly since the orientation of the axes was not specified rigorously in this development. With the other assumptions the equations of motion (Eq (93)) become, by use of Eq (96) and a change in notation,

$$\left.\begin{array}{l} \ddot{x}_{\epsilon\mathbb{C}} + \dfrac{G(M_\oplus + M_\mathbb{C})}{r^3_{\epsilon\mathbb{C}}} x_{\epsilon\mathbb{C}} = \dfrac{\partial R_1}{\partial x_{\epsilon\mathbb{C}}} \\[4mm] \ddot{y}_{\epsilon\mathbb{C}} + \dfrac{G(M_\oplus + M_\mathbb{C})}{r^3_{\epsilon\mathbb{C}}} y_{\epsilon\mathbb{C}} = \dfrac{\partial R_1}{\partial x_{\epsilon\mathbb{C}}} \end{array}\right\} \quad (103)$$

where

$$\left.\begin{array}{l} R_1 = n^2_\odot r^2_{\oplus\mathbb{C}} \left(-\dfrac{1}{2} + \dfrac{3}{2}\cos^2 S\right) \\[3mm] r^2_{\epsilon\mathbb{C}} = x^2_{\epsilon\mathbb{C}} + y^2_{\epsilon\mathbb{C}} \end{array}\right\} \quad (104)$$

Introduce a coordinate system $x_R\, y_R\, z_R$ rotating with angular velocity $n_\odot$ so that the x_R-axis is always in the direction of the sun. The equations of motion of the moon become in this coordinate system (compare with Eqs (74) and (75)):

$$\left.\begin{array}{l} \ddot{x}_{R\mathbb{C}} - 2n_\odot \dot{y}_{R\mathbb{C}} = \dfrac{\partial W}{\partial x_{R\mathbb{C}}} \\[4mm] \ddot{y}_{R\mathbb{C}} + 2n_\odot \dot{x}_{R\mathbb{C}} = \dfrac{\partial W}{\partial y_{R\mathbb{C}}} \end{array}\right\} \quad (105)$$

with

$$W = \dfrac{G(M_\oplus + M_\mathbb{C})}{r_{\epsilon\mathbb{C}}} + \dfrac{1}{2} n^2_\odot (x^2_{R\mathbb{C}} + y^2_{R\mathbb{C}}) + R_1 \quad (106)$$

Introduction of $r_{\epsilon\mathbb{C}} \cos S = x_{R\mathbb{C}}$ into the expression (Eq (104)) for R_1 permits us to write

$$W = \dfrac{G(M_\oplus + M_\mathbb{C})}{r_{\epsilon\mathbb{C}}} + \dfrac{3}{2} n^2_\odot x^2_{R\mathbb{C}}, \quad (107)$$

and yields for the equations of motion:

$$\left.\begin{array}{l} \ddot{x}_{R\mathbb{C}} - 2n_\odot \dot{y}_{R\mathbb{C}} + \dfrac{G(M_\oplus + M_\mathbb{C})}{r^3_{\epsilon\mathbb{C}}} x_{R\mathbb{C}} \\[4mm] \qquad - 3n^2_\odot x^2_{R\mathbb{C}} = 0 \\[6mm] \ddot{y}_{R\mathbb{C}} + 2n_\odot \dot{x}_{R\mathbb{C}} + \dfrac{G(M_\oplus + M_\mathbb{C})}{r^3_{\epsilon\mathbb{C}}} y_{R\mathbb{C}} = 0 \end{array}\right\} \quad (108)$$

To obtain a solution to Eq (108) that depends on $\dfrac{n_\odot}{n_\mathbb{C}}$ only, consider the initial conditions

$$x_{R\,\mathbb{C}}(t=t_0) = c_1$$

$$y_{R\,\mathbb{C}}(t=t_0) = 0$$

$$\dot{x}_{R\,\mathbb{C}}(t=t_0) = 0 \qquad\qquad (109)$$

$$\dot{y}_{R\,\mathbb{C}}(t=t_0) = c_2$$

that is, the moon is in conjunction with the sun at $t = t_0$.

Poincaré has shown that the initial conditions (Eq (109)) yield in the rotating coordinate system a periodic solution of the form

$$x_{R\,\mathbb{C}} = A_0 \cos (n_{\mathbb{C}} - n_{\odot})(t-t_0) + A_1 \cos 3$$

$$(n_{\mathbb{C}} - n_{\odot})(t-t_0) + A_2 \cos 5 (n_{\mathbb{C}} - n_{\odot})$$

$$(t-t_0) + \ldots$$

$$y_{R\,\mathbb{C}} = B_0 \sin (n_{\mathbb{C}} - n_{\odot})(t-t_0) + B_1 \sin 3 \qquad (110)$$

$$(n_{\mathbb{C}} - n_{\odot})(t-t_0) + B_2 \sin 5 (n_{\mathbb{C}} - n_{\odot})$$

$$(t-t_0) + \ldots$$

where A_i and B_i, $i = 0, 1, 2, \ldots$ are constants. This periodic solution is taken as the intermediate orbit in the Hill-Brown lunar theory. The intermediate orbit allows one to determine the coefficients with any accuracy in $\dfrac{n_{\odot}}{n_{\mathbb{C}}}$, which circumvents the slow convergence of the coefficients in the expansion of R in powers of $\dfrac{n_{\odot}}{n_{\mathbb{C}}}$ encountered in Delaunay's lunar theory (Ref. 13).

The first step for solving the main problem of lunar theory consists of determining the intermediate orbit, i.e., the coefficients A_i, B_i in Eq (110) in terms of the parameter $m = \dfrac{n_{\odot}}{n_{\mathbb{C}} - n_{\odot}}$ for which Hill adopted a numerical value of $m = 0.080848933808312$. Next the general solution of the differential equations (Eq (108)) is obtained, i.e., terms in R whose coefficients depend on m and $e_{\mathbb{C}}$ are considered. Then the simplification $e_{\odot} = 0$, $a_{\odot} = r_{\epsilon\odot}$ is lifted and terms in R whose coefficients depend on m and $e_{\odot}$ are considered. This procedure is continued by considering terms in R whose coefficients depend on m, $a_{\odot}^{-1}$; m, $\sin \frac{1}{2} i_{\epsilon m}$; as well as m and combinations of $e_{\odot}$, $e_{\mathbb{C}}$, $\sin \frac{1}{2} i_{\epsilon m}$, $a_{\odot}^{-1}$ and higher powers thereof.

The Hill-Brown lunar theory consists first of the development of a solution to the equations of

motion of the moon for the main problem of lunar theory as outlined above and secondly of the perturbations of this solution due to the direct and indirect gravitational attraction of the planets, the shape of the earth and tri-axiality of the moon. The obtained coordinates of the moon are expressed as explicit functions of time. Thirdly, Brown (Ref. 15) computed tables deriving coefficients of all periodic terms to an accuracy of the order of $0''.001$ in true orbital longitude $(\Omega + \ldots + f)$, celestial latitude φ_{ϵ}, and $0''.0001$ in sine parallax (Ref. 16) by keeping terms of the order $\left(\dfrac{n_{\odot}}{n_{\mathbb{C}}}\right)^6$, $e_{\mathbb{C}}^6$, $e_{\odot}^4$, $\sin^6 \frac{1}{2} i_{\epsilon m}$, $\left(\dfrac{a_{\mathbb{C}}}{a_{\odot}}\right)^3$ in the disturbing function R for the main problem in the lunar theory.

Brown's tables have been used for the calculation of lunar ephemerides from 1923 to 1959. However, in order to obtain the position of the moon to the desired precision of $0^s.001$ in right ascension and $0''.01$ in declination, the lunar ephemeris since 1960 is based on values of true orbital longitude, celestial latitude and horizontal parallax calculated directly from the trigonometric series obtained from the Hill-Brown theory, not Brown's tables. It has been shown in Ref. 16, pages 364 through 417, that there exist discrepancies in the calculation of the moon's position from the theory and from the tables which amount to an amplitude of approximately $0''.1$ in lunar true orbital longitude, $0''.15$ in lunar celestial latitude and $0''.01$ in sine parallax.

At present the position of the moon for ephemeris calculations is expressed in the form of a trigonometric series as given in the explanation in Brown's tables (Ref. 15). Each argument is a linear function of time with small secular and periodic additions due to the planetary attractions. Each coefficient of the series is a constant for the main problem of lunar theory with small secular and periodic additions due to the attractions of the planets.

Consider only the main problem of lunar theory. Each argument in the series expression is in turn a function of four fundamental arguments[*]

$$\ell = \mathbb{C} - \Gamma', \text{ mean anomaly of the moon}$$

$$\ell', \ell_{\odot}, g_{\odot} = L - \Gamma, \text{ mean anomaly of the sun}$$

$$F = \mathbb{C} - \Omega, \text{ argument of lunar perigee plus mean anomaly of the moon}$$

$$D = \mathbb{C} - L, \text{ mean elongation of the moon from the sun}$$

$$(111)$$

*The notation adopted in Ref. 1 has been used here, with the astronomical notation as well as the one used in Brown's tables indicated.

$\mathbb{C}$ (L) $= \Omega + \omega + \ell$ is the mean longitude of the moon, measured in the ecliptic from the mean equinox of date to the mean ascending node, then along the orbit

L (L') $= \tilde{\omega}_\odot + \ell_\odot$ ($g_\odot$) is the mean longitude of the sun, measured from the mean equinox of date

Γ' ($\tilde{\omega}$) = the mean longitude of lunar perigee, measured from the mean equinox of date along the ecliptic to the mean ascending node, then along the orbit

Γ ($\tilde{\omega}_\odot$) = the mean longitude of solar perigee measured from the mean equinox of date

Ω = the longitude of the mean ascending node of the lunar orbit on the ecliptic measured from the mean equinox of date

The arguments of each periodic term of the series can be expressed in the form

$$p_1 \ell + p_2 \, g_\odot + p_3 F + p_4 D \qquad (112)$$

where

$$p_i = 0, \pm 1, \pm 2, \pm 3, \ldots$$

If the attractions of the planets are taken into account, then secular and periodic terms are added to the solar arguments and for each planet a new argument appears which is a linear function of time. Effects of the shape of the earth and moon are included in the solar arguments.

The coefficients in the trigonometric series for the position of the moon are functions of four of the lunar and solar orbits:

e, $e_\mathbb{C}$ = 0.054900489, constant of the eccentricity of the moon's orbit

γ = $\sin \frac{1}{2} i_{\epsilon m}$ = 0.044886967, constant of the inclination of the moon's orbit

e', $e_\odot$ = eccentricity of the sun's orbit

α = 3422".5400, constant of sine parallax

$$\qquad (113)$$

The numerical value of $\dfrac{n_\odot}{n_\mathbb{C}}$, which can be obtained very accurately by observation, is introduced at the beginning of the theory. Each coefficient of the periodic terms consists of a numerical factor multiplied by the principal characteristic, which can be expressed in the form

$$e_\mathbb{C}^{q_1} \, e_\odot^{q_2} \, \gamma^{q_3} \, \alpha^{q_4} \qquad (114)$$

where $q_i = 0, 1, 2, 3, \ldots$ The gravitational attraction of the planets introduces secular and periodic terms in the parameters $e_\odot$, γ.

The independent variable is time counted from the epoch 1900, January 0.5 ET (Greenwich mean noon) which corresponds to the Julian Date 2415020.0. The position of the moon is usually given in spherical coordinates, i.e., true orbital longitude ($\Omega + \omega + f$), celestial latitude ϕ_ϵ, and horizontal parallax $\pi_\mathbb{C}$ (which is a measure of $r_{\epsilon \mathbb{C}}$). Its position in geocentric rectangular, or any other coordinate system can then be obtained by suitable transformations.

The trigonometric series as used for the calculation of the lunar position contains 1629 periodic terms which are tabulated in Ref. 16, together with 50 additive terms to the fundamental arguments.

Most of these periodic terms are very small but some of the principal ones, all due to the disturbing effects of the sun, have sizable coefficients. The better known terms are: The variation is a periodic perturbation in the moon's mean longitude $\mathbb{C}$ with a coefficient +39' 29".9 and a period of one-half mean synodic month (new moon to new moon), or approximately 14.8 days. Evection is the largest periodic perturbation in $\mathbb{C}$ due to periodic variations in the osculating eccentricity and longitude of perigee $\tilde{\omega}$ of the moon's orbit. Its coefficient is +1° 16' 26".4 and the period approximately 31.8 days. This term was known to Hipparchus from observations of the moon. The annual equation is another perturbation in $\mathbb{C}$ with coefficient -11'8".9 and period of an anomalistic year (the time between successive solar perigees in the orbit of the sun as seen from earth) of approximately 365.3 days. This perturbation is due primarily to the eccentricity of the earth's orbit around the sun. The parallactic inequality is a secondary perturbation in $\mathbb{C}$ (i.e., it comes from a term of R_2) with a coefficient -2'4".8 and period of mean synodic month (approximately 29.5 days). The principal perturbation in latitude has a coefficient of +10' 23".7 and a period of approximately 32.3 days.

d. Theory and observation

From lunar theory one can obtain the true coordinates of the moon as a function of time. This lunar position given by theory must be compared with observation and usually several corrections and coordinate transformations have to be applied before this comparison can be made accurately.

The geometric ephemeris is a table giving the actual or true position of the body at various times. However, actual positions cannot be observed directly since light emitted by the body takes a finite time to travel from the body to the observer (correction for light time), and during this time the body as well as the observer have been displaced from their original position (stellar aberration). These two corrections are known as planetary aberration, and if applied to the observed or apparent position of the body, they yield its true position. A table giving the apparent position of the body as a function of time

is known as an apparent ephemeris. Ephemerides of the sun, the principal planets, and the moon are usually apparent ephemerides. In the case of the moon the entire planetary aberration consists of the correction for light time which amounts to approximately $0''.7$ in geocentric mean orbital longitude $\mathbb{C}$ with a variation of $0''.05$ due to the eccentricity of the moon's orbit (Ref. 14), and will be neglected in this manual. For observations of the moon from the surface of the earth, such as moonrise and moonset, three additional corrections, the diurnal aberration due to the earth's rotation which is a part of the stellar aberration, the atmospheric refraction, and a parallax correction, must be applied to reduce the observation to an apparent ephemeris. Formulas for these corrections are given in Ref. 2.

Furthermore, the fundamental reference planes in celestial mechanics, the ecliptic and the celestial or earth's equatorial plane, as well as one of their points of intersection on the celestial sphere, the vernal equinox, are in constant motion. Hence, the geocentric coordinates of the body vary due to this motion. The secular terms of this motion, which are independent of the positions of the earth and moon, are termed precessional terms. There are also periodic terms in this motion with arguments ℓ, $\ell_\odot$, F, D, Ω which are termed nutational terms.

The principal term in nutation depends on Ω and has an amplitude of $9''.210$ and a period of 18.6 years.

The tabulated positions of the sun, moon, and planets in the ephemerides are usually <u>apparent positions</u>, that is, the coordinates of the body as an observer at the center of the earth would see them, and referred to a coordinate system defined by the instantaneous equator, ecliptic, and equinox. If the corrections for planetary aberration are applied to apparent positions, <u>true positions</u> are obtained. If the periodic effects of nutation are neglected, <u>mean positions</u> are obtained, which are the coordinates of the body referred to a coordinate system defined by the mean equator, ecliptic and equinox of date. Sometimes the effects of precession are removed for some time in order to provide a fixed reference for theoretical calculations. The selected epoch is usually chosen at the beginning of the year 1950.0 in order that data from various sources can most easily be combined. In Ref. 1 some positions are referred to the mean equator and equinox at the beginning of the year for which the ephemerides have been published. Transformations between the various reference systems are given in Ref. 6.

e. Available lunar ephemerides

The principal reference for lunar ephemerides is the <u>American Ephemeris and Nautical Almanac</u> (Ref. 1) which is published annually about two years in advance. On page 51 of Ref. 1 the following items are tabulated for every tenth day: the values of the fundamental arguments Γ', Ω, $\mathbb{C}$, and D (see the following sketch); $i_\mathbb{C}$, the inclination of the mean equator of the moon to the true equator of the earth; Δ, the angle along the mean equator of the moon from its

ascending node on the true equator of the earth to its ascending node on the ecliptic of date; $\Omega_\mathbb{C}$, the right ascension of the ascending node of the mean lunar equator measured from true equinox of date.
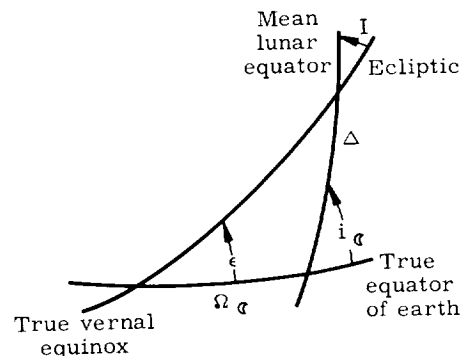
On pages 52 to 67, Ref 1 tabulates the following items for every half day: the apparent true orbital longitude referred to the mean equinox of date; the apparent celestial latitude referred to the ecliptic of date; the horizontal parallax, the semidiameter and ephemeris transit (time of crossing of the ephemerides meridian which is $1.002738 \Delta T$ east of the Greenwich meridian). In Ref. 1, pages 68 to 159, the apparent right ascension, the apparent declination referred to true equator and equinox of date, together with differences for interpolation and fully corrected for planetary aberration, are tabulated to the nearest $0^s.001$ and $0''.01$, respectively for each hour of ephemeris time (pages 68 through 159). This accuracy has been recommended for national ephemerides by a resolution of the International Astronomical Union in 1952 and has been introduced into the lunar ephemeris from 1960 on. The phases of the moon and lunar perigee and apogee have also been tabulated on page 159.

The ephemerides for physical observations of the moon are based on the apparent coordinates given in the fundamental ephemerides described above and tabulated to a lesser degree of accuracy, usually to $0.01°$.

The age, or number of days since the previous new moon, and the fraction of the illuminated disk, the earth's and sun's selenographic coordinates, the physical librations, and the position angles of the axis and bright limb, tabulated for 0^h Universal Time (UT) of each day, are given in Ref. 1, pages 310 through 317. The earth's selenographic coordinates are the sum of the optical and physical librations of the moon. They are the coordinates of the point on the lunar surface where the moon-earth line intersects it, and are given in the customary selenographic coordinate system described in Section A-2 of this Chapter. The sun's selenographic coordinates are the coordinates of the point of

intersection of the moon-sun line with the lunar
surface and are given in terms of selenographic
latitude (see Section A-2) and colongitude. The
selenographic colongitude, $\lambda'_{\mathbb{C}}$, $0° < \lambda'_{\mathbb{C}} < 360°$,
can be obtained by subtracting the selenographic
longitude, $0° < \lambda < 360°$, from 90° or 450°. The
sun's selenographic colongitude determines the
illuminated regions of the lunar surface because
the sun's selenographic latitude is small $|\phi_{\mathbb{C}}|$
$< 2°$: at new moon $\lambda'_{\mathbb{C}} \simeq 270°$, at first quarter
$\lambda'_{\mathbb{C}} \simeq 0°$, at full moon $\lambda'_{\mathbb{C}} \simeq 90°$, and at last
quarter $\lambda'_{\mathbb{C}} \simeq 180°$. The terminator is defined
as the orthogonal projection of the great circle
bounding the illuminated (by the sun) hemisphere
of the moon on a plane perpendicular to the line
of sight from the center of the earth or EML.
The selenographic colongitude of the sun can thus
be regarded as the selenographic longitude of the
morning terminator. The selenographic longitude
of the evening terminator differs by 180° from
that of the morning terminator. The position
angle of the axis is the angle between north on
the lunar meridian which passes through the
apparent central point of the lunar disk and the
declination circle through this central point,
measured positive eastward from the north point
of the disk. The position angle of the bright limb
is the angle between north on the same lunar
meridian and the moon-sun line. Both position
angles are analogous to the azimuth of topocentric
coordinates. In addition to the selenographic
coordinates of the earth, the physical librations
in longitude, latitude, and position angle are
tabulated separately.

For lunar mission planning purposes, positions
of the moon are often needed in advance of the
published ephemerides. In principle, it is pos-
sible to determine lunar ephemerides from the
Hill-Brown Lunar Theory for all time. However,

position of the moon can be determined with
essentially ephemeris accuracy for decades and
the Nautical Almanac Office of the United States
Naval Observatory is prepared to supply
ephemerides outside of the scope of Ref. 1 for
special purposes. To aid the lunar mission plan-
ner, a future addendum will give the geocentric
rectangular coordinates of the moon referred to
mean equator and equinox of date for the years
1965 through 1969 in half-day intervals. The
components of lunar position $x_{\oplus\mathbb{C}}$, $y_{\oplus\mathbb{C}}$, $z_{\oplus\mathbb{C}}$ are
given in units of earth radii.

Woolston (Ref. 17) gives additional lunar data
for the years 1961 through 1971 useful for the
mission planner: the phases of the moon are
tabulated to within approximately one minute of
time, and graphs giving the declination of the
moon with phases indicated as well as its radial
distance are presented for a rapid visualization
of trajectory and solar illumination data. From
the graphs the declination can be obtained to
within approximately 0.5° and the radial distance
to within 600 km for any given date. Some of
these graphs are presented in Chapter XI.

2. Librations of the Moon

An important factor in planning lunar missions,
whether they be circumlunar, reconnaissance,
or landing flights, is the libration of the moon,
or its orientation with respect to earth. Libration
is defined as the "position of the moon-earth line
with respect to the Moon's Mean Center point."
This mean center point* is the fundamental base
for the mapping of lunar features. The following
sketch illustrates the orientation of the mean
center point (MCP) and how latitude and longitude
are measured in the selenographic coordinate

Selenographic coordinates

Orbital motion

Prime meridian
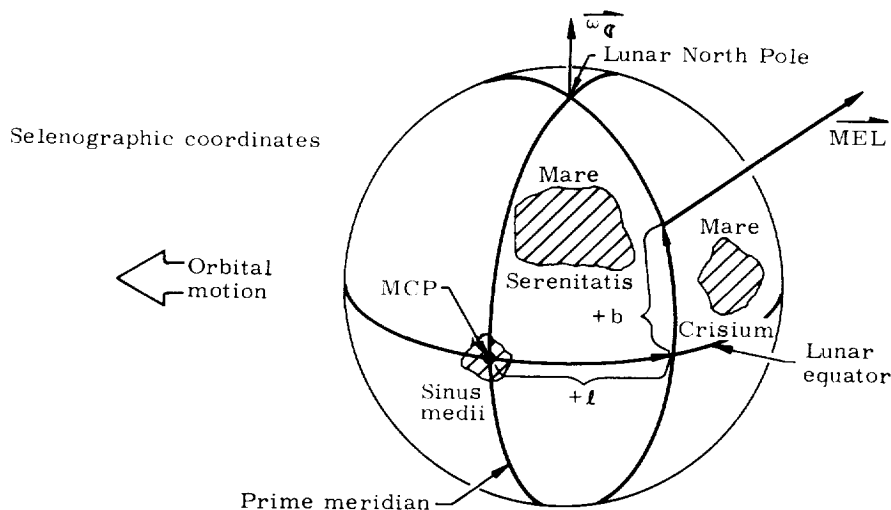
some parameters such as orbital elements and
the masses of the planets must be supplied by
observation, and due to observational inaccuracies,
the position computed from theory by use of these
observed parameters will differ more and more
from the true position at the same time the
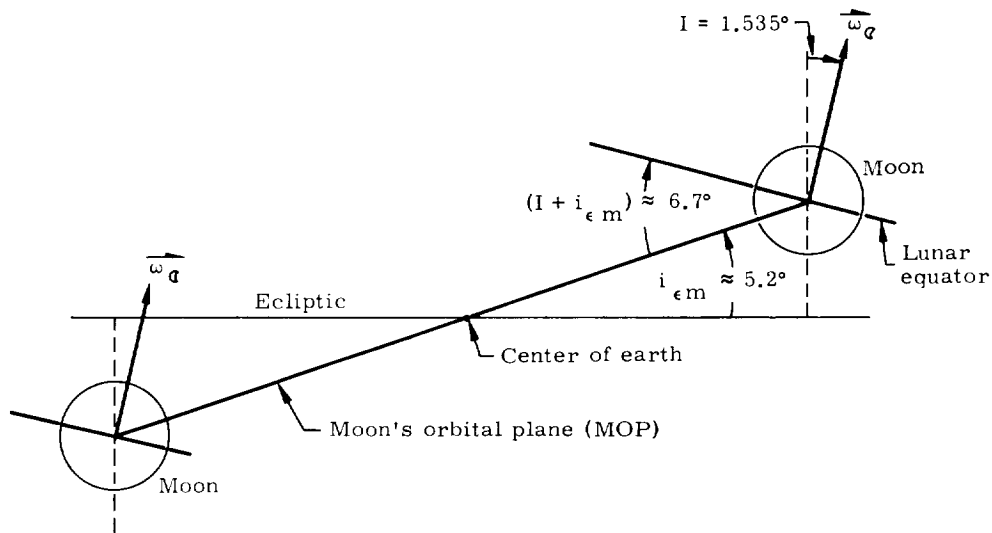farther ahead one tries to predict. However, the

*Definition of MCP: The mean center point
is the point on the lunar surface where the
surface is intersected by the radius of the
moon that would be directed toward the earth's
center, were the moon to be at the mean
ascending node when the node coincided with
either the mean perigee or mean apogee.

system. The lunar equatorial plane is per-
pendicular to the moon's spin axis and the
magnitude of the moon's angular velocity $\omega_{\mathbb{C}}$ is
practically constant.

Selenographic longitudes are measured from
the MCP (located in Sinus Medii-Central Bay)
positive in the direction toward Mare Crisium
(Sea of Crises). Selenographic latitudes are
positive in the hemisphere containing Mare
Serentatis (Sea of Serenity). Also in the sketch,
the positive librations in longitude (+ℓ) and
latitude (+b) are shown in the selenographic sys-
tem. These coordinates are the sum of both the
optical and physical librations in longitude and
latitude, respectively. Therefore as the position
of the moon-earth line (MEL) changes with
respect to the MCP so does any specific lunar
feature vary with respect to the MEL.

The causes of lunar librations are essentially
twofold: First there are the optical librations
which are the result of the dynamical properties
of the moon's orbit about the earth, and secondly,
the physical librations which are caused by the
motion of $\vec{\omega}_{\mathbb{C}}$ in inertial space due to the small
triaxiality in the moon's figure.

The following sketch is a view of the earth-
moon system as seen from a point in the ecliptic
plane. Effects of physical librations on I
($\rho < 0.045°$) are ignored for the purpose of this
demonstration.

has a constant rotational rate $\omega_{\mathbb{C}}$ and rotates
through an angle $\theta' = (t_1 - t_0) \omega_{\mathbb{C}}$. Because the
orbital motion of the moon about the earth is
elliptic, the central angle $\theta \neq \theta'$. The difference
(ℓ') is called the "optical libration in longitude"
with a variation from approximately $+8°$ to $-8°$
in a period of approximately 1 lunar month.

The much smaller physical librations (order
of 0.04°) are the result of rigid body dynamics

The inclination of the mean lunar equator to
the ecliptic is denoted by I and is constant
(1.535°). Now an observer at the earth's center
would note a more exposed northern hemisphere
at $(I + i_{em} \approx -6.7°)$ and one-half month later
would view a more exposed southern hemisphere
$(I + i_{em} = +6.7°)$. This apparent oscillation of
the moon is termed the "optical libration in
latitude" with a variation from approximately
$+7°$ to $-7°$ in a period of approximately 1 lunar
month.

The following sketch illustrates the earth-
moon system when viewed from above the
ecliptic. During the interval $(t_1 - t_0)$ the moon

and the moon's triaxial characteristics. These
characteristics cause the direction of the moon's
spin axis ($\vec{\omega}_{\mathbb{C}}$) to oscillate in inertial space about
a "mean" position. The periods of the physical
librations in longitude and latitude are approxi-
mately 1 year and 6 years, respectively. If these
minor librations are ignored, an uncertainty of
1000 m can arise for any given surface co-
ordinates. Thus it can be seen that for pre-
liminary mission planning, the physical librations
can be disregarded. However they cannot be
eliminated from detailed planning, especially for
"landing" type missions. This becomes more

evident when considering the fact that landing vehicles within this decade will be severely limited in hovering and translational capability. Furthermore, guidance inaccuracies may demand a large part of this capability. Physical librations can be compensated for prior to leaving earth or at a later time during flight depending on the guidance scheme. From the above discussion, it is seen that the librations are continually changing in magnitude. Also, the path traced by the $\overrightarrow{\text{MEL}}$ about the MCP is complex. This is evidenced in Fig. 3. In this figure the $\overrightarrow{\text{MEL}}$ loci are shown for the month of October in the years 1966 and 1967. Note the almost complete change in the trace characteristics and particularly the rapid movement across the moon's equatorial plane (up to 2°/day).

This movement has considerable influence on the planning of translunar and transearth trajectory orientations. Even during an earth launch time tolerance of 2 hr, a landing site can be displaced from a planned translunar trajectory to the site by 5000 m if librations are not accounted for during this time. Aborts occurring during a stay on the moon will markedly influence the earth return trajectories as compared to the original flight plan. Thus, the librations of the moon add both position and time constraints to the lunar mission.

Methods given in literature (Refs. 2 and 6) for determining librations can become cumbersome because interplanetary digital trajectory programs do and will most likely use stored positional data of the moon in geocentric rectangular coordinates. Thus, the following approach for simulating or determining librations on the computer is practical. The object is to obtain librations in longitude and latitude beyond published ephemeris data from geocentric equatorial coordinates of the moon using transformations of coordinates in terms of fundamental arguments.

First, the reference coordinate systems are shown in the following sketch. The numerical values in the following equations have been obtained from Ref. 1:

$\overrightarrow{\text{EML}}$ (earth moon line) has components $(x_{\mathbb{C}}, y_{\mathbb{C}}, z_{\mathbb{C}})$ in geocentric equatorial coordinates

ϵ (mean obliquity of the ecliptic)

$$\epsilon = 23.452294^\circ - 0.0130125^\circ \text{ T}$$
$$- 0.164^\circ \cdot 10^{-5} \text{ T}^2 +$$
$$0.0503^\circ \cdot 10^{-5} \text{ T}^3 \qquad (115)$$

T denotes the time measured in Julian centuries of 36525 ephemeris days from the epoch (1900 Jan 0.5 ET). See Table 1 for Julian day numbers for the years 1950 through 2000.
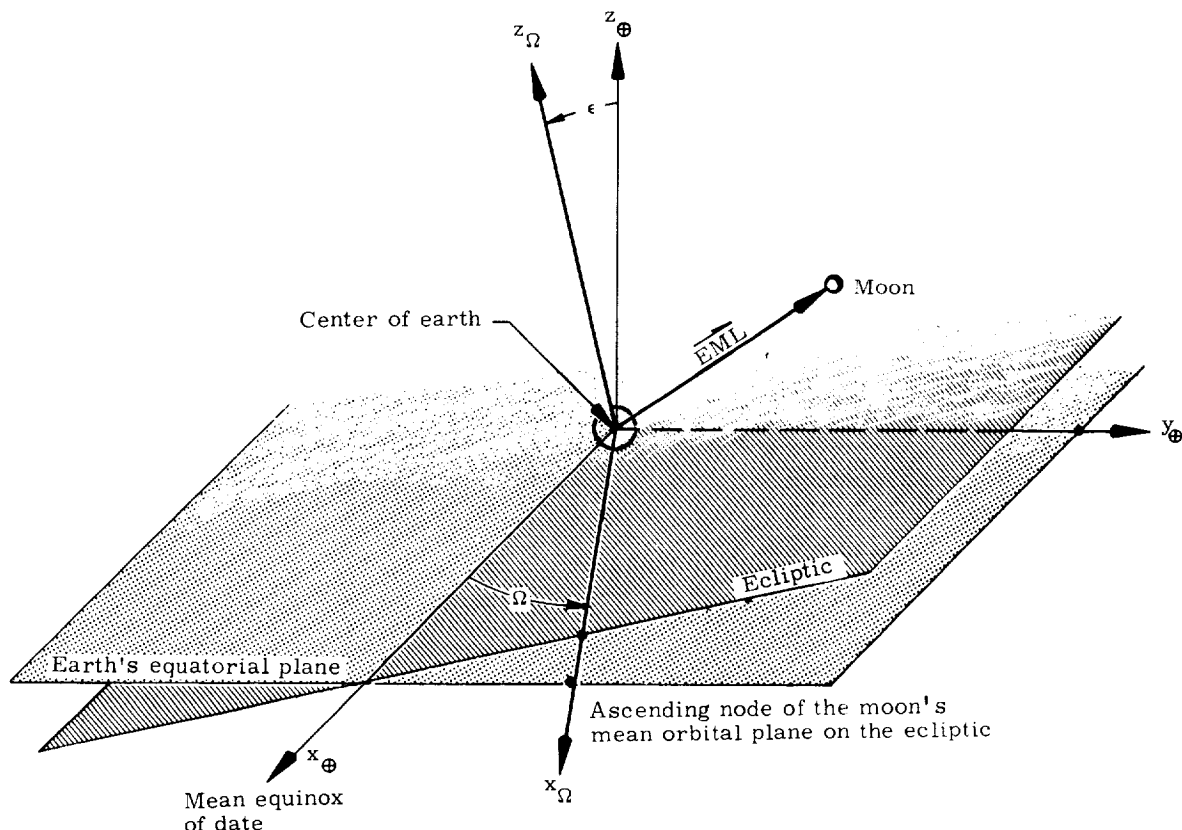
Center of earth

Moon

Earth's equatorial plane

Ecliptic

Ascending node of the moon's mean orbital plane on the ecliptic

Mean equinox of date

Ω (the longitude of the mean ascending node of the lunar orbit on the ecliptic, measured from the mean equinox of date)

$$\Omega = 259.183275° - 0.052953922° \, d$$
$$+ 0.002078° \, T^2 + 0.2° \cdot 10^{-5} T^3 \quad (116)$$

d denotes the number of ephemeris days from the epoch.

The transformation matrix giving $\overrightarrow{EML}$ in the ecliptic reference frame is:

$$(\overrightarrow{EML})_\Omega = \begin{pmatrix} x_\Omega \\ y_\Omega \\ z_\Omega \end{pmatrix} = \begin{bmatrix} \cos\Omega & \cos\epsilon\,\sin\Omega & \sin\epsilon\,\sin\Omega \\ -\sin\Omega & \cos\epsilon\,\cos\Omega & \sin\epsilon\,\cos\Omega \\ 0 & -\sin\epsilon & \cos\epsilon \end{bmatrix} \begin{pmatrix} x_{\oplus\mathbb{C}} \\ y_{\oplus\mathbb{C}} \\ z_{\oplus\mathbb{C}} \end{pmatrix} \quad (117)$$

In Ref. 2, optical librations are calculated using Hayn's value of 1.535° for the inclination (I) of the mean lunar equator to the ecliptic. The ascending node of the mean lunar equator on the ecliptic is at the descending node of the mean lunar orbit ($\Omega \pm 180°$). From the following sketch the $\overrightarrow{MEL}$ relative to the mean equatorial plane of the moon can be found.
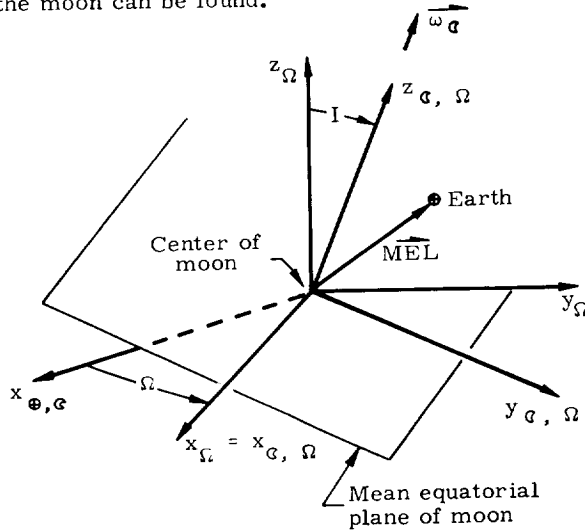
$\overrightarrow{MEL}$ (moon-earth line) = $- \overrightarrow{EML}$

The transformation is given by:

$$(\overrightarrow{MEL})_{\mathbb{C},\Omega} = \begin{pmatrix} x_{\mathbb{C},\Omega} \\ y_{\mathbb{C},\Omega} \\ z_{\mathbb{C},\Omega} \end{pmatrix} = \begin{bmatrix} 1 & 0 & 0 \\ 0 & \cos I & -\sin I \\ 0 & \sin I & \cos I \end{bmatrix} \begin{pmatrix} x_\Omega \\ y_\Omega \\ z_\Omega \end{pmatrix} \quad (118)$$

From the following sketch and the aforementioned definition of the MCP (the condition that the center of the apparent disk of the moon be at the mean center), the librations in longitude and latitude vanish simultaneously when $\mathbb{C} = \Omega$ and $\beta = 180°$.

Mean lunar equator →
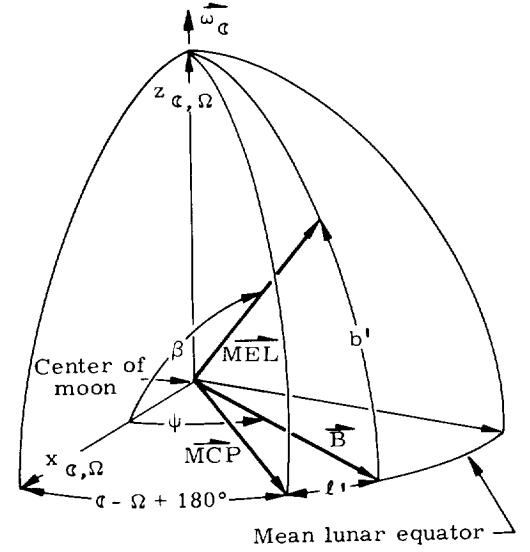
The symbols ℓ' and b' are the optical librations in longitude and latitude, respectively. The mean longitude of the moon $\mathbb{C}$, is given by the following series from Ref. 1.

$$\mathbb{C} = 270.434164° + 13.1763965286° \, d$$
$$- 0.001133° \, T^2 + 0.19 \cdot 10^{-5°} T^3 \quad (119)$$

and is measured in the ecliptic from the mean equinox of date to the mean ascending node of the lunar orbit and then along the orbit. The prime meridian rotates at a rate $(\omega_{\mathbb{C}})$ which is equal to the mean orbital motion $n_{\mathbb{C}}$ of the moon. The optical libration in latitude is given by:

$$b' = 90° - \cos^{-1}\left(\frac{z_{\mathbb{C},\Omega}}{|\overrightarrow{MEL}|}\right) \quad (120)$$

Now the vector $\vec{B}$ is found by taking the vector triple product $\hat{z}_{\mathbb{C},\Omega} \times (\overrightarrow{MEL} \times \hat{z}_{\mathbb{C},\Omega})$. Therefore ψ, the angle measured from $x_{\mathbb{C},\Omega}$ to $\vec{B}$ is

$$\psi = \cos^{-1}\left(\frac{\vec{B} \cdot \hat{x}_{\mathbb{C},\Omega}}{|\vec{B}|}\right)$$

or

$$\psi = \cos^{-1}\left(\frac{x_{\mathbb{C},\Omega}}{|\vec{B}|}\right) \quad (121)$$

Thus, the optical libration in longitude equals:

$$\ell' = \psi - (\mathbb{C} - \Omega) - 180°. \quad (122)$$

These librations must be adjusted to account for the 'wobble' motion mentioned previously of the lunar north pole $(\omega_{\mathbb{C}})$. Because of this

motion, the actual inclination and descending node of the lunar equator on the ecliptic are I + ρ and Ω + σ. It is well to note here that the physical librations are made up of forced and free librations. Free libration of the moon due to the gyroscopic motion has not been detected with certainty by observation and is neglected. The above equation represents the forced librations due to external torques (sun, earth, planets) on the moon.

From the Explanatory Supplement, Ref. 2, the physical librations (δl and δb) can be found by the use of the following formulas:

$$\delta l = 0.003 \sin (\mathbb{C} - \Gamma') - 0.005 \sin 2 (\Gamma' - \Omega)$$
$$\left. \begin{array}{l} - 0.016 \sin g_{\odot} + 0.018 \, \delta Cb' \\ \\ \delta b = M + N \sin l' \end{array} \right\} \quad (123)$$

where

$\Gamma' \sim$ the mean longitude of the lunar perigee, measured in the ecliptic from the mean equinox of date to the mean ascending node of the lunar orbit, and then along the orbit

$$\Gamma' = 334.329556° + 0.1114040803° \, d$$
$$- 0.010325° \, T^2 - 0.12° \cdot 10^{-4} T^3 \quad (124)$$

$l_{\odot} \sim$ mean anomaly of the sun

$$l_{\odot} = 358.47583 + 0.98560267° \, d$$
$$- 0.00015° \, T^2 - 0.3° \cdot 10^{-5} T^3 \quad (125)$$

$$\delta C = M \sin l' - N$$

$$M = 0.04° \sin (\Gamma' - \Omega) - 0.003° \sin (\mathbb{C} - \Omega)$$

$$N = 0.02° \cos (\Gamma' - \Omega) + 0.003° \cos (\mathbb{C} - \Omega) \quad (126)$$

The values of the fundamental arguments given in Eqs (115), (119), (124) and (125) have been calculated from the Hill-Brown lunar theory. The actual librations are the sums of the optical and physical librations in longitude and latitude, respectively

$$l \text{ (libration in longitude)} = l' + \delta l$$
$$b \text{ (libration in latitude)} = b' + \delta b \quad (127)$$

For reference and mission planning purposes, a future addendum will contain the actual librations in one-day intervals.

As mentioned in Section C-1 above, a future addendum will present the geocentric rectangular coordinates of the moon referred to the mean equinox of date in one-half day intervals. The components $(x_{\oplus \mathbb{C}}, y_{\oplus \mathbb{C}}, z_{\oplus \mathbb{C}})$ are in earth radii for

the years 1965 to 1969 and stored in the interplanetary trajectory program (Ref. 18). A continuous readout of librations can be obtained by curve fitting the positional data of the moon and utilizing the formulas presented in this section.

D. REFERENCES

1. "American Ephemeris and Nautical Almanac," published annually by the Nautical Almanac Office, United States Naval Observatory, Washington, D.C. (obtainable from the Supt. of Documents, U.S. Govt. Printing Office, Washington 25, D.C.)

2. "Explanatory Supplement to the Astronomical Ephemeris and the American Ephemeris and Nautical Almanac," Her Majesty's Stationery Office, London, 1961.

3. "Orbital Flight Handbook," Martin Company, Space Systems Division, Baltimore, Md., ER 12684, 1963.

4. Koskela, P., "Selenographic Coordinates for the Air Force Lunar Trajectory Program," Aeronutronic Systems Interim Technical Note 3 ASI Publication U-325, January 6, 1959.

5. Baker, R. M. L., and Makemson, M. W., "An Introduction to Astrodynamics," Academic Press, New York, 1960.

6. Kalensher, B. E., "Selenographic Coordinates," Jet Propulsion Laboratory, Pasadena, Calif., Technical Report 32-41, February 24, 1961.

7. Novak, D., "Simplified Lunar Trajectory Digital Program," Martin Marietta Corp., Space Systems Division, Baltimore, Md.

8. Moulton, F. R., "An Introduction to Celestial Mechanics," MacMillan, New York, 1914.

9. Finlay-Freundlich, E., "Celestial Mechanics," Pergamon Press, New York, 1958.

10. Egorov, V. A., "Certain Problems of Moon Flight Dynamics," Russian Literature of Satellites, Part 1, Intern. Phys. Index, New York, 1958.

11. Buchheim, R. W., "Lunar Flight Trajectories," The Rand Corp, Report P-1268, January 30, 1958.

    Also: Seifert, H. S., ed., "Space Technology," John Wiley and Sons, New York, Chapter 7, 1959.

12. Plummer, H. C., "An Introductory Treatise on Dynamical Astronomy," Dover Publications, New York, 1960.

13. Brown, E. W., "An Introductory Treatise on the Lunar Theory," Dover Publications, New York, 1960.

14. Brouwer, D., and Clemence, G. M.,
"Methods of Celestial Mechanics," Academic
Press, New York, 1961.

15. Brown, E. W., "Tables of the Motion of the
Moon," Yale University Press, New Haven,
Conn., 1919.

16. Anon., "Improved Lunar Ephemeris 1952
to 1959," Nautical Almanac Office, United
States Naval Observatory, Washington,
1954.

17. Woolston, D. S., "Declination, Radial
Distance and Phases of the Moon for the
Years 1961 to 1971 for Use in Trajectory
Considerations," NASA Technical Note
D-911, Washington, August 1961.

18. Pines, S., and Wolf, H., "Interplanetary
Trajectory by Encke Method Programmed
for the IBM 704," Republic Aviation Corp.,
Report RAC-656-450, December 15, 1959.

TABLE AND ILLUSTRATIONS

TABLE 1

Julian Day Numbers for the Years 1950-2000
(based on Greenwich Noon)

Year	Jan. 0.5	Feb. 0.5	Mar. 0.5	Apr. 0.5	May 0.5	June 0.5	July 0.5	Aug. 0.5	Sept. 0.5	Oct. 0.5	Nov. 0.5	Dec. 0.5
1950	243 3282	3313	3341	3372	3402	3433	3463	3494	3525	3555	3586	3616
1951	3647	3678	3706	3737	3767	3798	3828	3859	3890	3920	3951	3981
1952	4012	4043	4072	4103	4133	4164	4194	4225	4256	4286	4317	4347
1953	4378	4409	4437	4468	4498	4529	4559	4590	4621	4651	4682	4712
1954	4743	4774	4802	4833	4863	4894	4924	4955	4986	5016	5047	5077
1955	243 5108	5139	5167	5198	5228	5259	5289	5320	5351	5381	5412	5442
1956	5473	5504	5533	5564	5594	5625	5655	5686	5717	5747	5778	5808
1957	5839	5870	5898	5929	5959	5990	6020	6051	6082	6112	6143	6173
1958	6204	6235	6263	6294	6324	6355	6385	6416	6447	6477	6508	6538
1959	6569	6600	6628	6659	6689	6720	6750	6781	6812	6842	6873	6903
1960	243 6934	6965	6994	7025	7055	7086	7116	7147	7178	7208	7239	7269
1961	7300	7331	7359	7390	7420	7451	7481	7512	7543	7573	7604	7634
1962	7665	7696	7724	7750	7785	7816	7846	7877	7908	7938	7969	7999
1963	8030	8061	8089	8120	8150	8181	8211	8242	8273	8303	8334	8364
1964	8395	8426	8455	8486	8516	8547	8577	8608	8639	8669	8700	8730
1965	243 8761	8792	8820	8851	8881	8912	8942	8973	9004	9034	9065	9095
1966	9126	9157	9185	9216	9246	9277	9307	9338	9369	9399	9430	9460
1967	9491	9522	9550	9581	9611	9642	9672	9703	9734	9764	9795	9825
1968	9856	9887	9916	9947	9977	*0008	*0038	*0069	*0100	*0130	*0161	*0191
1969	244 0222	0253	0281	0312	0342	0373	0403	0434	0465	0495	0526	0556
1970	244 0587	0618	0646	0677	0707	0738	0768	0799	0830	0860	0891	0921
1971	0952	0983	1011	1042	1072	1103	1133	1164	1195	1225	1256	1286
1972	1317	1348	1377	1408	1438	1469	1499	1530	1561	1591	1622	1652
1973	1683	1714	1742	1773	1803	1834	1864	1895	1926	1956	1987	2017
1974	2048	2079	2107	2138	2168	2199	2229	2260	2291	2321	2352	2382
1975	244 2413	2444	2472	2503	2533	2564	2594	2625	2656	2686	2717	2747
1976	2778	2809	2838	2869	2899	2930	2960	2991	3022	3052	3083	3113
1977	3144	3175	3203	3234	3264	3295	3325	3356	3387	3417	3448	3478
1978	3509	3540	3568	3599	3629	3660	3690	3721	3752	3782	3813	3843
1979	3874	3905	3933	3964	3994	4025	4055	4086	4117	4147	4178	4208
1980	244 4239	4270	4299	4330	4360	4391	4421	4452	4483	4513	4544	4574
1981	4605	4636	4664	4695	4725	4756	4786	4817	4848	4878	4909	4939
1982	4970	5001	5029	5060	5090	5121	5151	5182	5213	5243	5274	5304
1983	5335	5366	5394	5425	5455	5486	5516	5547	5578	5608	5639	5669
1984	5700	5731	5760	5791	5821	5852	5882	5913	5944	5974	6005	6035
1985	244 6066	6097	6125	6156	6186	6217	6247	6278	6309	6339	6370	6400
1986	6431	6462	6490	6521	6551	6582	6612	6643	6674	6704	6735	6765
1987	6796	6827	6855	6886	6916	6947	6977	7008	7039	7069	7100	7130
1988	7161	7192	7221	7252	7282	7313	7343	7374	7405	7435	7466	7496
1989	7527	7558	7586	7617	7647	7678	7708	7739	7770	7800	7831	7861
1990	244 7892	7923	7951	7982	8012	8043	8073	8104	8135	8165	8196	8226
1991	8257	8288	8316	8347	8377	8408	8438	8469	8500	8530	8561	8591
1992	8622	8653	8682	8713	8743	8774	8804	8835	8866	8896	8927	8957
1993	8988	9019	9047	9078	9108	9139	9169	9200	9231	9261	9292	9322
1994	9353	9384	9412	9443	9473	9504	9534	9565	9596	9626	9657	9687
1995	244 9718	9749	9777	9808	9838	9869	9899	9930	9961	9991	*0022	*0052
1996	245 0083	0114	0143	0174	0204	0235	0265	0296	0327	0357	0388	0418
1997	0449	0480	0508	0539	0569	0600	0630	0661	0692	0722	0753	0783
1998	0814	0845	0873	0904	0934	0965	0995	1026	1057	1087	1118	1148
1999	245 1179	1210	1238	1269	1299	1330	1360	1391	1422	1452	1483	1513
2000	245 1544	1575	1604	1635	1665	1696	1726	1757	1788	1818	1849	1879

1900 Jan 0.5 ET = Julian Day 2,415,020.0 = Greenwich Noon, January 1, 1900, a common epoch
1950 Jan 0.5 ET = Julian Day 2,433,282.0 = Greenwich Noon, January 1, 1950, another common epoch and
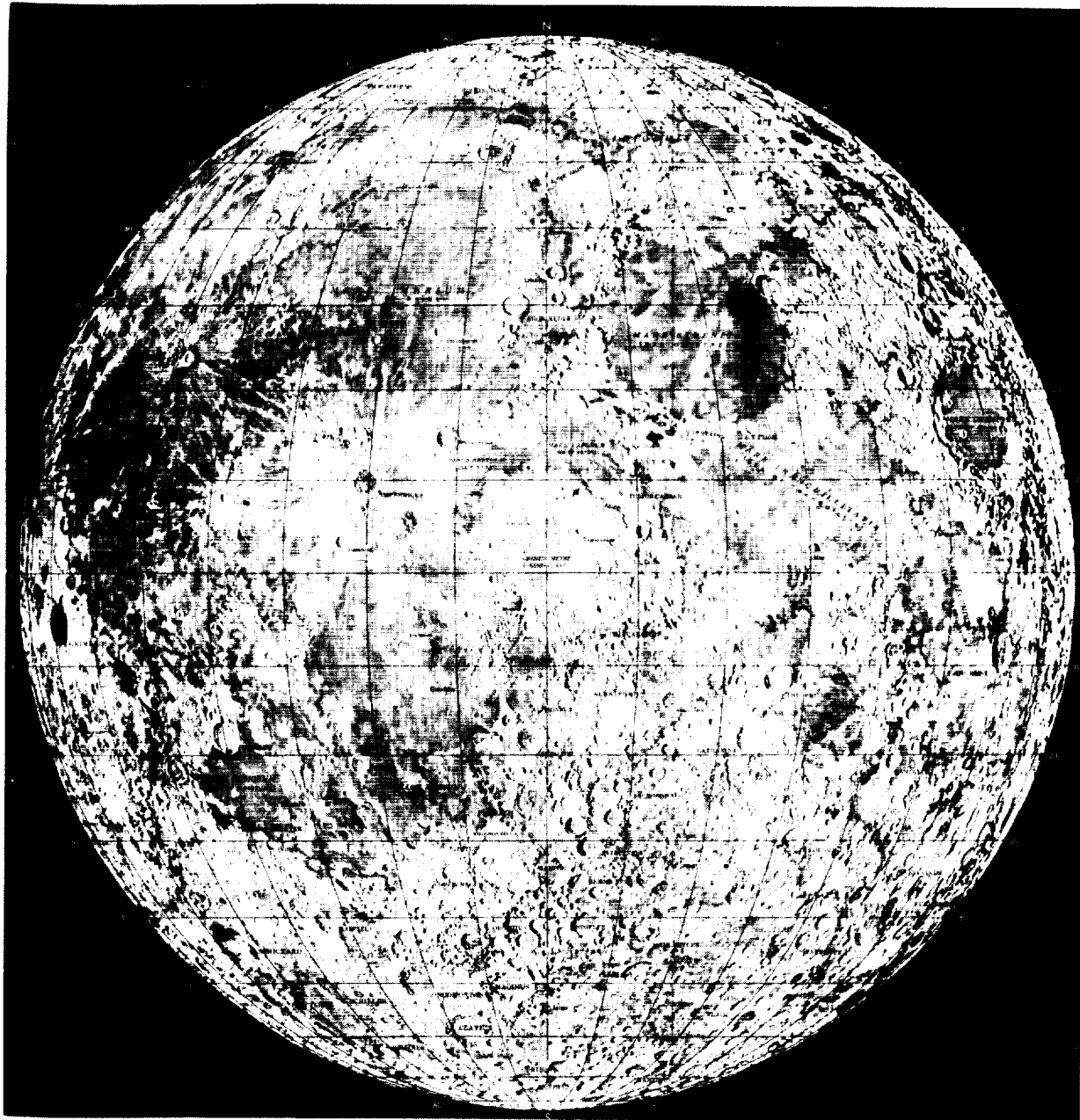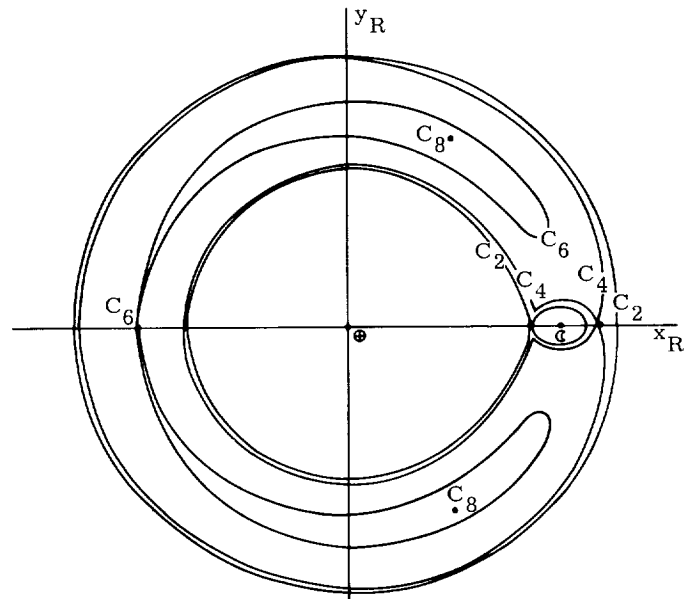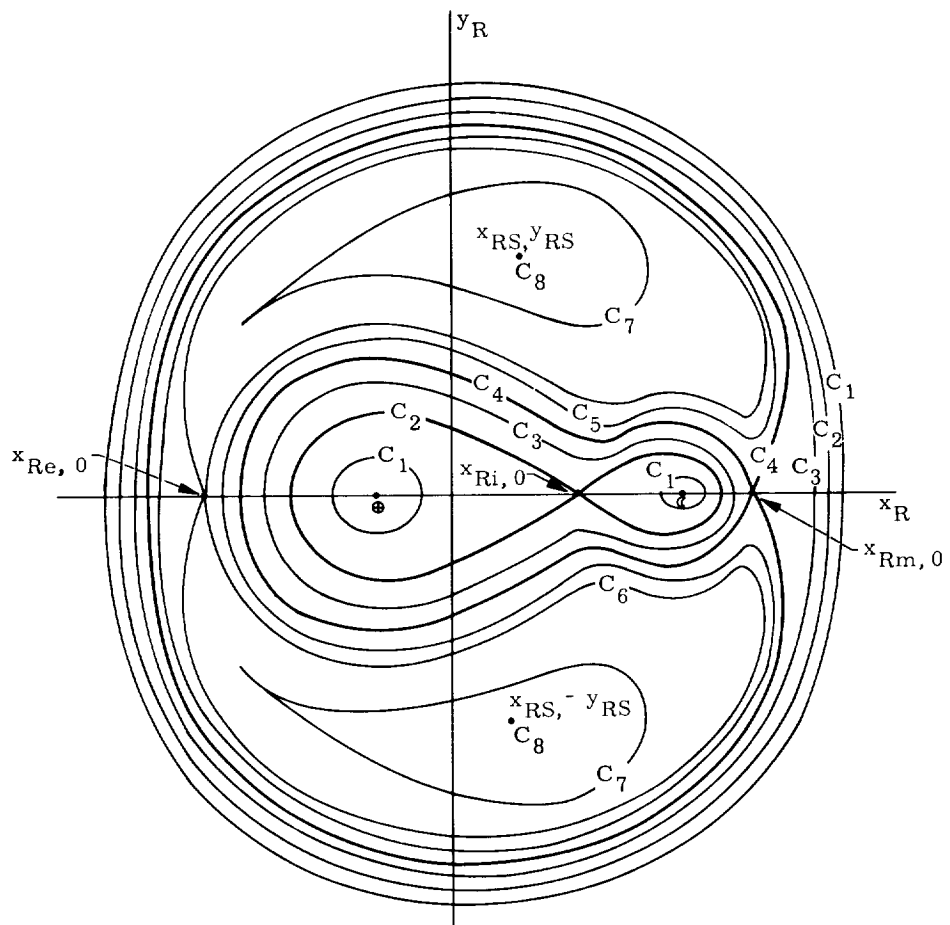first entry in this table

Fig. 1. Selenographic Coordinate System Superimposed on a Lunar Photograph

(a) Drawn to scale.

(b) Not drawn to scale.

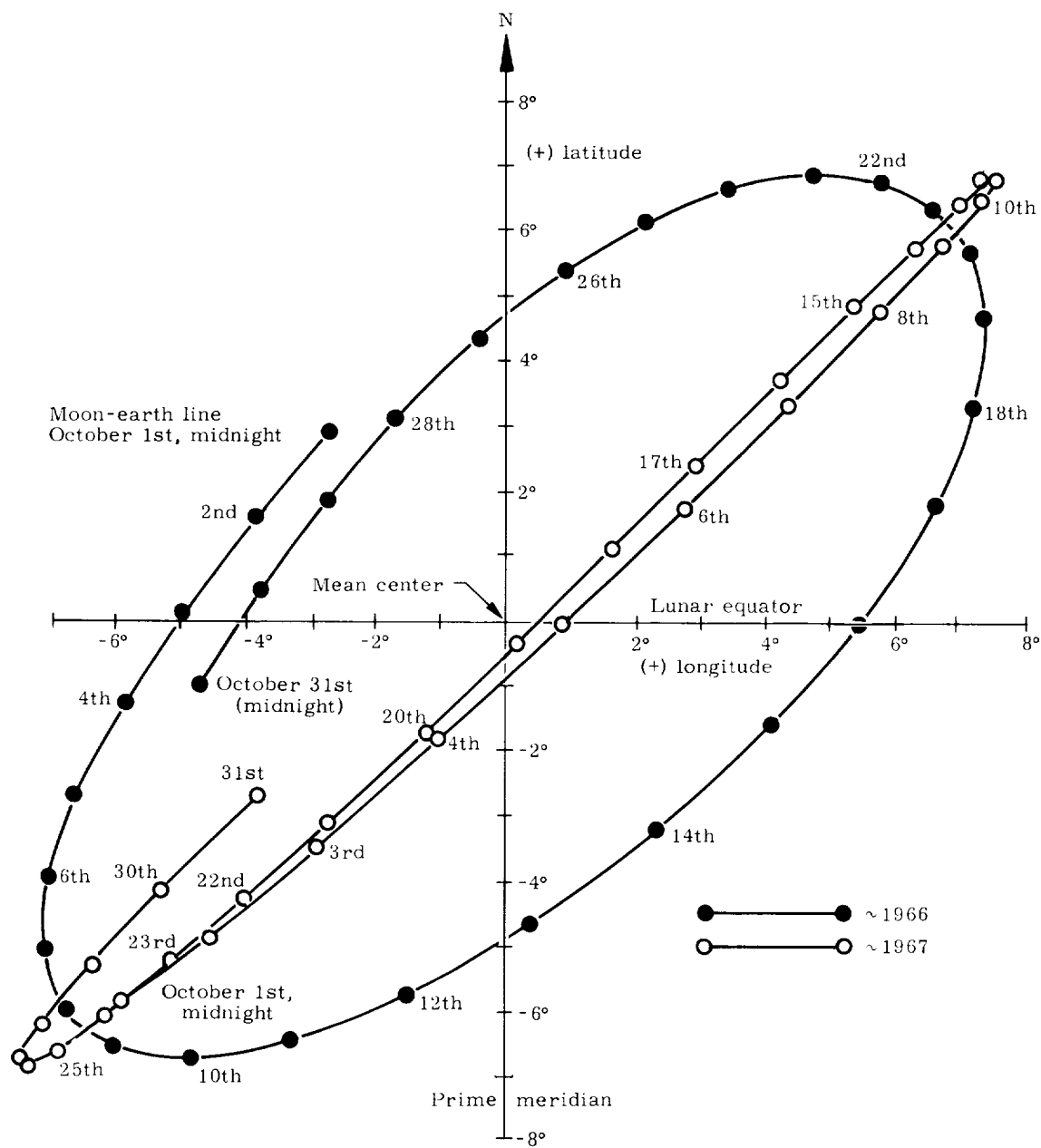Fig. 2. Curves of Zero Relative Velocity in the $x_R y_R$ Plane

Fig. 3. Lunar Librations During October 1966 and October 1967

CHAPTER IV

TRAJECTORIES IN THE EARTH-MOON SYSTEM

Prepared by:

F. Martikan, L. Emery, F. Santora,
T. Garceau and A. Jazwinski
Martin Company (Baltimore)
Aerospace Mechanics Department
March 1963

Page

This chapter will apply the introductory material on kinematics and dynamics of the earth-moon system from Chapter III to space vehicle trajectories in earth-moon space. The force models and methods of solving the equations of motion will be discussed with emphasis on the approximations introduced and the usefulness of various trajectory programs. Some typical trajectories in earth-moon space will be sketched and described briefly in order to illustrate the types of lunar missions to be contemplated in succeeding chapters.

Section A gives a classification of lunar trajectories, and introduces the nomenclature of lunar trajectories to facilitate their visualization when results will be presented later in the manual. Section B describes the various force models that are used in lunar trajectory calculation, i.e.:
(1) the restricted two-body trajectories for which analytical solutions are available, (2) their patching to form a complete earth-moon trajectory, (3) restricted three-body trajectories, (4) n-body trajectories with earth oblateness and triaxiality of the moon included, as well as a discussion of nongravitational forces and their simulation on the digital computer. Finally, Section C gives a description of the Voice trajectory computation technique which has been used extensively in obtaining lunar trajectories in this manual.

A. CLASSIFICATION AND NOMENCLATURE OF LUNAR MISSIONS AND TRAJECTORIES

1. General Considerations

Trajectory studies can be divided into two broad groups, feasibility and precision trajectories. Feasibility trajectories are used for preliminary vehicle performance studies such as injection requirements, maneuvering requirements, tolerances on flight parameters, guidance accuracies, observational constraints. Precision trajectories, on the other hand, are used for the detailed planning of an actual flight. In this latter approach the best values of parameters influencing the trajectory may be used to compute a nominal path, or to include correctional information, based on observations of the vehicle, in the trajectory calculation to obtain a path that is frequently updated during the flight. In this handbook most of the computed trajectories are of the feasibility type.

For the present qualitative discussion of lunar trajectories and missions it is not necessary to consider all the forces that act on the space vehicle, but only those which determine the characteristics of the lunar trajectories. The assumptions made in this section are:

(1) Gravitational effects of the sun and planets on lunar trajectories can be neglected because the region where the gravitational attraction of the earth and moon predominate extends in all directions about three times the earth-moon distance from earth.

(2) Atmospheric drag is neglected during the brief portion of the lunar trajectory in the earth's atmosphere, since the space vehicle reaches the required velocity for passage to the moon while it is more than 100 km above the surface of the earth.

(3) Lunar trajectories are assumed ballistic, i.e., no thrust forces act on the vehicle. Lunar missions, on the other hand, may include phases when large thrust forces alter the subsequent vehicle trajectory. Lunar missions with a continuous low thrust will not be considered here.

(4) The earth and moon are in circular orbits around the earth-moon barycenter (the small eccentricity of the lunar orbit can be neglected in qualitative trajectory discussions).

These facts suggest the use of the restricted three-body problem discussed in Chapter III as a force model for discussion of lunar trajectories. Sometimes an even simpler force model may describe the trajectory:

Two-body equations (earth-space vehicle) are used on most of the trajectory to the moon, and at some point near the moon a transformation to selenocentric coordinates is performed and two-body equations (moon-space vehicle) are used to describe the trajectory near the moon. This last simplification will be discussed further in Sections B-1 and C of the present chapter.

Any sketches of trajectories will be made either in nonrotating coordinates $x_e y_e z_e$ with origin at the center of the earth, nonrotating coordinates $x_m y_m z_m$ with origin at the center of the moon, or in rotating coordinates $x_R y_R z_R$ with origin at the barycenter and the x_R-axis along the earth-moon line in the direction of the moon (see sketch on page IV-20). A typical lunar trajectory is plotted to scale in geocentric nonrotating coordinates in Fig. 1 and in barycentric rotating coordinates in Fig. 2 with the time from injection indicated on each trajectory. The nonrotating trajectory shows the characteristic shape of a two-body conic section near the earth, and it is not until the moon is approached closely that the moon's gravitational attraction modifies the shape of this conic section. The path in the rotating coordinate system is approximately as it would appear to an observer at the center of the moon, since the moon's mean orbital motion is equal to the rotational rate about its axis. The qualification "approximately" is included because the difference between the true and mean orbital motion due to eccentricity $e_{\mathbb{C}}$ and the small inclination of the lunar spin axis to its orbital plane (both given by optical librations) cause the lunar observer to see a slightly different trajectory as the $x_R y_R$ coordinate trace.

As the title of this section indicates, lunar flights may be classified either into classes of trajectories, as was done notably by Egorov (Ref. 1) and Buchheim (Ref. 2), i.e., the trajectories are subdivided by their shape in an inertial or rotating coordinate system, or lunar flights may be classified into classes of missions according to the purpose of the flight. In general, the mission classification is broader since one mission, or one lunar flight, may consist of several trajectory classes. In this chapter, a lunar flight is defined as a space flight, on which the velocity at the initial point of the trajectory equals or exceeds the minimum velocity to leave the earth at the initial point and whose primary mission goal is in earth-moon space. Thus the boost or earth orbit phase of any trajectory will not be considered here, nor will any part of it outside of a region where the gravitational attraction of the earth and moon predominate. The table below classifies such lunar flights into the various mission and trajectory classes:

Mission Class	Trajectory Class
1. Lunar probes	Trajectories near minimum velocities
	Approach trajectories
	Impact trajectories (hard landing)
	Impact trajectories (soft landing)
2. Circumlunar and allunar missions	Circumlunar trajectories (nonperiodic and periodic)
	Allunar trajectories (nonperiodic and periodic)
3. Lunar orbit missions	Impact trajectories Approach trajectories Circumlunar trajectories Allunar trajectories Orbits around the moon
4. Landing missions	Approach trajectories Circumlunar trajectories Allunar trajectories Orbits around the moon Ascent and descent trajectories Impact trajectories
5. Space stations	Libration point buoys
6. Lunar passages to escape	Approach trajectories (accelerating or braking approaches)

The lunar missions in the classification above have been arranged chronologically, i.e., a planned exploration of the moon and solar system would at first involve lunar probes, then circumlunar (passing behind the moon) or allunar (passing in front of the moon) missions, lunar orbits, landings on the moon, establishment of long-term space stations in earth-moon space, and finally the use of the gravitational attraction of the moon to accelerate or decelerate space vehicles on their journey to the planets. Of course there may be a certain amount of overlapping so that for any given time the plan may call for lunar probes as

well as circumlunar missions, or for circumlunar, lunar orbit, as well as landing missions. Most of the classes of lunar missions may be used for research and exploration, for military roles, as well as exploitation and colonization of the moon. Since the lunar flight manual is essentially mission-oriented, it is preferable to discuss qualitatively each class of mission and describe the various types of trajectories associated with the mission in the order of their first appearance.

Prior to this classification it is instructive to compare approximate propulsion requirements for typical lunar missions from earth launch. These requirements are given below in terms of the characteristic velocity increment ΔV, or the velocity the space vehicle would attain in gravity-free space if it were accelerated in a straight line by the equivalent amount of rocket burning:

Mission	ΔV (km/sec)
1. Lunar probe without rocket burning near the moon	12.5
2. Circumlunar mission	12.5
3. Circumlunar mission with deceleration by rockets to earth orbit velocity	16
4. Establishment of a lunar orbit	13.5
5. Establishment of a lunar orbit return to earth and deceleration by rockets to earth orbit velocity	18
6. Landing on the moon	14.5
7. Landing on the moon with return to earth orbit velocity	20.0

The higher velocities in missions 3 through 7 reflect additional rocket burning in the vicinity of the moon or during earth return. The return to earth orbit and eventually to an earth landing base may be accomplished largely by aerodynamic maneuvering and hence reduce the total propulsion requirements for a mission with earth return.

2. Lunar Probes

A lunar probe is defined as a one-way, unmanned space vehicle for the collection of scientific data passing the vicinity of the moon but which does not pass behind the moon. The trajectory classes associated with probes are ballistic except for possible braking prior to lunar impact. Probes are used to obtain scientific data in earth-moon space, near the moon, and on the lunar surface as the name implies. Typical measurements may include (Ref. 2):

(1) A determination of the mass of the moon.

(2) Measurement of magnetic fields, electromagnetic and corpuscular radiation, meteoritic densities and of other environmental data in earth-moon space.

(3) Determination of the physical properties of the very tenuous lunar atmosphere.

(4) Determination of the composition, properties, temperature variation, and radioactivity of the lunar surface.

(5) Determination of the seismic properties of the lunar interior.

In addition, lunar probes may serve as engineering test vehicles for the evaluation of space vehicle systems such as tracking, communication, environmental control and power systems.

The associated trajectory classes may be:

(1) Trajectories near minimum velocities, or those which have just sufficient energy to eventually leave the earth, and will, at least initially, return to the vicinity of the earth several times.

(2) Approach trajectories, which have a higher energy, and are defined as trajectories which reach the vicinity of the moon on the first orbit but miss it by some distance.

(3) Impact trajectories which directly strike the moon either without rocket braking or with rocket braking near the moon. Impact trajectories can be classified further. If the impact velocity on the lunar surface is of the order of tens of m/sec, the impact can be classified as a soft landing while impact speeds of about 100 m/sec and above are called hard landings.

a. Trajectories near minimum velocities; transit time

In this section the results of the previous restricted three-body discussion will be applied to this trajectory class, its characteristics will be discussed in detail, and the strong effect of injection velocity on transit time near minimum velocities will be illustrated.

The ballistic trajectory of a space vehicle is completely determined by its initial position and velocity. These injection conditions (or initial conditions for lunar trajectories near earth) are usually given either in earth-centered trajectory coordinates $x_e y_e z_e$ and velocity components $\dot{x}_e \dot{y}_e \dot{z}_e$, where $\dot{x}_e = \dfrac{dx_e}{dt}$, or in terms of $r_{e\Delta}$, $V_{e\Delta}$, Y_e and η_e (for trajectories in the moon's orbital plane) as illustrated in the following sketch:
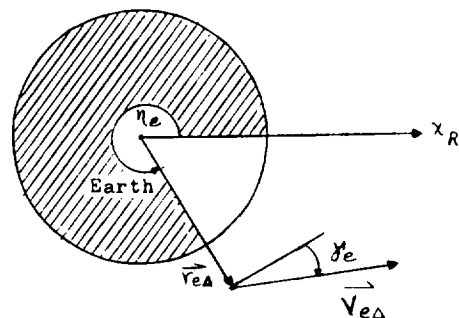
A subscript zero is used to specify injection conditions. Injection time must be held within close tolerances since the earth, moon, and space vehicle all move quite rapidly with respect to each other.

It was shown in Subsection B-2, Chapter III that the minimum velocity to reach the moon from earth corresponded to a value of $C_2 = 3.34367$ $(km/sec)^2$ for the Jacobi constant. This value was related to the injection velocity in the rotating $x_R y_R z_R$ coordinate system, $\vec{V}_{R\Delta}$, the magnitude of $V_{R\Delta}$ being independent of its direction and nearly independent of the angle between the initial radius vector $\vec{r}_{R\Delta} = \vec{r}_{e\Delta}$ and the x_R-axis. The maximum variation of $V_{R\Delta}$ with this angle was of the order of 0.1 m/sec for $r_{e\Delta} = 7378.2$ km and less for smaller values of $r_{e\Delta}$. However, a change in injection altitude from 100 km ($r_{e\Delta} = 6478.2$ km) to 1000 km ($r_{e\Delta} = 7378.2$ km) decreased the minimum $V_{R\Delta}$ from 10942.2 m/sec to 10233.2 m/sec.

It is now necessary to relate the injection velocity in rotating coordinates, $\vec{V}_{R\Delta 0}$ $(\dot{x}_{R\Delta 0}, \dot{y}_{R\Delta 0}, \dot{z}_{R\Delta 0})$ to the velocity in geocentric nonrotating coordinates $\vec{V}_{e\Delta 0}$ $(\dot{x}_{e\Delta 0}, \dot{y}_{e\Delta 0}, \dot{z}_{e\Delta 0})$. The general transformation between the velocity components of the two coordinate systems was given by Eq (86) of Chapter III,

$$\begin{Bmatrix} \dot{x}_{e\Delta} \\ \dot{y}_{e\Delta} \\ \dot{z}_{e\Delta} \end{Bmatrix} = \begin{bmatrix} \cos(\Phi + \omega_{\oplus\mathbb{C}}\, t) & -\sin(\Phi + \omega_{\oplus\mathbb{C}}\, t) & 0 \\ \sin(\Phi + \omega_{\oplus\mathbb{C}}\, t) & \cos(\Phi + \omega_{\oplus\mathbb{C}}\, t) & 0 \\ 0 & 0 & 1 \end{bmatrix}$$

$$\cdot \begin{Bmatrix} \dot{x}_{R\Delta} - \omega_{\oplus\mathbb{C}}\, y_{R\Delta} \\ \dot{y}_{R\Delta} + \omega_{\oplus\mathbb{C}}\,(x_{R\Delta} + \bar{r}_{\oplus\mathbb{C}}\, \nu) \\ \dot{z}_{R\Delta} \end{Bmatrix} \quad (1)$$

IV-3

where

$$\nu = \frac{M_{\mathcal{C}}}{M_{\oplus} + M_{\mathcal{C}}} = 0.01214216, \quad \bar{r}_{\oplus\mathcal{C}} = 384747.2 \text{ km}$$

is the lunar unit or earth-moon distance used for the circular restricted three-body problem,

$\omega_{\oplus\mathcal{C}} = 2.661699484 \times 10^{-6}$ rad/sec is the rotational rate of the earth-moon line around the barycenter, and Φ is the initial angle between the nonrotating and rotating coordinate systems.

If the matrix multiplication is performed $V_{e\Delta}^2$ is obtained as:

$$V_{e\Delta}^2 = V_{R\Delta}^2 + \omega_{\oplus\mathcal{C}}^2 \left[y_{R\Delta}^2 + (x_{R\Delta} + \bar{r}_{\oplus\mathcal{C}}\nu)^2 \right] + 2\omega_{\oplus\mathcal{C}} \left[\dot{x}_{R\Delta} \, y_{R\Delta} + \dot{y}_{R\Delta} \, (x_{R\Delta} + \bar{r}_{\oplus\mathcal{C}}\nu) \right] \tag{2}$$

This expression can be transformed further by reference to the following sketch:
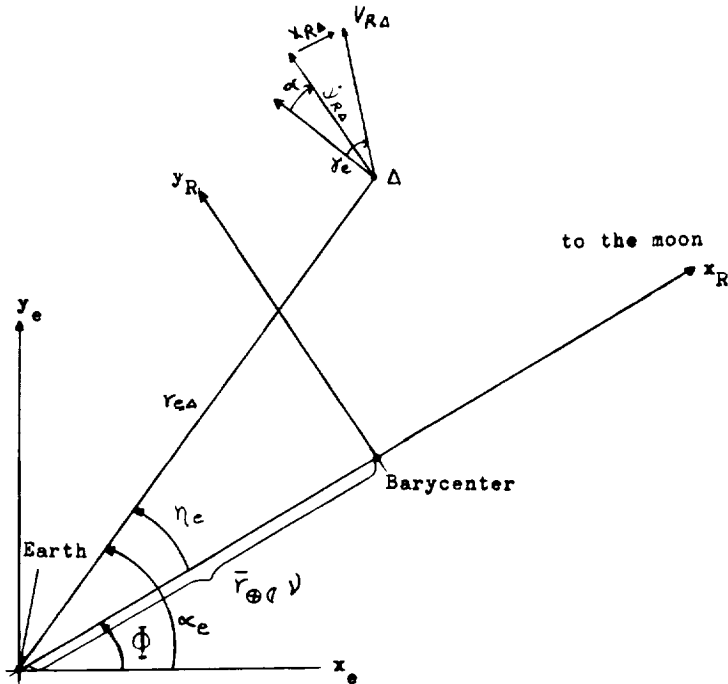
The following relations can be obtained from the previous sketch:

$$r_{e\Delta}^2 = x_{e\Delta}^2 + y_{e\Delta}^2 = (x_{R\Delta} + \bar{r}_{\oplus\mathcal{C}}\nu)^2 + y_{R\Delta}^2 \tag{3}$$

and

$$y_{R\Delta} = r_{e\Delta} \sin \eta_e, \quad x_{R\Delta} + \bar{r}_{\oplus\mathcal{C}}\nu = r_{e\Delta} \cos \eta_e \tag{4}$$

which yield, after substitution into Eq (2):

$$V_{e\Delta}^2 = V_{R\Delta}^2 + r_{e\Delta}^2 \omega_{\oplus\mathcal{C}}^2 + 2\omega_{\oplus\mathcal{C}} r_{e\Delta} (\dot{x}_{R\Delta} \sin \eta_e + \dot{y}_{R\Delta} \cos \eta_e) \tag{5}$$

In terms of the flight path angle relative to earth γ_e

$$\dot{x}_{R\Delta} \sin \eta_e + \dot{y}_{R\Delta} \cos \eta_e = V_{R\Delta} \cos \gamma_e,$$

so that the square of the velocity relative to earth becomes:

$$V_{e\Delta}^2 = V_{R\Delta}^2 + r_{e\Delta}^2 \omega_{\oplus\mathcal{C}}^2 + 2\omega_{\oplus\mathcal{C}} r_{e\Delta} V_{R\Delta} \cos \gamma_e. \tag{6}$$

For given values of $r_{e\Delta}$ and $V_{R\Delta}$ in the earth-moon system the velocity relative to earth $V_{e\Delta}$ is a maximum if $\cos \gamma_e = 1$ ($\gamma_e = 0°$) and it is a minimum if $\cos \gamma_e = -1$ ($\gamma_e = 180°$), or

$$\left[V_{R\Delta}^2 + r_{e\Delta}^2 \omega_{\oplus\mathcal{C}}^2 - 2\omega_{\oplus\mathcal{C}} r_{e\Delta} V_{R\Delta} \right]^{1/2} \leq V_{e\Delta} \leq \left[V_{R\Delta}^2 + r_{e\Delta}^2 \omega_{\oplus\mathcal{C}}^2 + 2\omega_{\oplus\mathcal{C}} r_{e\Delta} V_{R\Delta} \right]^{1/2} \tag{7}$$

For injection at 100-km altitude:

$$r_{e\Delta 0} = 6478.2 \text{ km}, \quad V_{R\Delta 0} = 10942.2 \text{ m/sec},$$

$$10925.0 \text{ m/sec} \leq V_{e\Delta 0} \leq 10959.4 \text{ m/sec},$$

and the minimum velocity relative to earth for sending a vehicle to the moon is 10925.0 m/sec, while for injection at 1000-km altitude:

$$r_{e\Delta} = 7378.2 \text{ km}, \quad V_{R\Delta 0} = 10233.2 \text{ m/sec},$$

$$10213.6 \text{ m/sec} \leq V_{e\Delta 0} \leq 10252.8 \text{ m/sec}$$

and the minimum velocity relative to earth for lunar injection at that altitude is 10213.6 m/sec. In each case the maximum value of $V_{e\Delta 0}$, $(V_{e\Delta})_{max}$, occurs when $V_{e\Delta 0}$ is perpendicular to $r_{e\Delta}$ in the direction of the moon's rotation as illustrated in the following sketch:
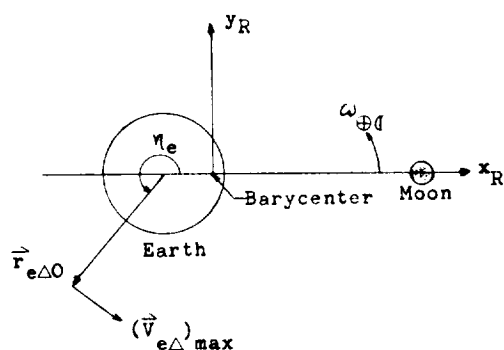
The injection flight path angle γ_{e0} may be used to classify lunar trajectories. Thus, a space vehicle trajectory in the direction of the earth-moon orbital motion($\gamma_{e0} < 90°$) illustrated in the previous sketch is known as a direct trajectory. Since the angular velocity vector of the earth $\bar{\omega}_\oplus$ has a component $\omega_\oplus \cos i_{em}$ perpendicular to the earth-moon orbital plane (MOP), a vehicle in a direct trajectory can capitalize on the rotation of the earth as well as the orbital motion of the earth in the MOP as illustrated above. Trajectories with injection in a sense opposite to $\omega_\oplus$ ($\gamma_{e0} > 90°$) are called retrograde trajectories. The ΔV penalty from launch for a retrograde trajectory as compared to a direct trajectory may be as high as 740 m/sec.

The gravitational attraction of the moon on the lunar trajectory near injection is very small, and it is possible to approximate the first stages of a lunar trajectory by a two-body earth-space vehicle problem. In a two-body approximation, the escape or parabolic velocity at 100 km is

$$V_{ep} = \sqrt{\frac{2\mu_\oplus}{r_{e\Delta}}} = 11093.2 \text{ m/sec}$$

which compares with a minimum restricted three-body velocity of

$$(V_{e\Delta})_{min} = 10925.0 \text{ m/sec.}$$

The corresponding minimum two and restricted three-body velocities for injection at 1000 km are:

$$V_{ep} = 10394.6 \text{ m/sec}, \quad (V_{e\Delta})_{min} =$$

$$10213.6 \text{ m/sec}$$

Thus, the minimum three-body velocity is only about 170 m/sec less than the two-body parabolic velocity. This indicates that lunar trajectories for near minimum velocities will approximate

two-body ellipses with initial eccentricities near 1 (i.e., when the gravitational effect of the earth is predominant). As the injection velocity is increased, the trajectories will approximate two-body parabolas and hyperbolas in their initial stages. The extent along the trajectory to the moon to which this two-body approximation can be carried will be discussed in Subsection B-1c.

Egorov (Ref. 1) has made a systematic study of trajectories in the MOP near minimum velocities. These trajectories with a Jacobi constant of C_3 (refer to Fig. 2, Chapter III) have the characteristic of an extremely long transit time in the order of months. For example, consider trajectories with $\gamma_{e0} = 0°$. In geocentric $x_e y_e$ coordinates these trajectories closely approximate two-body ellipses with large eccentricities (near 1). The apogee of these trajectories increases slowly due to lunar perturbations as illustrated in the following sketch; only the first several orbits of a typical earth-moon trajectory near minimum velocity are shown.
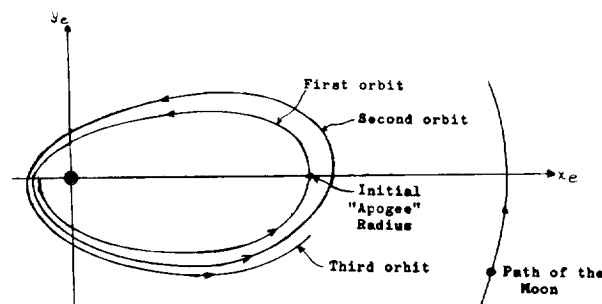
The space vehicle must traverse many such near-elliptical orbits before it can pass through the constriction in the C_3 contour near the double point between the earth and moon and approach the moon (Fig. 2, Chapter III). Increase of γ_{e0} will increase the required $V_{e\Delta0}$ as well as the initial apogee radius of the trajectory.

The time required for a passage from the earth to the moon depends strongly on the injection velocity. It has been estimated (Ref. 1) that trajectories at the minimum velocity reach the boundary of their region C_2 in about three years. This type of trajectory thus is impractical for most lunar missions. A slight increase in injection velocity reduces the transit time significantly as can be noted from the following trajectories to the moon in the MOP with an injection altitude of $h_{\oplus 0} = r_{e\Delta0} - R_e = 175.7$ km and with $\gamma_{e0} = 0°$:

Injection Velocity, $V_{e\Delta 0}$ (m/sec)		Transit Time to the Moon (hr)
γ_{e0} = 0° $r_{e\Delta 0}$ = 6478.2 km $h_{\oplus 0}$ = 100 km	γ_{e0} = 0° $r_{e\Delta 0}$ = 6553.9 km $h_{\oplus 0}$ = 175.7 km	
10,997	10,932	120
11,008	10,943	80
11,097	11,033	50
11,278	11,215	35
11,660	11,600	24
13,450	13,400	13

The injection velocity for an injection altitude of
100 km has been calculated from the energy integral
of a two-body force model, Eq (9) below, to allow
a direct comparison with the minimum restricted
three-body velocity of 10959 m/sec.

An increase in injection velocity of 100 m/sec
or about 1% near the minimum velocity decreases
the transit time from five to about two days, but for
any further significant decrease in transit time
the injection velocity must be increased consider-
ably. Hence, for each lunar mission there is a
tradeoff between a higher injection velocity and
the correspondingly higher fuel load and a longer
transit time with larger power requirements and
support systems.

b. Approach trajectories

Approach trajectories differ from trajectories
near minimum velocities in that with the former
class the vicinity of the moon may be reached
much quicker than with the latter. The transit
time for typical approach trajectories is approxi-

mately 120 hr at 40 m/sec above minimum re-
stricted three-body escape velocity. This time
is approximately 50 hr at parabolic velocity,
which is 170 m/sec above the minimum re-
stricted three-body escape velocity, and it decreases
to approximately 24 hr at 500 m/sec above
parabolic velocity. A further increase of injec-
tion velocity above the two-body escape or para-
bolic velocity will not reduce the transit time as
markedly as was possible near the two-body es-
cape velocity. Practical transit times for lunar
approach and impact trajectories vary from
about 30 to 80 hr, which seems to be a good com-
promise between rocket fuel requirements on one
hand, and power and support system requirements
on the other.

Approach trajectories may miss the moon by a
small or large distance, the major differences
between an approach trajectory from a trajectory
near minimum velocity being that the "initial
apogee" of the approach trajectory would be be-
yond the orbit of the moon and the transit time
for passage to the orbit of the moon is less than
five days. If the approach trajectory passes
near the moon, the concept of "apogee" becomes
illusory since the gravitational attraction of the
moon modifies the trajectory shape considerably.
Possible approach trajectories in the vicinity of
the moon are given in the following sketch in
selenocentric coordinates $x_m y_m$, where $\vec{V}_{m\Delta}$ is
constant vehicle velocity in selenocentric coor-
dinates at entry into the circular region around
the moon, and $\vec{V}_{e\text{◖}}$ is the velocity of the moon in
geocentric coordinates which is directed along
the negative y_m-axis:

Direct Trajectories
Around the Moon

Velocity Diagram

Retrograde Trajectories
Around the Moon
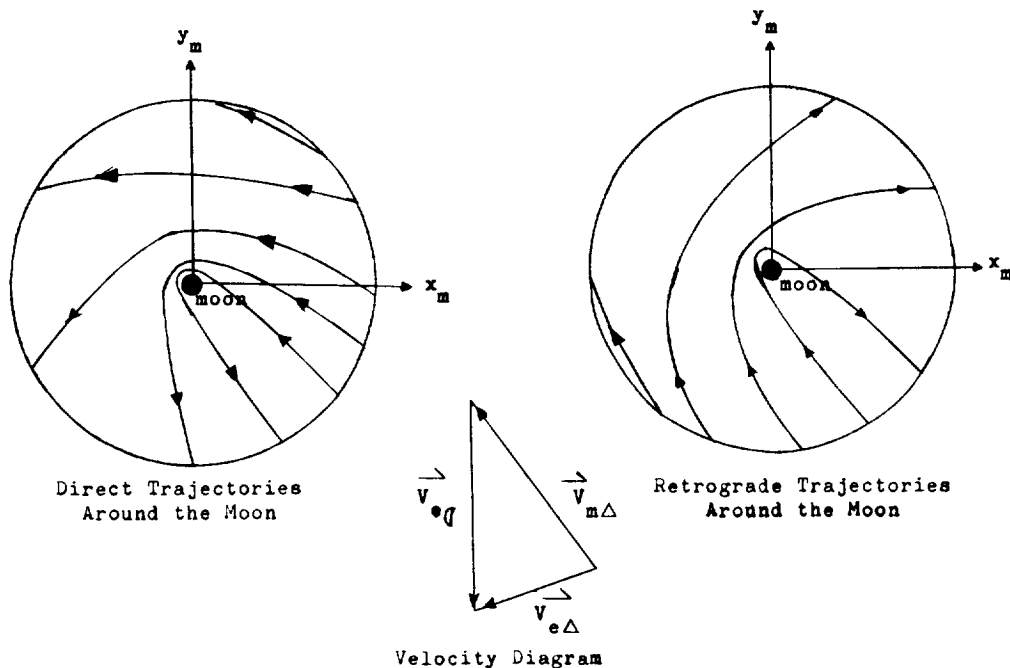
As can be seen from this sketch, the approach trajectory leaves the vicinity of the moon. It was shown by Egorov (Ref. 1) that the moon cannot capture a space vehicle on an approach trajectory since the vehicle energy corresponds to that of a hyperbolic selenocentric trajectory if the attraction of the earth is neglected. The preceding sketch also shows that the closer the approach to the moon, the greater is the "turning effect" of the moon on the trajectory. While in the vicinity of the moon, the approach trajectories may be either direct or retrograde, depending on whether they pass around the moon in the direction or against the direction of the lunar rotation, as illustrated in the preceding sketch. However, it is more common (Ref. 1, for example) to classify approach trajectories direct ($\gamma_{e0} < 90°$) or retrograde ($\gamma_{e0} > 90°$) at injection near earth.

c. Impact trajectories

In any study of lunar flight the first trajectory considered is usually an impact trajectory. Such a trajectory is simply an approach trajectory which intersects the surface of the moon. Since the impact may occur on the way out or on the return, there are now four types of impact trajectories as opposed to two types of approach trajectories:

The first type leaves the earth direct and intercepts the moon on an ascending arm. A second type leaves the earth direct but intercepts the moon on a descending arm. The following sketch depicts these two types of trajectories in the geocentric $(x_e y_e)$ coordinate system with t_0 denoting the injection time and t_i the impact time:
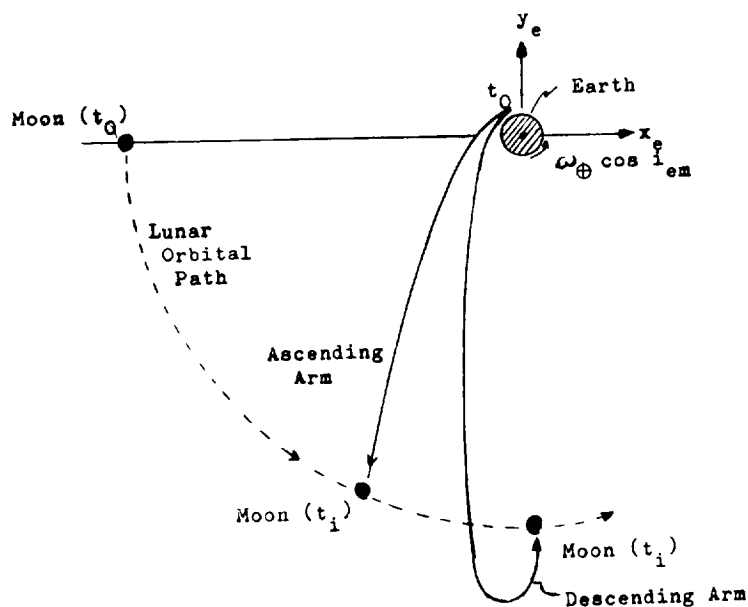
The third and fourth types are identical to the first two except that they leave the earth retrograde.

The retrograde trajectories are usually avoided due to the larger fuel requirements. Since interception of the moon on a descending arm has been shown to increase the required guidance accuracies by two to five times, the most practical impact probe trajectories are direct ones which strike the moon on the ascending arm.

Impact trajectories will hit the surface of the moon with a velocity of approximately 3000 m/sec unless they are retarded by rocket braking during the descent phase. Hard landings, with impact velocities approximately between 3000 and 100 m/sec, can be used for relatively simple experiments, while the impact velocity has to be braked to the order of tens of m/sec for soft landings of delicate equipment for experiments on the moon. Lunar impacts on the ascending arm are essentially limited to the visible disk while impacts on the descending arm occur essentially behind the moon. An impact trajectory with rocket burning before the landing will also require some control of the orientation of the vehicle before and during rocket burning.

### 3. Circumlunar and Allunar Missions

The next missions of interest are circumlunar and allunar missions, which may be manned or unmanned. Specific lunar and earth return conditions are somewhat more difficult to achieve than for lunar probes because of the tighter injection tolerances. A very desirable feature for these missions is that the vehicle returns to the vicinity of the earth ballistically after passing arbitrarily close to the lunar surface. The nomenclature of the associated trajectories is analogous to the mission nomenclature and the exact definition of each trajectory class will be given when it is discussed in detail.

Of primary interest are the nonperiodic circumlunar missions since they allow reconnaissance, surveillance and mapping of the back of the moon. The other trajectory classes are of less practical interest, but will nevertheless be mentioned briefly.

Trajectories that depart from earth, pass behind the moon while crossing the earth-moon line in the vicinity of the moon, and again return to earth ballistically are called nonperiodic circumlunar trajectories or circumlunar trajectories for short. Basically, these trajectories can leave the earth either direct as shown in the following sketch, or retrograde (not shown), where t_p is the time of pericynthion, or closest approach to the moon.

A circumlunar trajectory leaving the earth either direct or retrograde can return to earth by establishing either a direct or retrograde (and highly elliptic, parabolic or hyperbolic) orbit around it or impact the earth as indicated in the following sketch. This would account for six different types of circumlunar trajectories.

The general type of trajectory is one of the easiest to achieve, but specific conditions at the moon and on earth return are difficult to obtain due to the fact that error sensitivities are
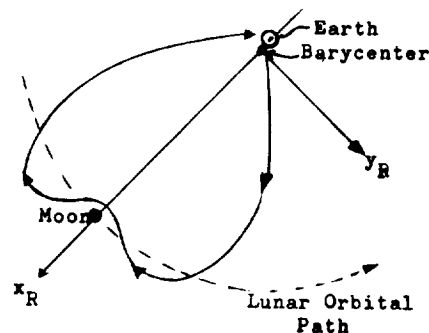
Moon (t_0)

Lunar Orbital Path
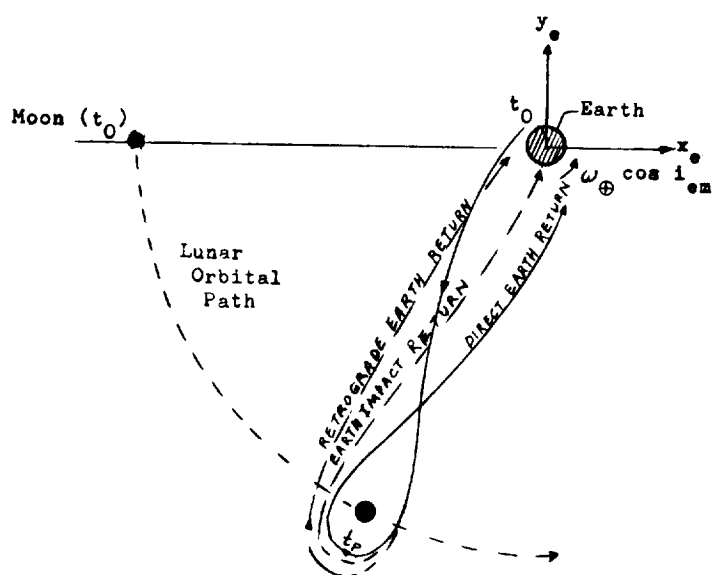
Orbit No.	$(r_{e\Delta})_{min}$ (km)	$(r_{m\Delta})_{min}$ (km)	Remarks
1	6,571	150	Lunar impact
2	42,203	825	Lunar impact
3	82,824	1500	Lunar impact
4	116,371	2000	A possible periodic orbit

As can be seen, the only case that does not impact the moon, $(r_{m\Delta})_{min}$ 1738 km, is Orbit No. 4. For this trajectory the closest approach to earth, $(r_{e\Delta})_{min}$, is almost 20 earth radii or about one-third of the distance to the moon. Such an orbit would seem to be of little practical interest, especially since this class of trajectories is also unstable, and small perturbations would cause the space vehicle to depart from this orbit.[**]

Opposed to the circumlunar classes of the corresponding nonperiodic and periodic trajectories described above are allunar trajectories, which pass only in front of the moon while they cross the earth-moon line in the vicinity of the moon. This feature is most clearly seen in rotating x_R y_R coordinates as shown in the following sketch of a direct nonperiodic allunar trajectory with an impact return to earth. Very frequently the descriptive term "nonperiodic" is dropped, and periodic allunar trajectories are referred to as allunar orbits to distinguish them from the allunar trajectories.

very high. For instance, an error of 1 m/sec in injection velocity (at t_0) can alter the miss distance by 870 km at the moon and 6650 km at earth. Although highly sensitive, these types of trajectories are especially suited for photographic missions on the back side of the moon. These missions may be manned or unmanned and may be highly desirable for future landing flights. In fact, actual landing missions may utilize such trajectories because of their inherent safety features (no lunar impact, ballistic departure and return). One drawback of circumlunar trajectories is the inaccessibility of higher lunar latitudes. This is due to the fact that their inclination to the lunar equatorial plane is limited to approximately 15° (see Chapter VI).

The total flight time for circumlunar missions is rather limited by the nature of the trajectory and depends strongly on the pericynthion altitude. The following figures are quoted for injection at an earth altitude of 200 km. For a pericynthion altitude of 200 km the total flight time to the moon and back can vary between 138 and 142 hr, for a pericynthion altitude of 1000 km it can vary between 147 and 152 hr, and for a pericynthion altitude of 2000 km it can vary between 155 and 165 hr. In each case the vacuum perigee of the return trajectory is at 50 km.

An interesting problem of lunar trajectories is the possibility of establishing periodic orbits around the earth and moon which pass behind the moon, or periodic circumlunar trajectories. The existence of such orbits was established and several orbits were calculated in Ref. 1. The closest approach to the earth, $(r_{e\Delta})_{min}$, and to the moon, $(r_{m\Delta})_{min}$, of several typical orbits is given below from Ref. 1[*]:

[*]These numerical values are based on Egorov's values of the earth-moon system constants and are to be regarded as illustrative rather than accurate.

Analogous to the six types of circumlunar trajectories one may distinguish six types of allunar trajectories. A typical mission employing an allunar trajectory is photography of the front face of the moon without the aid of lunar satellite orbits.

Although there is but one class of periodic circumlunar trajectories there are an unlimited number of possible periodic allunar trajectories.

[**]Note added in proof: A new class of circumlunar orbits has recently been described. A brief summary of this class of orbits is given as Section D.

Periods of these allunar orbits vary from 0.5 to
1.5 mo, and while they pass in front of the moon
as they cross the earth-moon line, their farthest
point from earth is well beyond the moon's orbit.
Circumlunar and allunar periodic orbits are of
interest, but it is doubtful that such orbits could
be established for a very long time due to their
unstable nature.

4. Lunar Orbit Missions

Lunar orbit missions are complex from a tra-
jectory viewpoint since a single mission may con-
sist of several phases, each utilizing a different
class of trajectories. The characteristic feature
of lunar orbit missions is that the primary purpose
of the mission is accomplished during the lunar
orbiting phase. In other respects the space ve-
hicle may be manned or unmanned; it may make
a one-way trip to the moon or eventually return
to earth if this is a manned mission.

The primary advantage of lunar orbits lies in
the almost unlimited time that the vehicle can
spend in the vicinity of the moon, time which can
be utilized for the gathering of scientific data, the
reconnaissance, surveillance, and mapping of the
moon. Also, no actual landing on the moon is
necessary, and all the attendant structural and
fuel problems do not appear.

The first question in a lunar orbit mission is
whether the moon can capture a space vehicle
launched with a velocity higher than the one cor-
responding to the Jacobi constant C_2 (see Chapter
III, Subsection B-2). It was shown by Egorov (Ref.
1) that it is impossible for the moon to capture a
vehicle on an approach trajectory, no matter
what the initial conditions. The question of lunar
capture without thrust remains open for trajec-
tories near minimum velocities which make more
than one orbit around earth before reaching the
vicinity of the moon. When the injection velocity
is between the one corresponding to the Jacobi
constants C_2 and C_4, then the space vehicle can
pass through the constriction near the critical
point between the earth and moon (see Fig. 2,
Chapter III) after more than one orbit around
earth and become a temporary satellite of the
moon before it returns to the vicinity of the
earth.

This class of trajectories is not very practical
since (1) the possible range of injection velocities
is about 1 m/sec (see table on page 21 in Chapter
III), and the trajectory is very sensitive to solar
and other perturbations, and (2) the transit time is
very long and the transit time is very sensitive to
injection velocity in the possible range of about
1 m/sec. Thus in practice a lunar orbit can only
be achieved by reducing the velocity of the space
vehicle through thrust application near the moon.

A typical lunar orbit mission with return to
earth, illustrated in the sketch at the top of the
next page, will consist of:

(1) An earth-to-moon transfer phase which
may be an approach, the first half of a
circumlunar, or, less likely, an impact
trajectory.

(2) An entry maneuver into the desired
lunar orbit.

(3) A lunar orbit phase which may last for
several revolutions.

(4) A departure maneuver from the lunar
orbit.

(5) A moon-to-earth transfer phase which
may be the second half of a circumlunar
trajectory, or an approach or impact
trajectory, and is illustrated in the fol-
lowing sketch in geocentric nonrotating
coordinates x_e y_e.

The different types of approach, impact, or
circumlunar trajectories have been discussed
above. Lunar orbits may be classified either into
direct or retrograde orbits; they may be either
circular or elliptical with respect to the moon,
but their actual shape is continually changing due
to perturbations of the earth, the sun, and the
moon's figure. A more quantitative characteri-
zation of orbits is by their elements (Chapter III,
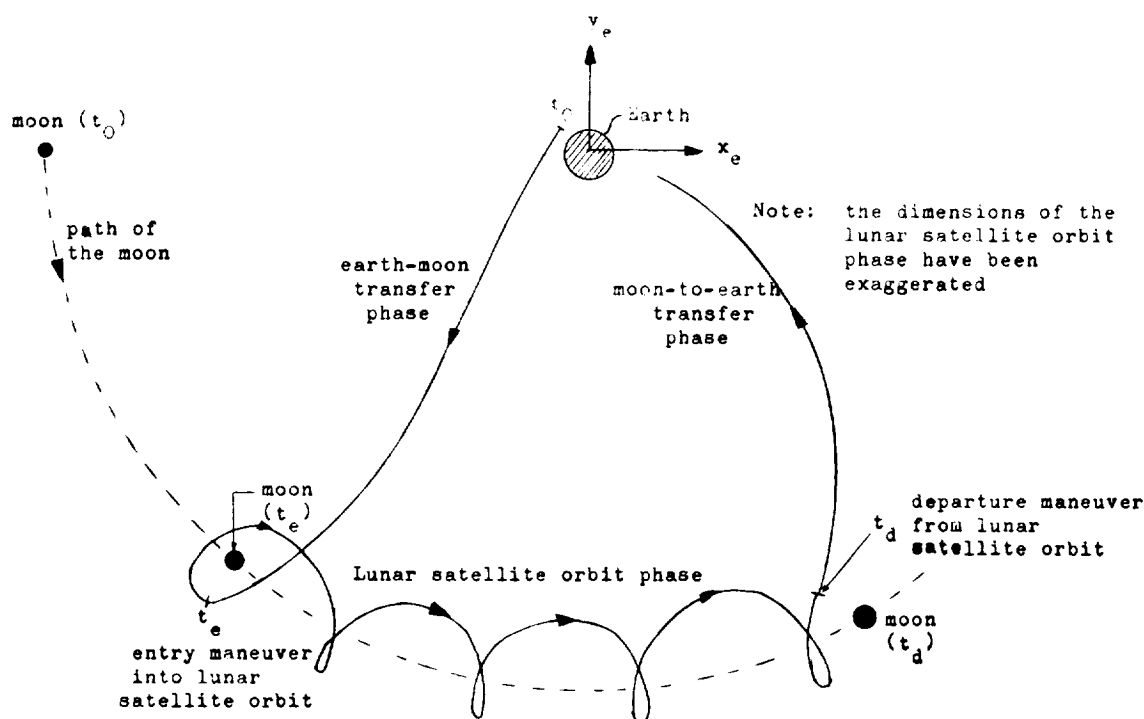Subsection A-3).

Entry to and departure maneuvers from lunar
orbits are generally characterized by the char-
acteristic velocity ΔV of the maneuver.

5. Landing Missions

Closely related to lunar orbit missions are the
lunar landing missions, in which the space vehicle
is on the lunar surface during one phase of the
mission where its primary purpose will be accom-
plished. Landing missions are the most complex
missions from a trajectory point of view. They
may be manned or unmanned, one-way or round
trip. Most likely the lunar landing mission will
use a circumlunar or approach trajectory in the
earth-moon transfer phase, and a lunar "parking"
orbit to reach the desired landing site, primarily
because of the flexibility in the choice of landing
site and because of the safety features of the cir-
cumlunar or approach trajectory. This type of
mission is known as lunar orbital landing. As
propulsion systems become more reliable, impact
trajectories with a soft landing may be used for
landing missions in areas of the moon which are
easily accessible for impact trajectories. The
latter type of mission is a lunar direct landing.
Lunar landing missions are used for exploration,
supply and logistics, and for establishment of
lunar bases.

A typical lunar landing mission with round trip
to earth consists of:

(1) An earth-to-moon transfer phase which
may be an approach, the first half of a
circumlunar, or, less likely, an impact
trajectory.

(2) An entry maneuver into the desired lunar
orbit (this phase is deleted for direct
landings).

(3) A lunar orbit phase which may last from
a fraction of one to several revolutions
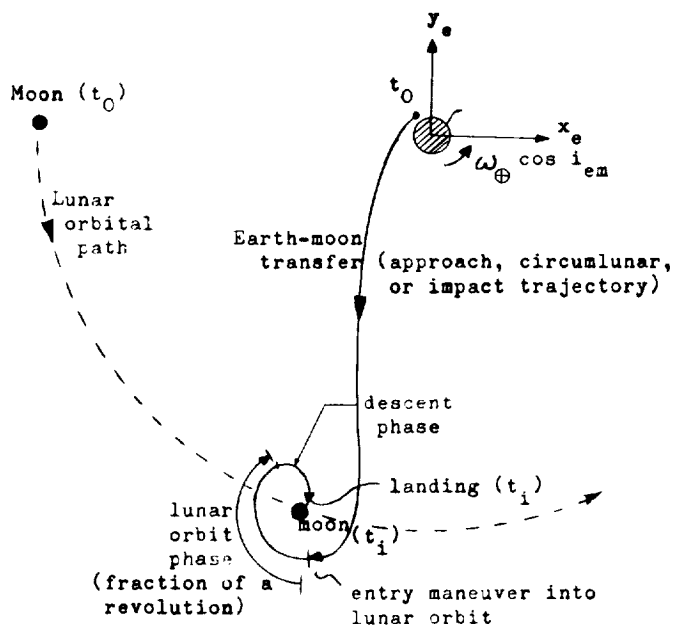(this phase is deleted for direct landings.)

moon (t_0)

v_e

t_0

Earth

x_e

path of the moon

earth-moon transfer phase

moon-to-earth transfer phase

Note: the dimensions of the lunar satellite orbit phase have been exaggerated

moon (t_e)

departure maneuver from lunar satellite orbit t_d

Lunar satellite orbit phase

moon (t_d)

t_e

entry maneuver into lunar satellite orbit

(4) A descent phase to the lunar surface and landing (possibly using lunar orbit rendezvous concept as described in the following paragraph).

(5) A lunar stay of arbitrary duration.

(6) An ascent phase from lunar surface.

(7) A lunar orbit phase which may last from a fraction of one to several revolutions (this phase is deleted for direct landings).

(8) A departure maneuver from lunar orbit (this phase is deleted for direct landings).

(9) A moon-to-earth transfer phase which may be the second half of a circumlunar trajectory, an approach or impact trajectory.

For one-way landing missions, phases (6) through (9) are deleted. The classes of trajectories utilized for each phase of the landing mission may be classified further as was discussed above.

A typical one-way lunar orbital landing mission has been illustrated in the following in geocentric nonrotating coordinates x_e y_e.

A mission which may be regarded as a hybrid between the lunar orbit and landing missions is the lunar orbit rendezvous mission (LOR). In this mission the space vehicle establishes a lunar orbit.

Moon (t_0)

y_e

t_0

x_e

$\omega_\oplus \cos i_{em}$

Lunar orbital path

Earth-moon transfer (approach, circumlunar, or impact trajectory)

descent phase

landing (t_i)

moon (t_i^-)

lunar orbit phase

lunar orbit phase (fraction of a revolution)

entry maneuver into lunar orbit

At the proper time a segment of the vehicle, called the shuttle vehicle, detaches itself, descends to and lands on the lunar surface. After the purpose of the mission on the lunar surface has been accomplished, the shuttle vehicle ascends to lunar orbit and makes a rendezvous with the orbiting space vehicle. The men and any equipment are

IV-10

transferred to the space vehicle, which then re-
turns to earth while the empty shuttle is abandoned
in lunar orbit.

6. Space Stations

It has been proposed by Buchheim (Ref. 2)
that space stations may be established at the five
double points in earth-moon space. He calls such
vehicles libration center buoys. These double
points are in the MOP, they rotate around the
barycenter with the same angular velocity as the
earth and moon, and their fixed location in the
rotating x_R y_R coordinate system is given in
Subsection B-2 of Chapter III.

Three of the five double points are on the earth-
moon line, two fairly near the moon and the third
is on the opposite side of the moon about one lunar
unit from earth. The double points on the earth-
moon lines are unstable and the space vehicle
would have to make corrective maneuvers to
counteract perturbing forces in order to stay near
the double points for a longer time. The other
two double points form equilateral triangles with
the earth and moon and they are stable. Thus,
a space vehicle could stay at these points indefi-
nitely. The sketch on page III-21 in the preceding
chapter shows the location of the double points.

Space stations at the double points have also
been called synodic or selenoid satellites. They
could be used for beacons in space, as astronomi-
cal observatories, for conducting long-term ex-
periments in earth-moon space and for space
surveillance.

7. Lunar Passages to Escape

The moon can be used to accelerate or decel-
erate a space vehicle for interplanetary missions
or solar probes since the moon and most planets
are very close to the plane of the ecliptic. Accel-
eration of the space vehicle can be accomplished
by planning the approach trajectory to pass very
close to the moon and pass out of the vicinity of
the moon in the general direction of the moon's
orbital motion around earth. The following sketch
in geocentric nonrotating coordinates illustrates
this special case.
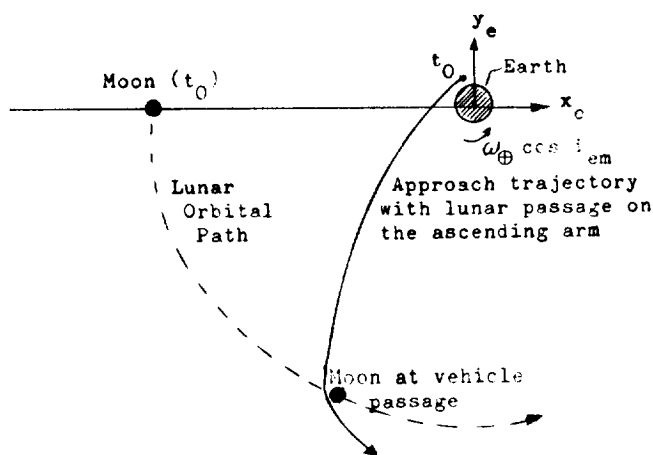
The maximum velocity increment that can be
gained is approximately 1480 m/sec. The vehicle
acceleration can be accomplished on a descending
arm as well. Retrograde trajectories can also
be used, but are not really practical because of
the larger ΔV required for earth departure. In
addition, the moon can be used to decelerate a
space vehicle. Deceleration would be obtained by
passing out of the moon's vicinity in a direction
opposite to the moon's orbital motion around the
earth.

The practicality of planning probes in this
fashion is debatable at this time due to the in-
creased guidance accuracy required. To take
full advantage of the gravitational attraction of
the moon, the following items are necessary:

(1) The approach to the moon should be as
close as possible.

(2) The pericynthion, or point of closest ap-
proach to the moon, has to be controlled
closely in order to turn the trajectory in
the desired direction (see the preceding
sketch.

(3) The launch time tolerance is very strin-
gent since both the moon and planet or
sun must be in a favorable position at
time of pericynthion.

8. Nomenclature and Characteristics of a Cir-cumlunar Trajectory

The ballistic lunar trajectories discussed above
behave very similarly during transit to and from
the moon. A fundamental plane of reference for
such trajectories is the moon's orbital plane
(MOP) used earlier in this section. For this dis-
cussion a circumlunar trajectory which is not
restricted to the MOP is used as an example.
The nomenclature used here is identical with that
given in the Voice discussion of Section C and
that describing all trajectory data throughout the
remaining chapters.

The outgoing trajectory to the moon is termed
a translunar trajectory. It is assumed that the
injection of the space vehicle into the translunar
trajectory occurs near earth, and a series of
two-body force models is used in the approxima-
tion of the entire trajectory. The connection or
patching between the different two-body trajectories
occurs near the moon. The eccentricity of the
translunar and transearth (a trajectory from the
vicinity of the moon to the vicinity of the earth)
trajectories is larger than 0.95.

The space vehicle can leave the earth in four
directions, direct north, direct south, retrograde
north, and retrograde south. These departure
directions are illustrated in the following sketch.
These departure directions are based on whether
the trajectory at injection is direct or retrograde,
above (north), or below (south) the MOP. The
injection position is given by the angle ψ_0 which
is measured from the intersection of the trans-
lunar trajectory plane with the MOP, which is
the x_E-axis, to the injection point. The vectors
$\vec{r}_{e\Delta 0}$ and $\vec{V}_{e\Delta 0}$ define the translunar trajectory
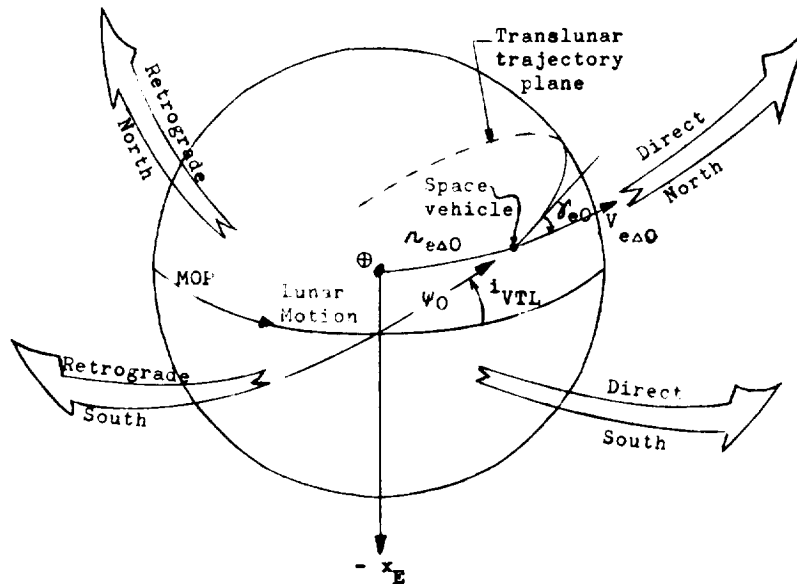
plane where $\vec{r}_{e\Delta 0}$ is the radius vector at injection. The injection flight path angle Y_{e0} is measured from the local horizontal (a plane perpendicular to $\vec{r}_{e\Delta 0}$) in the direction of the moon's motion to the velocity vector in the translunar plane (see preceding sketch). The positive x_E-axis is directed approximately toward the moon at the time of pericynthion while i_{VTL} is the inclination of the translunar plane to the MOP at the time of injection. In the vicinity of the earth ($r_{e\Delta} < 200,000$ km), i_{VTL} is essentially constant being affected primarily by the oblateness of the earth. As the vehicle nears the moon ($r_{e\Delta} \approx 200,000$ km), the trajectory is influenced to a greater degree by the gravitational attraction of the moon, thereby causing i_{VTL} to change. This is demonstrated in the following sketch.

Consider a space vehicle with a position vector $\vec{r}_{e\Delta}$ and a velocity vector $\vec{V}_{e\Delta}$ relative to earth. The space vehicle will be accelerated toward the moon by the lunar gravity $\vec{g}_q$. During a short time interval Δt the velocity of the vehicle will be changed by an amount ΔV_g along the line of action of $\vec{g}_q$.

By assuming that $\vec{r}_{e\Delta}$ remains unchanged, the resultant velocity of the space vehicle is $\vec{V}_{e\Delta 2} = \vec{V}_{e\Delta 1} + \Delta\vec{V}_g$. The plane formed by $\vec{r}_{e\Delta 1}$ and $\vec{V}_{e\Delta 1}$ is different from that formed by $\vec{r}_{e\Delta 1}$ and $\vec{V}_{e\Delta 2}$, and its translunar inclination differs from the original translunar inclination by Δi_{VTL}. Hence, lunar gravity causes the space vehicle to drift
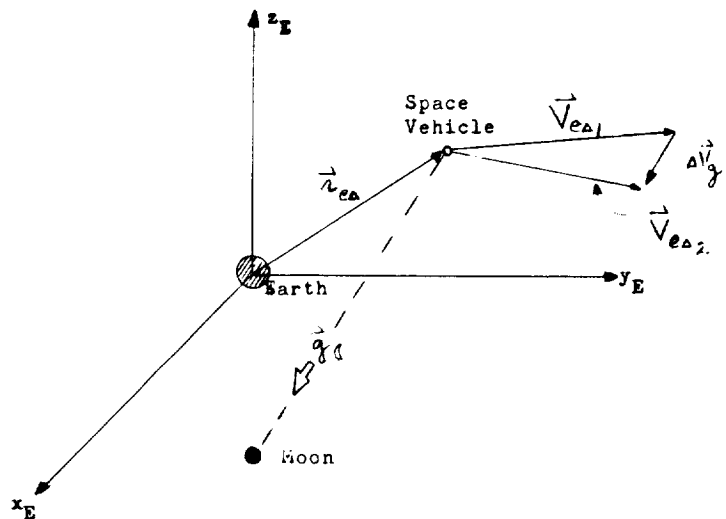
from the original translunar plane, and the rate of drift, directed toward the moon, increases as the moon is approached since $\vec{g}_q$ increases. This drift has occasionally been referred to as the focusing effect of the moon. In addition, the speed of the space vehicle relative to earth increases as the moon is neared. The following sketch shows the drift characteristic of a lunar trajectory.

A similar drift is experienced on the trip back to earth (transearth trajectory) except that the vehicle drifts into the final return inclination i_{VTE}.

On return to earth, the transearth trajectory may approach it from various directions. As was the case for the translunar injection, the directions

Initial translunar trajectory plane

Final transearth trajectory plane
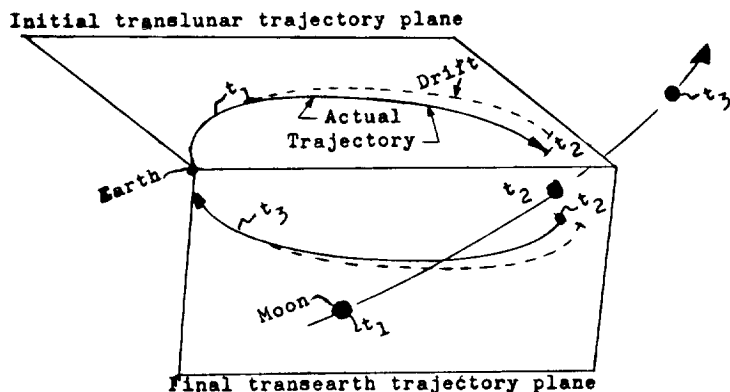
of return are classified as depicted in the follow-
ing sketch, where i_{VTE} is the final inclination of
the transearth trajectory:
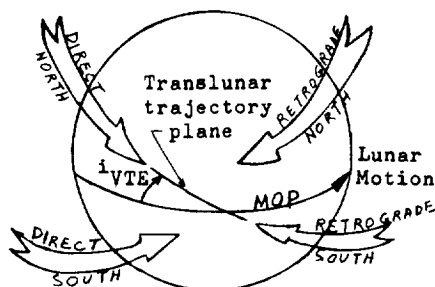
B. FORCE MODELS FOR LUNAR TRAJECTORY CALCULATIONS

In the preceding section the characteristics and
nomenclature of lunar trajectories were introduced.
These trajectory characteristics could be intro-
duced with very little attention to the physical and
mathematical background of how the position of
the space vehicle as a function of time, or its tra-
jectory, is obtained. However, in any quantitative
work, be it precise or approximate, it is necessary
to know what physical model underlies the calcula-
tions and by what mathematical method the trajec-
tory was obtained. The emphasis in the present
section will be on the assumed force model for
deriving the equations of motion since the analyti-
cal and numerical methods of solving these equa-
tions have been discussed in Chapter IV of Ref. 3.

Various degrees of sophistication are possible
in the description of the forces acting on a vehicle
in the earth-moon environment. These force
models vary in complexity as does the ease as
well as cost of generating trajectories and obtain-
ing values for trajectory parameters for a given
lunar mission. Rough approximations should not

be discarded simply because they are approxima-
tions. Different approximations in the force model
vary in their sensitivity to different parameters,
and a very crude approximation for one parameter
may be an excellent or at least an adequate one
for another, depending on the ultimate use of the
generated trajectories.

In general, the relative error between two
separate trajectories of a given force model is
smaller than the absolute error between a trajec-
tory using the given force model and one actually
flown in the earth-moon environment. Hence, a
very simple force model may be used to restrict
the range of each trajectory parameter for the
required lunar mission as well as to obtain the
allowable errors in initial conditions for success-
ful completion of the mission and to obtain guid-
ance sensitivities. Any conclusions drawn from
trajectories obtained from the simple model may
then be verified by generating a small number of
trajectories using a more sophisticated force
model.

In the following text, various force models
that have been employed in generating lunar tra-
jectories are discussed in the order of increasing
complexity, and quantitative differences between
the models are given whenever possible.

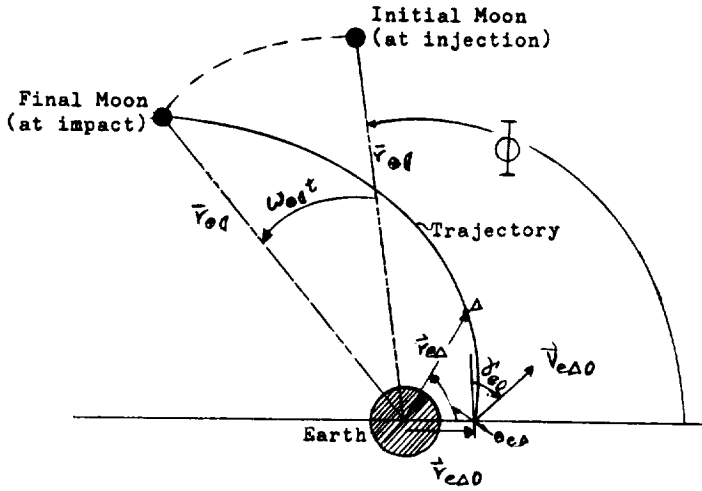### 1. Succession of Two-Body Trajectories

The simplest approach to lunar trajectory
studies is to treat the transit of a vehicle from
earth to moon as a succession of restricted two-
body problems. In the initial phase of flight the
vehicle is assumed to be in the earth's gravita-
tional field alone and its mass M_Δ is negligible
compared to the mass of the earth $M_\oplus$. At some
point along the trajectory the vehicle will pass into
a region where the moon's field is predominant.
It will then be assumed to be in the moon's field
alone and its mass M_Δ is negligible compared to
the mass of the moon $M_{\mathbb{C}}$. This approach allows
a splitting of the trajectory determination into
various phases, namely the study of (1) planar dy-
namics of the earth's field, (2) transition from
earth to moon influence where the criteria for
passing from phase (1) to the next phase are dis-
cussed, (3) planar dynamics of the lunar field,
and (4) three-dimensional effects when the vehicle
is not in the moon's orbital plane. Many char-
acteristics of lunar trajectories may be introduced
logically and studied on the basis of this approach.

It is obvious that this force model, like any
other model, will be more accurate for short
lunar missions than for longer ones, since the
neglected effects (discussed below) result from
accelerations acting over the entire transit time.
This approach is expected to be reasonably good
for lunar impact trajectories, and for circumlunar
flight. However, prolonged flights near the moon,
such as lunar satellites, should be analyzed by use
of more exact models.

a. Planar dynamics of the earth's field

For this two-body problem the vehicle moves
in a plane passing through the earth's center. The
moon revolves around the earth in the same plane

with an angular velocity $\omega_{\oplus\mathbb{C}}$ at a mean distance $\bar{r}_{\oplus\mathbb{C}}$ = 1 LU. The moon is treated here as a massless point without influence on the vehicle trajectory. Thus any nonrotating coordinate system at the earth's center of mass is inertial. In inertial plane polar coordinates $r_{e\Delta}$, $\theta_{e\Delta}$, as shown in the following sketch, the equations of motion of the space vehicle are:

$$\ddot{r}_{e\Delta} - r_{e\Delta}\dot{\theta}_{e\Delta}^2 = -\frac{\mu_\oplus}{r_{e\Delta}^2}$$
$$(8)$$
$$r_{e\Delta}\ddot{\theta}_{e\Delta} + 2\dot{r}_{e\Delta}\dot{\theta}_{e\Delta} = 0$$

Equation (8) yields two first integrals,

$$E_e = \frac{1}{2}\left\{\dot{r}_{e\Delta}^2 + \left(r_{e\Delta}\dot{\theta}_{e\Delta}\right)^2\right\} - \frac{\mu_\oplus}{r_{e\Delta}} =$$
$$\frac{1}{2} V_{e\Delta 0}^2 - \frac{\mu_\oplus}{r_{e\Delta 0}} \qquad (9)$$

$$h_e = r_{e\Delta}^2 \dot{\theta}_{e\Delta} = r_{e\Delta 0} V_{e\Delta 0} \cos \gamma_{e0}$$

where E_e and h_e are its energy and the magnitude of its angular momentum per unit mass, respectively. Equation (9) yields the final two integrals (see Ref. 4, for example)

$$t = \int_{r_{e\Delta 0}}^{\bar{r}_{\oplus\mathbb{C}}} \frac{dr}{\dot{r}} = \int_{r_{e\Delta 0}}^{\bar{r}_{\oplus\mathbb{C}}} \frac{dr}{\sqrt{2E_e + \dfrac{2\mu_\oplus}{r} - \dfrac{h_e^2}{r}}}$$
$$(10)$$

$$\theta_{0\mathbb{C}} = \int_{r_{e\Delta 0}}^{\bar{r}_{\oplus\mathbb{C}}} \frac{h_e\,dr}{r^2 \dot{r}} = \int_{r_{e\Delta 0}}^{\bar{r}_{\oplus\mathbb{C}}} \frac{h_e\,dr}{2E_e + \dfrac{2\mu_\oplus}{r} - \dfrac{h_e^2}{r^2}}$$
$$(11)$$

where t is the total time of flight and $\theta_{0\mathbb{C}}$ the total in-plane angle from $r_{e\Delta 0}$ to $\bar{r}_{\oplus\mathbb{C}}$.

As is well known, the trajectory obtained from Eq (8) is a conic section in the plane of the trajectory with focus at the center of the earth. It remains to orient the injection point on this conic section with respect to the moon at injection by the angle

$$\Phi = \theta_{0\mathbb{C}} \pm \omega_{\oplus\mathbb{C}}t. \qquad (12)$$

where the negative sign applies for direct and the positive sign for retrograde trajectories.

A consistent set of constants required in Eqs (8) through (11) is:

$$\mu_\oplus \equiv GM_\oplus = 398,601.5 \text{ km}^3/\text{sec}^2$$
$$\omega_{\oplus\mathbb{C}} = 2.661,699,484 \times 10^{-6} \text{ rad/sec} \quad (13)$$
$$\bar{r}_{\oplus\mathbb{C}} = 384,747.2 \text{ km}$$

Inspection of Eqs (10) and (11) in the light of Eq (9) reveals (Ref. 4) that the time of flight is insensitive to the burnout flight path angle γ_{e0}, but is a strong function of energy or burnout velocity $V_{e\Delta 0}$. The total in-plane angle $\theta_{0\mathbb{C}}$, on the other hand, is rather insensitive to $V_{e\Delta 0}$ and is a strong function of γ_{e0}. These relations are depicted in the following sketches for a representative injection radius of $r_{e\Delta 0}$ = 6740 km.
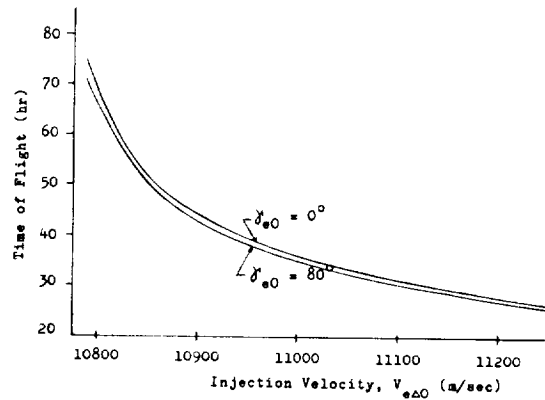
Since the effect of the moon has been ignored, the flight time and total in-plane angle for earth-moon transfer calculated from Eqs (10) and (11) are approximate. This approximation is relatively poor near minimum velocities $(V_{e\Delta})_{min}$ and becomes progressively better as the injection velocity $V_{e\Delta 0}$ is increased (for some comparison between these approximate and more exact results see Ref. 5). For the determination of visibility from earth, for instance, Eqs (10) and (11) are sufficiently accurate.

b. Transition from earth-to-moon influence

The transition from the earth to the lunar gravitational field may be made in various ways. Perhaps the simplest is to stop the translunar

Injection Flight Path Angle, $\gamma_{\oplus 0}$ (deg)
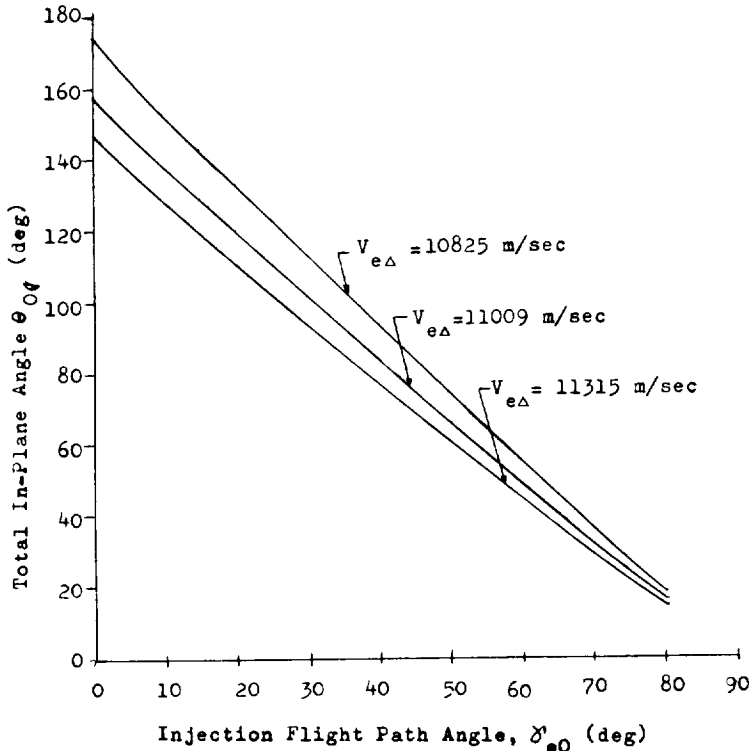
trajectory, as was done in the previous subsection, at a radius $\bar{r}_{\oplus\emptyset}$, the mean distance to the moon, and regard these conditions at $r_{e\Delta} = \bar{r}_{\oplus\emptyset}$ as occurring at infinity relative to the moon. This approach has been taken in Ref. 4, for example, and it may be referred to as the massless moon assumption.

However, a more natural transition from the earth's to the moon's gravitational field may be taken at the location in space when the ratio of the lunar disturbing force to the central force due to the earth's gravitational attraction becomes larger than the ratio of the earth's disturbing force to the central force of the lunar attraction. This region is called the sphere of influence of the moon, although it is slightly egg-shaped with the blunt end facing the earth, rather than spherical. The boundary of the sphere of influence of the moon can be found as follows.

Define distances by the following sketch: where the plane of the paper is the plane of the earth, moon, and space vehicle at its entry into the sphere of influence:
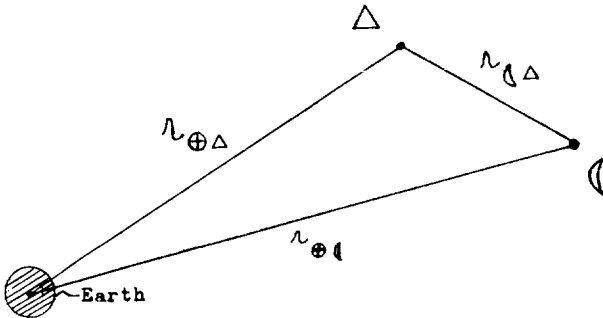
$r_{\oplus\emptyset}$ = earth-moon distance

$r_{\oplus\Delta}$ = earth-space vehicle distance

$r_{\emptyset\Delta}$ = moon-space vehicle distance

The gravitational acceleration or force per unit mass, on the space vehicle due to the moon, or the lunar gravitational field intensity at the space vehicle has the magnitude

$$ f_{\emptyset\Delta} = \frac{GM_\emptyset}{r^2_{\emptyset\Delta}} , \tag{14} $$

its acceleration due to the earth has the magnitude

$$ f_{\oplus\Delta} = \frac{GM_\oplus}{r^2_{\oplus\Delta}} , \tag{15} $$

and the gravitational acceleration of the moon due to the earth

$$ f_{\oplus\emptyset} = \frac{GM_\oplus}{r^2_{\oplus\emptyset}} \tag{16} $$

The ratio of the disturbing force of the earth to the attraction of the moon is given by

$$ \frac{f_{\oplus\Delta} - f_{\oplus\emptyset}}{f_{\emptyset\Delta}} = \left(\frac{M_\oplus}{M_\emptyset}\right) r^2_{\emptyset\Delta} $$
$$ \cdot \frac{(r_{\oplus\emptyset} + r_{\oplus\Delta})(r_{\oplus\emptyset} - r_{\oplus\Delta})}{r^2_{\oplus\Delta} \, r^2_{\oplus\emptyset}} \tag{17} $$

Similarly, the ratio of the disturbing force of the moon to the attraction of the earth is given by:

$$ \frac{f_{\emptyset\Delta} - f_{\emptyset\oplus}}{f_{\oplus\Delta}} = \left(\frac{M_\emptyset}{M_\oplus}\right) r^2_{\oplus\Delta} $$
$$ \cdot \frac{(r_{\oplus\emptyset} + r_{\emptyset\Delta})(r_{\oplus\emptyset} - r_{\emptyset\Delta})}{r^2_{\emptyset\Delta} \, r^2_{\oplus\emptyset}} , \tag{18} $$

where

$$ f_{\emptyset\oplus} = \frac{GM_\emptyset}{r^2_{\oplus\emptyset}} \tag{19} $$

is the gravitational acceleration of the earth due to the moon. The sphere of influence of the moon is the region

$$ \frac{f_{\oplus\Delta} - f_{\oplus\emptyset}}{f_{\emptyset\Delta}} < \frac{f_{\emptyset\Delta} - f_{\emptyset\oplus}}{f_{\oplus\Delta}} \tag{20} $$

and its boundary is given by

$$ \frac{f_{\oplus\Delta} - f_{\oplus\emptyset}}{f_{\emptyset\Delta}} = \frac{f_{\emptyset\Delta} - f_{\emptyset\oplus}}{f_{\oplus\Delta}} \tag{21} $$

IV-15

or, if we substitute from the right-hand sides of Eqs (17) and (18), the boundary is defined as:

$$r^4_{\unicode{x263D}\Delta} = \left(\frac{M_{\unicode{x263D}}}{M_\oplus}\right)^2 \cdot r^4_{\oplus\Delta} \cdot$$

$$\frac{(r_{\oplus\unicode{x263D}} + r_{\unicode{x263D}\Delta})(r_{\oplus\unicode{x263D}} - r_{\unicode{x263D}\Delta})}{(r_{\oplus\unicode{x263D}} + r_{\oplus\Delta})(r_{\oplus\unicode{x263D}} + r_{\oplus\Delta})} . \tag{22}$$

It can be deduced from the previous sketch that the disturbing effect is largest when the vehicle is on the earth-moon line between the earth and moon, and smallest when it is on the opposite side of the moon from the earth. Calling $r_{\unicode{x263D}\Delta}$ positive in the former case, negative in the latter, the radii at these two points of conjunction are:

$$r_{\oplus\Delta} = r_{\oplus\unicode{x263D}} - r_{\unicode{x263D}\Delta}$$

$$r_{\unicode{x263D}\Delta} = r_{\oplus\unicode{x263D}} - r_{\oplus\Delta}$$

and Eq (22) can be written:

$$r_{\unicode{x263D}\Delta} = \left(\frac{M_{\unicode{x263D}}}{M_\oplus}\right)^{2/5} r_{\oplus\Delta} \left(\frac{r_{\oplus\unicode{x263D}} + r_{\unicode{x263D}\Delta}}{2r_{\oplus\unicode{x263D}} - r_{\unicode{x263D}\Delta}}\right)^{1/5} . \tag{23}$$

Equation (23) can be solved by iteration, and the boundary of the "sphere of influence" of the moon on the earth-moon line is 51,870 km in front of the moon and 63,790 km behind the moon for a value of $\frac{M_\oplus}{M_{\unicode{x263D}}} = 81.357$. As can be seen from Eq (23), the "sphere" of influence is not a true sphere but has a bulge behind the moon.

It is instructive to compute the sphere of influence of the earth in its assumed circular orbit around the sun. Equation (23) can be used directly if we replace the earth symbol by the sun symbol and the moon symbol by the earth symbol in that equation:

$$r_{\oplus\Delta} = \left(\frac{M_\oplus}{M_\odot}\right)^{2/5} r_{\odot\Delta} \left(\frac{r_{\odot\oplus} + r_{\oplus\Delta}}{2 r_{\odot\oplus} - r_{\oplus\Delta}}\right)^{1/5} \tag{24}$$

In the sun-earth system $\frac{M_\odot}{M_\oplus} = 332,440$. Hence $r_{\odot\oplus} \gg r_{\oplus\Delta}$ and the spherical region approximating the earth's sphere of influence is given by

$$r_{\oplus\Delta} \approx \left(\frac{1}{2}\right)^{1/5} r_{\odot\oplus} \left(\frac{M_\oplus}{M_\odot}\right)^{2/5} . \tag{25}$$

For a mean solar distance of $r_{\odot\oplus} = 149.53 \times 10^6$ km, the "radius" of the earth's sphere of influence is

$$r_{\oplus\Delta} = 805,000 \text{ km.}$$

which is more than twice the mean distance of the moon from the earth. The moon, as well as lunar trajectories, is within the earth's sphere of influence, which justifies the omission of the gravitational attraction of the sun as a first approximation to the motion in earth-moon space.

When the space vehicle enters the lunar sphere of influence, its geocentric inertial position $(x_{e\Delta}, y_{e\Delta}, z_{e\Delta})$ and velocity $(\dot{x}_{e\Delta}, \dot{y}_{e\Delta}, \dot{z}_{e\Delta})$ will be transformed to a selenocentric inertial position $(x_{m\Delta}, y_{m\Delta}, z_{m\Delta})$ and velocity $(\dot{x}_{m\Delta}, \dot{y}_{m\Delta}, \dot{z}_{m\Delta})$ and its trajectory in the lunar gravitational field will be computed (see the sketch on page IV-40).

For typical lunar trajectory injection velocities, the velocity at the moon as given by the method of residual velocity at infinity is higher than that given by the method of sphere of influence by about 1%.

Another region around the moon that has been defined is the lunar gravisphere or sphere inside of which the gravitational attraction of the space vehicle by the moon exceeds the attraction by earth. On the boundary of the lunar gravisphere, from Eqs (14) and (15):

$$f_{\unicode{x263D}\Delta} = f_{\oplus\Delta} \quad \text{or} \quad r^2_{\unicode{x263D}\Delta} = \frac{M_{\unicode{x263D}}}{M_\oplus} r^2_{\oplus\Delta} \tag{26}$$

Numerically, this amounts in the earth-moon system to a ratio of the vehicle radii of

$$\frac{r_{\unicode{x263D}\Delta}}{r_{\oplus\Delta}} = \left(\frac{M_{\unicode{x263D}}}{M_\oplus}\right)^{1/2} = 0.1109 \tag{27}$$

It is more convenient to replace the vehicle distance from earth on the RHS of Eq (26) by application of the cosine law in the triangle shown in the following sketch (not drawn to scale).
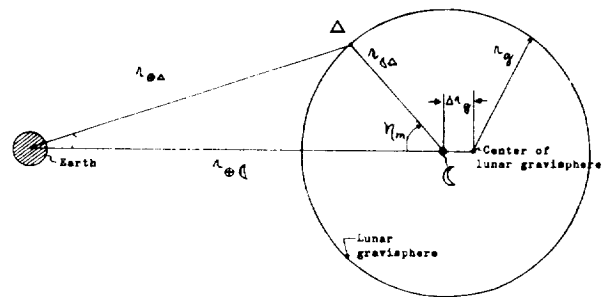
$$r^2_{\oplus\Delta} = r^2_{\oplus\unicode{x263D}} + r^2_{\unicode{x263D}\Delta} - 2r_{\oplus\unicode{x263D}} r_{\unicode{x263D}\Delta} \cos \eta_m$$

to obtain the boundary of the lunar gravisphere·

$$\frac{r_{\mathbb{C}\Delta}}{r_{\oplus\mathbb{C}}} = \frac{-\cos\eta_m + \left(\frac{M_\oplus}{M_\mathbb{C}}\sin^2\eta_m\right)^{1/2}}{\frac{M_\oplus}{M_\mathbb{C}} - 1}$$

(28)

From the preceding sketch it can be seen that the lunar gravisphere has a radius r_g and center at $r_{\oplus\mathbb{C}} + \Delta r_g$, where

$$r_g = r_{\oplus\mathbb{C}}\frac{\left(\frac{M_\oplus}{M_\mathbb{C}}\right)^{1/2}}{\frac{M_\oplus}{M_\mathbb{C}} - 1} =$$

$$43186.6 \text{ km}, \quad \frac{r_g}{r_{\oplus\mathbb{C}}} = 0.1122467 \text{ LU}$$

$$\Delta r_g = r_{\oplus\mathbb{C}}\frac{1}{\frac{M_\oplus}{M_\mathbb{C}} - 1} =$$

$$4788.0 \text{ km}, \quad \frac{\Delta r_g}{r_{\oplus\mathbb{C}}} = 0.0124445 \text{ LU}$$

(29)

The volume of influence of the moon, which is used in the Voice computer program, is defined by the relation

$$\frac{r_{\mathbb{C}\Delta}}{r_{\oplus\Delta}} < 0.175, \tag{30}$$

a number which was determined empirically from lunar trajectories. The boundary of the volume of influence is given by

$$\frac{r_{\mathbb{C}\Delta}}{r_{\oplus\Delta}} = 0.175 = k_v\left(\frac{M_\mathbb{C}}{M_\oplus}\right)^{1/2}, \tag{31}$$

where $k_v = 1.578$ is a constant of proportionality.
Hence, the volume of influence is a type of gravisphere with a scale factor k_v, larger than the lunar gravisphere, but one that gives the best location for transforming from earth to moon influence in typical lunar trajectories. Similar to the gravisphere, the volume of influence has a radius r_v and center at $r_{\oplus\mathbb{C}} + \Delta r_v$, where

$$r_v = r_{\oplus\mathbb{C}}\frac{k_v^{-1}\left(\frac{M_\oplus}{M_\mathbb{C}}\right)^{1/2}}{k_v^{-2}\frac{M_\oplus}{M_\mathbb{C}} - 1} =$$

(32)

$$69436.1 \text{ km}, \quad \frac{r_v}{r_{\oplus\mathbb{C}}} = 0.1804719 \text{ LU}$$

$$\Delta r_v = r_{\oplus\mathbb{C}}\frac{1}{k_v^{-2}\frac{M_\oplus}{M_\mathbb{C}} - 1} =$$

$$12147.7 \text{ km}, \quad \frac{\Delta r_v}{r_{\oplus\mathbb{C}}} = 0.0315732 \text{ LU}$$

At the boundary of the volume of influence the ratio of the lunar to the earth's gravitational attraction on the space vehicle is:

$$\frac{f_{\mathbb{C}\Delta}}{f_{\oplus\Delta}} = \frac{M_\mathbb{C}}{M_\oplus}\left(\frac{r_{\oplus\Delta}}{r_{\mathbb{C}\Delta}}\right)^2 \cong 0.4014 \tag{33}$$

The lunar gravisphere has little significance from the standpoint of trajectories. The erroneous belief that it is sufficient to reach the point of equal gravitational attraction or the boundary of the lunar gravisphere in order to hit the moon was revealed in trajectory calculations made by Egorov (Ref. 1). A much more significant region for trajectory calculations is the lunar volume of influence since it allows the use of two-body force models for the best approximation of three-body or n-body trajectories.

At this point it would be helpful to illustrate the lunar sphere of influence, gravisphere, and volume of influence as well as the boundary of the closed region around the moon obtained from the Jacobi integral of the restricted three-body problem (see also Fig. 2 of Chapter III). These regions around the moon are drawn to scale in Fig. 3. However, since their maximum and minimum radii are on the earth-moon line, the table below gives the intersection of these regions with the EML and their characteristics:

Region of Lunar Influence	EML Intersection		Description of Region
	(in front of moon) (km)	(behind moon) (km)	
Restricted three-body region from the Jacobi integral	57,890	48,350	Nearly elliptical region around the moon defined by the Jacobi constant C_2 (see Fig. 2 and Eq (77) of Chapter III). The boundary separates purely lunar orbits from moon escape trajectories.
Sphere of influence	51,870	63,790	Near-spherical region with the boundary given by Eq (23). The less the ratio of the mass of the smaller to that of the larger body, the more spherical this region.
Gravisphere	38,398.6	47,974.6	Region where the gravitational attraction of the moon exceeds that of the earth. It is spherical with center 4788.0 km behind the moon on the EML and with radius 43186.6 km.
Volume of influence	57,288.4	81,584.8	A type of gravisphere which gives the best successive two-body approximation for lunar trajectories. It is spherical with center 12147.7 km behind the moon on the EML and with radius 69436.1 km.

It should be remarked that the size of these various regions changes with the change of $\dfrac{M_\oplus}{M_\mathbb{C}}$ from the value 81.357 adopted in this manual and with any change in $\omega_{\oplus\mathbb{C}} = 2.661\ 699484 \times 10^{-6}\,\text{rad}/\text{sec}$.

(c) Planar dynamics of the lunar field

At the boundary of the lunar region of influence (sphere of influence, gravisphere or volume of influence) the geocentric (and so far inertial) position and velocity are transformed to the selenocentric system by the equations

$$\vec{r}_{m\Delta} = \vec{r}_{e\Delta} - \vec{r}_{e\mathbb{C}}$$
$$\vec{V}_{m\Delta} = \vec{V}_{e\Delta} - \vec{V}_{e\mathbb{C}} \tag{34}$$

In selenocentric coordinates, which are assumed inertial inside the lunar region of influence, the energy of the vehicle relative to the moon is positive and its approach trajectory in this region is a hyperbola (see sketch on page IV-6). The equation of this trajectory in plane polar coordinates ($r_{m\Delta}$, $0_{m\Delta}$) centered at the moon is given by

$$r_{m\Delta} = \dfrac{\dfrac{h_m^2}{\mu_\mathbb{C}}}{1 + e_{m\Delta} \cos 0_{m\Delta}} \tag{35}$$

where h_m is the magnitude of the angular momentum per unit mass of the vehicle relative to the moon, the angle $0_{m\Delta}$ is measured from pericynthion, and the eccentricity is given by

$$e_{m\Delta} = \left(1 + \dfrac{2\,E_m\,h_m^2}{\mu_\mathbb{C}^2}\right)^{1/2} \tag{36}$$

where E_m is the energy per unit mass of the vehicle relative to the moon. The value for the lunar gravitional constant is

$$\mu_\mathbb{C} = GM_\mathbb{C} = 4899.4\ \dfrac{\text{km}^3}{\text{sec}^2} \tag{37}$$

All the results of Keplerian motion (restricted two-body problem, i.e., infinitesimal mass of the space vehicle compared to the mass of the moon) are now available for further study of the trajectory.

When the method of "residual" velocities at infinity is used (Ref. 4), two useful parameters of the orbit are illustrated in the following sketch:

$V_{m\Delta\infty}$ = the velocity relative to the moon at infinity

b_m = the impact parameter, which is the perpendicular distance between the asymptote of the hyperbolic orbit (direction of $V_{m\Delta\infty}$) and the center of the moon.
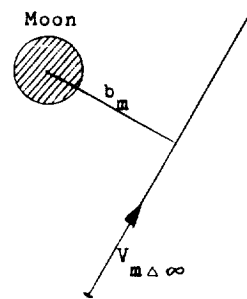
In the method of "residual" velocities at infinity the magnitude of the angular momentum and energy per unit mass of the vehicle are given by

$$h_m = b_m\ V_{m\Delta\infty}$$
$$E_m = \dfrac{1}{2}\ V_{m\Delta\infty}^2 \tag{38}$$
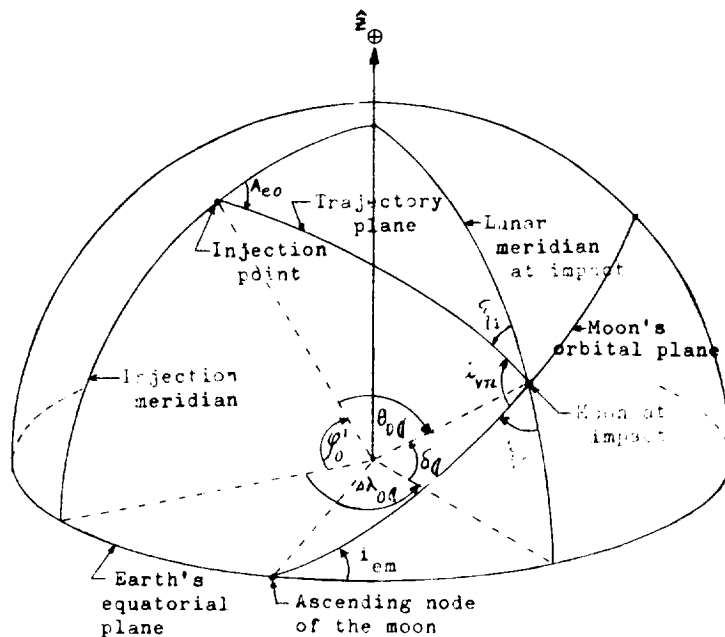
(d) Three-dimensional effects

It was seen in the previous sections that the planar trajectories were completely described by the injection conditions $r_{e\Delta 0}$, $V_{e\Delta 0}$, γ_{e0}. In addition, the orientation of the conic section with focus at the center of the earth (which is determined by the injection conditions) relative to the moon may be specified by the angle Φ (see sketch on page IV-14). Since the plane of the moon's motion is inclined to earth's equatorial plane, and the trajectory plane is, in general, inclined to both, three-dimensional effects must be considered (Refs. 4, 6, and 7). The geometry is portrayed in the following sketch.

A_{e0} = injection azimuth

ϕ_0' = injection latitude (geocentric)

$\Delta\lambda_{0\mathbb{C}}$ = longitude difference

$\delta_{\mathbb{C}}$ = instantaneous declination of the moon

i_{em} = inclination of the moon's orbital plane to the earth's equatorial plane or maximum declination of moon

$\theta_{0\mathbb{C}}$ = total in-plane angle

i_{VTL} = inclination of the translunar trajectory plane to the moon's orbital plane

Additional injection parameters required to describe three-dimensional trajectories are the geocentric injection latitude ϕ_0', the injection azimuth A_{e0}, the longitude difference between the injection point and the moon at impact $\Delta\lambda_{0\mathbb{C}}$, the instantaneous declination of the moon $\delta_{\mathbb{C}}$, and the inclination of the moon i_{em}.

From spherical trigonometry the total in-plane angle $\theta_{0\mathbb{C}}$ is given by

$$\cos\theta_{0\mathbb{C}} = \left[\sin\phi_0'\sin\delta_{\mathbb{C}} - \cos\phi_0'\cos A_{e0}\left(1 - \sin^2 A_{e0}\cos^2\phi_0' - \sin^2\delta_{\mathbb{C}}\right)^{1/2}\right]\left(1 - \sin^2 A_{e0}\cos^2\phi_0'\right)^{-1} \tag{39}$$

the longitude difference $\Delta\lambda_{0\mathbb{C}}$ is

$$\cos\Delta\lambda_{0\mathbb{C}} = \frac{\cos\theta_{0\mathbb{C}} - \sin\phi_0'\sin\delta_{\mathbb{C}}}{\cos\phi_0'\cos\delta_{\mathbb{C}}} \tag{40}$$

and the translunar inclination angle i_{VTL} in degrees is

$$i_{VTL} = 180° - (\xi_1 + \xi_2) \tag{41}$$

where

$$\xi_1 = \sin^{-1}\left(\frac{\cos\phi_0'\sin A_{e0}}{\cos\phi_0'}\right)$$

$$\xi_2 = \sin^{-1}\left(\frac{\cos i_{em}}{\cos\delta}\right)$$

In the following sketches, which have been taken from Ref. 6, the parameters $\theta_{0\mathbb{C}}$, $\Delta\lambda_{0\mathbb{C}}$, and i_{VTL} are plotted as functions of $\delta_{\mathbb{C}}$ and A_{e0}, respectively.

In each case injection is assumed to occur at ϕ_0' = +28.5°, the latitude of Cape Canaveral, and lunar inclination i_{em} is assumed to be 20°. Of course, in the general case, the injection latitude may vary between +90° and -90°, and the lunar inclination between 18° and 28.5°.
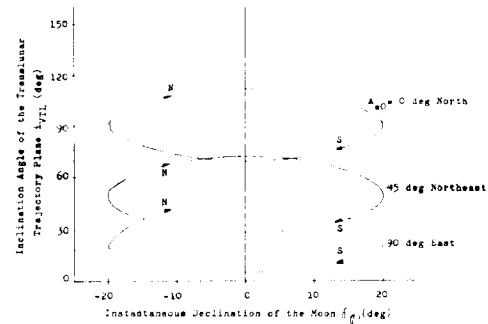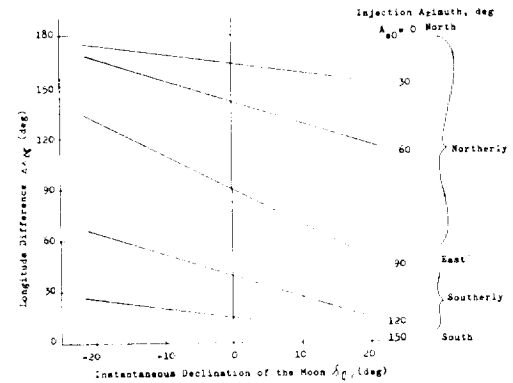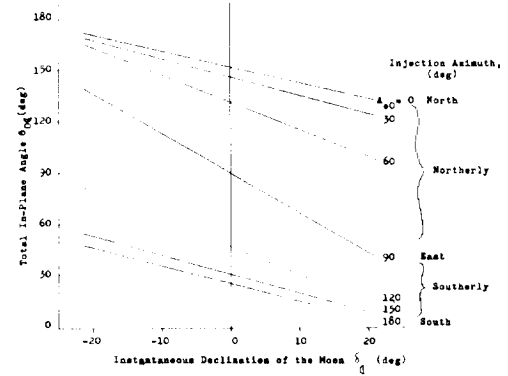
It is seen from the first of the previous three sketches, that $\theta_{0\!\!\!\!C}$ decreases with increasing declination of the moon, for an injection in the northern hemisphere. The total in-plane angle also decreases as the injection azimuth is increased. Since it is also a function of $V_{e\Delta0}$, $r_{e\Delta0}$, γ_{e0}, the injection time depends also on the trajectory initial conditions.

The longitude difference $\Delta\lambda_{0\!\!\!\!C}$ behaves similarly to the in-plane angle as can be noted from the middle sketch shown previously. In the first two sketches the abscissa coincides with the curve $A_{e0} = 180°$, or an injection toward the south. The last sketch shows that the minimum inclination angle i_{VTL} for lunar impact occurs when the moon is southbound in its orbit at zero declination. On the other hand, impact at the moon when it is at its maximum southern declination corresponds to a larger $\theta_{0\!\!\!\!C}$ and consequently for a given injection velocity a smaller flight path angle at injection, which means lower gravity losses during powered flight from launch to injection. The inclination angle in this case is somewhat larger, however, resulting in lower tolerances on initial velocity due to three-dimensional effects. Initial azimuths of 90° (east) take greatest advantage of the earth's surface rotational velocity. Thus some compromise in these parameters is necessary.

This brief discussion shows that the geometry of the earth-moon and vehicle planes places constraints on injection conditions and defines preferred launch times throughout the lunar month. It must be remembered that the above discussion does not consider the use of parking orbits to ease the aforementioned injection constraints. Chapters V, VI, IX and XI present data reflecting more practical aspects of the injection into lunar trajectories.

2. Restricted Three-Body Trajectories

The simplified model discussed in Subsection B-1, where analytical solutions of the equations of motion were possible, may be complicated by adding the moon to the earth-vehicle, restricted two-body problem. The resultant restricted three-body problem was discussed in some detail in Chapter III, Section B in terms of Jacobi's integral. An analytical solution of the equations of motion is no longer possible and recourse must be taken to numerical methods.

In this subsection, vehicle motion, in terms of the restricted three-body problem, will be considered, i.e., the mass of the vehicle is negligible in comparison to the mass of the earth and moon, and with the earth and moon as spherical bodies so that they may be considered as point masses. The earth-moon system is considered isolated in space, the two bodies revolving in circles about their center of mass with an angular velocity $\omega_{\oplus\!\!\!\!C}$.

The coordinate systems used in conjunction with this model have been defined in Section A of Chapter III and they are shown again in the following sketch.
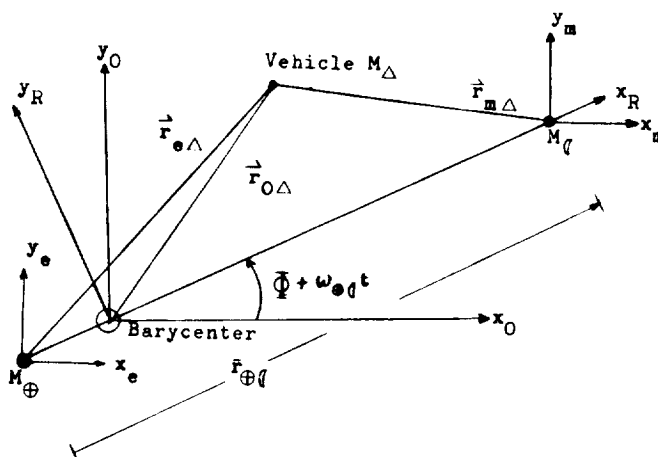
The transformations between the coordinates and velocity components of the various coordinate systems are summarized in Table 1. In the above sketch $\vec{r}_0$ (x_0, y_0, z_0) is an inertial reference system with origin at the barycenter (center of mass of the earth and moon system). The $\vec{r}_R$ (x_R, y_R, z_R) system rotates at the same rate as the earth and moon about the z_0-axis (up from the paper). The $\vec{r}_0$ and $\vec{r}_R$ systems have a common origin and coincident z_0, z_R axes. The $\vec{r}_e$ (x_e, y_e, z_e) system is a nonrotating system with origin at the center of mass of the earth, and the $\vec{r}_m$ (x_m, y_m, z_m) system is a nonrotating system with origin at the center of mass of the moon.

In the inertial reference system, where Newton's second law is valid, the equations of motion of a point mass representing the space vehicle are,

$$\ddot{\vec{r}}_{0\Delta} = - \frac{GM_\oplus}{r_{0,e\text{-}\Delta}^3} \vec{r}_{0,e\text{-}\Delta}$$

$$- \frac{GM_{\!\!\!\!C}}{r_{0,m\text{-}\Delta}^3} \vec{r}_{0,m\text{-}\Delta}, \tag{42}$$

where

$$\vec{r}_{0,e\text{-}\Delta} = \vec{r}_{0\Delta} - \vec{r}_{0e}$$

$$\vec{r}_{0,m\text{-}\Delta} = \vec{r}_{0\Delta} - \vec{r}_{0m} \tag{43}$$

It is convenient to transform the equations of motion (42) to the rotating coordinate system ($\vec{r}_R$) for the purpose of numerical calculations,

because in the latter system several terms are constant. This may be done with the aid of the rotation matrix $T(\Phi + \omega_{\oplus\text{☾}}\,t)$ given by Eq (47) of Chapter III and the equations of motion become,

$$\ddot{x}_{R\Delta} - 2\omega_{\oplus\text{☾}}\,\dot{y}_{R\Delta} = \omega_{\oplus\text{☾}}^2\,x_{R\Delta}$$

$$-\frac{GM_\oplus}{r_{R,e\rightarrow\Delta}^3}\,(x_{R\Delta} - x_{R\oplus})$$

$$-\frac{GM_\text{☾}}{r_{R,m\rightarrow\Delta}^3}\,(x_{R\Delta} - x_{R\text{☾}})$$

$$\ddot{y}_{R\Delta} + 2\omega_{\oplus\text{☾}}\,\dot{x}_{R\Delta} = \omega_{\oplus\text{☾}}^2\,y_{R\Delta}$$

$$\hspace{8cm}(44)$$

$$-\frac{GM_\oplus}{r_{R,e\rightarrow\Delta}^3}\,y_{R\Delta}$$

$$-\frac{GM_\text{☾}}{r_{R,m\rightarrow\Delta}^3}\,y_{R\Delta}$$

$$\ddot{z}_{R\Delta} = -\frac{GM_\oplus}{r_{R,e\rightarrow\Delta}^3}\,z_{R\Delta}$$

$$-\frac{GM}{r_{R,m\rightarrow\Delta}^3}\,z_{R\Delta}\ ,$$

compare with Eq (70) of Chapter III, where

$$\vec{r}_{R,e\rightarrow\Delta} = \vec{r}_{R\Delta} - \vec{r}_{R\oplus}\ , \quad \vec{r}_{R,m\rightarrow\Delta} = \vec{r}_{R\Delta} - \vec{r}_{R\text{☾}}$$

$$\hspace{8cm}(45)$$

$y_{Re} = y_{Rm} = 0$, and $(x_{Re},\ x_{Rm})$ are constants. The terms $2\omega_{\oplus\text{☾}}\,\dot{y}_{R\Delta}$ and $2\omega_{\oplus\text{☾}}\,\dot{x}_{R\Delta}$ are known as components of the Coriolis acceleration, and the terms $\omega_{\oplus\text{☾}}^2\,x_{R\Delta}$ and $\omega_{\oplus\text{☾}}^2\,y_{R\Delta}$ are components of the centrifugal acceleration. The equations of motion, Eq (44), can be integrated numerically subject to initial conditions on position and velocity $x_{R\Delta},\ y_{R\Delta},\ z_{R\Delta},\ \dot{x}_{R\Delta},\ \dot{y}_{R\Delta},\ \dot{z}_{R\Delta}.$

These equations are for ballistic flight. Space vehicles, however, may be subject to thrust forces. These can be included in the trajectory calculations in two different ways: The thrust forces on the vehicle may be simulated by additional terms in the equations of motion, or a large thrust of short

duration may also be simulated by an impulsive change $\Delta\vec{V}$ in inertial velocity $\vec{V}_{0\Delta}$ of the vehicle. This new vehicle velocity $\vec{V}_{0\Delta} + \Delta\vec{V}$ must be transformed to the rotating $x_R,\ y_R,\ z_R$ coordinate system and the new vehicle velocity components together with the position at the time of the simulated thrust can be regarded as new initial conditions for a ballistic trajectory.

Before Eq (44) can be solved numerically, values of the constants G, $M_\oplus$, $M_\text{☾}$, $\omega_{\oplus\text{☾}}$, and $\vec{r}_{\oplus\text{☾}}$ are required for the restricted three-body model. In reality, only four constants are needed since G never occurs alone. The following consistent set of constants is given for this model:

$$\mu_\oplus \equiv GM_\oplus = 398,601.5\ \text{km}^3/\text{sec}^2$$

$$\mu_\text{☾} = GM_\text{☾} = 4899.4\ \text{km}^3/\text{sec}^2$$

$$\hspace{8cm}(46)$$

$$\omega_{\oplus\text{☾}} = 2.661699484 \times 10^{-6}\ \text{rad/sec}$$

$$\vec{r}_{\oplus\text{☾}} = 384,747.2\ \text{km} \equiv 1\ \text{LU (lunar unit)}$$

The consistency of the above set of constants can be checked by Kepler's third law as applied to two-body (earth, moon) motion,

$$\tau_{\oplus\text{☾}}^2 = \frac{(2\pi)^2\,\vec{r}_{\oplus\text{☾}}^3}{\mu_\oplus + \mu_\text{☾}}\ ,$$

where $\tau_{\oplus\text{☾}}$ is the period of rotation of the earth-moon system. In terms of angular velocity

$$\omega_{\oplus\text{☾}} = \frac{2\pi}{\tau_{\oplus\text{☾}}}\ ,$$

the consistency relation becomes

$$\vec{r}_{\oplus\text{☾}}^3 = \frac{\mu_\oplus + \mu_\text{☾}}{\omega_{\oplus\text{☾}}^2}$$

$$\hspace{8cm}(47)$$

Since the angular velocity can be observed very accurately, it is customary to assume the angular velocity as well as the gravitational constants of the earth and moon as known, and to determine a consistent value of lunar unit $\vec{r}_{\oplus\text{☾}}$. The lunar unit may be regarded, from Eq (47), as the distance to a fictitious moon in a circular orbit around the earth (of mass as determined by experiment) whose mass and Keplerian period coincide with those observed for the moon.

3. Many-Body Trajectories (oblate earth, triaxial moon)

In the discussion of the previous two force models, several forces have been neglected. These can be conveniently divided into gravitational and nongravitational forces. Examples of gravitational forces to be considered in the earth-moon trajectories are the attraction of the sun and planets, the oblateness of the earth, the triaxiality of the

moon, any inhomogeneities in the earth, and the dynamical effect of the eccentricity and inclination of the moon's orbit around the earth. Nongravitational forces include solar radiation pressure, atmospheric and meteoritic drag, electromagnetic forces, rocket thrust, and relativistic effects. Many of these forces such as earth oblateness and atmospheric drag are strongly related to position, and are significant only in the vicinity of the earth.

The influence of these factors on translunar trajectories has been investigated (Refs. 2, 8). The integrated effect of these factors over the whole trajectory depends on trajectory shape transit time, and the actual magnitude of the forces varies throughout the trajectory. The corrections $\Delta V_{e \Delta 0}$ to the initial velocity near earth $V_{e \Delta 0}$ because of these effects are listed below. They are intended to convey the magnitude of each factor compared to the restricted three-body initial velocity of 10.7 km/sec.

Factor	$\Delta V_{e \Delta 0}$ m/sec*	Percent $V_{e \Delta 0}$
1. Gravitational field of the sun	3.0 (Ref. 8)	0.03*
2. Gravitational fields of planets	0.006	--
3. Oblateness of the earth	6.0 (Ref. 8)	0.06*
4. Asphericity of the moon	--	--
5. Eccentricity of moon's orbit	13.5 (Ref. 8)	0.13*
6. Inclination of orbit of moon	6.0 (Ref. 8)	0.06*
7. Solar radiation pressure	0.012 (Ref. 8)	--
8. Meteoroid disturbances	--	--

*Transit time, 2.5 days. Nominal injection velocity, 10.7 km/sec. Vehicle with projected area of about 1 m^2 and weighing 1300 newtons.

It is seen that the $\Delta V_{e \Delta 0}$ corrections for the sun, oblateness of the earth, eccentricity of moon's orbit, and the inclination of the orbit of the moon are significant enough to necessitate the inclusion of these effects in the determination of initial velocity in actual trajectory calculations. The asphericity of the moon will be important in near-moon trajectory computations. These, as well as the other factors, will be discussed in some detail later in this chapter.

The equations of motion even in the restricted three-body problem could not be integrated in closed form, and with the present more complicated force

model, numerical integration is necessary to obtain the position and velocity of the vehicle as a function of time. Since the integration technique can improve the speed and accuracy of obtaining a trajectory on the digital computer, a brief discussion of several techniques useful for lunar trajectory calculations will be included in this section.

a. Equations of motion

Consider the equatorial coordinate system described in Chapter III, Subsection A-1, with origin at the barycenter and unit vectors $\hat{x}_{\oplus \mathbb{C}}$, $\hat{y}_{\oplus \mathbb{C}}$, $\hat{z}_{\oplus \mathbb{C}}$, $\hat{x}_{\oplus \mathbb{C}}$ in the direction of the mean vernal equinox, and the $x_{\oplus \mathbb{C}}$ $y_{\oplus \mathbb{C}}$ -plane parallel to the mean equatorial plane of the earth. Let $M_{\oplus}$ represent the mass of the earth, $M_{\mathbb{C}}$ that of the moon, and M_{Δ} the mass of the vehicle, where $M_{\Delta} << M_{\mathbb{C}}$, $M_{\Delta} << M_{\oplus}$

Then, since $\hat{x}_{\oplus}$, $\hat{y}_{\oplus}$, $\hat{z}_{\oplus}$ constitute the unit vectors of an inertial coordinate system with origin chosen at the center of mass of the bodies considered in the physical model, the equations of motion of the space vehicle, or the equations of absolute motion, are

$$M_{\Delta} \ddot{\vec{r}}_{\oplus, 0 \to \Delta} = \sum_{i=\oplus}^{n} \left\{ (-G) \frac{\vec{r}_{\oplus, 0 \to \Delta} - \vec{r}_{\oplus, 0 \to i}}{r_{\oplus, i \to \Delta}^3} M_i M_{\Delta} + \vec{f}_i M_{\Delta} \right\} + \vec{n}_{\Delta} M_{\Delta} \quad (48)$$

$$i = \oplus, \mathbb{C}, 1, 2, \ldots, n$$

The term $\vec{r}_{\oplus, 0 \to \Delta}$ is the radius vector of the vehicle from the barycenter (center of mass) equatorial coordinates with origin of the barycenter, $\vec{r}_{\oplus, i \to \Delta} = \vec{r}_{\oplus, 0 \to \Delta} - \vec{r}_{\oplus, 0 \to i}$, $\vec{f}_i$ represents the forces per unit mass due to the asphericity of the celestial bodies, and $\vec{n}_{\Delta}$ are the nongravitational forces per unit mass acting on M_{Δ}.

To obtain the equations of motion of the space vehicle, Eq (48), in a coordinate system with the origin at the center of the earth, Eq (49), the equations of motion of the earth (neglecting the gravitational attraction of the space vehicle since $M_{\Delta} << M\oplus$),

$$\ddot{\vec{r}}_{\oplus,0\rightarrow\oplus} = \sum_{i=☽}^{n}\left[-GM_i\frac{\vec{r}_{\oplus,0\rightarrow\oplus}\ \vec{r}_{\oplus,0\rightarrow i}}{r_{i\oplus}^{3}}\right],$$

$$i = ☽,1,2,\ldots n \qquad (49)$$

is multiplied by M_Δ and subtracted from Eq (48) to yield Eq (50), the equations of relative motion.

$$M_\Delta \ddot{\vec{r}}_{\oplus\Delta} = -G\frac{\vec{r}_{\oplus\Delta}}{r_{\oplus\Delta}^{3}}M_\oplus M_\Delta$$

$$+ \vec{f}_\oplus M_\Delta \sum_{i=☽}^{n}\left[(-G)\left(\frac{\vec{r}_{\oplus\Delta}}{r_{\oplus\Delta}^{3}}-\frac{\vec{r}_{i\oplus}}{r_{i\oplus}^{3}}\right)M_i M_\Delta\right.$$

$$\left.+ \vec{f}_i M_\Delta\right] + \vec{n}_\Delta M_\Delta, \quad i=☽,1,2,\ldots n$$

$$(50)$$

where

$$\vec{r}_{\oplus\Delta} = \vec{r}_{\oplus,0\rightarrow\Delta} - \vec{r}_{\oplus,0\rightarrow\oplus}$$

$$\vec{r}_{i\oplus} = \vec{r}_{\oplus,0\rightarrow\oplus} - \vec{r}_{\oplus,0\rightarrow i}$$

Actually any other body, such as the moon, could have been chosen as a reference with an appropriate change of symbols in Eq (50). The geometry is illustrated in the following sketch:
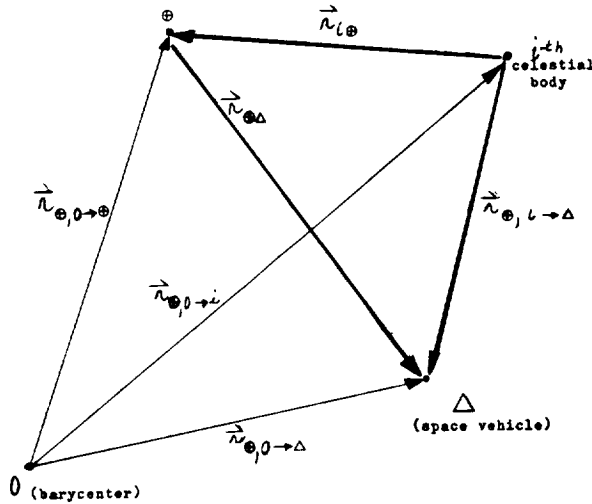
The unit vectors $\hat{x}_\oplus$, $\hat{y}_\oplus$, $\hat{z}_\oplus$ define the geocentric equatorial coordinate system in which the equations of motion, Eq (50), are given. The unit vector, $\hat{x}_\oplus$, is in the direction of the mean vernal equinox, and the $x_\oplus\ y_\oplus$ plane forms the mean equatorial plane of the earth. All vectors defined in the preceding sketch are assumed to be resolved into components in this coordinate system.

The vectors $\sum_{i=\oplus}^{n}\vec{f}_i$, representing the forces acting on M_Δ due to asphericity of the i celestial bodies, $i = \oplus,☽,1,2,\ldots n$ can be written:

$$\vec{f}_i = \vec{f}_\oplus + \vec{f}_☽ + \vec{f}_1 + \vec{f}_2 + \ldots + \vec{f}_n \qquad (51)$$

Any asphericity of the sun and planets f_i, $i = 1$, $2,\ldots n$, is insignificant in its effect on lunar trajectories since even the effect of the central force is small, as can be seen in the preceding table.

Consider $\vec{f}_\oplus$ first. It arises from the expansion terms of the earth's gravitational potential in terms of spherical harmonics. In theory a large number of harmonic terms should be included; however, the coefficient of the oblateness term (second zonal harmonic) is larger by three orders of magnitude than the others (i. e., of order 10^{-3} as compared to the order 10^{-6} for the others). Thus all but the oblateness term can be neglected in lunar trajectory studies. The effect of local gravitational anomalies of the earth on the lunar trajectory is very small and will also be neglected.

If $U_\oplus$ represents the earth's gravitational potential, then the expansion of $U_\oplus$ in terms of zonal spherical harmonics (tesseral and sectoral harmonics have not yet been determined well enough for their inclusion) can be written

$$U_\oplus = \frac{GM_\oplus}{r_{\oplus\Delta}}\left[1 - \sum_{n=1}^{\infty}J_n\left(\frac{R_e}{r_{\oplus\Delta}}\right)^{n}P_n(\sin\phi')\right]$$

$$(52)$$

where $r_{\oplus\Delta}$ is the distance of the vehicle from the earth, J_n, $n = 1, 2, \ldots$ are empirical constants (determined from geodetic and satellite measurements) and given in Chapter II, R_e is the mean equatorial radius of the earth ($R_e = 6,378,163$ m), ϕ' is the geocentric latitude, and $P_n(\sin\phi')$ is the associated Legendre polynomial of $\sin\phi'$. The above form of $U_\oplus$ has been adopted by the International Commission on Celestial Mechanics (Ref. 9). Let $U_\oplus = U_0 + U_2 + U_3$, where, by comparison with Eq (51)

$$U_0 = \frac{GM_\oplus}{r_{\oplus\Delta}}$$

$$U_2 = -\frac{GM_\oplus}{r_{\oplus\Delta}}J_2\left(\frac{R_e}{r_{\oplus\Delta}}\right)^{2}\frac{3\sin^{2}\phi' - 1}{2} \qquad (53)$$

$$U_3 = -\frac{GM_\oplus}{r_{\oplus\Delta}}\sum_{n=3}^{\infty}J_n\left(\frac{R_e}{r_{\oplus\Delta}}\right)^{n}P_n(\sin\phi')$$

U_0 represents the spherically symmetric earth, which has already been acounted for by the term $-G \dfrac{\vec{r}_{\oplus\Delta}}{r_{\oplus\Delta}^3} M_{\oplus}$ in Eq (50). U_1, the term corresponding to $n = 1$ in Eq (52), vanishes if the center of gravity of the earth coincides with the origin of coordinates (Ref. 10, p 43).

U_2 is the oblateness term (or second zonal harmonic) which is the largest term in the expansion, while U_3 represents the higher order zonal harmonics of the earth which may be neglected for lunar trajectory studies as mentioned above. The numerical value for

$$J_2 = 1082.28 \times 10^{-6}.$$

Let $f_{\oplus x}$, $f_{\oplus y}$ and $f_{\oplus z}$ be the $x_{\oplus}$, $y_{\oplus}$, $z_{\oplus}$ components of $\vec{f}_{\oplus}$ as defined by Eq (50), respectively. Then these components are given by

$$f_{\oplus x} = \frac{\partial U_2}{\partial x}, \quad f_{\oplus y} = \frac{\partial U_2}{\partial y}, \quad f_{\oplus z} = \frac{\partial U_2}{\partial z} \tag{54}$$

Next we turn to $\vec{f}_{\mathcal{C}}$. To obtain $\vec{f}_{\mathcal{C}}$, it is convenient to find an expression for the lunar gravitation potential $U_{\mathcal{C}}$ and define the gravitational force as the gradient of the potential. $U_{\mathcal{C}}$ is defined by

$$U_{\mathcal{C}} = G \int_{\mathcal{C}} \frac{dM_{\mathcal{C}}}{s} \tag{55}$$

where $dM_{\mathcal{C}}$ is an element of mass of the moon, s is the distance from $dM_{\mathcal{C}}$ to the space vehicle, and $\int_{\mathcal{C}}$ indicates integration over the total mass of the moon. The function $\frac{1}{s}$ can be expanded in terms of Legendre polynomials,

$$U_{\mathcal{C}} = U_{\mathcal{C}0} + U_{\mathcal{C}1} + U_{\mathcal{C}2} + \cdots \tag{56}$$

where Alexandrov (Ref. 11) and Baker, Makemson (Ref. 12) have given the following values for $U_{\mathcal{C}0}$, $U_{\mathcal{C}2}$ and $U_{\mathcal{C}3}$, after a slight change in notation*.

$$U_{\mathcal{C}0} = \frac{GM_{\mathcal{C}}}{r_{S\Delta}}$$

$$U_{\mathcal{C}1} = 0$$

$$U_{\mathcal{C}2} = \frac{GM_{\mathcal{C}} \, a^2}{2r_{S\Delta}^3} \left[\frac{I_b - I_a}{I_c} (1 - 3\cos^2 \beta_{\mathcal{C}}) \right. \tag{57}$$
$$\left. + \frac{I_c - I_a}{I_c} (1 - 3\sin^2 \phi'_{\mathcal{C}}) \right]$$

The term a is the semiaxis of inertia of the moon, in the direction of the earth, $r_{S\Delta}$ is the distance from the center of the moon to the vehicle, $U_{\mathcal{C}0}$ is the central force term arising from the spherically symmetric moon, $U_{\mathcal{C}1}$ shows that the moment about the center of mass vanishes by symmetry, and $U_{\mathcal{C}2}$ comes about since the moon is a triaxial ellipsoid (i.e., an ellipsoid with different semimajor axes in three mutually orthogonal directions from the center). I_a, I_b and I_c are the moments of inertia about the three principal semiaxes of inertia, a, b and c of the moon, such that c is along the lunar polar axis, a is in the earth's direction (excluding small librations) and b completes the right-hand system in the lunar equatorial plane.

The selenographic coordinate axes x_S, y_S, z_S coincide with the principal axes of inertia a, b, c. The angles $\phi'_{\mathcal{C}}$ and $\beta_{\mathcal{C}}$ are then defined to be the angle between the radius vector to the vehicle and the lunar equatorial plane (or the selenographic latitude), and the angle between the y_S-axis and the radius vector, respectively. These relationships are illustrated in the following sketch:
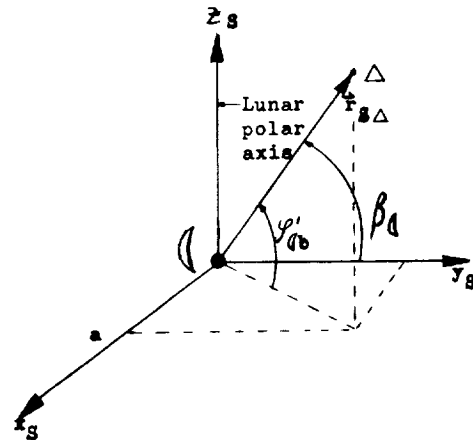
The expressions for $U_{\mathcal{C}2}$ given by Pines and Wolf (Ref. 13) agree with this expression if their symbol γ_{VM}^3 is replaced by R_{VM}^3 (which corresponds to $r_{S\Delta}^3$ in the notation of the present chapter).

*Actually, Baker and Makemson (Ref. 11) define a unit vector $\hat{r}_{S\Delta}$ in the direction of the vehicle radius vector $\vec{r}_{S\Delta}$ with components $x_{S\Delta}$, $y_{S\Delta}$, $z_{S\Delta}$ along the selenographic axes. Clearly,

$$\frac{y_{S\Delta}}{r_{S\Delta}} = \cos \beta_{\mathcal{C}}, \quad \frac{z_{S\Delta}}{r_{S\Delta}} = \cos (90 - \phi_{\mathcal{C}}) = \sin \phi_{\mathcal{C}}.$$

The form of $U_{\mathfrak{C}2}$ in Eq (57) is given in the selenographic coordinate system which rotates with the moon (see preceding sketch). From this point one may proceed in two different ways. The first would be to transform $U_{\mathfrak{C}2}$ to the geocentric equatorial coordinates used in the equations of motion, Eq (50). Since the influence of $U_{\mathfrak{C}2}$ on the trajectory is strongest near the moon, it is more practical to write the equations of motion in a selenocentric equatorial or, preferably, lunar equatorial system and consequently transform $U_{\mathfrak{C}2}$ to that coordinate system. If the second approach is taken, and the new perturbative expression is denoted by $U'_{\mathfrak{C}2}$, then the components of the perturbative acceleration $\vec{f}_{\mathfrak{C}}$ in the lunar equatorial system are given formally by

$$f_{\mathfrak{C}\,x} = \frac{\partial U'_{\mathfrak{C}2}}{\partial x_{\mathfrak{C}\Delta}}, \quad f_{\mathfrak{C}\,y} = \frac{\partial U'_{\mathfrak{C}2}}{\partial y_{\mathfrak{C}\Delta}}, \quad f_{\mathfrak{C}z} = \frac{\partial U'_{\mathfrak{C}2}}{\partial z_{\mathfrak{C}\Delta}} \tag{58}$$

Expressions for $\vec{f}_{\mathfrak{C}}$ and $U'_{\mathfrak{C}2}$ will be given in Chapters VII and II.

At this time the knowledge of the lunar shape and the density distribution inside of the moon is slight and terms beyond $U_{\mathfrak{C}2}$ in the expansion of $U_{\mathfrak{C}}$ given by Eq (56) are too uncertain for their inclusion. In the expressions for $U_{\mathfrak{C}}$, Eqs (56 and (57), the numerical values of a, b, c, I_a, I_b, I_c given in Chapter II, are based on observations of the moon and the assumption that the lunar density is constant over concentric ellipsoidal shells. More accurate numerical values and expressions for $U_{\mathfrak{C}}$ together with local lunar gravity anomalies will become available as soon as a long-term lunar satellite can be observed from the lunar surface and when gravity measurements can be made on the moon.

b. Brief discussion of integration methods and techniques

Expressions for all gravitational terms in the equation of motion of the space vehicle, Eq (50), have been given previously. Before turning to the nongravitational force term $\vec{n}_\Delta\, M_\Delta$ in Eq (50), it is helpful to discuss the method of solution of this vector differential equation which corresponds to three second-order scalar differential equations, or an equivalent system of six first-order differential equations.

The problem is to find the position of the space vehicle as a function of time subject to its position and velocity at some initial time $t = t_0$, or its motion or trajectory. Mathematically speaking, this is an initial value problem in ordinary differential equations with time t as the independent variable and the coordinates $x_\oplus$, $y_\oplus$, $z_\oplus$ as the dependent variables. In order to proceed with the solution, the positions of the moon, sun and planets must be known in geocentric equatorial coordinates. These positions can be obtained from the yearly American Ephemeris (Ref. 14). If earth oblateness and the triaxiality of the moon are included in the physical model, then numerical values for certain other constants of the shape and density distribution of these celestial bodies are required as described in the previous subsection.

For lunar trajectories, the differential equation, Eq (50), is solved numerically on a digital computer. There are several methods of integration available (Cowell's method, Encke's method, for example), each with its own advantages and disadvantages for a specific physical problem. In addition one can use various numerical integration techniques (Runge-Kutta technique, for example), in which the integrand is represented by a polynomial of finite order at each computation step. Two types of errors arise from the integration technique, one due to the finite number of terms in the series, called the truncation error, and an error due to the finite number of digits carried on the computer, called the round-off error. In general it can be stated that the fewer the total number of computation steps in a given physical problem, the less the error. The term special perturbations is given to the determination of a trajectory by numerical integration; a more complete discussion of special perturbations can be found in Chapter IV of Ref. 3.

The numerical integration of space vehicle trajectories and the orbits of celestial bodies is based upon one of three methods, and variations thereof. The most direct in concept is Cowell's method. In this method the rectangular components of acceleration in the equations of motion are integrated directly, yielding the rectangular components of velocity and position. One disadvantage of the method is that the acceleration term in the integration changes rapidly with time, thereby necessitating the use of small computation steps (or time intervals). A second method, and the one most often used in ballistic trajectory computations, is Encke's method. Here, instead of obtaining the actual position and velocity coordinates, the difference between the actual position and velocity coordinates and that of a Keplerian orbit are computed. Some time, designated the epoch of osculation, is utilized to define the reference curve. This implies that for times near the epoch of osculation, the effects of the perturbations are small and can thus be summed over relatively large time intervals. A disadvantage lies in the fact that a new epoch of osculation must be introduced when the effects of the perturbations become large. This procedure is known as rectifying the Keplerian reference orbit. Another method is the Variation of Parameters which is discussed by Brouwer and Clemence (Ref. 15). There have been some recent studies (Baker et al., Ref. 16, Pines et al., Ref. 17, for example) of the advantages of the various integration methods in terms of simplicity, area of applicability and computing time, as well as accuracy and interpretation.

For long-term ephemerides, such as long-term artificial satellites of the earth and moon and periodic circumlunar and allunar trajectories, numerical methods are not well suited since a

very large number of computation steps are required and hence the accumulated error becomes excessive. In these cases one must resort to general perturbations, which is the analytical integration of series expansions of the perturbing forces, or a combination of special and general perturbations. Examples of general perturbations are the various lunar theories discussed in Chapter III. A discussion of general perturbations can be found in Chapter IV of Ref. 3.

For short transit trajectories as envisioned for approach, impact, lunar landing, the accuracy afforded by general perturbation theory is offset by its following inadequacies: (1) the theories have not yet included a complete analysis of all perturbing accelerations such as solar radiation pressure, and (2) the theories are very complicated to program (although short in machine time) and almost impossible to check. For these reasons general perturbation theories will not be discussed any further in this chapter.

In order to compare the various special perturbation methods, the following table taken primarily from page F-2 of Ref. 18 is useful:

Method	Advantages	Disadvantages
Cowell's	Simplicity in programming and analysis Universally applicable Coordinate conversion unnecessary	Increased number of integration steps Excessive error accumulation Increased computing time Detection of small perturbations difficult
Encke's	Smaller number of integration steps than Cowell's method Reduced computing time as compared with Cowell's method Improved accuracy Detection of small perturbations	Increased computing time for each step Complex program Special program for near-parabolic orbits
Variation of Parameters	Smaller number of integration steps than Cowell's Reduced computing time relative to Cowell's Improved accuracy as compared with Cowell's (about same as Encke's) Detection of small perturbations	Most complex to program Most computing time Most useful for earth-satellites of moderate eccentricity

Another consideration in numerical calculations is the integration technique to be used. The choice is between use of a single computation step technique such as the Runge-Kutta, a fourth-order multistep predictor-corrector technique such as Milne's and Adams-Moulton's or a higher order multistep technique such as Adams' Backward Difference, Obrechkoff, and Gauss-Jackson. There exist also special techniques for second-order differential equations such as the special Runge-Kutta and Milne-Stormer. For each multistep technique special formulas (for example, a Runge-Kutta technique or a Taylor series expansion) must be devised for starting the scheme at the given initial conditions. The most important factors in the choice of an integration technique for space vehicle trajectories are high speed and good accuracy. The latter involves low truncation or round-off error, ease of changing step size and little error growth. The round-off error can be reduced by using a double precision process, i.e., by carrying all dependent variables in double precision. The advantages and disadvantages of the various schemes are discussed more fully in Chapter IV of Ref. 3 (see also Refs. 15 and 18).

For ballistic lunar trajectories Encke's integration method or a variation thereof seems to be best suited due to the smallness of the perturbations throughout the trajectory (this can be seen by the way successive two-body problems can be used to describe the trajectory relatively accurately). The epoch of osculation should be changed whenever the sphere or volume of influence of the moon is entered or left. For an accurate simulation of large thrusts during the flight, Cowell's method is preferable during rocket burning. Of the various integration techniques Ref. 18 seems to favor slightly the Gauss-Jackson scheme over the others, while the Obrechkoff scheme has been found useful in the reduction of computing time. The interplanetary (and lunar) trajectory program described in Ref. 13 uses a modified Encke's method with an Adams' sixth-order backward difference integration technique which is initiated by a Runge-Kutta scheme.

Encke's method. Due to its widespread use in ballistic lunar trajectories, Encke's method will be described in this subsection. This method is used with some modifications in the trajectory program described in Ref. 13. This trajectory program, in turn, has been used with some minor modifications for the calculation of n-body lunar trajectories in this manual.

For the discussion of the basic Encke's method without modifications, consider Eq (50) repeated here:

$$M_\Delta \, \ddot{\vec{r}}_{\oplus \Delta} = -G \, \frac{\vec{r}_{\oplus \Delta}}{r_{\oplus \Delta}^3} \, M_\oplus M_\Delta$$

$$+ \vec{f}_\oplus M_\Delta \sum_{i=1}^{n} \left[(-G) \left(\frac{\vec{r}_{\oplus \Delta}}{r_{\oplus \Delta}^3} - \frac{\vec{r}_{i\oplus}}{r_{i\oplus}^3} \right) M_i M_\Delta \right.$$

$$\left. + \vec{f}_i M_\Delta \right] + \vec{n}_\Delta M_\Delta, \quad i = 1, 1, 2, \ldots n$$

Dividing this equation by M_Δ and taking the dot product with $\hat{x}_\oplus$, $\hat{y}_\oplus$, $\hat{z}_\oplus$, respectively, yields the $x_\oplus$ $y_\oplus$ $z_\oplus$ components of vehicle acceleration. The $x_\oplus$ -component of vehicle acceleration becomes

$$\ddot{x}_{\oplus\Delta} = -G\,\frac{x_{\oplus\Delta}}{r_{\oplus\Delta}^3}\,M_\oplus + f_{\oplus x}$$

$$+ \sum_{i=\emptyset}^{n}\left[(-G)\left(\frac{x_{\oplus\Delta}}{r_{\oplus\Delta}^3} - \frac{x_{i\oplus}}{r_{i\oplus}^3}\right)M_i + f_{ix}\right] + n_{\Delta x}$$

$$i = \emptyset, 1, 2, \ldots n \qquad (59)$$

with similar expressions for $\ddot{y}_{\oplus\Delta}$ and $\ddot{z}_{\oplus\Delta}$.

Here f_{ix} represents the $x_\oplus$ -component, in $x_\oplus$ $y_\oplus$ $z_\oplus$ coordinates, of the aspherical gravitational terms of the ith body affecting vehicle motion, and $n_{\Delta x}$ is the x-component of the resultant of all nongravitational accelerations acting on the vehicle in $x_\oplus$ $y_\oplus$ $z_\oplus$ coordinates.

For brevity neglect all but the spherical gravitational terms, i.e., n-body motion, since the other may be superimposed at the end. Then Eqs (59) become:

$$\ddot{x}_{\oplus\Delta} = -\frac{Gx_{\oplus\Delta}}{r_{\oplus\Delta}^3}\,M_\oplus + \sum_{i=\emptyset}^{n}(-G)\left(\frac{x_{\oplus\Delta}}{r_{\oplus\Delta}^3} - \frac{x_{i\oplus}}{r_{i\oplus}^3}\right)M_i,$$

$$i = \emptyset, 1, 2, \ldots n \qquad (60)$$

with similar expressions for $\ddot{y}_{\oplus\Delta}$ and $\ddot{z}_{\oplus\Delta}$.

Consider the path that the vehicle would follow if acted on only by the gravitational attraction of the earth. Let the vehicle radius vector, its components of position and acceleration in this unperturbed restricted two-body motion be $\vec{r}_{\oplus u}$, $x_{\oplus u}$, $y_{\oplus u}$, $z_{\oplus u}$, and $\ddot{x}_{\oplus u}$, $\ddot{y}_{\oplus u}$, $\ddot{z}_{\oplus u}$, respectively. The unperturbed vehicle equations of motion for this case are:

$$\ddot{x}_{\oplus u} = -\frac{Gx_{\oplus u}}{r_{\oplus u}^3}\,M_\oplus \qquad (61)$$

and similar expressions for $\ddot{y}_{\oplus u}$ and $\ddot{z}_{\oplus u}$.

Subtract Eqs (61) from Eqs (60), and define new coordinates $\xi_{\oplus\Delta}$, $\eta_{\oplus\Delta}$, $\zeta_{\oplus\Delta}$ by the relations $x_{\oplus\Delta} - x_{\oplus u} = \xi_{\oplus\Delta}$, $y_{\oplus\Delta} - y_{\oplus u} = \eta_{\oplus\Delta}$, $z_{\oplus\Delta} - z_{\oplus u} = \zeta_{\oplus\Delta}$.

Then

$$\ddot{\xi}_{\oplus\Delta} = -GM_\oplus\left(\frac{x_{\oplus\Delta}}{r_{\oplus\Delta}^3} - \frac{x_{\oplus u}}{r_{\oplus u}^3}\right)$$

$$+ \sum_{i=\emptyset}^{n}(-G)\left(\frac{x_{\oplus\Delta}}{r_{\oplus\Delta}^3} - \frac{x_{i\oplus}}{r_{i\oplus}^3}\right)M_i,$$

$$i = \emptyset, 1, 2, \ldots n \qquad (62)$$

and similar expressions hold for $\ddot{\eta}_{\oplus\Delta}$ and $\ddot{\zeta}_{\oplus\Delta}$.

Consider the first term in Eq (62). Taking only the term in parentheses and multiplying by (-1), it can be written

$$-\left(\frac{x_{\oplus u}}{r_{\oplus u}^3} - \frac{x_{\oplus\Delta}}{r_{\oplus\Delta}^3}\right) = -\frac{1}{r_{\oplus u}^3}\left(x_{\oplus u} - \frac{r_{\oplus u}^3}{r_{\oplus\Delta}^3}x_{\oplus u}\right)$$

$$= -\frac{1}{r_{\oplus u}^3}\left(x_{\oplus\Delta} - \xi_{\oplus\Delta} - \frac{r_{\oplus u}^3}{r_{\oplus\Delta}^3}x_{\oplus\Delta}\right)$$

$$= -\frac{1}{r_{\oplus u}^3}\left[\left(1 - \frac{r_{\oplus u}^3}{r_{\oplus\Delta}^3}\right)x_{\oplus\Delta} - \xi_{\oplus\Delta}\right]$$

$$(63)$$

Now, expressing $r_{\oplus\Delta}$ in terms of $x_{\oplus 0}$, $y_{\oplus 0}$, $z_{\oplus 0}$, $\xi_{\oplus\Delta}$, $\eta_{\oplus\Delta}$, $\zeta_{\oplus\Delta}$

$$r_{\oplus\Delta}^2 = x_{\oplus\Delta}^2 + y_{\oplus\Delta}^2 + z_{\oplus\Delta}^2$$

$$= (x_{\oplus u} + \xi_{\oplus\Delta})^2 + (y_{\oplus u} + \eta_{\oplus\Delta})^2 + (z_{\oplus u} + \zeta_{\oplus\Delta})^2$$

$$= r_{\oplus u}^2 + 2x_{\oplus u}\xi_{\oplus\Delta} + 2y_{\oplus u}\eta_{\oplus\Delta} + 2z_{\oplus u}\zeta_{\oplus\Delta}$$

$$+ \xi_{\oplus\Delta}^2 + \eta_{\oplus\Delta}^2 + \zeta_{\oplus\Delta}^2 \qquad (64)$$

Then

$$\frac{r_{\oplus\Delta}^2}{r_{\oplus u}^2} = 1 + 2\frac{(x_{\oplus u} + 1/2\,\xi_{\oplus\Delta})\xi_{\oplus\Delta} + (y_{\oplus u} + 1/2\,\eta_{\oplus\Delta})\eta_{\oplus\Delta} + (z_{\oplus u} + 1/2\,\zeta_{\oplus\Delta})\zeta_{\oplus\Delta}}{r_{\oplus u}^2}$$

$$(65)$$

Put

$$q = \frac{(x_{\oplus u} + 1/2\,\xi_{\oplus\Delta})\xi_{\oplus\Delta} + (y_{\oplus u} + 1/2\,\eta_{\oplus\Delta})\eta_{\oplus\Delta} + (z_{\oplus u} + 1/2\,\zeta_{\oplus\Delta})\zeta_{\oplus\Delta}}{r_{\oplus u}^2}$$

$$(66)$$

Then

$$\left(\frac{r_{\oplus\Delta}}{r_{\oplus u}}\right)^2 = 1 + 2q$$

and

$$\left(\frac{r_{\oplus u}}{r_{\oplus\Delta}}\right)^3 = (1 + 2q)^{-3/2}$$

Assume that the true orbit, Eq (60), does not differ much from the Keplerian orbit, Eq (61), so that $\xi_{\oplus\Delta}, \eta_{\oplus\Delta}, \zeta_{\oplus\Delta}$, are very small in comparison to $x_{\oplus u}, y_{\oplus u}, z_{\oplus u}$. In that case the squares of the increments can be neglected. Thus,

$$q \approx \frac{x_{\oplus u}\,\xi_{\oplus\Delta} + y_{\oplus u}\,\eta_{\oplus\Delta} + z_{\oplus u}\,\zeta_{\oplus\Delta}}{r^2_{\oplus u}} \qquad (67)$$

Further, assume q is small compared to unity, thus enabling the first few terms of the binomial expansion to approximate the term $\left[1 - \left(\dfrac{r_{\oplus u}}{r_{\oplus\Delta}}\right)^3\right]$ in Eq (63).

Then,

$$\left[1 - \left(\frac{r_{\oplus u}}{r_{\oplus\Delta}}\right)^3\right] = 1 - (1 + 2q)^{-3/2}$$

$$\approx 3q - \frac{15}{2}q^2 \qquad (68)$$

The series used in the expansion of Eq (68) can be shown to converge for $-\frac{1}{2} < q < \frac{1}{2}$ which is well outside its practical limit of applicability in the n-body trajectory program.

Define

$$f = \frac{1 - (1 + 2q)^{-3/2}}{q} \qquad (69)$$

Note that f changes much less rapidly than q, staying very close to 3 when q is small. It is thus easy to interpolate giving q as a function of f.

Equation (63) then becomes by use of Eqs (64), (67) and (69):

$$-\frac{x_{\oplus u}}{r^3_{\oplus u}} - \frac{x_{\oplus\Delta}}{r^3_{\oplus\Delta}} = -\frac{1}{r^3_{\oplus u}}\left(fqx_{\oplus\Delta} - \xi_{\oplus\Delta}\right) \qquad (70)$$

Substitution of Eq (70) into Eq (62) and addition of the terms that have been neglected yields the following perturbation equations of motion:

$$\ddot{\xi}_{\oplus\Delta} = -\frac{GM_\oplus}{r^3_{\oplus u}}\left(fqx_{\oplus\Delta} - \xi_{\oplus\Delta}\right)$$

$$+ f_{\oplus x} + \sum_{i=1}^{n}\left[(-G)\left(\frac{x_{\oplus\Delta}}{r^3_{\oplus\Delta}} - \frac{x_{i\oplus}}{r^3_{i\oplus}}\right)M_i + f_{ix}\right] + n_{\Delta x}$$

$$\ddot{\eta}_{\oplus\Delta} = -\frac{GM_\oplus}{r^3_{\oplus u}}\left(fqy_{\oplus\Delta} - \xi_{\oplus\Delta}\right)$$

$$+ f_{\oplus y} + \sum_{i=1}^{n}\left[(-G)\left(\frac{y_{\oplus\Delta}}{r^3_{\oplus\Delta}} - \frac{y_{i\oplus}}{r^3_{i\oplus}}\right)M_i + f_{iy}\right] + n_{\Delta y} \qquad (71)$$

$$\ddot{\zeta}_{\oplus\Delta} = -\frac{GM_\oplus}{r^3_{\oplus u}}\left(fqz_{\oplus\Delta} - \zeta_{\oplus\Delta}\right)$$

$$+ f_{\oplus z} + \sum_{i=1}^{n}\left[(-G)\left(\frac{z_{\oplus\Delta}}{r^3_{\oplus\Delta}} - \frac{z_{i\oplus}}{r^3_{i\oplus}}\right)M_i + f_{iz}\right] + n_{\Delta z}$$

These are the fundamental equations of Encke's method. Sometimes they will be encountered having been multiplied by the constant factor, h^2, where h represents the width of the interpolation interval. An actual numerical example using this method is given by Brouwer (Ref. 15, p 179).

The reference orbit used in this description of Encke's method is the restricted two-body orbit, Eq (61). The method may be modified to use other types of reference orbits which would be more advantageous for the particular geometry and force model.

d. Description of the n-body trajectory program

The trajectory program used for obtaining n-body integrated lunar trajectories in this manual is described in detail in Ref. 13. Some additions have been made, so that the program at present is able to give the motion of a point mass with mass M_Δ (simulating the space vehicle) under the gravitational attraction of the oblate earth, the triaxially ellipsoidal moon, the sun, Venus, Mars and Jupiter. The positions of these celestial bodies as obtained from the U. S. Naval Observatory are stored in the program in geocentric equatorial rectangular coordinates $(x_\oplus, y_\oplus, z_\oplus)$ for 12-hr intervals for the moon and for 24-hr intervals for the sun and planets. A special input variable allows the use of this position data for the specified time period. In addition a subroutine for computing lunar librations from the rectangular position coordinates of the moon exists, and is described in Section C of Chapter III. It will be incorporated in the program as soon as a satisfactory interpolation routine can be established.

The force model for this trajectory has also provisions for including drag due to a spherically symmetric atmosphere rotating with the earth. The atmospheric drag terms in the equations of motion are described in the next subsection. There are plans to include solar radiation pressure and other nongravitational forces.

The n-body trajectory program uses a modified Encke numerical integration method as described in Subsection 3d. The unperturbed restricted two-body orbit is rectified as soon as the ratios of the perturbative distance, speed, or numerical

value of acceleration exceeds 1% of the respective restricted two-body reference orbit. The procedure is essentially as follows:

(1) The most significant body in the system is selected (initially this is the earth, and if the trajectory approaches the moon, the moon); Eqs (61) are solved numerically on the computer. This numerical solution can always be checked by the known analytical solution.

(2) Equations (60) are then solved using a sixth-order Adams backward difference technique which is started by a Runge-Kutta scheme.

(3) The corrected coordinates of the body are then obtained by using the relations:
$x_{\oplus\Delta} = x_{\oplus u} + \xi_{\oplus\Delta}$, $y_{\oplus\Delta} = y_{\oplus u} + \eta_{\oplus\Delta}$, $z_{\oplus\Delta} = z_{\oplus u} + \zeta_{\oplus\Delta}$ and similar ones for velocity and acceleration components. When the perturbations exceed the above limits, new solutions are obtained for Eq (61), and the orbit is rectified.

4. Nongravitational Forces

Having discussed all gravitational terms appearing in Eq (50), which are significant for lunar trajectories, let us turn our attention to the nongravitational forces acting on the vehicle, the resultant of which was termed $\vec{n}_\Delta M_\Delta$ in Eq (50).

It should be noted that if the forces discussed subsequently are to be used in Eq (50) and the trajectory program, they must be expressed in component form in equatorial geocentric coordinates.

Let

$$\vec{n}_\Delta M_\Delta = \vec{D}_S + \vec{D} + \vec{D}_E + \vec{D}_M + \vec{T} + \vec{R}_{rel} \tag{72}$$

where

$\vec{D}_S$ = force due to the solar radiation pressure

$\vec{D}$ = atmospheric drag force

$\vec{D}_E$ = electromagnetic forces

$\vec{D}_M$ = meteoritic drag force

$\vec{T}$ = rocket thrust force

$\vec{R}_{rel}$ = relativistic corrections to the equations of motion.

These forces will be discussed more fully in the above order in the following subsections.

a. Solar radiation pressure

Outside the confines of the earth's atmosphere, the most significant natural nongravitational force acting on a vehicle arises from solar radiation pressures can be seen from the table on page IV-22. It is due to the absorption and emission of photons by the space vehicle and is a consequence of the photon nature of light. Studies have been made previous to the launching of space vehicles concerning the effects of this solar radiation pressure on the orbits of micrometeorites around the sun. These studies by Poynting and Robertson indicated that the orbits of micrometeorites became more cir-

cular due to solar radiation, while simultaneously, slowly spiraling into the sun. More recently investigators have studied the effects of this force on satellites and, have found that for a vehicle mass to area ratio $\frac{M_\Delta}{A_\Delta} \leq 0.04$ gm/cm^2, a sizable perturbation occurs in the orbital elements (see Ref. 12). The essential qualitative effect of radiation pressure is a displacement of the center of the orbit, which is especially evident for circular and near-circular orbits (Ref. 19).

In these studies one of two possible approaches is taken. Either this force is obtained neglecting those times when the space vehicle is eclipsed by the earth or moon and hence the radiation pressure does not act (this is termed the shadow time), or the shadow time is included by expressing the force as a function of the orbital elements of the vehicle (i.e., as a perturbation in the variation of parameters method).

For the present analysis, the shadow time will be neglected and the rectangular components of the radiation pressure will be given in terms of vehicle-centered coordinates. This analysis essentially follows Kochi and Staley (Ref. 20).

Let P be the magnitude of the momentum of a photon, E_P its energy, m its equivalent mass, and c the speed of light; then

$$P = mc \tag{73}$$

and

$$E_P = h\nu_P = mc^2 \tag{74}$$

where $h = 6.625 \times 10^{-39}$ joule-sec is Planck's constant and ν is the frequency of the radiation. From Eqs (73) and (74)

$$P = \frac{h\nu_P}{c} \tag{75}$$

The magnitude of the force per unit area due to radiation pressure, p_s, then is

$$p_s = \frac{h\nu_p}{c} N \tag{76}$$

where N is the number of photon collisions with the vehicle per unit time on a unit area. If W_Δ is the radiated power arriving at the space vehicle per unit area of the vehicle, then $N = \frac{W_\Delta}{E_P} = \frac{W_\Delta}{h\nu_P}$

and

$$p_s = \frac{h\nu_P}{c} \cdot \frac{W_\Delta}{h\nu_P} = \frac{W_\Delta}{c} .$$

The type of photon collision with the vehicle must also be taken into consideration. To do this, a factor q_s will be introduced such that $0 \leq q_s \leq 1$ where $q_s = 0$ represents total momentum transfer, or perfect absorber, black body, i.e., an inelastic photon collision, and $q_s = 1$ represents a perfect

reflector, i.e., an elastic photon collision. Hence

$$p_s = \frac{W_\Delta}{c} (1 + q_s) \qquad (77)$$

Let $W_\odot$ represent the total radiated power (in watts/cm^2 per hemisphere) of the sun at all frequencies. Then by the Stefen-Boltzmann Law:

$$W_\odot = \epsilon \sigma T^4 A_\odot \qquad (78)$$

where ϵ is the total empirically determined emissivity of the sun ($\epsilon = 1.0$, i.e., the sun is a perfect radiator), $\sigma = 5.67 \times 10^{-8}$ watts/m^2 ($^\circ$K)^4

is the Stefan-Boltzmann constant, a constant of proportionality determined experimentally and defined by Eq (78),

T is the absolute temperature in $^\circ$K,

$A_\odot$ is the surface area of the sun.

Now the radiant energy per second, W_Δ, impinging upon a unit area of the vehicle perpendicular to the line-of-sight to the sun, which is regarded as a point source, at a distance $r_{\oplus,\odot \to\Delta}$ is given by

$$W_\Delta = \frac{W_\odot}{\pi r^2_{\oplus,\odot \to\Delta}} = \frac{\epsilon \sigma T^4 A_\odot}{\pi r^2_{\oplus,\odot \to\Delta}} \qquad (79)$$

The point source approximation is reasonable since any trajectory in the vicinity of the earth is more than 100 solar diameters from the sun. Hence the solar radiation pressure per unit area is given by

$$p_s = \frac{\epsilon \sigma T^4 A_\odot}{\pi c r^2_{\oplus,\odot \to\Delta}} (1 + q_s) \times 10^7 \frac{\text{dynes}}{\text{cm}^2} \qquad (80)$$

where p_s is in the opposite direction from the sun along the vehicle-sun line, and 10^7 is a conversion factor from watts to $\frac{\text{dyne-cm}}{\text{sec}}$. An approximate value for the solar radiation pressure at the distance of the earth is $p_s = 4.5 \times 10^{-5} \frac{\text{dynes}}{\text{cm}^2}$ for a black body space vehicle (Ref. 21).

The acceleration of the vehicle due to the solar radiation pressure, $\vec{D}_s$, is given by

$$\frac{\vec{D}_s}{M_\Delta} = \frac{p_{s0}(1 + q) A_s}{M_\Delta r^2_{\oplus,\odot \to\Delta}} \frac{\vec{r}_{\oplus,\odot \to\Delta}}{r_{\oplus,\odot \to\Delta}} \qquad (81)$$

where

$$p_{s0} = \frac{\epsilon \sigma T^4 A_\odot \times 10^7}{\pi c} \simeq 10^{22} \text{ dynes}$$

is the total force due to solar radiation divided by π, q_s, $0 \leq q_s \leq 1$, is the space vehicle

reflectivity, zero for a black body and 1 for a perfect reflector, A_s the area of the vehicle perpendicular to the vehicle-sun line, M_Δ its mass, and $\vec{r}_{\oplus,\odot \to\Delta}$ is the radius vector of the vehicle from the sun. Next write $\vec{r}_{\oplus,\odot \to\Delta} = \vec{r}_{\oplus\Delta} - \vec{r}_{\oplus\odot}$ so that Eq (81) becomes

$$\frac{\vec{D}}{M_\Delta} = \frac{p_{s0}(1 + q_s) A_s}{M_\Delta |\vec{r}_{\oplus\Delta} - \vec{r}_{\oplus\odot}|^3} (\vec{r}_{\oplus\Delta} - \vec{r}_{\oplus\odot}) \qquad (82)$$

Since the position of the vehicle is continually computed during a trajectory run on the computer and since the positions of the sun are stored, Eq (82) may be solved as soon as A_s is specified.

For all but spherical space vehicles the computation of A_s requires a knowledge of vehicle orientation with respect to the vehicle-sun line. This line can be given with respect to body axes x_b, y_b, z_b with origin at the vehicle center of gravity, and these axes can be transformed to the geocentric equatorial coordinates by the transformation given in Table 2. The following sketch illustrates the geometry in this case.

Equation (82) shows that $\frac{\vec{D}_s}{M_\Delta}$ depends very strongly on the area-to-mass ratio $\frac{A_s}{M_\Delta}$. It is quite negligible for the moon and planets, small for dense space vehicles, and becomes sizable for light and unorthodox vehicles such as balloons. The term $\frac{\vec{D}_s}{M_\Delta}$ also depends on the type of surface-- thus q_s may approach 0.98 for highly polished metals. The shadow time may be neglected for lunar trajectory studies since the trajectory will be in sunlight during most approach, impact, and circumlunar trajectories. However, during earth or moon orbital phase the shadow time may approach half of the total time in orbit for low-altitude orbits. A discussion and graphical presentation of shadow time as a function of orbital elements is given in Chapter XIII of Ref. 3.

b. Atmospheric drag and lift

In connection with lunar trajectories, the contribution of atmospheric drag need only be considered in the short time period when the vehicle is in the immediate vicinity of the earth. Thus, its significance is much less important than in the case of earth satellite vehicles. However, during parking orbits around the earth, atmospheric drag becomes of decisive importance in the selection of orbital radius and eccentricity; a discussion of this force will be included here.

The acceleration of a space vehicle due to the drag force can be expressed as

$$\frac{\vec{D}}{M_\Delta} = -\frac{1}{2} C_D \frac{A_a}{M_\Delta} \rho V_a^2 \frac{\vec{V}_a}{V_a} \qquad (83)$$
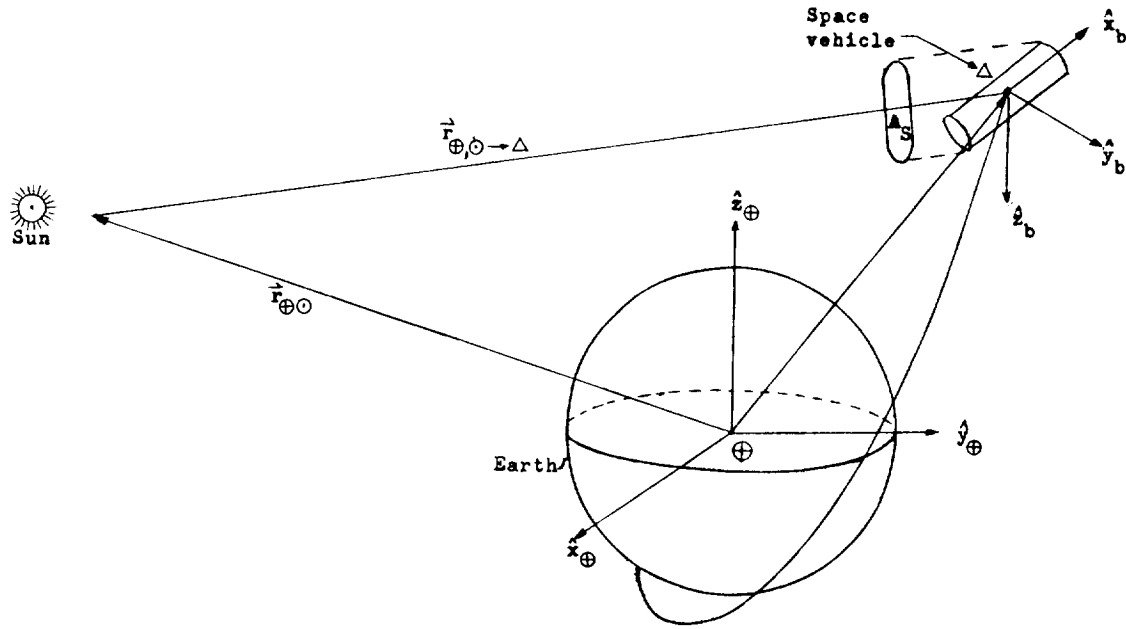
where

C_D is the drag coefficient (usually the one for free molecular flow in the case of earth satellites and space vehicles)

A_a is the area of the space vehicle perpendicular to V_a

ρ_a is the density of the atmosphere

$\vec{V}_a$ is the velocity of the vehicle relative to the atmosphere.

For parametric studies it is useful to introduce a ballistic coefficient $B = \dfrac{C_D A_a}{2 M_\Delta}$ which gives for the drag acceleration

$$\frac{\vec{D}}{M_\Delta} = -B \rho\, V_a\, \vec{V}_a \tag{84}$$

The drag coefficient C_D can be calculated from free molecular flow assumption in the kinetic theory of gases. It depends on the geometry and orientation of the vehicle as well as the interaction of the air molecules with its surface. The value of C_D is 2.0 for spherical vehicles, and slightly larger for other vehicle shapes. For all but spherical vehicles A_a as well as C_D will vary with the orientation of the vehicle relative to $\vec{V}_a$.

In the case of a vehicle in a random tumble with a short period of tumble compared to the orbital period or compared to the time in the atmosphere for lunar trajectories, a good approximation is $A_a = \dfrac{A_\Delta}{4}$, where A_Δ is the surface area of the vehicle.

$\vec{V}_a$ can be written as the difference of the vehicle velocity with respect to the geocentric equatorial system frame $\vec{V}_{\oplus \Delta}$ and the velocity of the atmosphere $\vec{V}_{\oplus a}$. Thus,

$$\vec{V}_a = \vec{V}_{\oplus \Delta} - \vec{V}_{\oplus a} \tag{85}$$

At altitudes below 500 km, the atmosphere can be assumed to rotate with the earth so that under this assumption the velocity of the atmosphere with respect to the equatorial system is given by

$$\vec{V}_{\oplus a} = \vec{\omega}_\oplus \times \vec{r}_{\oplus \Delta} \tag{86}$$

Substituting (86) into (85)

$$\vec{V}_a = \vec{V}_{\oplus \Delta} - \vec{\omega}_\oplus \times \vec{r}_{\oplus \Delta} \tag{87}$$

In order to express V_a in rectangular geocentric coordinates, note that

$$\vec{V}_{\oplus \Delta} = \dot{x}_{\oplus \Delta}\, \hat{x}_\oplus + \dot{y}_{\oplus \Delta}\, \hat{y}_\oplus + \dot{z}_{\oplus \Delta}\, \hat{z}_\oplus \tag{88}$$

$$\vec{\omega}_\oplus \times \vec{r}_{\oplus \Delta} = \begin{vmatrix} \hat{x}_\oplus & \hat{y}_\oplus & \hat{z}_\oplus \\ 0 & 0 & \omega_\oplus \\ x_{\oplus \Delta} & y_{\oplus \Delta} & z_{\oplus \Delta} \end{vmatrix} = \omega_\oplus\, x_{\oplus \Delta}\, \hat{y}_\oplus - \omega_\oplus\, y_{\oplus \Delta}\, \hat{x}_\oplus$$

If Eqs (88) are substituted into Eq (87) and the result into Eq (84), the magnitude of the drag acceleration is given by:

$$\frac{D}{M_\Delta} = -B \rho \left(\dot{r}_{\oplus \Delta}^{2} - 2\omega_\oplus\, \dot{x}_{\oplus \Delta}\, y_{\oplus \Delta} + 2\omega_\oplus\, x_{\oplus \Delta}\, \dot{y}_{\oplus \Delta} + \omega_\oplus^{2}\, x_{\oplus \Delta}^{2} \right) \tag{89}$$

The number of molecules per unit volume, N_0, can be obtained from the kinetic theory of gases. In the case of an isothermal atmosphere (T = constant) and constant molecular weight and composition

$$N_0 = N_1 \exp\left[-\frac{mg_\oplus}{kT}(h_e - h_{e1})\right] \qquad (90)$$

where

m = the constant mass of each molecule

h_e = altitude above earth

$g_\oplus$ = the constant value of the gravitational acceleration

k = 1.380 x 10^{-23} joules/°K, Boltzmann's constant

T = absolute temperature in °K

h = altitude.

Subscript 1 designates some reference condition. The atmospheric density is then given by $\rho = N_0 m$. However, this is a very poor approximation of the atmosphere, and usually a variation of temperature T, $g_\oplus$, as well as molecular weight is assumed with altitude and the density, pressure, and any other quantities are computed from this assumption. The latest such "standard atmosphere" is the 1961 U.S. Standard Atmosphere, which is used in all work in this manual. The density in this atmosphere varies with altitude and is given to an altitude of 700 km. Actually the density varies additionally with latitude due to the latitude-dependence of the earth's gravitational potential $U_\oplus$ by about +2% and with the solar activity (which at the higher altitudes may cause very large deviations from the standard density). These variations from the standard atmospheric density may be neglected, however, as long as only lunar trajectories or a few orbits near the earth are considered.

Just as in the case of solar radiation pressure the drag acceleration is small for small area-to-mass ratio or dense vehicles and becomes more significant for light vehicles such as balloons. The drag force decreases very substantially with altitude and may be neglected for all but long-time operations above 700 km.

For accurate drag computations and when the vehicle orientation is significant it is more convenient to express the drag force $\vec{D}$ in component form along the body axes x_b, y_b, z_b.

$$D_x = -\frac{1}{2} C_x A_{ref} \rho V_a^2$$

$$D_y = -\frac{1}{2} C_y A_{ref} \rho V_a^2 \qquad (91)$$

$$D_z = -\frac{1}{2} C_z A_{ref} \rho V_a^2$$

where all the variations in the force are absorbed in the coefficients C_x, C_y, C_z and A_{ref} is a constant reference area characterizing the space vehicle. Once the orientation of the vehicle is known, the transformation from body axes to

geocentric equatorial coordinates as given in Table 2 can be performed.

Atmospheric lift will be neglected for parking orbits and lunar trajectories since it is several orders of magnitude less than the drag at orbital altitudes. However, during the intermediate stages of ascent to orbit or injection, and in the initial stages of a nonballistic re-entry, this force becomes important. The magnitude of the lift L is defined, analogously to the magnitude of the drag D, by the equation

$$L = \frac{1}{2} C_L A_a \rho V_a^2. \qquad (92)$$

where C_L is the lift coefficient which can be computed similarly to C_D from free molecular assumption in the kinetic theory of gases. The lift force $\vec{L}$ is in a plane perpendicular to $\vec{V}_a$ by definition, and its direction in this plane is specified by the bank angle ξ. Consider a unit vector in this plane perpendicular to $\vec{r}_{\oplus\Delta}$ and $\vec{V}_a$, namely $\hat{y}_w \equiv \frac{\vec{r}_{\oplus\Delta}}{r_{\oplus\Delta}} \times \frac{\vec{V}_a}{V_a}$. A unit vector orthogonal to $\hat{y}_w$ is given by $\hat{z}_w \equiv \frac{\vec{V}_a}{V_a} \times \frac{\vec{r}_{\oplus\Delta}}{r_{\oplus\Delta}} \times \frac{\vec{V}_a}{V_a}$

The unit vectors $\hat{x}_w \equiv \frac{\vec{V}_a}{V_a}$, $\hat{y}_w$ and $\hat{z}_w$ define wind axes, where a rotation about the x_w-axis is defined as the bank angle ξ, a rotation about the y_w-axis is the angle of attack α, and a rotation about the z_w-axis is the yaw angle β. Wind axes and the bank angle ξ between $\hat{z}_w$ and $\vec{L}$ are illustrated in the following sketch:

Perpendicular Plane
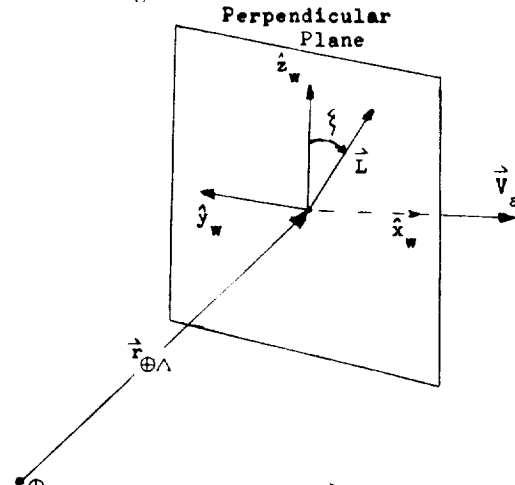
The drag acceleration $\frac{\vec{D}}{M_\Delta}$ as given by Eq (83) is in the negative $\hat{x}_w$-direction.

c. Electromagnetic forces

In most trajectory calculations the vehicle on a lunar trajectory is assumed to be electrically neutral, and beyond some altitude (700 km), which is regarded as the upper limit of the atmosphere, it is assumed to move in a vacuum. This ideal condition does not exist in space, and the effects of several electromagnetic phenomena will influence the vehicle trajectory very slightly. Even though these effects are small, upper limits to the deceleration of space vehicles should be determined and they should be considered in a detailed trajectory analysis.

The medium through which the space vehicle moves consists of charged particles. Baker (Ref. 12) states that even interplanetary space contains between 100 and 1000 charged particles per cubic centimeter which originate from solar eruptions (flares and solar winds), cosmic ray ionization (the ionization of neutral particles caused by cosmic rays and gamma radiation). Higher concentrations of charged particles occur near earth in the inner and outer Van Allen belts which consist of solar particles trapped in the earth's magnetic field. Recently a temporary radiation belt was created by a high-altitude hydrogen bomb explosion of July 9, 1962 which is expected to last for several years.

A space station in a stationary plasma (an electrically neutral medium containing charged particles) will collide with both slow moving positive ions and fast moving electrons and build up a small excess of net negative change on its surface.

Another factor affecting the potential of the vehicle, ϕ_Δ, stems from its motion with respect to the plasma.

As the vehicle travels at several km/sec, its collision rate with the positive ions, which move more slowly, increases as compared to the stationary plasma collision rate, whereas the collision rate with the electrons, which move much faster than the positive ions, remains essentially unaltered. Thus, vehicle motion tends to decrease the induced negative voltage from the source discussed above.

Beard and Johnson (Ref. 21) have derived an expression for the potential, ϕ_Δ, of a satellite moving through such a plasma with speed V_p. It is:

$$\phi_\Delta = - \frac{kT}{q_e} \ln\left(\frac{1}{2} \frac{\overline{V}_{e\ell}}{V_p}\right) \tag{93}$$

where

    k = 1.380 x 10^{-23} joules/° K, Boltzmann's constant

    T = absolute temperature of the plasma in ° K

    q_c = 1.602 x 10^{-19} coulomb, the charge of an electron

V_p = speed of space vehicle relative to the plasma

$\overline{V}_{e\ell}$ = the average thermal speed of an electron in the medium, given by

$$\overline{V}_{e\ell} = 0.145 \quad T/m_e$$

where m_e is the atomic weight of an electron.

This negative potential obtained from Eq (93) amounts to only a few volts in typical cases.

Singer and Walker (Ref. 22) have proposed that the ejection of electrons caused by high-energy solar radiation striking the vehicle need not be considered due to the buildup of a screen of ejected electrons surrounding the vehicle, thus reducing any further electron ejection.

An expression for the total force on a space vehicle which is electrically conductive and magnetically permeable has been given by M. Z. V. Krzywoblocki, et al., in Ref. 23. Starting from Maxwell's equation for moving media he derived the force on a body due to the electrostatic field, the magnetic field and a final expression for the force acting on a moving body in an electromagnetic field.

Due to our scant knowledge of the cislunar and interplanetary medium and the large and unpredictable fluctuation of its number-density with solar eruptions, the material given in this subsection has been primarily of an illustrative nature. The presence of these particles and the radiation will influence the trajectory of the lunar vehicle only slightly; their pressure, however, is of primary importance from the standpoint of shielding requirements for any human occupants in the space vehicle.

d. Meteoritic drag

In the attempts to analyze the force acting upon a space vehicle due to meteoritic drag, experimental evidence is taken primarily from past observation of meteoritic contact with the earth (Ref. 20) to which some space probe data has been added recently. Due to the rarity of large meteorites impinging even upon a body the size of the earth, it can be assumed that the probability of a small lunar vehicle being hit by such a meteorite would be extremely small; therefore, it will be neglected. Hence, it will be assumed that micrometeorites contribute the only significant meteoritic drag perturbation. Ideally one would like to know meteor density, mass flux, velocity and spatial distribution as a function of position and time for the sporadic background as well as for meteoritic showers. Only the sporadic background flux can be considered here. Estimates of the accretion of meteoritic material by the earth vary widely, but extensive geophysical evidence from both optical and radio experiments indicates that the maximum amount of meteoritic material hitting the earth per day is 2000 tons (Refs. 20, 24). This would correspond to a meteoritic density of ρ_M = 5 x 10^{-21} g/cm^3 outside of the atmosphere. Furthermore, it is believed that micrometeorites (i.e., meteorites

with magnitudes between the ranges 20 and 30 or radii less than about 100 microns) constitute 95% of the meteoritic material hitting the earth (Ref. 20). Also, meteorites can enter the earth's atmosphere only with velocities between 11 and 72 km/sec relative to the earth. The lower limit on velocities of entry is due to the gravitational acceleration of the particle by the earth, while the upper limit is the sum of the parabolic velocity for a solar orbit at the distance of the earth (42 km/sec) and the earth's orbital velocity (30 km/sec).

Assume that the direction of motion of the meteorites is random along the lunar trajectory (this hypothesis is invalid near the surface of the earth or the moon which shield the vehicle from below) and that the meteorites are so small as to evenly distributed in space. Then the mass, M_M of meteorites striking the vehicle in the time interval Δt from any one direction is:

$$M_M = \frac{1}{6} \rho_M A_M V_{\oplus M} \Delta t \qquad (94)$$

where

ρ_M = is the average density of meteoritic material in space

A_M = the cross-sectional area of the vehicle perpendicular to the particular direction

$V_{\oplus M}$ = the average speed of the meteorites

and it has been assumed that the velocity of the micrometeorites is much larger than the velocity of the vehicle. The net momentum imparted to the vehicle sides per second is zero since the momentum of the micrometeoritic hits from the left is cancelled by those from the right, and similarly for the top and bottom of the vehicle. However, the micrometeorites striking the space vehicle from behind have a relative velocity of $(V_{\oplus M} - V_{\oplus \Delta})$ with respect to the vehicle, and those from the front have a relative velocity of $-(V_{\oplus M} + V_{\oplus \Delta})$. The net rate of momentum transfer, or the magnitude of the force on the vehicle due to meteoritic impact is

$$D_{M1} = -\frac{1}{3} \rho_M A_M V_{\oplus M} V_{\oplus \Delta} \qquad (95)$$

where the negative sign indicates that this force is directed against the vehicle geocentric velocity vector $\vec{V}_{\oplus \Delta}$. As an illustrative example, for $\rho_M = 5 \times 10^{-21}$ g/cm^3, $A_M = 10 m^2 = 10^5$ cm^2, an average meteoritic speed of $V_{\oplus M} = 40$ km/sec $= 4 \times 10^6$ cm/sec and a representative vehicle speed of 3 km/sec $= 3 \times 10^5$ cm/sec, the magnitude of the force due to meteoritic impacts is $D_{M1} = -2 \times 10^{-4}$ dynes.

Also to be considered is the type of meteoritic impact. In a perfectly elastic collision the micrometeorite will leave the space vehicle with the same relative speed as that at which it hit and

the magnitude of this total force on the space vehicle becomes

$$D_M = 2D_{M1} = -4 \times 10^{-4} \text{ dynes}.$$

In a perfectly inelastic collision, on the other hand, all the micrometeorites stay with the vehicle and must be accelerated to its speed. In this case the magnitude of the total force on the space vehicle becomes

$$D_M = D_{M1} - \rho_M A_M V_{\oplus M} V_{\oplus \Delta} = 4D_{M1}$$

$$= -8 \times 10^{-4} \text{ dynes}.$$

In the case where the micrometeorite blasts material from the skin of the space vehicle, and where it, together with some satellite material, is left behind, the meteoritic drag force should probably be decreased.

This discussion shows that regardless of the type of collision and even for the maximum meteoritic density assumed for these calculations the force on the satellite is extremely small. The major importance of meteoritic impacts lies in their effect on the material of the satellite skin, i.e., the probability of puncture with resulting fuel or gas losses, or damage to some subsystem, and the sandblasting or pitting of the skin or of optical surfaces such as lenses, windows, etc. The probabilities of a catastrophic encounter between a space vehicle and a large meteor are extremely small. A more complete discussion of meteoritic densities, representative values for fluxes, classifications, models, and the effect of micrometeorites on space vehicle materials is given in Chapter II and Chapter II of Ref. 3.

e. Rocket thrust

The thrust due to rocket burning is another force acting on the space vehicle which must be considered in the complete analysis of a lunar trajectory. As a first approximation it is possible to assume that the vehicle is accelerated by an initial large thrust during the boost stage to the predetermined injection velocity, and that the lunar trajectory approaches the moon ballistically on a path determined by the injection conditions. In this case thrust forces need not be considered. However, even the earliest lunar vehicles had provisions for applying corrective accelerations by both midcourse and terminal thrust to overcome any errors in initial conditions and due to our imperfect knowledge of the physical environment. More sophisticated missions such as lunar orbit and landing missions require one or several large decelerations and accelerations of the space vehicle during the mission. Thus at some time in the planning of any lunar mission the simulation of thrust becomes necessary.

In most cases the thrust force is large and the time for rocket burning is small compared to the transit time. Then Encke's integration method should be stopped at the onset of rocket burning (since the perturbing acceleration by the thrust force is too large), and Cowell's method of integration should be used to simulate vehicle motion

during rocket burning. The end conditions, i.e., the time when the thrust is terminated, can be used to define a new rectified orbit and the numerical calculations of the subsequent trajectory can be continued by use of Encke's integration method. Since the trajectory after injection is outside the denser parts of the atmosphere, low-thrust propulsion by ion engines or other devices is possible. The thrust perturbation will then act during the major part of the lunar trajectory, but it will be small enough so that Encke's method of integration may be used throughout for some small thrust accelerations, without large errors arising from rectification.

Let $\vec{T}$ be the thrust force acting on the space vehicle. It enters the equations of motion Eq (50) through the term n_Δ which is defined by Eq (72) where the mass M_Δ of the vehicle is its instantaneous mass, which decreases due to the exhaust of mass in a stream of particles during rocket burning. The magnitude, direction, and time-variation of $\vec{T}$ must be specified. A natural coordinate system in which the components of $\vec{T}$ might be given is the body-axis system defined in Chapter III since the rocket engine is mounted in the body of the space vehicle. With the orientation of the vehicle known, it is possible to obtain the $x_\oplus$, $y_\oplus$, $z_\oplus$ components of $\vec{T}$ by the transformation of Table 2.

In some cases such as in lunar landing optimization studies the thrust force will be resolved into components in and normal to the vehicle trajectory plane. The transformation from these thrust components to $x_\oplus$, $y_\oplus$, $z_\oplus$ components of $\vec{T}$ is given below.

Define a coordinate system x_v y_v z_v with origin at the center of gravity of the vehicle, the z_v-axis in the direction of the radius vector (or up), the x_v-axis perpendicular to the z_v-axis in the general direction of vehicle motion in the trajectory plane, and the y_v-axis perpendicular to the instantaneous trajectory plane to complete the right-handed Cartesian coordinate system. Denote the thrust components in the $x_v y_v z_v$ directions by T_u, T_v, T_w respectively. The problem, then, is to transform the T_u, T_v, T_w components to T_x, T_y, T_z components in the $x_\oplus$, $y_\oplus$, $z_\oplus$ directions, respectively (see the following sketch):
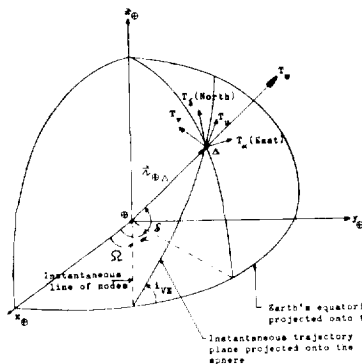
Define thrust components T_δ and T_α in the north and east directions, respectively. Then, as can be seen from the preceding sketch, the angle between T_v and T_δ as well as T_u and T_α is $(360° - A_e)$, where A_e is the azimuth of the T_v direction measured from geographic north. A rotation about T_w by the angle A_e will transform from T_u, T_v, T_w components to T_α, T_δ, T_ω components. Further rotations about T_α by the angle $-(90-\delta) = \delta - 90$ and then about T_z by the angle $(270-\alpha)$ will yield the following transformation equations:

$$\begin{Bmatrix} T_x \\ T_y \\ T_z \end{Bmatrix} = \begin{bmatrix} T(270-\alpha) \end{bmatrix} \cdot \begin{bmatrix} T(\delta-90) \end{bmatrix} \cdot \begin{bmatrix} T(A_e) \end{bmatrix} \begin{Bmatrix} T_u \\ T_v \\ T_w \end{Bmatrix}$$

$$= \begin{bmatrix} -\sin\alpha & -\cos\alpha & 0 \\ \cos\alpha & -\sin\alpha & 0 \\ 0 & 0 & 1 \end{bmatrix} \begin{bmatrix} 1 & 0 & 0 \\ 0 & \sin\delta & -\cos\delta \\ 0 & \cos\delta & \sin\delta \end{bmatrix}$$

$$\begin{bmatrix} \cos A_e & \sin A_e & 0 \\ -\sin A_e & \cos A_e & 0 \\ 0 & 0 & 1 \end{bmatrix} \begin{Bmatrix} T_u \\ T_v \\ T_w \end{Bmatrix} \qquad (96)$$

In the above equation

$$\sin\alpha = \frac{y_{\oplus\Delta}}{\left(x^2_{\oplus\Delta} + y^2_{\oplus\Delta} \right)^{1/2}} \qquad (97)$$

$$\cos\alpha = \frac{x_{\oplus\Delta}}{\left(x^2_{\oplus\Delta} + y^2_{\oplus\Delta} \right)^{1/2}}$$

$$\sin\delta = \frac{z_{\oplus\Delta}}{r_{\oplus\Delta}}$$

$$\cos\delta = \frac{\left(x^2_{\oplus\Delta} + y^2_{\oplus\Delta} \right)^{1/2}}{r_{\oplus\Delta}}$$

(compare with the preceding sketch). It remains to give $\cos A_e$ and $\sin A_e$ in terms of $x_{\oplus\Delta}$ $y_{\oplus\Delta}$ $z_{\oplus\Delta}$. We have

$$\cos A_e = \frac{\cos i_{VE}}{\cos \delta}$$

$$\sin A_e = -\left(1 - \frac{\cos^2 i_{VE}}{\cos^2 \delta}\right)^{1/2} \tag{98}$$

where

$$\cos i_{VE} = \frac{\left(\vec{r}_{\oplus\Delta} \times \vec{V}_{\oplus\Delta}\right) \cdot \hat{z}_\oplus}{r_{\oplus\Delta} \times V_{\oplus\Delta}}$$

$$= \frac{x_{\oplus\Delta}\,\dot{y}_{\oplus\Delta}}{\left[\left(y_{\oplus\Delta}\,\dot{z}_{\oplus\Delta} - \dot{y}_{\oplus\Delta}\,z_{\oplus\Delta}\right)^2\right.}$$

$$\frac{-\dot{x}_{\oplus\Delta}\,y_{\oplus\Delta}}{+\left(z_{\oplus\Delta}\,\dot{x}_{\oplus\Delta} - \dot{z}_{\oplus\Delta}\,x_{\oplus\Delta}\right)^2}$$

$$\left.+\left(x_{\oplus\Delta}\,\dot{y}_{\oplus\Delta} - \dot{x}_{\oplus\Delta}\,y_{\oplus\Delta}\right)^2\right]^{1/2} \tag{99}$$

The expressions (98) become, by use of (99):

$$\cos A_e = \left\{\left(x_{\oplus\Delta}\,\dot{y}_{\oplus\Delta} - \dot{x}_{\oplus\Delta}\,y_{\oplus\Delta}\right)\ r_{\oplus\Delta}\right\}$$

$$\left\{\left(x^2_{\oplus\Delta} + y^2_{\oplus\Delta}\right)\right.$$

$$\left[\left(y_{\oplus\Delta}\,\dot{z}_{\oplus\Delta} - \dot{y}_{\oplus\Delta}\,z_{\oplus\Delta}\right)^2\right.$$

$$+\left(z_{\oplus\Delta}\,\dot{x}_{\oplus\Delta} - \dot{z}_{\oplus\Delta}\,x_{\oplus\Delta}\right)^2$$

$$\left.\left.+\left(x_{\oplus\Delta}\,\dot{y}_{\oplus\Delta} - \dot{x}_{\oplus\Delta}\,y_{\oplus\Delta}\right)^2\right]\right\}^{-1/2} \tag{100}$$

$$\sin A_e = -\left[1 - \left\{\left(x_{\oplus\Delta}\,\dot{y}_{\oplus\Delta} - \dot{x}_{\oplus\Delta}\,y_{\oplus\Delta}\right)^2\right.\right.$$

$$r^2_{\oplus\Delta}\Big\}\Big\{\left(x^2_{\oplus\Delta} + y^2_{\oplus\Delta}\right)\Big[\left(y_{\oplus\Delta}\,\dot{z}_{\oplus\Delta}\right.$$

$$\left.-\dot{y}_{\oplus\Delta}\,z_{\oplus\Delta}\right)^2 + \left(z_{\oplus\Delta}\,\dot{x}_{\oplus\Delta}\right.$$

$$\left.-\dot{z}_{\oplus\Delta}\,x_{\oplus\Delta}\right)^2 + \left(x_{\oplus\Delta}\,\dot{y}_{\oplus\Delta} - \dot{x}_{\oplus\Delta}\right.$$

$$\left.\left.\left.y_{\oplus\Delta}\right)^2\right]\right\}^{-1}\right]^{1/2} \tag{101}$$

Equations (96), (97), (100) and (101) completely define T_x, T_y, T_z in terms of T_u, T_v, T_w and the instantaneous position and velocity coordinates $x_{\oplus\Delta}$, $y_{\oplus\Delta}$, $z_{\oplus\Delta}$, $\dot{x}_{\oplus\Delta}$, $\dot{y}_{\oplus\Delta}$, $\dot{z}_{\oplus\Delta}$. This latter method of determining the components of the thrust force is advantageous since the vehicle orientation does not enter the computations explicitly but rather implicitly as an input through the specification of the time variation of T_u, T_v, T_w.

When one starts with the components of thrust in the body axis, the vehicle orientation must be specified explicitly.

f. Relativistic effects

Before relativistic effects are mentioned, a brief description of the various systems of mechanics which deal with the motion of bodies on the astronomical scale is required. The earliest formulation of mechanics in mathematical form is due to Newton. Two postulates underlie his formulation of the laws of motion: (1) there exists a universal absolute time t in terms of which all events can be described, (2) any particle can be placed in an absolute euclidean three-dimensional space. The metric, or distance ds between any two neighboring points, of this space is given by

$$ds^2 = dx^2 + dy^2 + dz^2 \tag{102}$$

where x, y, z are the three cartesian coordinates of this space, and time t is regarded as a parameter. An inertial system in newtonian mechanics is defined as a coordinate system in which Newton's laws of motion preserve their mathematical form during a transformation of coordinates. Newton avoided complications by not specifying this absolute space and this absolute time (i. e., the inertial system). They have to be specified for each experiment that is performed.

Newtonian mechanics was very successful in interpreting experimental data, and it was not until two centuries later that this theory was modified by Einstein. Einstein's special theory of relativity is based on (1) the postulate of relativity, which states that it is impossible to detect unaccelerated motion through space and (2) the velocity of light in vacuo is the same for all observers, regardless of the relative velocity of the light source with respect to the observer. The most striking distinction between special relativity and newtonian mechanics is the introduction of a finite maximum velocity c in special relativity while the maximum velocity in newtonian mechanics does not have any limit. As a tribute to the success of newtonian mechanics the absolute euclidean three-dimensional space has been retained by special relativity. However, the notion of an absolute time which could be fixed in some way by two observers at two different places has been abandoned. Each event now needs four numbers to specify it: three space coordinates and time, and they can be plotted as points in the four-dimensional space-time with metric.

$$ds^2 = dt^2 - \frac{1}{c^2}\left(dx^2 + dy^2 + dz^2\right) \tag{103}$$

(Eq 103 is called the Minkowski space-time.)

Similar to its definition in newtonian mechanics, an inertial system in special relativity is defined as a coordinate system in which the laws of mathematical physics retain their form during a transformation of coordinates. The most general transformation between two inertial system S (x, y, z, t) and S' (x', y', z', t') in newtonian mechanics is given by the Galileo transformation

$$t' = t, \quad x' = x - Vt, \quad y' = y, \quad z' = z \tag{104}$$

where V is the uniform speed with which S' moves parallel to the x-axis with respect to S. In special relativity the most general transformation between

S and S' is given by the Lorentz transformation

$$t' = \beta \left(t - \frac{V}{c^2} x\right), \quad x' = \beta(x - Vt),$$

$$y' = y, \quad z' = z, \tag{105}$$

where $\beta = \left(1 - \frac{V^2}{c^2}\right)^{-1/2}$, and c is the velocity of light in vacuo. Both of these transformations are invariants, i.e., we may exchange the primed and unprimed coordinate systems without altering the form of the equations.

The theory of general relativity attempts to extend the postulate of relativity to accelerated types of motion (not only to unaccelerated motion as in special relativity) such as to motion in a gravitational field. The euclidean geometry of the previous systems of mechanics has been abandoned, and all events can be plotted as points in some four-dimensional riemannian (curved) space-time with the metric

$$ds^2 = \sum_{i=1}^{4} \sum_{j=1}^{4} g_{ij}(x_i) \, dx_i \, dx_j, \tag{106}$$

where x_i are the coordinates and $g_{ij}(x_i)$ are the components of the fundamental metric tensor characterizing the particular space-time used in the problem. The coordinates x_i are not necessarily known a priori but will be assigned in some way later, the only restriction being that the same method of assigning coordinates be used throughout. The laws of physics are assumed to be unaffected by the choice of coordinates and can therefore be expressed in an invariant form. This means that as a guide one uses the principle of covariance: There must be no preferred coordinate system. This principle of covariance can be insured by use of tensors and tensor equations which have the same form in all coordinate systems.

The equations of mathematical physics in special relativity and general relativity should reduce to the corresponding equations in newtonian mechanics if the finite maximum velocity c in the relativistic equations is replaced by an infinite one. Thus, in the problem of space vehicle motion, special relativity may be regarded as a "correction" to newtonian mechanics at high space vehicle speeds and general relativity as a "correction" to Newton's law of gravitation.

Contributions to special relativistic rocket kinematics and dynamics have been made by many investigators and the fundamental equations have been presented by many authors, for example by Krause in Ref. 25. To illustrate special relativistic effects, the following summary of equations for the motion of a rocket in a straight line and without any external forces acting on it has been taken from Ref. 25.

The following table shows that special relativistic effects on a space vehicle become important when its velocity or the velocity of the exhaust gases are an appreciable fraction of the speed of light, c = 299792.5 km/sec. It should be noted that by letting $c \to \infty$, $\beta \to 1$ the above relativistic rocket equations reduce to the newtonian rocket equations. For lunar vehicles these relativistic corrections are very small and can be neglected in most practical cases.

Since the theories of special nor general relativity do not employ a universal absolute time as newtonian mechanics does, the readings of clocks moving relative to each other and/or being in a different gravitational field will not agree. It is therefore possible to employ the different gravitational environment and the relative velocity between an earth observer and a space vehicle to measure special and general relativistic "time dilation" effects.

The problem of rocket motion has not yet been attacked in the theory of general relativity. However, equations of motion analogous to the n-body and restricted n-body problems of newtonian mechanics have been obtained in general form by Einstein, Fock, and Papapetrou among others. The general relativistic equations of motion are so complicated that no method of solution has as yet been given. By using a simplified dynamical system of a massive body and a space vehicle analogous to the classical restricted two-body problem of newtonian mechanics, three general relativistic effects have been deduced:

(1) The advance of perihelion (closest approach to the sun) of the planets.

(2) The deflection of light by gravitational fields.

(3) The red-shift of spectral lines by the gravitational field near its source.

Krause derived in Ref. 25, by use of the above simplifying assumption, the secular and long-periodic perturbations in the osculating orbital elements of a near-earth satellite.

The theory of general relativity gives the effect of gravitational fields, and the stronger the field, the more pronounced its effect on the trajectory. But, just as in the case of special relativity, general relativistic effects are very small for lunar vehicles and can be neglected in practical trajectory calculations. For example, the advance of perigee of a near-earth satellite, as calculated by LaPaz (Ref. 26) amounts only to several hundreds of seconds of arc per century.

5. Accuracy of Computed Trajectories

Before closing the discussion on force models and trajectory calculations it is helpful to summarize the deviations of a computed from an actual trajectory. The main sources of error in a computed trajectory are:

Rocket in Rectilinear Motion

Quantity	Expression in Coordinate System $S_\oplus$ of Stationary Earth Observer	Expression in Body-Fixed Coordinate System S_Δ Centered in the Moving Rocket
Velocity	$\vec{V}$	0
Mass	$M = \dfrac{M_\Delta}{\left(1 - \dfrac{V^2}{c^2}\right)^{1/2}} \equiv \beta M_\Delta$	M_Δ
Time element	$dt = \beta\, dt_\Delta$	dt_Δ
Acceleration	$\vec{f}_c = \dfrac{1}{\beta^2}\left[\vec{f}_\Delta - \left(1 - \dfrac{1}{\beta}\right)\dfrac{\vec{f}_\Delta \cdot \vec{V}}{V}\,\dfrac{\vec{V}}{V}\right]$	$\vec{f}_\Delta$
Exhaust velocity	$\vec{V}_{ex} = \left\{\dfrac{\vec{V}_{ex\Delta}}{\beta} + \vec{V}\left[\left(1 - \dfrac{1}{\beta}\right)\dfrac{\vec{V}_{ex\Delta}\cdot\vec{V}}{V^2} - 1\right]\right\}\left\{1 - V_{ex}\right\}^{-1}$	$\vec{V}_{ex\Delta}$
Element of mass flow after ejection	$dM = \dfrac{dM_\Delta^{*}}{\left(1 - \dfrac{V_{ex}^2}{c^2}\right)^{1/2}}$	$dM_\Delta = \dfrac{dM_\Delta^{*}}{\left(1 - \dfrac{V_{ex\Delta}^2}{c^2}\right)^{1/2}}$
Mass flow rate	$-\dfrac{dM}{dt} = \dfrac{\dfrac{-1}{\beta}\dfrac{dM_\Delta^{*}}{dt_\Delta}}{\left(1 - \dfrac{V_{ex}^2}{c^2}\right)^{1/2}}$	$-\dfrac{dM_\Delta}{dt_\Delta} = \dfrac{-\dfrac{dM_\Delta^{*}}{dt_\Delta}}{\left(1 - \dfrac{V_{ex\Delta}^2}{c^2}\right)^{1/2}}$
Thrust force	$\vec{T} = -\dfrac{dM}{dt}V_{ex} = \dfrac{-\dfrac{1}{\beta}\dfrac{dM_\Delta^{*}}{dt_\Delta}}{\left(1 - \dfrac{V_{ex}^2}{c^2}\right)^{1/2}}\vec{V}_{ex}$	$\vec{T}_\Delta = \dfrac{dM_\Delta}{dt_\Delta}V_{ex\Delta} = \dfrac{\dfrac{dM_\Delta}{dt_\Delta}}{\left(1 - V_{ex\Delta}^2/c^2\right)^{1/2}}\vec{V}_{ex\Delta}$

where M_Δ or M_Δ^{*} is the rest mass (i.e., mass if $\vec{V} = 0$) of the rocket,

$\beta = \dfrac{1}{1 - \dfrac{V^2}{c^2}}$, c is the speed of light in

vacuo, $\vec{V}_{ex}$ is the exhaust velocity, $\vec{V}$ is the velocity of the rocket and $\vec{f}$ its thrust acceleration.

a. Use of simplified force models

In the discussion of the various force models it is pointed out what approximations have been made in each. One would expect to use a simpler force model for preliminary trajectory selection and then use a more complicated model to verify some more desirable trajectories. It is to be expected that the many-body force model with the inclusion of nongravitational forces yields the most accurate trajectory. With each force model, many questions of computer simulation arise, such as the type of buildup and tail-off of thrust, the drag and lift coefficients, the reflectivity of the vehicle skin, the type of interaction between neutral and charged particles with the skin, etc. The computer simulation of some forces presents major problems and may be costly in programming and computation time.

b. Use of approximate physical constants

With each force there are in general some associated constants. Thus we need the gravitational constants of the moon $\mu_{\mathbb{C}} = GM_{\mathbb{C}}$, the earth $\mu_{\oplus} = GM_{\oplus}$, the mean angular velocity of the moon $\omega_{\oplus\mathbb{C}}$, constants associated with the expansion of the earth's and the moon's gravitational potentials, the variation of atmospheric temperature and molecular weight with altitude above the earth and many more constants depending on the force model. Each one of these constants is known imprecisely; this fact will cause errors in the computed trajectories. There should ideally be a balance between our knowledge of these constants and the type of force model to be used on the computer. The constants in any force model should be consistent among each other; and if they are not, a justification of each such departure should be given.

c. Errors in the lunar, solar, and planetary positions

The coordinates of celestial bodies have been obtained at the US Naval Observatory by use of general perturbation theories with certain values of physical constants which may differ from the values of the same constants used in the trajectory program.

d. Errors in initial conditions

The initial conditions of the vehicle, the celestial bodies and the launch site on earth as used in the computer simulation may be in error.

e. Computational errors

The programming of a trajectory computer program requires careful attention to the accumulation of error during the numerical integration of the equations of motion. Computational errors include those due to round-off, truncation, approximation, cancellation, and due to the presence of small divisors.

f. Human error

Last, but not least there is the possibility of human error in the handling of the data from assembling the machine input to the evaluation of the trajectory output.

C. THE VOICE TECHNIQUE

The discussion of the accuracy of computed trajectories in the preceding subsection pointed out the need of a simplified force model for parametric studies of lunar trajectories. The n-body force model is very complex because of the number of trajectory variables involved and the lack of exact solutions to the equations of motion. In fact, even the restricted three-body model (Subsection B-1) does not afford solutions for lunar trajectories efficiently. Although computer programs exist that determine trajectories by use of various integration schemes, the inputs to these programs are the unknown position and velocity of the spacecraft at some time. Since lunar trajectories are very sensitive to these initial conditions, these unknowns must be estimated very accurately. For example, a typical trajectory that passes behind the moon and returns to earth (circumlunar) requires an initial speed at the earth of approximately 11,000 m/sec. Perturbing this speed by 1 m/sec can change pericynthion (closest approach to moon) altitude by hundreds of kilometers, and the return perigee by thousands of kilometers. Thus, systematic studies using computer programs that integrate numerically can become long, tedious, and expensive, if the initial conditions are determined by a trial and error approach. The most desirable means around this problem is via a simplified technique that is relatively accurate and free of integration logic.

1. Description

To this end, a three-dimensional patched conic program using a succession of two-body trajectories, and with a transition region similar to the gravisphere transition to lunar influence was developed. However, instead of a gravisphere or sphere of influence, a lunar "volume of influence" is used which is defined by the locus of points that satisfy $r_M / r_E = 0.175$ (see Subsection B-1b). This volume, empirically determined to give the best results, is a sphere as was shown in the referenced subsection.

The following assumptions are made in any patched conic program: The earth and moon are spherical homogeneous bodies with the moon rotating about the earth's center. Motion within the lunar volume of influence is free of gravitational forces from the earth and sun. Likewise, motion toward or away from the volume is free of forces due to the moon and sun. Thus, a trajectory in this earth-moon model can be described by the classic two-body equations which are "patched" at the boundary of the lunar volume of influence.

Figure 4 presents a definition of the terms and the coordinate system used in the Voice (Volume of Influence-Calculated Envelopes) trajectory program. A geocentric coordinate system is employed with the positive x_E-axis defined by the vector lying along the intersection of the translunar trajectory plane and the moon's orbital plane in the direction of the moon. The z_E-axis is normal to the moon's orbital plane, i.e., in the direction of the angular momentum vector of the moon with the y_E-axis completing the right-handed system in the MOP. The lead angle of the moon, ϕ *, is measured from the x_E-axis to the position of the moon at the time of injection.

The relative inclination of the translunar trajectory plane i_{VTL} and the transearth trajectory plane i_{VTE} to the MOP are determined at the time of injection and volume of influence exit, respectively.

The program first computes the translunar trajectory to the point of entry into the volume of influence, at which point the velocity and position vectors are determined relative to the geocentric coordinate system. At volume entry the velocity and position vectors are transformed to a selenocentric reference frame as illustrated in the following sketch for the simple case of a trajectory in the MOP (i_{VTL} = 0):
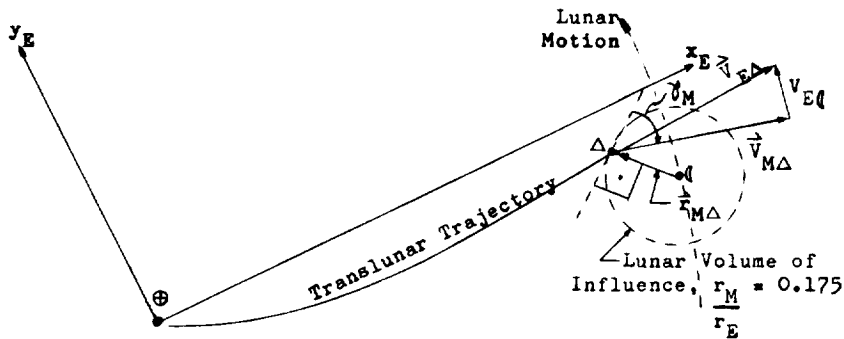
where $\vec{V}_{EA}$ is the velocity of the space vehicle and $\vec{V}_{E(}$ is that of the moon relative to earth. From the preceding sketch it can be seen that the velocity of the space vehicle relative to the moon $\vec{V}_{MA}$ is given by $\vec{V}_{MA} = \vec{V}_{EA} - \vec{V}_{E(}$.

The geocentric vehicle position and velocity at entry into the lunar volume of influence ($\vec{r}_{EA}$, $\vec{V}_{EA}$) are transformed to a selenocentric coordinate system $x_M\, y_M\, z_M$, i.e. to ($\vec{r}_{MA}$, $\vec{V}_{MA}$) for the trajectory computation around the moon. The $x_M\, y_M\, z_M$ coordinate system is illustrated in the following sketch:
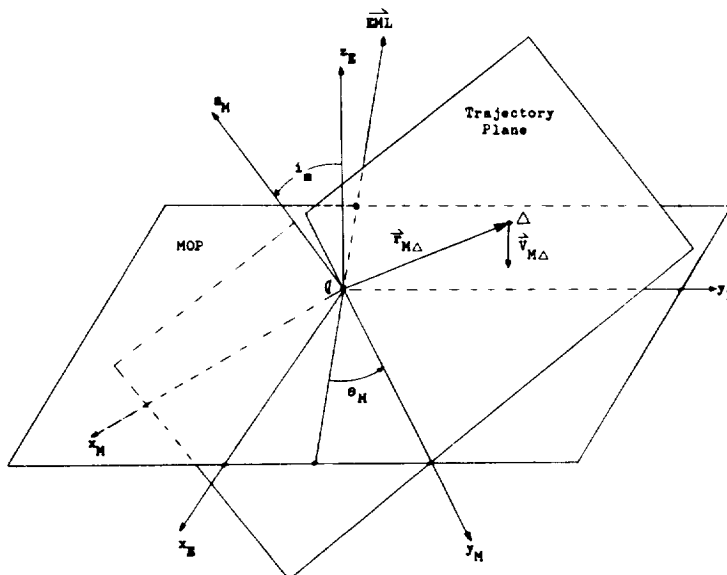
The z_M-axis is in the direction of $\vec{V}_{M\triangle} \times \vec{r}_{M\triangle}$ or perpendicular to the trajectory plane around the moon. The y_M axis defines the intersection between the trajectory or $x_M y_M$-plane and MOP (or the $x_E y_E$-plane), with the x_M axis completing the right-handed coordinate system. The inclination i_m of the trajectory to the moon's orbital plane inside the volume of influence is given by $i_m = \cos^{-1}\left(\dfrac{\vec{z}_M \cdot \vec{z}_E}{z_M \, z_E}\right)$. Knowing the direction of the earth-moon line $\overrightarrow{EML}$ at the time of entry into the volume, the time to reach pericynthion and the moon's rotational rate about the earth, $\omega_{\oplus\mathbb{C}}$, the orientation θ_M of the lunar trajectory with respect to the earth-moon line $\overrightarrow{EML}$ at pericynthion can be found.

Upon leaving the lunar volume of influence, the vehicle position and velocity are again transformed to the $x_E y_E z_E$ coordinate system and the transearth trajectory is then computed.

The above discussion acquaints the reader with the technique. In order to understand exactly what the Voice program can do, one must look at the inputs and outputs. The following trajectory variables are specified in the input for circumlunar mission trajectories:

(1) Earth launch base position (geocentric latitude and longitude).

(2) Injection altitude h_{e0} and flight path angle γ_{e0} for the translunar trajectory.

(3) Pericynthion altitude h_{PL}, closest approach to moon.

(4) Return vacuum perigee altitude h_{PE} or the closest approach to the earth if the earth's atmosphere is neglected.

(5) Translunar trajectory inclination i_{VTL} to the MOP.

(6) Transearth trajectory inclination i_{VTE} to the MOP.

(7) Declination of the moon when the spacecraft is at pericynthion.

(8) Return base geocentric latitude.

As can be seen, the major characteristics of the entire lunar trajectory are specified. The essence of the program is thus a matter of iteration within the program in order to satisfy these desired characteristics or trajectory variables, thus allowing one to explicitly state mission parameters as input.

The program output consists of other requirements to fulfill the mission and additional pertinent data as listed below:

(1) Injection position ρ_0 and geocentric latitude and longitude. The injection position ρ_0 is measured from the MOP along the translunar trajectory plane to the point of injection.

(2) Injection velocity $V_{E\triangle 0}$.

(3) Lunar lead angle ψ^* at injection.

(4) Position and velocity of the space vehicle at pericynthion.

(5) Inclination i_m of the vehicle trajectory to the MOP in the lunar volume of influence.

(6) Orientation θ_M of the trajectory with respect to the $\overrightarrow{EML}$ at pericynthion.

(7) Position and velocity at return vacuum perigee.

(8) Flight time to pericynthion and to return vacuum perigee.

(9) Longitude of first two intersections of the return trajectory.

(10) Range angle in parking orbit and range to return base latitude extended beyond perigee to the return base latitude.

Another program exists using the same principles as the Voice technique wherein one-way transearth trajectories from lunar orbit can be determined. Entitled, "Ejection from Lunar Orbit," this program has the following inputs and outputs which are illustrated in the following sketch:

Inputs:

(1) Inclination of the circular lunar orbit to the moon's orbital plane i_m. The program is restricted to circular lunar orbits.

(2) Orientation of the circular lunar orbit with respect to the earth-moon line θ_M.

(3) Altitude of the circular lunar orbit h_{PL}.

(4) Ejection point from lunar orbit β_{M0}.

(5) Flight path angle at ejection γ_{M0}.
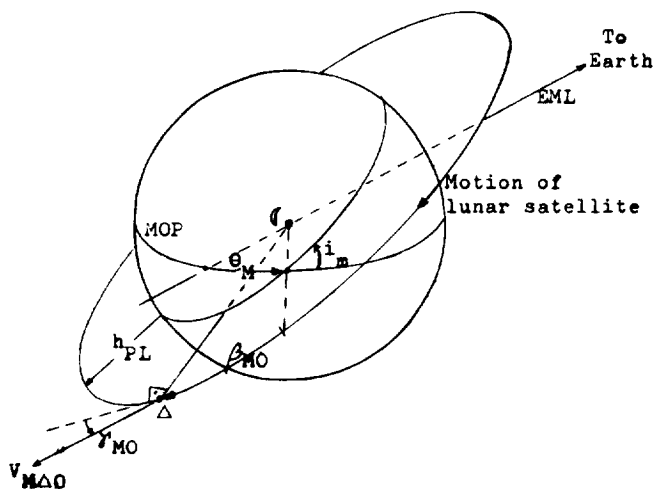
(6) Desired vacuum perigee altitude h_{PE}.

Outputs:

(1) Ejection velocity $V_{M\triangle 0}$.

(2) Transearth inclination i_{VTE}.

(3) Time to return to vacuum perigee.

(4) Position and velocity at perigee.

With proper interpretation this program is also used for one-way translunar trajectories. Again note the ease by which specific mission requirements can be obtained.

2. Comparison with Integrated Trajectories

The Voice technique, although an approximation to a complex physical model, compares very favorably with integrated restricted three-body and n-body trajectories. The following table illustrates this point by comparing two typical integrated trajectories (one restricted 3-body and one n-body) with their respective Voice trajectories. The integrated trajectories were obtained by an iterative scheme utilizing the Voice program. The table, which is self-explanatory, shows that there is good agreement between the initial conditions obtained with the Voice technique and the initial conditions for the actual integrated trajectory. All mission constraints are closely matched, thereby proving trends established by Voice.

Thus the Voice technique can be used with reasonable accuracy to perform parametric studies of lunar trajectory characteristics. In addition the technique can be used for obtaining actual n-body integrated trajectories.

Further comparisons between Voice trajectory characteristics and those using the restricted 3-body and n-body force models for various types of lunar trajectories are given in Chapters VI and IX.

### Comparison of Voice Trajectories with Integrated Trajectories

Inject North--Direct Item			Restricted 3-Body Force Model Comparison		n-Body Force Model Comparison	
			Voice	Integrated	Voice	Integrated
Injection into translunar orbit	Altitude (h_{e0})	km	231.648	231.648	182.88	182.88
	Velocity ($V_{E\Delta0}$)	m/sec	10905.545	10903.951	10962.32	10963.786
	Flight path angle (γ_{e0})	deg	3.0	3.0	2.6682	2.6682
	Inclination to MOP (i_{VTL})	deg	30.	30.	29.2495*	29.3822*
	Injection position (ψ_0)	deg	12.259	11.94	13.502125	13.198678
	Lunar lead angle (ϕ*)	deg	44.0596	45.0258	37.3314	38.02945
At moon	Pericynthion altitude (h_{PL})	km	1852.	1851.44	185.015	186.867
At earth	Vacuum perigee altitude (h_{PE})	km	46.72	46.086	36.81	37.5
	Total flight time (t)	hr	154.31	154.3	147.736	147.078
	Inclination to MOP (i_{VTE})	deg	7.92	6.95	35.206*	35.387*
	Direction and mode of return		Direct from south	Direct from south	Direct from south	Direct from south

*i_{VTL} and i_{VTE} are relative to earth equatorial plane, i.e., they are actually i_{VE} and i_{VTEQ}, respectively.

D. ADDITIONAL CLASS OF CIRCUMLUNAR ORBITS

A new class of circumlunar orbits, i.e., periodic circumlunar trajectories, has been described and an outline of the proof of existence for these orbits had been given by Arenstorf (Ref. 27) just as the Lunar Flight Manual went to press. These orbits were obtained for the restricted three-body problem, and they exist for small mass ratios of the two primary bodies. The circumlunar orbits exist near Keplerian, or restricted two-body, ellipses which represent a zero mass ratio between the two primary bodies or the existence of

only one primary body. Two typical circumlunar orbits as calculated by Arenstorf have been plotted below for the earth-moon-space vehicle system in rotating $x_R y_R$ coordinates:

By a judicious choice of trajectory parameters these orbits can be made to pass arbitrarily close to the earth and moon, and small perturbations from forces arising outside of the framework of the restricted three-body problem can be counteracted by thrust. Reference 27 suggests the use of circumlunar orbits for shuttling passengers and materials from the vicinity of the earth to the vicinity of the moon.
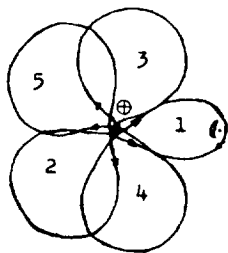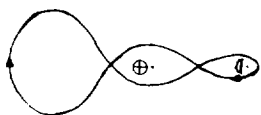
E. REFERENCES

1. Egorov, V. A., "Certain Problems of Moon Flight Dynamics," The Russian Literature of Satellites, Part I International Physics Index, Inc., New York, 1958.

2. Buchheim, R. W., "Lunar Flight Trajectories," Report P 1268, Rand Corporation, January 30, 1958. Also Chapter 7, "Lunar Flight Trajectories," in H. S. Seifert, ed. "Space Technology," John Wiley and Sons, Inc., New York, 1959.

3. Anonymous, "Orbital Flight Manual," ER 12684, Martin Marietta Corporation, Space Systems Division, Baltimore, 1963.

4. Mickelwait, A. B., "Lunar Trajectories," ARS Journal, Vol. 29, December 1959, pp 905 to 914.

5. Mickelwait, A. B., and Booton, R. C., Jr., "Analytical and Numerical Studies of Three-Dimensional Trajectories to the Moon," Journal of Aerospace Sciences, Vol. 27, August 1960, pp 561 to 573.

6. Koelle, H. H., Editor-in-Chief, "Handbook of Astronautical Engineering," McGraw-Hill, New York, 1961.

7. Weber, R. J., Pauson, W. M., and Burley, R. R., "Lunar Trajectories," NASA Technical Note TN D-866, August 1961.

8. Buchheim, R. W., "Motion of a Small Body in Earth-Moon Space," RM 1726, Rand Corporation, June 4, 1956.

9. Hagihara, Y., "Recommendations on Notation of the Earth Potential," Astronomical Journal, Vol. 67, February 1962, p 108.

10. Heiskanen, W. A., and Vening-Meinesz, F. A., "The Earth and Its Gravity Field," McGraw-Hill, New York, 1958.

11. Alexandrov, I., "The Lunar Gravitational Potential," in "Astronautical Science," Vol. 9, Plenum Press, New York, 1960, pp 320 to 324.

12. Baker, R. M. L., Jr., and Makemson, M. W., "An Introduction to Astrodynamics," Academic Press, New York, 1960.

13. Pines, S., and Wolf, H., "Interplanetary Trajectory by the Enckes Method Programmed for the IBM 704 and 7090," Republic Aviation Corporation, New York.

14. Anonymous, "American Ephemeris and Nautical Almanac," published annually by the Nautical Almanac Office, United States Observatory, Washington, D. C. (obtainable from Superintendent of Documents, U. S. Government Printing Office, Washington 25, D. C.).

15. Brouwer, D., and Clemence, G. M., "Methods of Celestial Mechanics," Academic Press, New York, 1961.

16. Baker, R. M. L., Jr., Westrom, G. B., et al., "Efficient Precision Orbit Computation Techniques," ARS Journal, August 1960, pp 740 to 747.

17. Pines, S., Payne, M., and Wolf, H., "Comparison of Special Perturbation Methods in Celestial Mechanics," Report No. 60-281, Aero Research Laboratory, Wright-Patterson AFB, Ohio, August 1960.

18. Anonoymous, "Flight Performance Handbook for Orbital Operations," Space Technology Laboratories, Inc., Redondo Beach, Calif., September 1961.

19. Parkinson, R. W., Jones, H. M., and Shapiro, I. J., "Effects of Solar Radiation Pressure on Earth Satellite Orbits," Science, Vol. 131, 1960. pp 920 and 921.

20. Kochi, K. C., and Staley, R. M., "Methods for Analysis of Satellite Trajectories," Aeronautical Research Laboratories, Wright-Patterson AFB, Ohio, September 1960.

21. Beard, D., and Johnson, F., "Charge and Magnetic Field Interaction with Satellites," Journal of Geophysical Research, Vol. 65, No. 1, 1960, pp 1 to 7.

   Singer, S. F., and Walker, E. H., "Electrostatic Screening of Bodies in Space," Report of the Physics Department, University of Maryland, College Park, September 1961.

23. Krzywoblocki, M. Z. v., et al., "A Study of Special Interplanetary Flight Problems," Report No. 2, PR-DW-58-43, IOD 2446-58, Engineering Experiment Station, Aeronautical Engineering Department, University of Illinois, Urbana, June 1959.

24. Lovell, A. C. B., "Meteor Astronomy," Clarendon Press, Oxford, 1954.

25. Krause, H. G. L., "Astrorelativity," Report MTP-P & VE-F-62-4, NASA, George C. Marshall Space Flight Center, Huntsville, Alabama, May 22, 1962. Also Chapter II, H. H. Koelle, Editor-in-Chief, "Handbook of Astronautical Engineering," McGraw-Hill, New York, 1961.

26. LaPaz, L., "Advances of the Perigees of Earth Satellites Predicted by General Relativity," Publications of the Astronautical Society of the Pacific, Vol. 66, 1954, pp 13 to 18.

27. Arenstorf, R. F., "Existence of Periodic Solutions Passing Near Both Masses of the Restricted Three-Body Problem," AIAA Journal, Vol. 1, No. 1 (January 1963), pp 238 to 240.

TABLES AND ILLUSTRATIONS

LIST OF TABLES

LIST OF ILLUSTRATIONS

TABLE 1

Transformations Between Position and
Velocity Components of the
Restricted Three-Body
Problem

Define the following rotation matrices:

$$[T_1] \equiv [T(\phi + \omega_{\oplus\mathbb{C}} t)] =$$

$$\begin{bmatrix} \cos(\phi + \omega_{\oplus\mathbb{C}} t) & -\sin(\phi + \omega_{\oplus\mathbb{C}} t) & 0 \\ \sin(\phi + \omega_{\oplus\mathbb{C}} t) & \cos(\phi + \omega_{\oplus\mathbb{C}} t) & 0 \\ 0 & 0 & 1 \end{bmatrix}$$

$$[T_2] \equiv [T^{-1}(\phi + \omega_{\oplus\mathbb{C}} t)] =$$

$$\begin{bmatrix} \cos(\phi + \omega_{\oplus\mathbb{C}} t) & \sin(\phi + \omega_{\oplus\mathbb{C}} t) & 0 \\ -\sin(\phi + \omega_{\oplus\mathbb{C}} t) & \cos(\phi + \omega_{\oplus\mathbb{C}} t) & 0 \\ 0 & 0 & 1 \end{bmatrix}$$

Position and velocity components in the three nonrotating coordinate systems are related to the rotating systems by the transformations:

$$\begin{Bmatrix} x_0 \\ y_0 \\ z_0 \end{Bmatrix} = [T_1] \begin{Bmatrix} x_R \\ y_R \\ x_R \end{Bmatrix} \quad ,$$

$$\begin{Bmatrix} \dot{x}_0 \\ \dot{y}_0 \\ \dot{z}_0 \end{Bmatrix} = [T_1] \begin{Bmatrix} \dot{x}_R - \omega_{\oplus\mathbb{C}} y_R \\ \dot{y}_R + \omega_{\oplus\mathbb{C}} x_R \\ \dot{z}_R \end{Bmatrix}$$

$$\begin{Bmatrix} x_e \\ y_e \\ z_e \end{Bmatrix} = [T_1] \begin{Bmatrix} x_R + \bar{r}_{\oplus\mathbb{C}} \nu \\ y_R \\ z_R \end{Bmatrix} ,$$

$$\begin{Bmatrix} \dot{x}_e \\ \dot{y}_e \\ \dot{z}_e \end{Bmatrix} = [T_1] \begin{Bmatrix} \dot{x}_R - \omega_{\oplus\mathbb{C}} y_R \\ \dot{y}_R + \omega_{\oplus\mathbb{C}} (x_R + \bar{r}_{\oplus\mathbb{C}} \nu) \\ \dot{z}_R \end{Bmatrix}$$

$$\begin{Bmatrix} x_m \\ y_m \\ z_m \end{Bmatrix} = [T_1] \begin{Bmatrix} x_R - \bar{r}_{\oplus\mathbb{C}} (1 - \nu) \\ y_R \\ z_R \end{Bmatrix}$$

$$\begin{Bmatrix} \dot{x}_m \\ \dot{y}_m \\ \dot{z}_m \end{Bmatrix} = [T_1] \begin{Bmatrix} \dot{x}_R - \omega_{\oplus\mathbb{C}} y_R \\ \dot{y}_R + \omega_{\oplus\mathbb{C}} [x_R - \bar{r}_{\oplus\mathbb{C}} (1 - \nu)] \\ \dot{z}_R \end{Bmatrix}$$

and the inverse transformations must be given since the initial conditions are usually given in nonrotating coordinates, while the computation is performed in rotating coordinates:

$$\begin{Bmatrix} x_R \\ y_R \\ z_R \end{Bmatrix} = [T_2] \begin{Bmatrix} x_0 \\ y_0 \\ z_0 \end{Bmatrix} \quad ,$$

$$\begin{Bmatrix} \dot{x}_R \\ \dot{y}_R \\ \dot{z}_R \end{Bmatrix} = [T_2] \begin{Bmatrix} \dot{x}_0 + \omega_{\oplus\mathbb{C}} y_0 \\ \dot{y}_0 - \omega_{\oplus\mathbb{C}} x_0 \\ \dot{z}_0 \end{Bmatrix}$$

$$\begin{Bmatrix} x_R + \bar{r}_{\oplus\mathbb{C}} \nu \\ y_R \\ z_R \end{Bmatrix} = [T_2] \begin{Bmatrix} x_e \\ y_e \\ z_e \end{Bmatrix} ,$$

$$\begin{Bmatrix} \dot{x}_R \\ \dot{y}_R \\ \dot{z}_R \end{Bmatrix} = [T_2] \begin{Bmatrix} \dot{x}_e + \omega_{\oplus\mathbb{C}} y_e \\ \dot{y}_e - \omega_{\oplus\mathbb{C}} x_e \\ \dot{z}_e \end{Bmatrix}$$

$$\begin{Bmatrix} x_R - \bar{r}_{\oplus\mathbb{C}} (1 - \nu) \\ y_R \\ z_R \end{Bmatrix} = [T_2] \begin{Bmatrix} x_m \\ y_m \\ z_m \end{Bmatrix} ,$$

$$\begin{Bmatrix} \dot{x}_R \\ \dot{y}_R \\ \dot{z}_R \end{Bmatrix} = \begin{bmatrix} T_2 \end{bmatrix} \begin{Bmatrix} \dot{x}_m + \omega_\oplus \text{C} \ y_m \\ \dot{y}_m - \omega_\oplus \text{C} \ x_m \\ \dot{z}_m \end{Bmatrix}$$

*The coordinate systems are defined by the
sketch on page IV-20.

TABLE 2

Transformation Between Body-Axes and Vehicle-Centered Equatorial Coordinates

The coordinates in the body-axis (x_b, y_b, z_b) coordinate system with origin at the instantaneous center of mass of the vehicle are related to nonrotating coordinates $(x_{\oplus, \Delta}, y_{\oplus, \Delta}, z_{\oplus, \Delta})$ fixed in the vehicle with origin at the instantaneous center of mass and axes parallel to the $x_\oplus, y_\oplus, z_\oplus$ directions by the relations (where the order of rotation is ψ, θ, ϕ around the z, y, and x axes, respectively)

$$\begin{Bmatrix} x_b \\ y_b \\ z_b \end{Bmatrix} = \begin{bmatrix} T(\phi) \end{bmatrix} \begin{bmatrix} T(\theta) \end{bmatrix} \begin{bmatrix} T(\psi) \end{bmatrix} \begin{Bmatrix} x_{\oplus, \Delta} \\ y_{\oplus, \Delta} \\ z_{\oplus, \Delta} \end{Bmatrix}$$

or

$$\begin{Bmatrix} x_b \\ y_b \\ z_b \end{Bmatrix} = \begin{bmatrix} 1 & 0 & 0 \\ 0 & \cos\phi & \sin\phi \\ 0 & -\sin\phi & \cos\phi \end{bmatrix} \begin{bmatrix} \cos\theta & 0 & -\sin\theta \\ 0 & 1 & 0 \\ \sin\theta & 0 & \cos\theta \end{bmatrix} \begin{bmatrix} \cos\psi & \sin\psi & 0 \\ -\sin\psi & \cos\psi & 0 \\ 0 & 0 & 1 \end{bmatrix} \begin{Bmatrix} x_{\oplus, \Delta} \\ y_{\oplus, \Delta} \\ z_{\oplus, \Delta} \end{Bmatrix}$$

The inverse transformation is given by

$$\begin{Bmatrix} x_{\oplus, \Delta} \\ y_{\oplus, \Delta} \\ z_{\oplus, \Delta} \end{Bmatrix} = \begin{bmatrix} T(\psi) \end{bmatrix}^{-1} \begin{bmatrix} T(\theta) \end{bmatrix}^{-1} \begin{bmatrix} T(\phi) \end{bmatrix}^{-1} \begin{Bmatrix} x_b \\ y_b \\ z_b \end{Bmatrix}$$

or

$$\begin{Bmatrix} x_{\oplus, \Delta} \\ y_{\oplus, \Delta} \\ z_{\oplus, \Delta} \end{Bmatrix} = \begin{bmatrix} \cos\psi & -\sin\psi & 0 \\ \sin\psi & \cos\psi & 0 \\ 0 & 0 & 1 \end{bmatrix} \begin{bmatrix} \cos\theta & 0 & \sin\theta \\ 0 & 1 & 0 \\ -\sin\theta & 0 & \cos\theta \end{bmatrix} \begin{bmatrix} 1 & 0 & 0 \\ 0 & \cos\phi & -\sin\phi \\ 0 & \sin\phi & \cos\phi \end{bmatrix} \begin{Bmatrix} x_b \\ y_b \\ z_b \end{Bmatrix}$$

or, when the matrix multiplication is performed,

$$\begin{Bmatrix} x_{\oplus, \Delta} \\ y_{\oplus, \Delta} \\ z_{\oplus, \Delta} \end{Bmatrix} = \begin{bmatrix} (\cos\psi \ \cos\theta) & (\cos\psi \ \sin\theta \ \sin\phi - \sin\psi \ \cos\phi) & (\cos\psi \ \sin\theta \ \cos\phi + \sin\psi \ \sin\phi) \\ (\sin\psi \ \cos\theta) & (\sin\psi \ \sin\theta \ \sin\phi + \cos\psi \ \cos\phi) & (\sin\psi \ \sin\theta \ \cos\phi - \cos\psi \ \sin\phi) \\ (-\sin\theta) & (\cos\theta \ \sin\phi) & (\cos\theta \ \cos\phi) \end{bmatrix} \begin{Bmatrix} x_b \\ y_b \\ z_b \end{Bmatrix}$$

This can also be written formally in the form of direction cosines

$$
\begin{Bmatrix} x_{\oplus,\Delta} \\ y_{\oplus,\Delta} \\ z_{\oplus,\Delta} \end{Bmatrix}
=
\begin{bmatrix} \ell_{11} & m_{11} & n_{11} \\ \ell_{12} & m_{12} & n_{12} \\ \ell_{13} & m_{13} & n_{13} \end{bmatrix}
\begin{Bmatrix} x_b \\ y_b \\ z_b \end{Bmatrix}
$$

which are given by direct comparison of the preceding two equations

$$\ell_{11} = \cos\psi\,\cos\theta$$

$$\ell_{12} = \sin\psi\,\cos\theta$$

$$\ell_{13} = -\sin\theta$$

$$m_{11} = \cos\psi\,\sin\theta\,\sin\phi - \sin\psi\,\cos\phi$$

$$m_{12} = \sin\psi\,\sin\theta\,\sin\phi + \cos\psi\,\cos\phi$$

$$m_{13} = \cos\theta\,\sin\phi$$

$$n_{11} = \cos\psi\,\sin\theta\,\cos\phi + \sin\psi\,\sin\phi$$

$$n_{12} = \sin\psi\,\sin\theta\,\cos\phi - \cos\psi\,\sin\phi$$

$$n_{13} = \cos\theta\,\cos\phi$$

and must satisfy

$$\ell_{11}^2 + m_{11}^2 + n_{11}^2 = 1$$
$$\ell_{12}^2 + m_{12}^2 + n_{12}^2 = 1$$
$$\ell_{13}^2 + m_{13}^2 + n_{13}^2 = 1$$

and

$$\ell_{11} m_{11} + \ell_{12} m_{12} + \ell_{13} m_{13} = 0$$

$$m_{11} n_{11} + m_{12} n_{12} + m_{13} n_{13} = 0$$

$$n_{11} \ell_{11} + n_{12} \ell_{12} + n_{13} \ell_{13} = 0$$

$$\ell_{11} \ell_{12} + m_{11} m_{12} + n_{11} n_{12} = 0$$

$$\ell_{12} \ell_{13} + m_{12} m_{13} + n_{12} n_{13} = 0$$

$$\ell_{13} \ell_{11} + m_{13} m_{11} + n_{13} n_{11} = 0$$

$$
\begin{vmatrix} \ell_{11} & \ell_{12} & \ell_{13} \\ m_{11} & m_{12} & m_{13} \\ n_{11} & n_{12} & n_{13} \end{vmatrix} = 1
$$

$$\ell_{11}^2 + \ell_{12}^2 + \ell_{13}^2 = 1$$

$$m_{11}^2 + m_{12}^2 + m_{13}^2 = 1$$

$$n_{11}^2 + n_{12}^2 + n_{13}^2 = 1$$

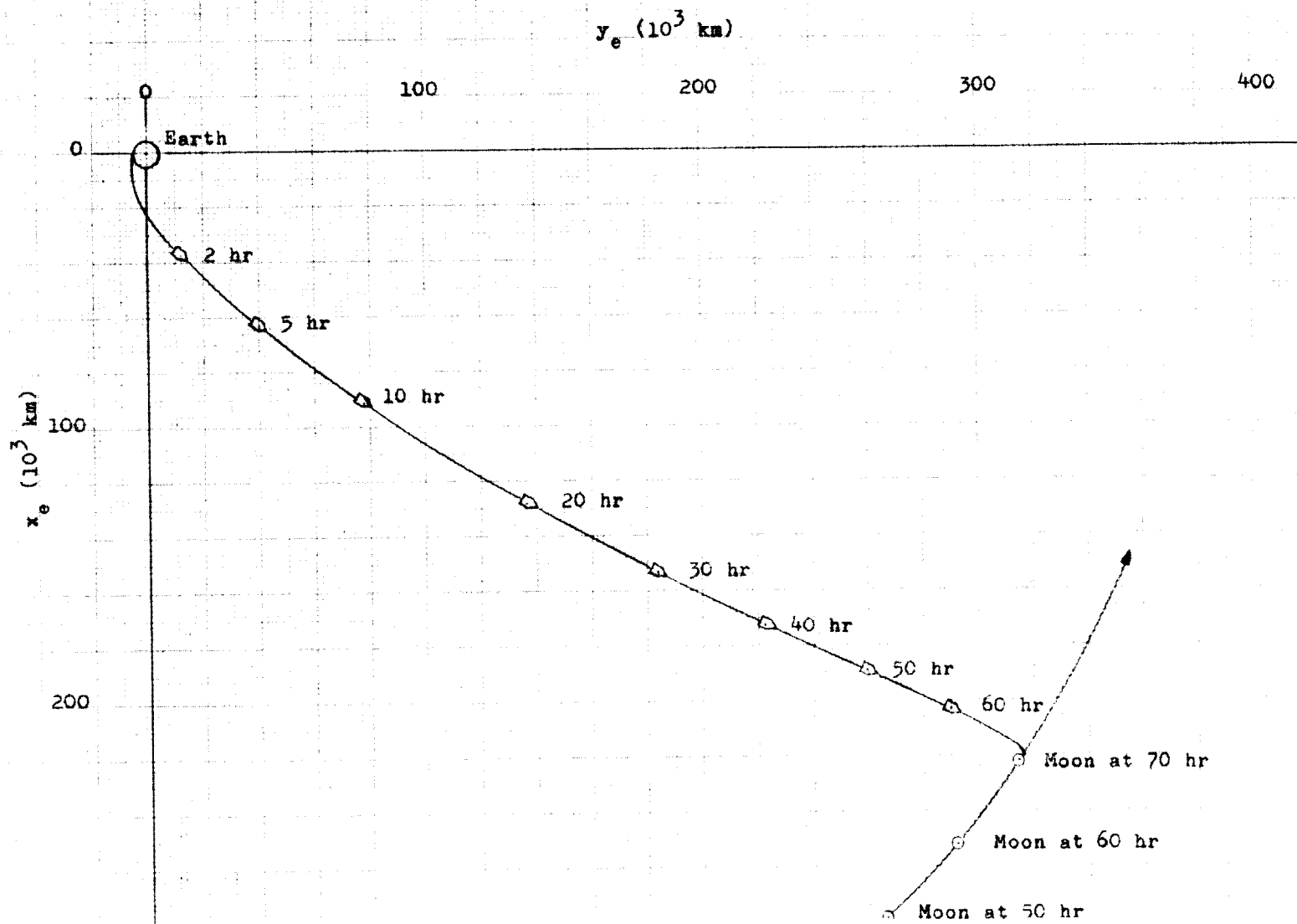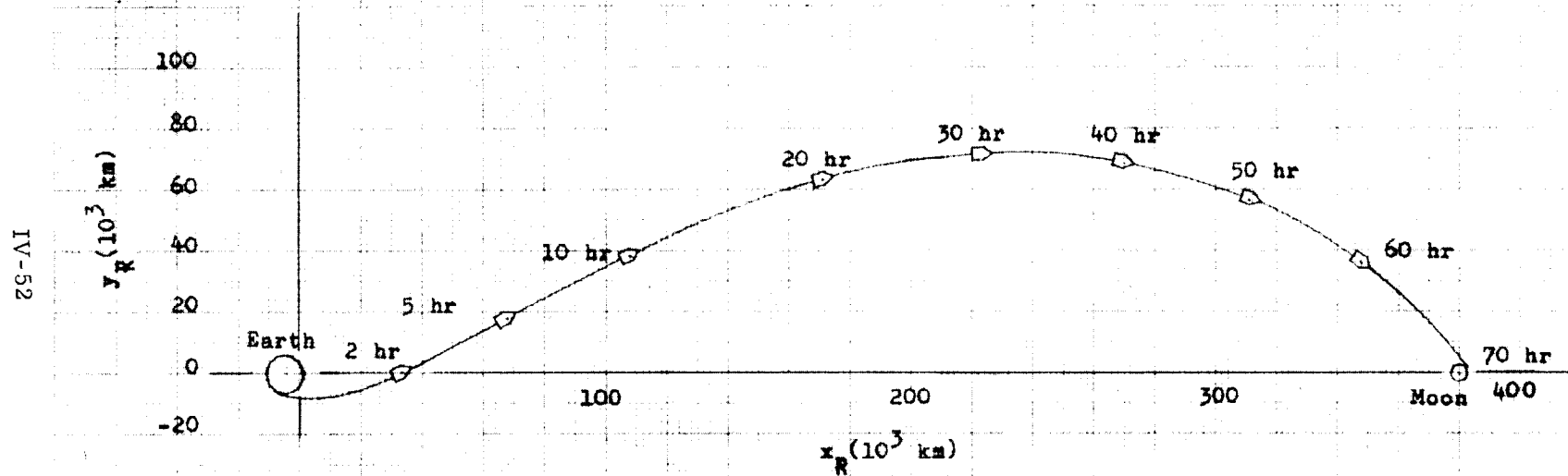Fig. 1. Typical Earth-Moon Trajectory in Nonrotating $x_e y_e$ Coordinates

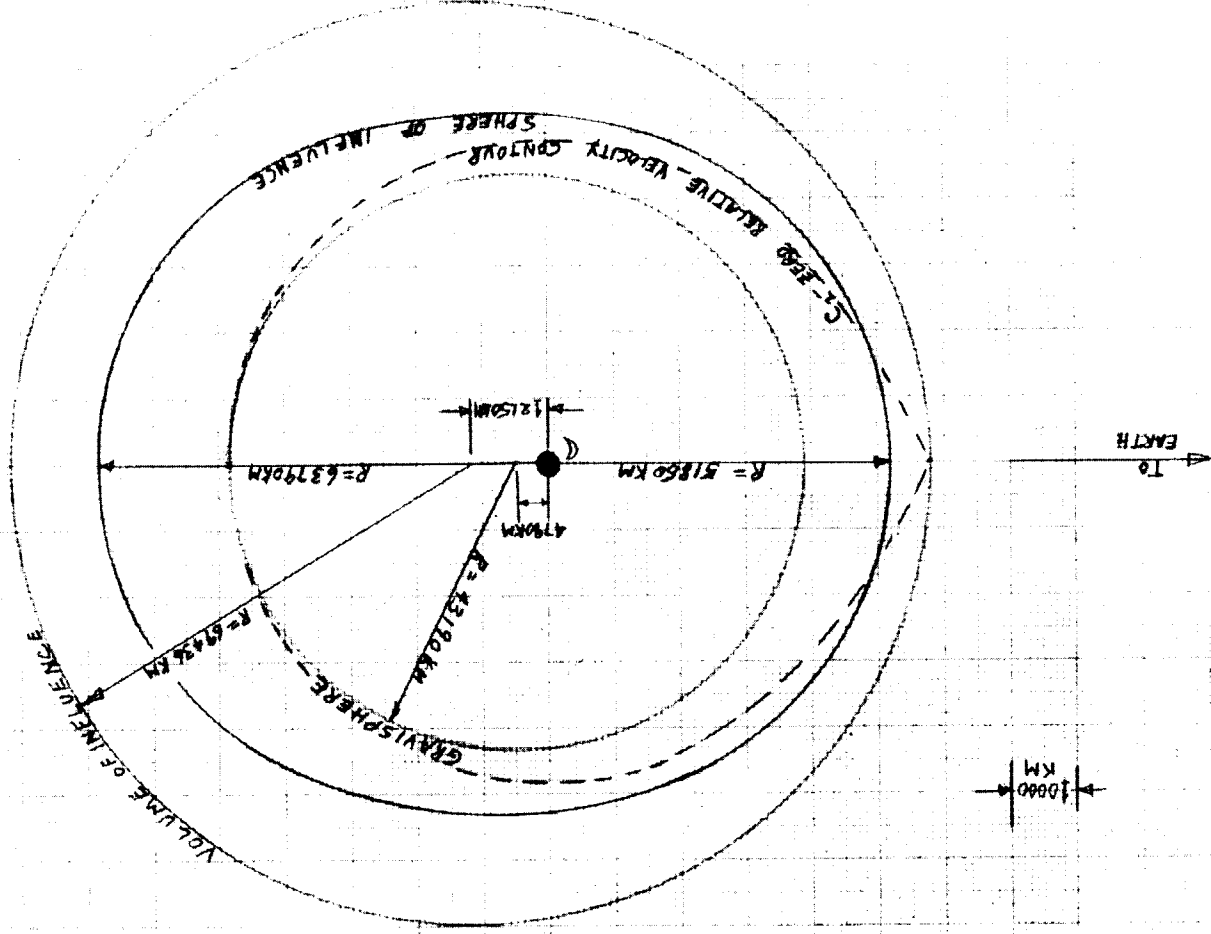Fig. 2. The Earth-Moon Trajectory of Fig. 1 in Rotating $x_R y_R$ Coordinates

IV-52

Fig. 3. Gravitational Regions Around the Moon

IV-53

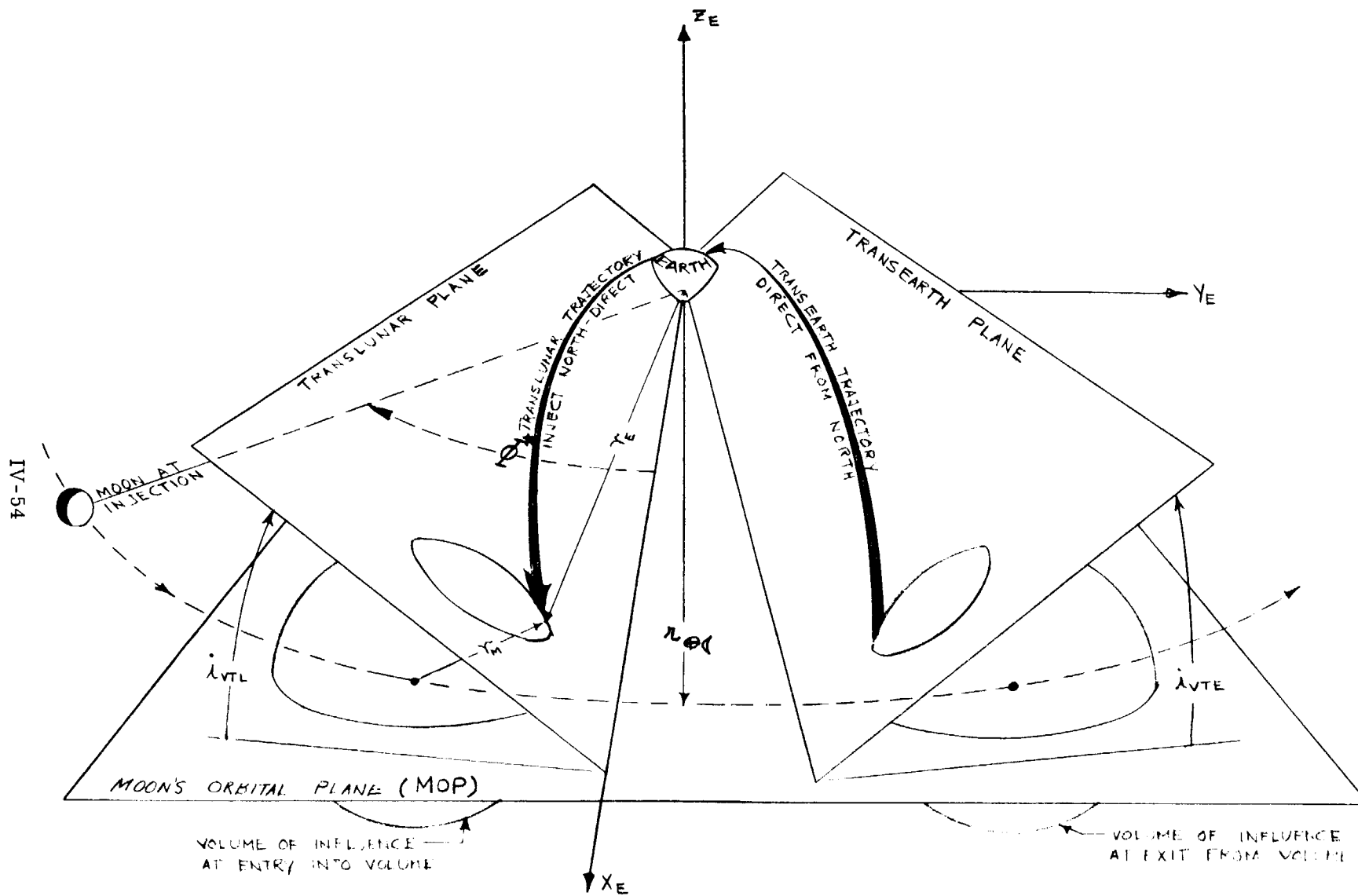FIG 4 VOICE GEOMETRY